AD 63 600

DISCLAIMER NOTICE

THIS DOCUMENT IS BEST QUALITY PRACTICABLE. THE COPY FURNISHED TO DTIC CONTAINED A SIGNIFICANT NUMBER OF PAGES WHICH DO NOT REPRODUCE LEGIBLY.

OR are
Blank pgs
that have
Been Removed

BEST AVAILABLE COPY

RESEARCH AND DEVELOPMENT LABORATORIES

HUGHES AIRCRAFT COMPANY

Microwave Laboratory
Research and Development Laboratories

WAVEGUIDE SLOT ARRAY DESIGN

Technical Memorandum No. 348

by
Ivan P. Kaminow
and
Robert J. Stegen

1 July 1954

This technical memorandum constitutes partial fulfillment of the work under Contract AF19(604)-262, Change C.

ACKNOWLEDGEMENT

The authors are deeply indebted to the members of the Microwave Laboratory of the Hughes Aircraft Company whose work we have drawn upon freely. We are further indebted to the members of the Antenna Research Section of the Antenna Department for their invaluable suggestions and conversations. In particular, we should like to acknowledge the assistance of Dr. R. S. Wehner, who directed the writing of this paper, and of Dr. R. W. Bickmore, Dr. R. S. Elliott, T. T. Taylor, I. K. Williams, R. H. Reed, and C. H. Wilcox, who were kind enough to read the manuscript and eliminate many errors.

ACKNOWLEDGEMENTS FOR ILLUSTRATIONS

Fig. II-50 (p.147) S. Silvo, "Microwave Antenna Theory and Design," Radiation Laboratory Series, vol. 12, McGraw Hill, p. 301.

Fig. III-2 (p.153) W. H. Watson, "Waveguide Transmission and Antenna Systems," Clarendon Press, p. 136.

Fig. III-4 (p.155) A. L. Cullen and F. K. Goward, "The Design of a Wave-Guide-Fed Array of Slots to Give a Specified Radiation Pattern," Journal of the Institute of Electrical Engineers, (III A) 93 (1946), p. 684.

Fig. III-15 (p.166) P. M. Woodward, "A Method of Calculating the Field over a Plane Aperture Required to Produce a Given Polar Diagram," Journal of the Institute of Electrical Engineers, (III A) 93 (1946), p. 1554.

Ivan P. Kaminow
Robert J. Stegen

TABLE OF CONTENTS

TABLE OF CONTENTS (Continued)

LIST OF ILLUSTRATIONS

LIST OF ILLUSTRATIONS (Continued)

LIST OF ILLUSTRATIONS (Continued)

ABSTRACT

A slot cut in the wall of a hollow waveguide forms an interesting and useful type of radiator of electromagnetic energy. The slots which are discussed in this report are resonant or nearly resonant; that is, the slots are approximately one-half wavelength long. By positioning a series of these slots along a length of waveguide, a linear array antenna can be formed which has excellent electrical characteristics and which has mechanical advantages over other types of antennas. To design such an array, the radiation and impedance characteristics of the individual slots must be known. It is one purpose of this report (Chapter II) to present in complete form the theory of operation of individual slot radiators, methods of measuring their characteristics, and an extensive collection of useful slot design data. The second portion of this report (Chapter III) presents some of the theoretical and experimental aspects of arrays which use slot radiators as exciting elements. Much of the data presented have not been previously published but have appeared in the form of laboratory technical memoranda. An attempt has been made to correlate and evaluate these data.

WAVEGUIDE SLOT ARRAY DESIGN

1. INTRODUCTION

Arrays of slots cut into the walls of waveguides form an interesting and useful type of antenna. These waveguide slot arrays evolved naturally as the result of two important developments in the early 1940's. The first was the development of practical microwave generators; the second was the need for highly directive and shaped beam antennas for radar applications. With microwave generators available, the use of hollow waveguide transmission lines became feasible and, because of their low losses, desirable. Since the aperture distribution (and consequently the radiation pattern) can be controlled quite accurately in an array of radiating elements, it was felt that highly directive and shaped beam antennas could be produced more easily by antenna arrays than by certain optical-type antennas such as lenses, horns, or point sources feeding reflectors.

Dipoles, probe-coupled to the field in a rectangular waveguide, were first used as the radiating elements in these arrays. Generally, a linear array of these dipoles was used in connection with a cylindrical reflector for search radar antennas. The array was designed to give a narrow beam in azimuth and the reflector was shaped to give a fan beam in elevation. These dipole arrays, however, exhibited a number of undesirable characteristics:

1) It was difficult to adjust the probe coupling accurately.
2) The probe-fed dipole presented a complex impedance to the wave in the guide, which resulted in low efficiency.
3) The stem of the dipole radiated, producing cross polarization.
4) At high frequencies, the electrical design of the dipoles did not permit rugged mechanical qualities.
5) The cost of producing these arrays was excessive.

During the early years of World War II, W. H. Watson recognized the fact that a slot cut into the wall of a waveguide would radiate if positioned so as to interrupt the wall currents on the guide. He and his co-workers (E. W. Guptill, J. W. Dodds, R. H. Johnston, M. Telford, and F. R. Terroux) at McGill University later succeeded in developing techniques for designing slot arrays in rectangular waveguide. Since Watson's early investigations, a good deal of theoretical and experimental work has been done on slot radiators in rectangular and other types of guide. Slot antennas are now finding applications as zero-drag antennas which can be faired into the skin of high speed aircraft.

Watson's work is described in his book[87] and in his paper[88] in the Journal of the Institution of Electrical Engineers. Therefore, emphasis in this report has been placed on more recent work which may not be readily available in the public literature. In particular, most of the slot studies conducted at the Microwave Laboratory of the Hughes Aircraft Company will be outlined.

Section 2 contains a description of the characteristics of the slot radiator--the slot radiation pattern (or element factor), slot impedance and techniques for measuring it, and available design data on slots. In Section 3 are described the general characteristics of the slot array, methods for determining the proper excitation coefficients of the elements to produce a specified radiation pattern, techniques for producing this aperture distribution on the slot array, and finally some practical considerations appropriate to slot arrays.

2. SLOT RADIATORS

Slot radiators are the building blocks that make up a slot array, and, as such, their characteristics must be known before an array can be designed. In the first section the radiation patterns of slot radiators are discussed; techniques for measuring slot impedances are described next; and in the last section design data for various types of slots are presented.

2.1 THE ELEMENT FACTOR

It is well known in antenna theory that, for certain types of arrays, the mathematical equation which describes the radiation pattern can be factored into two parts: the element factor and the space (or array) factor. The element factor is nothing more than the radiation pattern of a single element of the array (assuming no mutual coupling[33]), and the space factor is the radiation pattern of an array of isotropic radiators that are excited by the same currents as the elements which comprise the actual array. The term radiation pattern, as it is used in this report, means the amplitude and phase variation of the radiated field at the surface of a very large sphere centered at the antenna. Since amplitude and phase are of interest, it is convenient to think of the radiation pattern as being complex. Thus, in the equation relating antenna pattern, $R(\theta, \phi)$, element factor, $E(\theta, \phi)$, and space factor, $S(\theta, \phi)$,

$$R(\theta, \phi) = E(\theta, \phi)\, S(\theta, \phi) \tag{1}$$

R, E, and S are not only space vectors but are also complex functions. It is also true that the antenna power pattern can be factored; thus,

$$\left| R(\theta, \phi) \right|^2 = \left| E(\theta, \phi) \right|^2 \cdot \left| S(\theta, \phi) \right|^2 \tag{2}$$

Since the array designer is generally interested in the power pattern rather than the field pattern, the phase of the element factor is not of great importance. However, it should be emphasized that equations (1) and (2) hold only for a special class of arrays known as "parallel arrays." Parallel arrays are characterized by the fact that any element (or element pattern) may be made to coincide with any other by translation without rotation. From another point of view, it can be said that, for a parallel array, the far field pattern for any element in its regular position in the array and radiating by itself is similar to the far field pattern for any other element in the array except for a phase difference which depends only on the element spacing and current phases.

Fortunately, the majority of practical arrays are of the parallel variety, including for all practical purposes linear arrays of slots cut in the same face of a waveguide. Arrays of slots on the periphery of conducting cylinders or tangent to curves on a flat surface, however, are not parallel arrays. For these nonparallel types of array, the amplitude and phase of the element factor are both important for analyzing or synthesizing an array pattern whether the designer is interested in the power pattern or

in the field pattern. The reason is that the radiation pattern of an array element does not appear as a factor in the mathematical formulation for the array pattern[83]. Consequently, both amplitude and phase data for the element factor are presented whenever they are available.

2.1.1 The Electromagnetic Babinet's Principle

It is often true that accurate analogies simplify the solution of unfamiliar and complex problems by allowing the investigator to solve them in terms of their familiar analogs. The electromagnetic Babinet's Principle is such a tool; it can be extended to describe the dual relationship between a radiating slot and the familiar dipole.

Babinet's Principle is a theorem in physical optics which can be stated as follows:

> Consider a thin plane screen which is "black" (that is, nonreflecting) and infinite in extent. Suppose now that apertures of any size, shape, or distribution are cut in the screen, and that in front of the screen there are one or more optical sources. Let the screen produced by interchanging holes and obstructions be called the complementary screen. Then Babinet's Principle states that the optical disturbances at any point behind the plane of each of two complementary screens, exposed in turn to the same incident waves, would, if superposed, produce the same effect at the given point as if no screen were present.

For example, a thin nonreflecting disc, interposed between a lamp and a white screen, would cast a shadow pattern on the screen consisting of a small black shadow directly behind the disc, a grey area surrounding the shadow which is produced by diffraction at the edges of the disc, and a white area which is exposed to the direct rays from the lamp. If, now, the disc is replaced by a large nonreflecting screen containing an aperture identical with the disc in which the aperture occupies the former position of the disc, the shadow pattern will be just the reverse of that previously described; and if the two patterns were superposed, the image would be white as though the nonreflecting screen were not present at all.

In electromagnetism (as opposed to physical optics), however, the propagation of scalar waves or the use of nonreflecting screens is not considered, as has been done above. The description of electromagnetic waves in terms of an electric and a magnetic vector which obey certain well known boundary conditions at a perfectly conducting surface must be taken into account if Babinet's Principle is to be applied to electromagnetic waves at microwave frequencies. H. G. Booker[7] has succeeded in restating the theorem for the purpose of deducing some of the properties of a resonant slot in an infinite ground plane from known properties of a

complementary strip dipole,* and E. T. Copson[14] has rigorously proved the electromagnetic Babinet's Principle.

Booker observed that Babinet's Principle in optics would hold for electromagnetism provided that, in passing from one screen to its complement, one also made the transformation $\vec{E}_i \rightarrow \vec{H}_i'$, $\vec{H}_i \rightarrow -\frac{\epsilon}{\mu}\vec{E}_i'$ in the incident fields. The mathematical statement of the electromagnetic Babinet's Principle (in rationalized MKS units) is:

> Let the electromagnetic field $\vec{E}_i$, $\vec{H}_i$ be incident in $z > 0$ on a perfectly conducting screen in the plane $z = 0$; the holes in the screen are denoted by R_1, the metal of the screen by R_2. Let the total field in $z < 0$ be $\vec{E}$, $\vec{H}$. Further, let the complementary electromagnetic field $\vec{E}_i'$, $\vec{H}_i'$ be incident in $z > 0$ on the complementary perfectly conducting screen in the plane $z = 0$; the holes in the screen are R_2 and the metal R_1. Let the total field in $z < 0$ be $\vec{E}'$, $\vec{H}'$.

Then, if

$$k\vec{H}_i' = \vec{E}_i$$
$$k\vec{E}_i' = -\frac{\mu}{\epsilon}\vec{H}_i \qquad (3)$$

and

k = one ohm (to keep the equations dimensionally consistent);

Babinet's Principle is:

$$\vec{E} + k\vec{H}' = \vec{E}_i$$
$$\vec{H} - \frac{\epsilon}{\mu}k\vec{E}' = \vec{H}_i \qquad (4)$$

for all $z < 0$ and

$$\vec{E} - k\vec{H}' = \vec{E}_r$$
$$\vec{H} + \frac{\epsilon}{\mu}k\vec{E}' = \vec{H}_r \qquad (5)$$

---

*Booker assumes that a thin strip of width b (small compared with a wavelength) behaves like a circular wire of diameter b/2 from the point of view of frequency selectivity.

for all $z > 0$, where $\vec{E}_r$, $\vec{H}_r$ is the reflected field for a completely closed screen.

As an application of Babinet's Principle, the radiation from a strip dipole fed at the center by a parallel wire transmission line can be compared with a complementary slot antenna. (See arrangement illustrated in Figure II-1.) If the parallel wire line is ideal (an infinitesimal distance between wires), then the line when open-circuited or short-circuited will not radiate. In other words, if this line terminates in free space or in an infinite ground plane, the incident and reflected fields, respectively, external to the parallel wire line will be zero; or, in terms of equations (4) and (5), $E_i = H_i = 0$ and $E_r = H_r = 0$. In Figure II-1B the plane containing the transmission line has been rotated 90 degrees from the position illustrated in Figure II-1A to conform to the conditions of equation (3). Applying equations (4) and (5), in which the primed fields refer to the slot,

$$E_\theta = k H'_\theta$$
$$H_\phi = -\frac{\epsilon}{\mu} k E'_\phi \qquad (6)$$

for $z > 0$, and

$$E_\theta = -k H'_\theta$$
$$H_\phi = \frac{\epsilon}{\mu} k E'_\phi \qquad (7)$$

for $z < 0$. Thus, the radiation pattern of a center-fed slot antenna is simply the pattern of the complementary center-fed dipole with the polarization rotated 90 degrees.

2.1.2 Infinite Ground Plane

A slot in a ground plane can be excited in a number of ways. Feeding the slot at the center by a two-wire line is one method; another is to cut a slot in a waveguide. A study of the latter technique is the purpose of this report.

It is generally assumed that the magnetic current distribution in a radiating slot is sinusoidal, just as it is assumed that the electric current distribution on a dipole is sinusoidal. In both cases, calculations based on this assumption are supported by experiment.

Since the distribution in a slot cut in a waveguide is assumed to be the same as that for a slot in an infinite ground plane and fed by a parallel wire line, the electromagnetic Babinet's Principle can be used to deduce the pattern of a waveguide slot radiating into an infinite ground plane. In fact, the manner in which the slot is fed is irrelevant as far as its radiation pattern is concerned, as long as the sinusoidal assumption holds. Thus,

the pattern of a waveguide slot in an infinite ground plane is the same as the pattern of the complementary center-fed strip dipole with the exception that the $\vec{E}$ and $\vec{H}$ vectors are rotated 90 degrees. Stated another way, $\vec{E}$ for the dipole becomes $\vec{H}$ for the slot and $\vec{H}$ for the dipole becomes $-\vec{E}$ for the slot. Thus, the far field pattern of a narrow resonant slot is given by[64]

$$H_\theta(\theta) = j\left(\frac{\epsilon}{\mu}\right)^{1/2} \frac{V_o(m) \sin \frac{m\pi}{2}}{2\pi R} e^{-jkR} \left[\frac{\cos\left(\frac{m\pi}{2}\right) \cos\theta)}{\sin\theta}\right], \quad (8)$$

$$m = 1, 3, 5. \ldots$$

or

$$H_\theta(\theta) = \left(\frac{\epsilon}{\mu}\right)^{1/2} \frac{V_o(m) \cos \frac{m\pi}{2}}{2\pi R} e^{-jkR} \left[\frac{\sin\left(\frac{m\pi}{2} \cos\theta\right)}{\sin\theta}\right], \quad (9)$$

$$m = 2, 4, 6, \ldots$$

and

$$E_\phi(\phi) = \text{constant for a given R.} \quad (10)$$

In these equations

$V_o(m)$ = the value of the voltage at voltage maximum

$\ell = m\lambda/2$ = the length of the slot

R = the distance from the center of the slot to an observer in space

θ = the angle measured from the longitudinal axis of the slot to the observer.

From equations (8), (9) and (10), it is apparent that the surfaces of constant R are equiphase surfaces (provided that the amplitude is both positive and negative).

A comparison of radiation patterns for the "half-wave dipole" and complementary "half-wave slot" (m = 1) is illustrated in Figure II-2. In the event that the slot can radiate on only one side of the ground plane, the dashed portion of the pattern does not exist. This condition is the case of interest for waveguide slot radiators.

2.1.3 Finite Ground Plane

The fields at the surface of the ground plane into which a slot radiates must obey the boundary conditions imposed by Maxwell's equations. As a result, the radiation pattern for a slot is a function of its ground plane configuration.

The H-plane pattern for an ideal slot in a finite ground plane is practically the same as that for a slot in an infinite ground plane since the fields vanish in the $\theta = 0$ and $\theta = \pi$ directions. The E-plane pattern, on the other hand, is modified due to reflections at the edges of the ground plane. The resultant pattern will consist of undulations superimposed on the original semicircular pattern. The angular location of the maxima and minima of these undulations can be determined by assuming that the far field is produced by three sources, one at the slot and one at each edge of the ground plane.[55] These angles are given by

$$\phi = \arccos \frac{n\lambda}{L} \tag{11}$$

where n is an integer and L is the dimension of the ground plane normal to the slot axis. The successive deterioration of the pattern as L becomes small is shown in Figure II-3. It can be seen from Figure II-3 that as L becomes large, the undulations become more numerous but their magnitudes decrease, so that for very long ground planes the pattern approaches a semicircular shape.

2.1.4 Rectangular Waveguide

Radiating slots can be located at a number of different positions on a rectangular waveguide. If no auxiliary ground plane is provided, the shape of the radiation pattern will depend on the orientation of the slot with respect to the edges and faces of the guide. A cylinder of rectangular cross section does not in general lend itself to mathematical description so that the pattern of a slot in a rectangular waveguide cannot be readily predicted.

A measured E-plane pattern for a longitudinally oriented slot in the broad face of the guide is shown in Figure II-4. The backward lobe is produced by reflections from the two lower edges of the guide. As the slot is displaced from the centerline of the broad face, the maximum of the pattern tilts off the normal, as shown in Figure II-5, due to the asymmetry of the currents on the guide face.

2.1.5 Slot Pairs

A slot pair is defined as a radiating element consisting of two equally excited slots located diametrically opposite each other on the surface of a cylinder.

If the electric vectors across the slots point in the same direction proceeding around the cylinder, the slots are said to be "in-phase." The theoretical E-plane pattern for an in-phase longitudinal slot pair on a thin elliptic cylinder with its major axis less than two wavelengths is a circle.[10] Mathematical and computational difficulties have prevented reliable prediction of results for larger sizes of elliptic cross section. The measured patterns of in-phase slot pairs on a thin elliptic cylinder taken from the work of Carter[10] are shown in Figure II-6. These patterns illustrate the changes which occur as the cylinder thickness increases.

If the electric vectors across the slots point in opposite directions proceeding around the cylinder, the slots are said to be in "phase opposition." A plane conducting sheet with a slot opening on both sides is the equivalent of a thin elliptic cylinder with slots in phase opposition. If the sheet is infinite in extent, the E-plane pattern is a circle. For finite thin elliptic cylinders (or finite sheets), however, the pattern has a null in the direction of the major axis of the elliptic cross sections, a fact which can be verified by applying the simple boundary conditions of Maxwell's equations. Carter observed that for small elliptic cylinders the E-plane patterns are similar to the patterns of wire dipoles oriented in the direction of the major axis and having a corresponding length. Figure II-7A illustrates the measured E-plane patterns for a thin cylinder and Figure II-7B, the patterns for a thick cylinder. The difference in some of these patterns when compared with the patterns of the corresponding wire dipoles is due to the fact that the current distribution on the elliptic cylinder is far from sinusoidal. The approximation, however, is useful for small cylinders.

The comments made above for elliptic cylinders hold approximately for other shapes such as flat ground planes, cylinders of rectangular cross section, and aircraft wings and stabilizers.

2.1.6 Circular Cylinders

Much theoretical work has been done on the radiation from axial and circumferential slots in infinite circular cylinders. (References 3, 46, 47, 49, 50, 62, 65-67.) However, no attempt to evaluate or assemble the results of these investigations will be made here.

The solutions for the far fields are generally harmonic series of integer order Hankel functions, which converge rapidly for sufficiently small cylinders. However, for cylinders which have a circumference greater than approximately 12 wavelengths, the convergence is very slow and the computation tedious. Furthermore, tabulations of the Hankel function are not complete. Simplified expressions for certain regions of cylinder size are presently being sought[62]

Bailin[3] has applied the equations of Silver and Saunders[65] to the special cases of a narrow circumferential half-wave slot and a narrow axial half-wave slot. From these special equations, Bailin has calculated a number of radiation patterns for slots on a 12 and an 8 wavelength circumference cylinder. Figure II-8 is the $\theta = 30$ degrees pattern for a circumferential slot. E_θ is the principal component and E_ϕ the cross-polarized component; both amplitude and phase are shown. The cross polarization is due to asymmetry in the current pattern on the cylinder when viewed in planes other than the $\theta = 90$ degrees plane. Figures II-9 and II-10 show the principal component and cross-polarized component patterns respectively, for different values of θ.

Figure II-11 shows the deterioration of the E-plane pattern as a function of θ for the axial slot. For this slot $E_\theta = 0$. Figures II-12 and

II-13 describe the H-plane patterns in the ϕ = 180 degrees and ϕ = 0 degree planes for an 8 and a 12 wavelength circumference cylinder. For these large cylinders the pattern at ϕ = 0 is very nearly given by the radiation field of a half-wave dipole which is indicated by the dashed lines.

The patterns in Figures II-8 through II-13 are for slots in an infinitely long cylinder and it is to be expected that a finite cylinder will exhibit a somewhat modified pattern.

2.1.7 Elliptic Cylinder

The circular cylinder is a special case of the elliptic cylinder; however, the problem of determining the radiation fields for a slot in an elliptic cylinder is a good deal more difficult. On the other hand, the elliptic cylinder is a good approximation to rectangular waveguide and is better adapted to mathematical treatment than rectangular guide.

The results of investigations on elliptic cylinders are too complicated to be presented here, and as in the previous section the reader is directed to the appropriate references.[10, 68, 85] The applicability of the theoretical solutions depends on the size of the cylinder with respect to the wavelength and the eccentricity of the elliptic cross section. A large number of measured and theoretical patterns for a variety of elliptic cross sections and slot locations have been published.[10] The largest cylinder considered, however, had a maximum dimension of 2 wavelengths. The various slot configurations considered are a single slot at the vertex of the ellipse, an in-phase slot pair with slots located on opposite broad sides of the ellipse, a single slot in the side, and a slot pair in phase opposition.

Sinclair[68] and Taylor[85] show that in the equatorial plane the radiation pattern of an infinite axial slot is identical with that of a finite slot. This fact is useful in applying theoretical data (which is often for infinite slots) to the practical case of resonant slots.

2.1.8 The Effect of Dielectric Covers

Dielectric covers are often used to protect the slots and waveguide from the weather or to allow the waveguide system to be pressurized. If the covers are thin, the radiation pattern will not differ noticeably from that of the uncovered slot. On the other hand, if the dielectric cover is thick and large in extent, some energy will be "trapped" by the dielectric and directed along the ground plane.

The curves of Figure II-14 describe the deterioration of the pattern for increasing dielectric thickness. The undulations in the pattern become more violent as more energy is trapped by the dielectric and reflected from the edges of the ground plane.

2.2 MEASUREMENT TECHNIQUES

When slots are used as elements in an array, their characteristics are affected by their neighbors. For certain slot array configurations, this mutual interaction is not very serious and the slot characteristics are practically the same for a single slot as for a similar slot in the presence of a number of other like slots in the array. On the other hand, slots that will experience strong mutual coupling in the array must be measured in the presence of a large number of similar slots. For this reason measurement techniques are discussed in three sections: Equivalent Circuit Representation (introductory), Negligible Mutual Coupling, and Effective Mutual Coupling.

2.2.1 Equivalent Circuit Representation

Figure II-15 illustrates the distribution of current lines on the inner surfaces of a rectangular waveguide propagating the TE_{01} mode. If the guide is matched along its length, this current pattern travels down the guide with a velocity equal to the phase velocity in the guide. If the guide is terminated in a short or open circuit (that is, if there are only standing waves in the guide), this pattern remains stationary. The current lines in the pattern may be resolved conveniently into two components: A longitudinal component parallel to the longitudinal guide axis and a transverse component in a plane normal to the guide axis. In terms of lumped networks, one may think of the longitudinal currents as series currents and the transverse currents as shunt currents. Thus, at an open circuit termination, the series current vanishes and the shunt (transverse) current is a maximum; and at short circuit termination, the shunt current vanishes while the series (longitudinal) current is a maximum.

A consideration of the wall currents offers a convenient and intuitive means for determining whether or not a slot will radiate, and if so, what type of equivalent circuit representation it will have. In Figure II-16 the position of slots on rectangular guide is shown. Slots b and g do not intercept any lines of current so that no electric field intensity will be developed in these slots (provided that the slots are sufficiently narrow), and they will not radiate. On the other hand, slots c, h, i and j will intercept only shunt currents and can be represented by shunt elements in an equivalent circuit; slots d, e and f will intercept only series currents and are represented by series elements; slot a intercepts both series and shunt currents and can be represented, in general, only by a four terminal network (that is, by a T or a π-section). The degree of coupling or excitation of these slots depends on the current density intercepted by the slot and the component of the length transverse to the current lines. Thus, the coupling at a given position in the guide can be adjusted by the orientation of the slot: For slots d and i the coupling increases with θ, for c the coupling increases with x, and for a the series coupling increases with θ and the shunt coupling increases with x. It is important to note that if the guide is not matched, the coupling also depends on the position of the slot along the guide. A shunt slot located $\lambda g/2$ from a short or $\lambda g/4$ from an open circuit (that is, at a node of the transverse currents) will not radiate nor will a series slot radiate at a node of the longitudinal currents. A slot of the type a can be made to look like a simple shunt or series

element by locating it at a node of the series current or a node of the shunt current.

It is possible to change the phase of the electric field in the slot by 180 degrees by the simple expedient of relocating the slot in its mirror image position with respect to the appropriate guide axis. This phenomenon is illustrated in Figure 17.

Since a radiating slot represents a loss of power from the transmission line, the slot can be represented by a lumped resistive element located at the center of the slot on the equivalent transmission line. In general, there is also reactive power associated with the slot. Experimental frequency measurements of slot impedance show that it behaves like a resonant circuit near the frequency at which the slot impedance is real. The series slot looks like a parallel resonant circuit in series with the line and the shunt slot looks like a series resonant circuit in parallel with the line as shown in Figure II-18. Thus it is possible to define a slot bandwidth in terms of the Q of the resonant circuit representation. Broad band slots will be considered in the discussion of slot bandwidth, section 2.3.5.

For high efficiency, it is desirable to minimize the reactive power associated with the slot since high reactive power makes for high currents and consequent wall losses. Thus, from a practical standpoint, the "resonant slot" (approximately a multiple of $\lambda g/2$ in length) is the most interesting. Furthermore, the power radiated from a slot is proportional to the value of resistance R or conductance G for its equivalent circuit. A. F. Stevenson[64, 75] has developed equations for determining the value of G or of R for the appropriate resonant slots. The theory is based on the following assumptions:

1) The slot is narrow; that is, $2 \log_{10} (\text{length/width}) \gg 1$.
2) The slot is cut so as to be near the first resonance (length $\approx \lambda g/2$).
3) The field in the slot is transverse to the long dimension (due to assumption 1) and varies sinusoidally along the slot, independent of the exciting system.
4) The guide walls are perfectly conducting and infinitely thin.
5) The field in the region behind the guide face containing the slot is negligible with respect to the field outside the guide; physically, this assumption means extending the face containing the slot into an infinite perfectly conducting ground plane.

The third assumption corresponds to an approximation often made for the current on a resonant dipole and is in close accord with experimental conditions. The fifth assumption in general is not valid in the physical situation except when very large ground planes are employed. Assumptions (1) and (4) are generally slightly in error. Nonetheless, the equations are quite valuable in that they give approximate values for G and R and also indicate the manner in which the slot parameters affect G and R. Furthermore, good experimental agreement is found in many cases. More exact theoretical investigations have been performed on certain types of practical slots and

can be found in the literature.[43]

Figure II-19 illustrates the rectangular guide dimensions, the four types of slots considered by Stevenson, and their equivalent circuit representation at resonance. The relations for the appropriate resonant slot conductances, G, and resonant slot resistances, R, normalized to the characteristic impedance for the waveguide are given below:

1) Longitudinal shunt slot in the broad face (Figure II-19B):

$$G = G_o \sin^2 \frac{\pi x}{a} \tag{12}$$

where

$$G_o = 2.09 \frac{\lambda_g}{\lambda} \frac{a}{b} \cos^2\left(\frac{\pi\lambda}{2\lambda_g}\right) \tag{13}$$

2) Transverse series slot in the broad face (Figure II-19C):

$$R = R_o \cos^2\left(\frac{\pi x}{a}\right) \tag{14}$$

where

$$R_o = 0.523 \left(\frac{\lambda_g}{\lambda}\right)^3 \frac{\lambda^2}{ab} \cos^2\left(\frac{\pi\lambda}{4a}\right) \tag{15}$$

3) Centered inclined series slot in the broad face (Figure II-19D):

$$R = 0.131 \left(\frac{\lambda}{\lambda_g}\right) \frac{\lambda^2}{ab} \left[I(\theta) \sin\theta + \frac{\lambda_g}{2a} J(\theta) \cos\theta \right]^2 \tag{16}$$

where

$$\left.\begin{matrix} I(\theta) \\ J(\theta) \end{matrix}\right\} = \frac{\cos\left(\frac{\pi\xi}{2}\right)}{1-\xi^2} \pm \frac{\cos\left(\frac{\pi\eta}{2}\right)}{1-\eta^2} \tag{17}$$

and

$$\left.\begin{matrix} \xi \\ \eta \end{matrix}\right\} = \frac{\lambda}{\lambda_g} \cos\theta \mp \frac{\lambda}{2a} \sin\theta \tag{18}$$

4) Inclined shunt slot in the narrow face (edge slot) Figure II-19E:

$$G = \frac{30}{73\pi} \left(\frac{\lambda_g}{\lambda}\right) \frac{\lambda^4}{a^3 b} \left[\frac{\sin\theta \cos\left(\frac{\pi\lambda}{2\lambda_g} \sin\theta\right)}{1 - \left(\frac{\lambda}{\lambda_g}\right)^2 \sin^2\theta} \right]^2 \qquad (19)$$

These equations are cumbersome, and, as previously noted, not exact for practical slots. Thus, slots are not usually designed by these equations. The equations do indicate quite well the manner in which G or R varies with θ or x, as the case may be, so that data on a few slots can be extended reasonably accurately. In addition, some of the Stevenson equations lend themselves to simplification in special cases.

It may be worth while to mention here an application of Babinet's Principle to slot admittance. Booker[7] has shown that the radiation (driving-point) impedance Z_w, of a center-fed wire dipole near resonance and the radiation admittance, Y_s, of the complementary narrow center-fed slot in an infinite ground plane are related by

$$Y_s = 4 Z_w / Z_o^2$$

in which Z_o is the intrinsic impedance of the surrounding medium. The admittance which a waveguide-fed slot presents to the wave in the guide is not the same as the admittance Y_s, above, because the method of feeding the slots is different.

2.2.2 Negligible Mutual Coupling

Slotted Line Method

General techniques for measuring voltage standing wave ratio (VSWR) and impedance are described in Silver[64] and Ragan[51]. More specialized treatments are given by Stegen[73] and Oliner.[44] The following discussion is based on Stegen's paper.

Two techniques may be used to obtain the impedance of a slot by VSWR measurements: One is to terminate the waveguide by a movable termination which is almost a match to the waveguide, and the other is to use a near-perfect movable short circuit. The latter method is quicker and more accurate for slot measurement and, therefore, is the method which is generally used.

The movable short-circuiting plunger must have a very low loss, a wide bandwidth, and an accurately calibrated movement. The plunger found to be most desirable for waveguide slots is the noncontacting type.[51] The contacting type, however, is more convenient for use in the TEM transmission lines. Usually the shorting plunger is placed inside the waveguide section containing the slot, thus keeping attenuation to a minimum and

avoiding a junction between the slot and plunger. The slotted-line and the test slot are either machined in the same section of transmission line or the junction between the two is designed to have a minimum effect on the measurements. (For longitudinally polarized slots care must be taken to minimize the reflections outside the guide from connecting flanges.) The distance between the slotted line and the radiating element is kept as small as possible with the limitations: 1) that the slotted line should be isolated from the fields radiated by the slot, and 2) that there should be no external objects in the vicinity of the slot to affect the impedance measurements. The r-f source must be frequency stabilized to one part in 10^5 for precision measurements. Frequency instability of 10^5 cps at X-band has been found to give a phase error of 3 percent of the maximum node shift for a slot which has a resonant conductance of 0.02. This frequency stability is not needed for the usual impedance measurements, however. Usually the source is isolated from the slot by attenuators and the frequency is continuously monitored by a transmission-type cavity lightly coupled to the main transmission line. Figure II-20 illustrates a typical impedance measuring setup.

The step-by-step procedure for measuring the admittance of a pure shunt slot on a transmission line follows.

1) A movable short-circuiting plunger is placed at two adjacent positions in the waveguide beyond the slot in such a way that there is no radiation from the slot as indicated by a sensitive pick-up device. The pick-up device is usually a horn feeding the energy into a crystal detector. Care must be exercised in placing the pick-up device symmetrically about the slot because of the presence of a small amount of energy in the form of the second slot mode which may cause erroneous readings. These two positions of the shorting plunger are a half guide wavelength apart, and for a shunt slot they represent a short circuit across the waveguide at the electrical center of the slot. If the plunger is moved to a position exactly half way between these two points, the waveguide will appear to be terminated in an open circuit beyond the slot center.

2) With zero radiation from the slot, two adjacent node positions on the standing wave in the slotted line are noted. The distance between these nodes is a half wavelength in the slotted section.

3) A second node position is obtained on the slotted line when an open circuit termination is placed at the slot.

4) The VSWR is determined by either of two methods. The usual method is to use a calibrated crystal or a bolometer rectifier and to read the VSWR on a meter. The requirement that the traveling probe be coupled very weakly to the waveguide results in the node being near the noise level, and, therefore, VSWR's greater than about 10 become increasingly difficult to measure. A method which determines VSWR greater than 10, which is almost independent of probe insertion, is frequently used. This method has the advantage that sufficient probe insertion may be used to provide a well-defined node. In the vicinity of the node the shape of the standing wave is parabolic. If the distance between two points on the standing wave at n times the

minimum power level is ΔX, then the VSWR is given by

$$\rho = \frac{\lambda g \sqrt{n-1}}{\pi \Delta X} \quad \text{for } \Delta X \text{ small.} \tag{20}$$

The distance ΔX is measured very accurately by using a dial indicator attached to the slotted line.

The admittance of the slot may now be determined from the distance the node has moved and from the VSWR in the waveguide (see Figure II-21).

The procedure for measuring the impedance of a pure series slot is the same except that an open circuit at the slot results in no radiation. This difference must be remembered when the phase of the impedance is calculated from the distance the node shifts. For the case of the inclined displaced waveguide slots which may be represented by a four-terminal network, the technique must be modified. The electrical center of the slot must be determined by physical measurement. This modification also applies to edge waveguide slots which cut into the broad face of the waveguide and which may have an appreciable series component.

The length of waveguide from the shunt slot to the slotted section is often great enough to require compensation in the admittance for the losses in the waveguide. The short circuiting plunger may also be lossy and require that the slot admittance be adjusted accordingly. The loss in the short, a_s, may be represented as a low admittance across the shunt element and may therefore be subtracted directly from the measured value. If one now neglects the short and assumes that the guide wall losses are all between the slot and slotted section, a distance ℓ, then the VSWR of the slot relative to the measured VSWR, ρ_m, is

$$\rho_s = \frac{\rho_m - \tanh a\ell}{1 - \rho_m \tanh a\ell} \tag{21}$$

where a = the attenuation constant of the waveguide. The normalized conductance of a resonant slot, neglecting the loss in the short, is (for $G_s < 1.0$)

$$G'_s = \frac{G_m - \tanh a\ell}{1 - G_m \tanh a\ell} \tag{22}$$

where $G_m = \frac{1}{\rho_m}$. For the usual case of G_m and $a\ell$ small,

$$G'_s \approx G_m - a\ell \tag{23}$$

The normalized conductance of the slot, taking the transmission line and short into account, is approximately

$$G_s = G_m - (a_s + a\ell) \tag{24}$$

where $a_s + a\ell$ is the loss measured without the slot in the waveguide. It should be noted that the attenuation in an unslotted guide is slightly different from that in a slotted guide since the slots distort the wall current distributions.

A similar analysis may be made for series slots where the slots of interest are those having resistances less than unity in which case

$$R_s = \frac{R_m - \tanh a\ell}{1 - R_m \tanh a\ell} - a_s \tag{25}$$

$$\approx R_m - (a\ell + a_s) \tag{26}$$

Radiation Pattern Method

Slots whose normalized conductances (or resistances in the case of series slots) are greater than 0.1 can be measured very accurately by the direct measurement technique; however, direct measurement of lower conductance slots becomes increasingly difficult. As the slot admittances become smaller, waveguide attenuation becomes a larger part of the measured admittance. The difficulty is enhanced by the high VSWR's that are associated with the low slot admittances. A new admittance measuring technique is therefore desirable. Since the phase of the radiation from a slot is of interest, a system has been developed to measure the radiation pattern of two slots and from this pattern to calculate the phase of the radiated field, as well as the admittance (or impedance) of the slot.

Two isotropic radiators whose radiated fields differ in phase by ϕ and whose magnitudes are proportional to A_1 and A_2 will have a power pattern proportional to

$$\begin{aligned} P &= \left| A_1 + A_2\, e^{j(kd\cos\theta + \phi)} \right|^2 \\ &= A_1^2 + A_2^2 + 2A_1A_2\cos(kd\cos\theta + \phi) \end{aligned} \tag{27}$$

where d is the spacing between elements and θ is the angle measured from endfire to an observer. This power pattern is maximum (P_{max}) when the cosine term has a value of +1.0 (at the angle θ_{max}) and is minimum (P_{min}) when the cosine term has a value of -1.0 (at the angle θ_{min}). The ratio of the magnitudes of the excitation coefficients is

$$\frac{A_2}{A_1} = \frac{\left(\frac{P_{max}}{P_{min}}\right)^{1/2} - 1}{\left(\frac{P_{max}}{P_{min}}\right)^{1/2} + 1} \tag{28}$$

The relative phase between the elements is

$$\phi = (2n - 1)\pi - kd\cos\theta_{min} \tag{29}$$

or

$$\phi = 2n\pi - kd\cos\theta_{max} \tag{30}$$

If the spacing between two shunt slots is an integral number of guide wavelengths, then the power radiated by each slot is (neglecting guide attenuation and external coupling) proportional to its conductance and it is also proportional to the square of the magnitude of the excitation coefficients. It follows then that

$$G_2 = G_1 \left(\frac{A_2}{A_1}\right)^2 \tag{31}$$

for shunt slots, or

$$R_2 = R_1 \left(\frac{A_2}{A_1}\right)^2 \tag{32}$$

for series slots.

Since the phase of the radiated field with respect to the field in the guide for a shunt slot is the phase of the slot admittance[73], the susceptance of the unknown slot when measured with a known resonant slot is

$$B_2 = G_2 \tan\phi \tag{33}$$

for shunt slots, or

$$X_2 = R_2 \tan\phi \tag{34}$$

for series slots.

The slot conductance can be calculated from equation (31) using the ratio A_2/A_1 from equation (28). The susceptance can be calculated from equation (33) using the angle ϕ from equations (29) or (30).

A series of measurements, made as the length of the unknown shunt (series) slot is varied, will result in values of the components which are then plotted in the rectangular coordinate admittance (impedance) plane. These points will determine a circle. The point of maximum admittance and/or zero susceptance is called the resonant conductance. A plot of the susceptance of the slot as a function of length may be used to determine the resonant length of the slot.

2.2.3 Effective Mutual Coupling

Impedance Method

Consider a transmission line with an unloaded characteristic impedance Z_o and an unloaded propagation constant $\gamma = \alpha + j\beta$, loaded at regular intervals ℓ with identical radiating elements. Reference planes may be taken midway between radiating elements so that this loaded line may be considered to consist of N units in cascade, each unit consisting of a radiating element centered in a length of line ℓ. This loaded transmission line can be represented by a four-terminal network. The series and shunt elements of the equivalent tee of this network are $Z_{11} - Z_{12}$ and Z_{12}, respectively, as shown in Figure II-22A. The impedances Z_{11} and Z_{12} may be measured in any manner, the usual one being to place a short circuit and an open circuit in turn across the output. The input impedance for an open circuit termination is

$$Z_{inoc} = Z_{11} \tag{35}$$

and for a short circuit termination

$$Z_{insc} = Z_{11} - \frac{Z_{12}^2}{Z_{11}} \tag{36}$$

Bartlett's bisection theorem[29] states that if Z_o' and γ' are the characteristic impedance and propagation function, respectively, of a symmetrical network, then

$$Z_{oc} = Z_o' \coth \frac{\gamma' N}{2} = Z_{11} + Z_{12} \tag{37}$$

and

$$Z_{sc} = Z_o' \tanh \frac{\gamma' N}{2} = Z_{11} - Z_{12} \tag{38}$$

are the open- and short-circuit impedances of half the network as shown in Figure II-22B. Solving equations (37) and (38),

$$\gamma' = \frac{2}{N} \text{ arc tanh } \frac{Z_{11} - Z_{12}}{Z_{11} + Z_{12}} \tag{39}$$

The loaded-line expressions[64c]

$$\cosh \gamma' \ell = \cosh \gamma \ell + \frac{Y}{2Y_o} \sinh \gamma \ell \tag{40}$$

$$\cosh \gamma' \ell = \cosh \gamma \ell + \frac{Z}{2Z_o} \sinh \gamma \ell \tag{41}$$

may be used to obtain the admittance Y of a shunt element or the impedance Z of a series element.

The procedure for determining the impedance of a slot in the presence of a number of like slots by the present method is:

1) Place a short circuit and an open circuit in turn across the slotted guide at a distance $\ell/2$ from the last slot. The guide should contain a large number of equally spaced like slots (spacing equals ℓ) so that end effects may be neglected and mutual coupling will be taken into account. Adjacent slots are generally coupled to the guide in opposed phase.

2) Measure the input impedances: short circuit and open circuit.

3) Use equations (35) and (36) to determine the parameters of the equivalent tee.

4) Substitute these values of Z_{11} and Z_{12} into equation (39) and solve for γ'.

5) Calculate $\frac{Y}{Y_o}$ or $\frac{Z}{Z_o}$ from equation (40) or (41) using the value of γ' obtained in equation (39) and the complex propagation constant γ of the unloaded transmission line.

Special Cases: Incremental Conductance

For N identical shunt elements of admittance Y, spaced $\lambda_g/2$ apart with the termination at a half wavelength from the last slot,

$$Y_{insc} = 0$$

$$Y_{inoc} = NY$$

and

$$Y = \frac{Y_{inoc}}{N} \tag{42}$$

For N identical series elements of impedance Z spaced $\lambda_g/2$ apart

$$Z_{insc} = N\,Z$$

$$Z_{inoc} = 0$$

and

$$Z = \frac{Z_{insc}}{N} \tag{43}$$

Watson has measured the input admittance Y_{inoc} for an array of N identical edge slots at $\lambda_g/2$ spacing and has plotted the conductance per slot versus the number of slots[88] as shown in Figure II-23A. The curve approaches a limiting value which Watson called the "incremental conductance," that is, the increase in conductance due to adding one more slot.

The length of the slot for resonance is found by trial and error. The input admittance is measured and plotted as shown in Figure II-23B for various slot lengths. The length for which the susceptance becomes constant as N is increased represents resonance. This susceptance is generally tuned out in the final array. A simpler method is to measure the input admittance for an array of a sufficiently large number of elements as the length of all the slots is varied. The length for zero susceptance and/or maximum admittance can be defined as the resonant length. This method yields substantially the same results.

Power Methods

The incremental conductance can be measured for an array of at least twelve identical slots, at the appropriate spacing by measuring the power in the guide before (P_1) and after (P_2) the slots, by the relation

$$\text{Power} = Y_o(V_{max} \times V_{min}) \tag{44}$$

The experiment is repeated with an added n slots, and the power before and after is now P_1 and P_2'. Thus, after n slots a fraction f_n of the power incident on the n slots remains where

$$f_n = P'_2/P_2 \tag{45}$$

Now if the slotted guide is matched at all points, for a single slot,

$$\text{(Power radiated)/(power incident)} = 1 - g_i \tag{46}$$

where g_i is the incremental conductance in terms of the guide admittance (Y_o). For $\underline{n}$ slots therefore

$$f_n = (1 - g_i)^n \tag{47}$$

But $\log_e \left[\frac{1}{1 - g_i}\right] = \log_e \left[1 + \frac{g_i}{1 - g_i}\right] \approx g_i$ if $g_i << 1$, and therefore, equation (47) becomes

$$g_i = \frac{1}{n} \log_e \frac{1}{f_n} \tag{48}$$

f_n being defined by equation (45).

The measured value of g_i will not correspond to resonance unless the slot length for resonance is known; the experiment must therefore be repeated using various slot lengths, and the maximum value of g_i found. With 12 edge slots, for example, the incremental conductance may be measured to better than 1 percent on adding a few extra slots. The incremental conductance is often very different from the conductance of a single slot, for example, three times as high in a particular case quoted by Watson.

The method of measurement outlined above obtains the incremental conductance using the minimum number of slots, but two arrays comprising different numbers of slots must be constructed for each measurement. An alternative technique is merely to measure the mean conductance of a large number of slots. It is necessary to take at least 24 slots to make such a measurement, and to measure the power in (P_1) and the power out (P_2) writing

$$g_i = \frac{1}{N} \log_e \frac{P_1}{P_2} \tag{49}$$

It is obvious that the array of measured slots must be terminated by a matched load. Criteria for insuring a match in the slotted guide are mentioned in section 3.

Limitations on Methods

The impedance method (page 19) leads to some very involved computations especially when guide attenuation is taken into account. If the slots are spaced $\lambda_g/2$ apart, the simplified equations (42) and (43) may be used. The data obtained for $\lambda_g/2$ spacing cannot, of course, be used for any spacing which differs much from $\lambda_g/2$.

The power methods (page 21) allow for any spacing provided the slotted guide is matched at all points. This condition holds only for lightly

coupled slots and spacing off $\lambda_g/2$ (so that the reflections from the slots do not add in phase).

The power measurements are simpler than the impedance measurements. On the other hand, the impedance method gives a direct measure of conductance and reactance so that it is obvious if the radiator is longer or shorter than resonant length.

Nonetheless, it should be recognized that any method of measurement of slot impedance in the presence of strong mutual interaction is an approximation, since all the slots in the measured array will not "see" the same mutual impedance even though all the slots are exactly alike. For a long experimental array, the calculated impedance holds for slots near the center of the array. Slots near the ends do not have as many neighbors and therefore experience less mutual interaction than central slots. An array designed with these data will have errors in the aperture distribution near the ends.

Experience has shown that the above methods can be used to design successful arrays when the array has a large number of elements, a uniform progressive phase distribution, and an amplitude distribution that is not very peaked.

2.3 EXPERIMENTAL AND DESIGN DATA

2.3.1 Rectangular Waveguide Slots

The impedance of a rectangular waveguide slot depends on a number of factors: the guide dimensions (a/b ratio and wall thickness), slot length and width, operating frequency, and the orientation of the slot on the guide. The problem of the designer is the following.

> Given the operating frequency (the TE_{10} mode is assumed here), guide dimensions, a particular slot type, and the required slot impedance, find the slot orientation on the guide and the slot dimensions.

Unfortunately, there is not a great deal of systematic slot design data available. The specialized data to follow, however, may be extended by scaling frequencies and dimensions, with a fair degree of accuracy. It is advisable to check these approximations with a few experimental measurements. Where the shape of a particular design curve is known for a given set of conditions, it may be possible to draw a reasonably accurate similar curve for another set of conditions by measuring only a few points for the new curve.

Most of the data to be presented here are taken from unpublished technical memoranda of the Hughes Aircraft Company. Only a small part of Watson's data is presented since it is readily available in the public literature.

Longitudinal Shunt Slots

The longitudinal shunt slot (sometimes called shunt-displaced) is one of the most widely used types of slot. This slot has the advantages that the mutual admittance between adjacent slots on a guide is negligible and that large conductances, of the order of the guide characteristic admittance, may be obtained without complication. However, off-axis sidelobes may be present due to the staggering of the slots in an array. (Section 3.4.5.) The radiation from the slot is polarized transverse to the guide axis.

An investigation of six shunt-displaced slots was carried on by one of the authors.[72] The admittances of the six slots were calculated from radiation pattern measurements at a number of frequencies and then plotted in the complex admittance plane. The maximum conductance of each slot was obtained from the curves (circles) determined by these experimental points. The points of Figures II-24 and II-25 were then determined from these measurements. The ratios G/G_m and B/G_m and the phase of the radiation are apparently independent of the centerline displacement of the slots.

The measurements were made on longitudinal shunt slots in standard 1.0 by 0.5 inch (0.050-inch wall) waveguide at 9375 mc/s and the G values obtained differed from the value obtained from equation (13) by the factor 0.96. A similar correction factor was obtained from experimental results with series slots in waveguide and in that case was shown to be due almost entirely to the finite thickness of the waveguide wall. The semi-empirical expression for the resonant conductance of the longitudinal shunt slot at 9375 mc/s,

$$G_m = 0.96G = 1.19 \sin^2 \left(\frac{\pi x}{a} \right) \tag{50}$$

is plotted in Figure II-26 with measured points indicated. Radiation pattern measurements with a large ground plane about the slots gave essentially the same results as direct admittance measurements without a ground plane.

The length of a narrow resonant slot having a given displacement has been shown empirically to be approximately directly proportional to the free-space wavelength at the resonant frequency and is therefore plotted as shown in Figure II-27. Figure II-28 shows that, for small displacements, the resonant length of a longitudinal shunt slot increases parabolically with its displacement from the center of the broad face.

Impedance measurements on slots have shown that the conductance of a resonant slot with a particular displacement has a frequency variation which is proportional to the terms in equation (13) which are frequency-sensitive, that is,

$$G \propto \frac{\lambda_g}{\lambda} \cos^2 \left(\frac{\pi}{2} \cdot \frac{\lambda}{\lambda_g} \right) \tag{51}$$

The frequency dependence of the resonant conductance is shown in Figure II-29. The curve was calculated from Stevenson's equation corrected by the factor 0.96.

The frequency dependence of the conductance and susceptance of longitudinal slots measured by Watson as a function of slot width is shown in Figure II-30, which also shows the improvement in bandwidth with increasing slot width. It can be seen that resonance, defined here as the frequency for zero susceptance, does not occur at the point of maximum conductance. As in the case of wire dipoles which exhibit the same phenomenon, this discrepancy may be attributed to end effects in the slot and to frequency variations in the R, L, and C of the equivalent circuit representation.[34a]

The design data for a resonant slot may be extended to other frequencies (different from 9375 mc/s) as follows:

1) If the guide to be used is the same as the experimental guide and the desired operating frequency is in the range 8400 to 10,800 mc/s, find the conductance, G, at the operating frequency, f, from Figure II-29. This curve is for a displacement X = 0.1833 inch. Substitute for G and X in

$$G = K \sin^2 \left(\frac{\pi x}{a} \right) \tag{52}$$

to find K. Equation (52) relates the resonant conductance and slot displacement at the operating frequency. The resonant slot length can be determined with the aid of Figures II-27 and II-28. The original slot width (0.0625 inch) should be retained (although slot width has a second-order effect on G).

2) If the new a/b ratio is the same as for the experimental guide and if the frequency is not in the range 8400 to 10,800 mc/s, the slot and guide dimensions (including wall thickness) can be scaled directly.

3) If the new a/b ratio is different from that for the experimental guide, it is possible to correct equation (52) according to equation (13); that is, multiply K by the b/a ratio for the experimental guide and by the a/b ratio for the new guide.

Other data on resonant longitudinal shunt slots can be found in Watson's paper. He finds, for example, that

$$G = 1.40 \sin^2 \left(\frac{\pi X}{a} \right) \tag{53}$$

at $\lambda = 3.2$ cm. Cullen[16] has derived a semianalytical expression for G:

$$G = K \frac{\lambda \lambda_g \ell^2}{a^3 b} \sin^2 \left(\frac{\pi x}{a} \right) \tag{54}$$

in which K is a constant which must be determined experimentally. For example, at $\lambda = 3.2$ centimeters, K was experimentally determined to be 0.454. Cullen presents a number of K values in his paper.

The results of various investigators differ by as much as 10 percent, (and more in some cases) which will give the designer an idea of the reliability of the data presented here. Nonetheless, an accuracy of about 10 percent is sufficiently good for many practical arrays.

Longitudinal Shunt Slots Radiating into Parallel Plate Horns: For purposes of reducing off-axis sidelobes and for beam shaping in the transverse plane, it is sometimes useful to allow the slots in an array to radiate into a parallel plate or a flared parallel plate horn. The presence of this horn modifies the slot conductances so that slots to be used in conjunction with a horn system should be measured in the presence of the horn. Gruenberg[28] presents theoretical equations and curves for the conductances of longitudinal shunt slots radiating into parallel plate horns. Other horn configurations have also been used but little data are available.

Edge Slots

The edge (or shunt-inclined) slot is probably as widely used as the longitudinal shunt slot but has different advantages to recommend it. The edge slot gives longitudinal polarization, which is the normal requirement; and the slot is easy to construct. The simple edge slot can be cut in a single milling operation, the slot length being determined by the depth of cut; the "dumbbell" and extended edge slot can be produced by drilling two holes and milling the slot between them. Furthermore, it will be found that machining tolerances are not so critical for edge slots as for longitudinal shunt slots. On the other hand, the edge slot has a large mutual effect on the admittance of its neighbors which complicates the array design procedure considerably (see page 19). Further, high conductances cannot be obtained without introducing cross polarization due to excessive inclination of the slot. For long arrays, however, low individual slot conductances are required and the edge slot is usually satisfactory.

Stevenson's expression for the conductance of a resonant edge slot, equation (19), may be modified for small inclination:

$$G = G_1 \sin^2\theta \tag{55}$$

for θ small, for example, less than 15 degrees. However, the edge or b dimension of a standard guide is usually less than a half-wavelength so that the slot must be extended to the broad face to obtain resonance as shown in Figure II-31. The section of the slot on the broad face adds a series component to the slot equivalent circuit so that the slot is represented by a four-terminal network. In most cases, however, the series component is neglected since it is generally small. Another expedient is to "load" the slot with dielectric or, by a dumbbell configuration, to make it resonant for a shorter physical length and thus fit completely on the narrow face of the guide.

Stevenson's equation holds only for a single slot and does not take mutual admittance into account. Since edge slots are generally nearly parallel side-by-side in an array, the mutual coupling is very strong. Thus, if the slot is to be used in an array, admittance measurements must be made which include the coupling, (section 2.2.3). In this case, the slot conductance is an "incremental conductance," that is, the increase in conductance of a large group of similar slots at a particular spacing when another slot is added. The incremental conductance is accurate only for slots near the center of the large group; slots near the ends are subject to less mutual interaction nce they have fewer near neighbors. The measurement of a slot having a strong mutual admittance is a difficult and inaccurate procedure. The methods described (section 2.2.3), however, have produced reasonably successful arrays. Array designs using few elements, nonuniform phase distributions, or peaked amplitude distributions will probably result in failure, however.

Simple Edge Slot: The incremental and single slot conductances versus slot inclination for a particular edge slot are shown in Figure II-32. Both curves approximate a $G = G_1 \sin^2\theta$ curve for a range of about 0 to 15 degrees, thereby substantiating equation (55). For these slots the variation of susceptance with frequency is small compared with that for slots in other positions on the guide. The variation of admittance with slot depth (that is, length of cut into the broad face) is also small, as indicated in Figure II-33.

Since the design data for simple edge slots are not adequate, it may be expedient to measure the incremental conductance for a slot of a particular angle and draw a $\sin^2\theta$ curve through the measured point to obtain a design curve. Several successful arrays have been built using this technique.

Edge-Slot Coupling into Waveguide:[37] In order to reduce cross polarization due to slot inclination and to cut down on mutual coupling, the arrangement pictured in Figure II-34 may be employed. The open end of the auxiliary waveguide can be matched to free space by appropriate E-plane flares[64d] and the measurement of slot conductance becomes a measurement of guide-to-guide coupling.[87,88]

In the present experiment, mutual coupling was neglected; that is, single slot conductance was measured. Figure II-35 shows plots of the depth of cut and resonant conductance versus frequency for the slot coupling into an auxiliary waveguide with a reflectionless termination. The electric field excited in the slot is proportional to $\sin\theta$ and the field propagated by the auxiliary guide is proportional to $\cos\theta$. Thus, the radiated power (and consequently, the slot conductance) should be proportional to $\sin^2\theta \cos^2\theta$. Unfortunately, insufficient measurements were made to verify the relationship.

The resonant lengths of the three measured slots (15, 20 and 30 degrees) were within 0.010 inch of the same value.

The variations in resonant frequency and normalized conductance of a 30-degree edge slot as a function of wall thickness are shown in Figure II-36. The thickness of the entire wall within the auxiliary waveguide was

reduced for the measurements. These curves are useful for scaling the edge slot data to other frequencies at which the wall thicknesses do not scale.

Dumbbell Edge Slots: The dumbbell slot offers a useful solution when a low conductance radiating element has to be cut into the narrow wall of a waveguide and either the broad faces are not accessible for cutbacks or it is not desirable to weaken the waveguide structure by cutting back into the broad faces.

The use of the resonant dumbbell slot in linear array design requires an extension of the slot into a solid metal block as shown in Figure II-37. This arrangement introduces an additional variable, the depth to which the dumbbell is cut. To reduce the number of variables and simplify the investigation, three slot parameters were kept constant at the following values: length = 0.700 inch, depth of dumbbell = 0.328 inch ($\lambda/4$ at 9000 mc/s so that an open circuit will appear at the face of the guide), width of slot = 0.062 inch. Furthermore, since these slots were to be used for an array on a helical waveguide in which the slots would be end to end (negligible mutual coupling), single slot conductances only were considered.

Values of normalized conductances as a function of slot inclination and frequency are presented in Figure II-38. The corresponding resonant dumbbell sizes are plotted in Figure II-39. From these two families of curves, one can obtain the array design curves consisting of resonant dumbbell diameter and resonant conductance as a function of any frequency within the spectrum covered and at other frequencies by scaling all dimensions. A particular set of curves is presented in Figures II-40 and II-41. A comparison with Stevenson's equation is also made in Figure II-40. By correction for wall thickness, the correlation between the two curves can be improved.

Inclined Series Slot in the Broad Face

A slot inclined slightly about the centerline of the broad face of a waveguide is transversely polarized. Aside from the requirement for maintaining high machining tolerances, the inclined series slot presents a cross-polarization component which often must be eliminated. If the angle of inclination is increased to 90 degrees, the slot will be longitudinally polarized. This transverse series slot has a high resonant resistance and cannot be used in long arrays because the first few slots extract most of the power from the guide. The slot coupling may be adjusted by offsetting the slot from the guide centerline and making the slot resonant by loading or by extending the slot to the narrow face. (See Figure II-16, page 112.) The mutual coupling problem is also serious in transverse series slots in the broad face.

Simple Series Slot: Measurements of resonant length and normalized resistance as a function of frequency have been made for 15°, 20° and 30° resonant slots of the type shown in Figure II-42, over a frequency range of 8600 to 9800 megacycles. The measurement techniques used are described in the discussion of negligible mutual coupling, section 2.2.2, and the experimental data are shown in Figure II-43. It can be seen that resistance and resonant length are very nearly linear functions of the frequency. The width of these

slots was chosen to be 1/16 inch. A change in this value of slot width, for power breakdown or other considerations, would cause a slight change in the resonant length and resistance but would not change appreciably their behavior as a function of the frequency.

A comparison of the measured values of resistance with the theoretical values as given by Stevenson is shown in Figure II-44. The measured values of resistance are lower than the calculated values due to the finite thickness of the waveguide wall. The variations in resonant frequency and resistance with varying wall thickness are shown in Figure II-45 for a 30 degrees slot. When the wall thickness of this slot is reduced from 0.050 to 0.013 inch and the length is varied to maintain resonance at 8700 megacycles, the change in resistance is + 10 percent as calculated from Figures II-43 and II-45. This percent change applied to the measured values of resistance in Figure II-44 brings them into agreement with the theoretical values of resistance. This agreement is based on the assumption that the resistance will not change appreciably when the wall is reduced from 0.013 inch to zero thickness.

The measurements indicate that the resonant length remains nearly constant as the angle of inclination is changed; hence all slots were cut to the lengths given in Figure II-44.

Series Slot with Horn: A linear array of slots of the type shown in Figure II-42 (page 138) will radiate a longitudinal component of electric field in addition to the transverse component. In some applications it may be desirable to eliminate this cross-polarized component of electric field. In one instance this component has been eliminated by allowing the slots to radiate into a flared, parallel-plate horn similar to that shown in Figure II-46. The plates are spaced such that the cross-polarized electric fields are suppressed, and the flare of the horn is such that reflections from the throat and aperture very nearly cancel each other. The horn also can be used to control the radiation pattern in the transverse plane.

The addition of the parallel-plate horn produces an increase in both the resonant frequency and resistance of the series slots. Also, any reflections from the throat or aperture of the horn will produce small variations in the resonant frequency and resistance. Reflections from the aperture, however, should become negligible compared with those from the throat when the E-plane aperture dimension is larger than about three-fourths of a wavelength. Thus, for a given flare angle there is a flare length beyond which any increase in flare length will produce a negligible change in slot characteristics. Reflections from the throat of the horn, on the other hand, will cause variations in slot characteristics, and these have a frequency sensitivity dependent upon the separation of the slots from the throat of the horn. It is important, therefore, that the electrical length from the slots to the throat of the horn be as small as possible consistent with effective suppression of the cross-polarized component of electric field, or that the reflections from the throat of the horn be matched out in some manner. The resonant lengths and resistances versus frequency for a 20-degree slot with two different horns are shown in Figure II-47. The slopes of these curves are approximately the same as those of Figure II-43 (page 139); however, more data are necessary

to establish the correspondence. The measured values of resistance for 15-degree and 20-degree slots with horns have been found to follow closely a $\sin^2\theta$ curve, and it has been assumed that this shape will hold for angles less than 15 degrees. This assumption is substantiated by a successful array which has been built with the present data.

The General Inclined-Displaced Slot in the Broad Face

An inclined laterally displaced slot cut in the broad face of the guide is illustrated in Figure II-16A (page 112). For the displacement, x, equal to zero, the general slot becomes a series slot; and for the inclination, θ, equal to zero the general slot becomes a shunt slot. Furthermore, the load across the slot (the waveguide termination) determines the wall current pattern at the slot, that is, the proportion of series and shunt currents at the slot. Thus, the general inclined-displaced slot is quite versatile. Unfortunately, this slot is very difficult to measure and manufacture. For this reason, the slot is primarily of academic interest and will not be discussed at great length here.

Watson and Guptill have studied this slot and, in fact, did build an array of such slots with probe compensation. The slot can be so adjusted that, after a small residual susceptance has been cancelled out by a probe opposite the slot, it gives a perfect match before and after the slot. Thus, a pure traveling wave is obtained in the guide, and a nonresonant array (see Resonant and Nonresonant Arrays, section 3.1) which radiates at right angles to the guide may be constructed. A very large bandwidth array may be obtained using this type of slot, particularly since the mutual interaction among neighboring slots is small. The slot is a combination of series and shunt slots and therefore acts as a π-network; thus, there is an appreciable phase retardation at the slot, and the slots must be placed closer than $\lambda_g/2$ to give a broadside array. Watson gives a complete set of design data for the general slot in his book and paper.

Slot in an End Plate

If an open waveguide propagating the TE_{10} mode is short-circuited by a metal plate at the open end, currer s will be excited in the shorting plate. The current lines in the plate will be normal to the broad faces of the guide; that is, they will be transverse (shunt) currents. A slot cut parallel to the broad faces in the plate will therefore radiate and will look like a shunt element on the equivalent line. In the extreme, the "slot" aperture may be the open end of the guide itself. Theoretical admittance data for open-ended waveguides radiating into an infinite ground plane are given by Lewin.[40] For narrow slots, the radiation can be controlled by inclining the slot to the current lines in the shorting plate. Since the shorting plate is of limited size and since inclining the slot would result in cross polarization, the slot radiation is more often controlled by the amount of power fed to the section of guide containing the slot. In this case, the feed might be matched by an iris or similar device.

Slot Pairs

An experimental investigation of in-phase longitudinal shunt slot pairs has been made by E. P. McDowell and N. Namerow at the Hughes Aircraft Company. The arrangement of the slots on the guide is illustrated in Figure II-48. Design curves for resonant slots in the frequency range 8400 to 10,200 megacycles are presented in Figure II-49. In Figure II-49A a family of curves of resonant conductance versus resonant frequency is plotted with slot displacement as the parameter; and in Figure II-49B a family of curves of resonant length versus resonant frequency is plotted with slot displacement as the parameter. From these curves more specialized design curves can be drawn. Thus, at a particular operating frequency, the designer can find five points on a curve of normalized conductance versus slot displacement from Figure II-48, and he can find five points on a curve of resonant length versus slot displacement from Figure II-49.

2.3.2 Probe-Excited Slots[64e]

There are various slot positions on a guide for which no radiation takes place. (See discussion, section 2.2.1.) It is possible; however, to make any slot of this type radiate by inserting a suitable probe into the guide in the vicinity of the slot. The probe introduces the necessary asymmetry in the field and in the current distributions for excitation of a field across the slot.

An important advantage of an array of probe-excited slots is that all the slots will have the same relative positions on the guide except, of course, for a longitudinal displacement. In this way, the off-axis sidelobes common to longitudinal shunt slot arrays can be eliminated. Instead of effecting phase reversals by displacing adjacent longitudinal shunt slots on opposite sides of the waveguide centerline, for example, the direction of the field across the slot can be controlled by the position of the probe. The phase of a given slot can be shifted 180 degrees by switching the probe position as illustrated in Figure II-50A.

Another advantage of the probe-excited slot is that cross polarization due to slot inclination can be eliminated. The amount of energy radiated by the slot is controlled by the probe insertion rather than by slot inclination. For the case illustrated in Figure II-51A, where the probe is parallel to the field, the coupling is adjusted by the probe depth. To excite an edge slot a bent probe is used as shown in Figure II-51B. The coupling can be varied by the angle between the hook of the probe and the electric field. In some cases the screw head on the outside of the guide introduces undesirable impedance characteristics, but the head can be ground off after the desired coupling has been obtained, or the unit can be balanced externally by a dummy screw head.

Other variations of probe-excited slots in other types of rectangular guides are, of course, possible. Some of these are described by Clapp[13].

Despite their advantages, probe-excited slots have been used only occasionally because they are extremely sensitive electrically and mechanically; generally, the bandwidth is small and the probe tolerances tight. Some

probe-fed antennas in circular and elliptical guide, however, are described by Silver.[64f]

2.3.3 TEM Line Slots

The wall currents on a TEM transmission line are longitudinal. Thus, an inclined or a transverse slot cut in the outer wall of the TEM line would radiate and could be represented by a series impedance. An advantage of the TEM line over waveguide is the fact that, at a given frequency, the TEM line can have a smaller cross section.

Circular Coaxial Transmission Line

The most familiar type of TEM line is the circular coaxial type. Nevertheless, very little practical work has been done with slots on circular coax with the exception of a few arrays of probe-fed slots. The reasons for the lack of interest in circular coax include the difficulty of predicting the radiation pattern for an array of slots on a small circular cylinder and the difficulty of machining slots on curved surfaces.

Rectangular TEM Line

A TEM transmission line with a rectangular outer conductor eliminates some of the difficulties posed by the circular coax. Experimental data have been obtained for a single slot in two types of rectangular line: 1) a rectangular outer conductor with a coaxial round inner conductor, and 2) a rectangular outer conductor with an offset strip inner conductor.[77]

In the first type of line, dumbbell-loaded slots were cut in the broad face of the outer conductor and were inclined about the centerline to vary the excitation. A reasonably successful 16-element array was constructed with this type of slot. Since the slot data for this array are quite specialized, they will not be presented here. The data do show, however, that the slot resistance varies approximately as $\sin^2\theta$, where θ is the angle of inclination. The slots were dumbbell-loaded to avoid having adjacent slots overlap when spaced approximately $\lambda_g/2$ apart.

In the second type of line, transverse slots were cut in the broad face of the guide and were displaced from the centerline of the offset inner conductor to control the excitation. Since the dimensions of the rectangular outer conductor must be designed to suppress modes different from the TEM, the width of the broad face is limited and the slots must be loaded (dielectric or dumbbell) if they are to be resonant on the broad face. The greatest objections to this type of slot are the mutual coupling problem and the inability to make the slot resistances very small.

2.3.4 Circular and Elliptic Waveguide Slots

It is possible to construct slot radiators in circular or elliptic waveguide by proper arrangement of the slots with respect to the wall currents. However, very little work, practical or theoretical, has been done along this line.

Wong has developed analytic expressions for the radiation conductance of transverse slots in elliptic cylinders and presents some theoretical curves.[95] The radiation conductance is the conductance at the terminals of a parallel wire line feeding the slot, not the conductance seen by the wave in an elliptic guide. He shows that the radiation conductance is influenced considerably by the degree of curvature of the surface on which the slot is located.

Feiker and Clark have measured the admittances of a number of resonant longitudinal slots in circular guide propagating the TE_{11} mode.[24] The results indicate properties similar to those of longitudinal shunt slots in the broad face of rectangular guide. The equivalent circuit representation for the longitudinal slot in circular guide is a shunt conductance. Feiker and Clark have derived a formula (similar to Stevenson's for the longitudinal shunt slot in rectangular guide) for this conductance:

$$g = \frac{480}{73(2.38)} \left(\frac{\lambda g}{\lambda o}\right) \cos^2 \left(\beta_{11} \frac{\lambda o}{4}\right) \sin^2 \phi_o \qquad (56)$$

where β_{11} is the phase constant for the circular TE_{11} mode and ϕ_o is the angle between the direction of polarization of the waveguide mode and the radius vector to the center of the slot.

Lucke[39] has derived relations for the mutual admittance of slots in a circular cylinder in terms of infinite series and integrals of cylinder harmonics.

2.3.5 Slot Bandwidth

The bandwidth of a slot array depends to some extent upon the bandwidth of the individual slots, that is, on the frequency characteristic of the slot admittance. The bandwidth may be conveniently defined in terms of a slot "quality factor," Q:

$$Q = \frac{f_o}{\Delta f} \qquad (57)$$

where f_o = resonant frequency and

Δf = difference between frequencies at which slot admittance is one-half times the resonant admittance.

This definition of Q requires the use of a large band of frequencies when measuring very broadband slots. An alternative expression which permits measurement over a narrower band is[15]

$$Q_B = \frac{fo}{2G_o} \left(\frac{\partial B}{\partial f}\right)_{fo} \qquad (58)$$

where G_o = resonant slot conductance,

B = slot susceptance;

or, in terms of directly measurable quantities,

$$Q_B = \frac{\pi f_o (\rho^2 - 1)}{G_o} \left(\frac{d\Delta}{df} \right)_{f_o} \qquad (59)$$

where ρ = voltage standing wave ratio

and Δ = difference in wavelengths between the standing wave node positions at f and f_o.*

Effect of Slot Width

In an experiment conducted by R. H. Reed,[21] the slot bandwidth and resonant frequency as a function of slot width was measured for a large number of longitudinal shunt slots. During the investigation, it was discovered that slots which overlap the waveguide centerline (central slots) possess a very peculiar impedance characteristic. However, further study of this phenomenon was not undertaken. Although only longitudinal shunt slots were measured, some of the data may be extended to other types of slot.

Figure II-51 is the curve of Q_B as a function of slot width. The measured values of Q_B are given approximately by the empirical relation

$$Q_B = \frac{K}{\sqrt{W}}$$

where K = constant of proportionality

and W = slot width. As the slot width is increased to the point where it crosses the centerline, an abrupt change is noted and the measured values depart quite severely from the approximation.

The curve of susceptance as a function of frequency for a wide slot with a slight centerline excursion (shown in Figure II-52) further illustrates experimental difficulties in an accurate determination of Q_B for those central slots. A small error in the measurement of B is accompanied by a large error in the determination of f_o with a resultant large error in computation of $Q_B = \frac{f_o}{2G_o} \left(\frac{\partial B}{\partial f} \right)_{f_o}$. As a consequence, an estimate of the mean value of $\left(\frac{\partial B}{\partial f} \right)_{f_o}$ about f_o was used rather than a measurement of the slope at resonance.

The resonant length of a longitudinal shunt slot has been found to increase with slot width until the slot crosses the waveguide centerline, as

*In this discussion, resonance is defined as the frequency giving zero slot susceptance (not necessarily maximum admittance).

shown in Figure II-53. This curve was obtained with a relatively high conductance slot ($G_o = 0.32$) in order to have a large number of measurements. Lower conductance slots have been found to give curves which had the same shape but which shifted vertically downward from that of Figure II-53. This vertical shift is caused by the dependence of resonant length upon slot displacement from the waveguide centerline.

As noted above, a large drop in slot Q occurs as a longitudinal shunt slot is widened to the point at which it becomes central. At the same point, Figure II-53 shows that there is a marked drop in resonant frequency. In fact, if the ratio of the slot width to centerline displacement exceeds approximately 2.35, there are indications that the slot may not become resonant. This absence of resonance was observed for the entire range of conductances tested. Study of the effect of shortening the slot was not completed.

Figures II-52 and II-54 show the frequency characteristics of a low Q slot having a width to centerline displacement ratio of 2.30 (this slot is therefore a borderline case). Comparison of the susceptance characteristics with those of a narrow slot shows a reduction in variation with frequency coupled with a tendency for the susceptance values to oscillate near zero. There are some experimental difficulties in obtaining the susceptance values shown in Figure II-52, and therefore, the curves are to be regarded as an indication of trend rather than a precise quantitative measurement.

Absence of resonance should not be serious, however, provided the susceptance does not vary markedly with frequency and remains small compared with the conductance. A further investigation of the admittance behavior as a function of frequency of the low Q slot was made for several slot lengths. The results are also shown in Figures II-52 and II-54. As can be seen, lengthening the slot not only lowered the resonant frequency appreciably but also raised the normalized conductance about 20 percent for a 2.6-percent increase in slot length. In addition, the conductance reached a peak at a frequency far from resonance. These characteristics tend to make a slot this wide of little interest for array applications.

Effect of Slot Loading

Reducing slot length by various methods of loading tends to increase the Q of the slot. The various types of loaded slots include dumbbell-shaped slots and dielectric loaded slots (here the loading increases with the amount of dielectric present and the dielectric constant of the loading material).

The results of Q measurements on transverse slots in a TEM line (rectangular outer and flat center conductor) are presented in Table I.

TABLE I

RESULTS OF Q MEASUREMENTS ON TRANSVERSE SLOTS IN TEM LINE

Type of Slot	Resonant Frequency (mc/s)	Q
5 by 1/6 inch straight unloaded	1200	24
3 by 1/8 inch straight, dielectric loaded, $\epsilon_r = 7.2$	1150	33
3 by 1/16 by 1 inch diameter dumbbells	1200	37
2-1/2 by 3/16 by 7/8 inch diameter dumbbells, dielectric in straight section only, $\epsilon_r = 7.4$	1220	27
3 by 5/8 inch straight, dielectric loaded, $\epsilon_r = 7.2$	1390	14
2 by 1/16 by 1/2 inch diameter dumbbells, dielectric in straight section only, $\epsilon_r = 7.4$	1000	110
1-5/8 by 1/16 by 1/2 inch diameter dumbbells, dielectric in straight section only, $\epsilon_r = 7.4$	1300	118

The dielectric loading described in the data in the table consisted of a slug of dielectric which filled the slot rather than covered it. Dielectric weatherizing covers have a loading effect which is not so large as the dielectric slugs.

The tabulated data indicate that, with the proper choice of slot width, dielectric material, and dumbbell size, the over-all length of a slot can be appreciably reduced while satisfactory broadband operation is still maintained.

Multiple Slots

Ehrlich and others[21] have investigated the possibility of increasing the bandwidth of a slot element by the use of several closely spaced slots as a single element. It was found that the broadbanding effect was a function of the lengths of the slots and their separation. For large differences in slot lengths, it was found that closely spaced slots acted independently; that is, the slots, despite their close spacing, have the separate impedance characteristics of the individual slots. Broadbanding by this method can be compared with the stagger-tuning of coils.

3. SLOT ARRAYS

The primary advantage of an array of individual radiators (slots, dipoles, polyrods, etc.) as opposed to an optical type of antenna such as a point source and reflector is that the aperture distribution which determines the radiation pattern may be readily controlled. In this section, the types of arrays are named and described, and methods for producing a given amplitude and phase distribution in the aperture are given. Methods for determining the aperture distribution which will produce a required radiation pattern are presented in the third section; and, finally, practical problems encountered in the design of slot arrays are discussed.

3.1 RESONANT AND NONRESONANT ARRAYS

3.1.1 Resonant Arrays

Linear arrays have been divided into two classes: resonant and nonresonant. In the resonant array, the slots are spaced $\lambda_g/2$ apart along the guide with adjacent slots coupled in opposed phase, or λ_g apart for in-phase slots. For example, in a longitudinal shunt slot array, the slots would all be displaced on the same side of the guide axis. The resonant array is terminated by a short circuit at the last slot for an array of series slots and by an open circuit for an array of shunt slots. All the slots may be considered to be located at a single point on an equivalent transmission line (for negligible attenuation). Thus, the problem of distributing power to the various elements is a simple network problem; for shunt slots, the slot conductances are all in parallel, and for series slots, the slot resistances are all in series. The input conductance of a shunt slot resonant array is $\sum_{k=1}^{n} g_k$, and the input resistance of a series slot array is $\sum_{k=1}^{n} r_k$, where g_k and r_k are the resonant conductance and resistance, respectively, of the k^{th} slot and n is the number of slots in the array. The array is generally designed for unity input impedance so that the array will be matched at its feed.

The resonant array is useful for short arrays and has the advantages that no power is dissipated in the reflecting termination and that its beam is normal to the array. As the length increases, however, a very small change in frequency is sufficient to destroy the necessary phase relationship down the guide and change the input impedance and radiation pattern radically (the main beam may split due to the reflected wave). For example, an array of n radiators, 1/2 n guide wavelengths long, would probably be useless if the frequency were changed to make it 1/2 n $\pm$ 1/4 guide wavelengths long since this would make the end radiator roughly in quadrature with the first, which would invalidate the principle of resonant operation. The bandwidth, therefore, would be approximately $\pm$ 50/n percent. This criterion is reasonably good for $n > 10$. A more accurate means for determining the bandwidth of a resonant array is afforded by the curves of Figure III-1. Long resonant arrays also require accurate spacing between slots so that stringent mechanical tolerances are required.

3.1.2 Nonresonant Arrays

The sensitivity of long resonant arrays has led to the development of arrays with slot spacings other than $\lambda_g/2$ or λ_g; these are the nonresonant arrays. In these arrays, since the slots do not radiate in phase, the beam emerges at an angle to the array, and the angle changes with frequency according to the relation

$$\sin \theta = \frac{\lambda}{\lambda_g} - \frac{\lambda}{2d} \tag{60}$$

where θ = position of the main beam relative to broadside
d = element spacing
λ = free space wavelength
λ_g = guide wavelength

and adjacent slots are coupled with opposed phase. Further, a small percentage of the input power (approximately 5 percent) must be wasted in a dummy load at the far end of the array. The advantages of the nonresonant array are improved impedance and pattern bandwidth, and an easing of mechanical tolerances.

The important characteristic of the nonresonant array (sometimes called a traveling wave array) is that it is matched along its whole length. This matching is accomplished by having the slots loosely coupled (which is generally the case for long arrays), by spacing the slots far enough off $\lambda_g/2$ or λ_g so that the reflections from individual slots add randomly (not in phase), and by terminating the guide in a matched load. A criterion for ensuring a correct match and uniform phase along the array has been developed by a number of investigators (see References 87, 88, 26a) and is

$$g_s^2 \csc^2 \beta d \ll 1 \tag{61}$$

where g_s is the largest slot conductance, $\beta = 2\pi/\lambda_g$, and d is the interelement spacing. For practical purposes

$$g_s^2 \csc^2 \beta d \leq 0.2 \tag{62}$$

may be used; this condition gives a maximum VSWR of 1.2. The effect of slot spacing on SWR is indicated clearly in Figure III-2. It can be seen that the impedance bandwidth is limited by the proximity to resonant spacing.

The efficiency bandwidth is generally less than the input impedance bandwidth. The power into the load varies due to the slots going off resonance, change of normalized slot conductance, and change of mutual interaction in the case of edge slots. The effect of frequency variation on the radiation pattern, except for shifting the main beam as indicated in equation (60), is generally not great as long as the guide is matched. The reflections from a secondary reflector or discontinuities in the parallel plate or horn system into which the array radiates may strongly affect the impedance and

efficiency. The seriousness of the reflections depends on whether the discontinuity lies parallel to the array or along the wave front. In the first instance the reflections cause little trouble, while in the latter, the effect is rather serious.[26b]

3.2 METHODS FOR CONTROLLING THE APERTURE ILLUMINATION

3.2.1 General Expressions

The following analysis is for shunt slots with negligible external mutual interaction among slots. For series elements, currents simply replace voltages and impedances replace admittances. If mutual coupling is serious, incremental admittance may be used with reasonable success in the resonant array and, near broadside, in the nonresonant array.

Figure III-3 is the equivalent circuit representation for a shunt slot array consisting of n elements, the first being nearest the generator. $Y_r = G_r + jB_r$ is the normalized admittance of the r^{th} element and Y_L the normalized admittance of the termination; Y_r^+ and Y_r^- are the normalized admittances looking toward the load on the right and left sides of the r^{th} element, respectively; V_r is the voltage across the equivalent transmission line at the position of the r^{th} element; P_r is the power radiated by the r^{th} element; and d is the distance between elements.

The equations satisfied by the voltages are

$$V_{n-1} = V_n (\cosh \gamma d + Y_n^- \sinh \gamma d) \tag{63}$$

$$V_{n-2} = V_{n-1} (2 \cosh \gamma d + Y_{n-1} \sinh \gamma d) - V_n \tag{64}$$

and

$$V_r = V_{r+1} (2 \cosh \gamma d + Y_{r+1} \sinh \gamma d) - V_{r+2} \tag{65}$$

where $\gamma = \alpha + j\beta$, the complex propagation constant of the unloaded line,

$$Y_r^+ = G_r^+ + jB_r^+ = \frac{Y_{r+1}^- \cosh \gamma d + \sinh \gamma d}{\cosh \gamma d + Y_{r+1}^- \sinh \gamma d} \tag{66}$$

and

$$Y_r^- = Y_r + Y_r^+ \tag{67}$$

The relation between power radiated by an element and its conductance is readily determined from Figure III-3;

$$G_r = G_r^+ \frac{P_r}{P_r^+} \tag{68}$$

where

$$P_r^+ = P_{r+1}^- \left[e^{2\alpha d} + \frac{\left|2\Gamma_{r+1}\right|^2 \sinh 2\alpha d}{1 - \left|\Gamma_{r+1}\right|^2} \right] \tag{69}$$

and $\left|\Gamma_r\right|$ is the absolute value of the total reflection coefficient at the r^{th} element.

It has been shown[73] that the ratio of the field across a longitudinal shunt slot, E_s, to the total field across the waveguide is

$$\frac{E_s}{E_t} = \frac{jK_1 Y}{\cos \frac{\pi x}{a}} \tag{70}$$

where K_1 = a positive real quantity

Y = the slot admittance
x = the displacement of the slot off the waveguide centerline
a = the wide dimension of the waveguide

Equation (70) illustrates an important point: the phase of E_s/E_t equals the phase of the slot admittance (plus $\pi/2$). The phase of the slot admittance,

$$\phi = \arctan \frac{B}{G} \tag{71}$$

may be determined from the desired phase of radiation, the phase of V_r and (72).

3.2.2 Resonant Spacing

The design of a broadside resonant array to produce a real (not complex) aperture distribution in lossless waveguide is a relatively simple matter. If the aperture distribution is complex and the guide is lossy, the problem is more involved; and a number of schemes for its solution have been proposed. (See References 26c, 74, 87a, and 88.)

For an n element array of longitudinal shunt slots in rectangular waveguide with an interelement spacing of a half-guide wavelength and adjacent elements placed on opposite sides of the waveguide centerline, equation (65) becomes

$$V_r = V_n \left[1 + \alpha d \sum_{s=1}^{n-r} s\, Y_{r+s} \right] \tag{73}$$

where terms of order higher than αd have been neglected. For the usual case of low attenuation and short arrays, equation (73) reduces to

$$V_r = V_n \tag{74}$$

In addition, since

$$P_r = V_r^2 G_r \tag{75}$$

$$G_r = G_n \frac{P_r}{P_n} = P_r \frac{\sum_{r=1}^{n} G_r}{\sum_{r=1}^{n} P_r} \tag{76}$$

The input admittance for an open circuit termination at the end slot is (attenuation neglected)

$$Y_{in} = \sum_{r=1}^{n} G_r + j \sum_{r=1}^{n} B_r \tag{77}$$

In general, the input admittance is designed to be either unity or a large real value (overloading).[64g] For resonant slots, $B_r = 0$.

An example of the design of a resonantly spaced array of longitudinal shunt slots with a complex aperture distribution follows:

1) Decide upon the input impedance to the array from the position of feeding (end, center, or other) and bandwidth considerations (broadbanding techniques). For this example, assume an open circuit termination and a desired real input admittance of unity, that is,

$$Y_{in} = 1.0 + j0$$

or

$$\sum_{r=1}^{n} G_r = 1.0, \quad \sum_{r=1}^{n} B_r = 0 \tag{78}$$

2) Determine the relative phase, ϕ_r', and the relative power, P_r, required to be radiated by each slot to produce the desired radiation pattern. (See Methods of Linear Array Synthesis, section 3.3.)

3) Calculate G_r from equation (76).

4) Calculate a new set of phase angles

$$\phi_r = \phi'_r + \phi_o \tag{79}$$

where ϕ_o is the constant phase change which will result in

$$\sum_{r=1}^{n} B_r = \sum_{r=1}^{n} G_r \tan (\phi'_r + \phi_o) = 0 \tag{80}$$

Then

$$Y_r = G_r + jB_r = G_r (1 + \tan \phi_r) \tag{81}$$

Equation (80) is in general a complicated transcendental equation but since ϕ_o is the only unknown, equation (80) does have a solution. If $\phi'_r = 0$ for all r, the beam will be broadside and the slots resonant; if $\phi'_r = k\phi$, the beam will be off broadside.

The values of G_r and ϕ_r will determine the dimensions of the slots to be used. If series slots are to be used, the resistance and phase of each slot will be the same as the conductance and phase of the shunt slots. To obtain the proper phase of the waveguide field at the slots, adjacent elements must be given 180-degree phase reversals.

3.2.3 Nonresonant Spacing

The design of arrays using elements with nonresonant spacing has been given by Watson[87a], Fry and by Goward.[26d] Watson assumes a pure traveling wave and indicates the corrections to be made for waveguide attenuation. Fry and Goward give a more direct approach and also assume a pure traveling wave but indicate no corrections for waveguide attenuation. Begovich presents the theory for a nonresonant array without assuming a pure traveling wave but does not give the corrections for waveguide attenuation. It can be shown that for medium length arrays the wave in the guide differs considerably from a pure traveling wave and the design is altered very appreciably from that calculated with the assumption of a pure traveling wave. For long arrays, the guide attenuation will produce a power loss which is a relatively large part of the total input power. This situation is especially true at X- and K-bands.

The voltages for a lossless transmission line are, from equations (63) and (65),

$$V_{n-1} = V_n (\cos \beta d + jY_n^- \sin \beta d) \tag{82}$$

and

$$V_r = V_{r+1} (2 \cos \beta d + jY_{r+1} \sin \beta d) - V_{r+2} \tag{83}$$

This expression shows that the magnitude and phase of the voltage at the r^{th} element are functions of both the distance between elements and the admittance introduced at the $(r+1)^{th}$ element.

For the usual cases of slots spaced less than a guide wavelength apart and for the reflection coefficients small, equations (69) and (66) simplify to

$$P_r^+ = P_{r+1} (1 + 2\alpha d) \tag{84}$$

and

$$Y_r^+ = \frac{Y_{r+1}^- \cos \beta d + j \sin \beta d}{\cos \beta d + j Y_{r+1}^- \sin \beta d} \tag{85}$$

This admittance equation may be solved graphically very quickly by use of the Smith Admittance Chart. The reflection coefficient to the right of the r^{th} slot is

$$\Gamma_r^+ = \Gamma_{r+1}^- e^{-2\gamma d} = \Gamma_r^+ \Big|_{\alpha=0} \cdot e^{-2\alpha d} \tag{86}$$

This relation shows that, compared with the case in which the attenuation is zero, only the amplitude of the reflection coefficient at the r^{th} slot is altered by transmission line attenuation. If it is necessary to take attenuation into account, equation (86) may be used.

For a pure traveling wave and no mutual interaction, the phase of radiation can be controlled by the slot position along the guide and/or by the phase of the slot admittance. Since the measurement of incremental conductance depends on the presence of a number of slots of equal conductance and spacing, control of phase by slot position is not feasible in the presence of mutual coupling except for uniform progressive phase (that is, equally spaced slots). Figure III-4 illustrates a graphical method for determining slot spacings; if the guide is not matched, the phase does not vary linearly in the guide and a correction must be made[15].

The following is an example of the design procedure for an n-element nonresonantly spaced array of longitudinal shunt slots.

1) Determine the relative phase, ϕ_r', of the field and the relative power, P_r, to be radiated by each slot (see Methods of Linear Array Synthesis, section 3.3).

2) Determine the spacing between elements based on a knowledge of the required phase shift and waveguide dimensions, the desired position of the main beam relative to the normal to the array, bandwidth considerations, etc.

3) Except for a few special cases, the termination will be a match to the waveguide.

4) To insure good input admittance properties for a short array and a broadband matched operation for long arrays, the normalized admittance of the n^{th} slot, Y_n, is made 0.1 or lower.[10] The greater the conductance of the last slot, however, the less power will be lost in the load.

5) Calculate the admittance Y_{n-1} and the voltage V_{n-1} using equations (68) or (85) and (63) or (82), respectively, depending on whether or not the waveguide attenuation is negligible. For the array with a matched termination

$$Y_n^- = Y_n + 1.0 \tag{87}$$

6) Using equations (66) and (67) or (84), calculate G_{n-1}

$$G_{n-1} = G_{n-1}^+ \frac{P_{n-1}}{P_{n-1}^+} \tag{88}$$

where

$$P_{n-1}^+ = P_n + P_n^+ \tag{89}$$

under the assumption that the waveguide attenuation is zero; P_n^+ is the power dissipated in the termination and is obtained from equation (66).

7) The phase of the admittance of the $(n-1)^{th}$ slot is

$$\phi_{n-1} = \arctan \frac{B_{n-1}}{G_{n-1}} \tag{90}$$

ϕ_{n-1} is found using equation (70), step 1, and the results of step 5, taking into account the progressive phase shift desired.

8) The other G_r and ϕ_r are determined progressively in a similar manner.

3.3 METHODS OF LINEAR ARRAY SYNTHESIS

3.3.1 Introduction

Methods for effecting a specified amplitude and phase distribution on a linear slot array have been described. The present section will be concerned with prescribing an amplitude and phase distribution to produce a specified far field radiation pattern. Only parallel linear arrays will

be considered. (See the Element Factor, section 2.1.) A two-dimensional array can be designed by considering it to be a linear array of linear arrays. Nonparallel arrays are described elsewhere in the literature. This process, known as array synthesis, is the inverse of array analysis, and is, in general, rather complicated*. However, a number of reasonably successful methods of array synthesis have been devised and a few of them will be described. Only the methods will be presented; the mathematical justification can be found in the appropriate reference.

A working knowledge of array theory is assumed here.[64] It may be worthwhile, however, to recall a few important concepts pertinent to the discussion to follow.

1) The far field radiation pattern of an antenna oriented in space with respect to some coordinate system is the field measured on a sphere (or, for a pattern in a principal plane, on a great circle of the sphere) of large radius centered at the origin of the coordinate system.

2) The radiation pattern of an array can be expressed as the product of two factors, the element factor and the space factor. The element factor is the radiation pattern of an element of the array,** and the space factor is the radiation pattern of the array with the elements of the array replaced by isotropic radiators. Only synthesis of the space factor S is of concern in this discussion. The effect of the element factor, E, on the array radiation pattern, R, can be taken into account by the relation

$$S = \frac{R}{E} \tag{91}$$

in which R, E and S may be complex.

3) The relationship between the space factor and the aperture distribution, A, for a linear array of N equally spaced discrete elements can be written

$$S(\nu) = e^{jkx_o(\nu - k_1/k)} \sum_{m=0}^{N-1} A_m e^{jkmd(\nu - k_1/k)} \tag{92}$$

*Aperture distributions to produce suitable patterns are often determined empirically; one calculates the pattern produced by some distribution and notes how closely it approximates the desired pattern.

**In certain instances where the elements of an array are subject to mutual interaction by their neighbors, the element factor is the pattern of an element measured in the presence of all the other radiators in the array. (See Reference 59.)

where $S(\nu)$ is a complex number proportional to the field strength at a point ν on a great circle in the plane containing the array on an infinite sphere centered at the origin. A_m is a complex coefficient to which the currents at corresponding points in the several elements are respectively proportional (the phase of A_m is measured with respect to the uniform progressive phase e^{-jk_1md}); k is the free space phase factor ($=2\pi/\lambda$); k_1 is the array phase factor ($=2\pi/\lambda_1$); λ_1 is the wavelength along the array; $\nu = \cos\theta$; and the remaining symbols are defined in Figure III-5.

4) For a discrete array with an odd number of elements, N, centered at the origin, equation (92) becomes

$$S(\nu) = \sum_{m=0}^{N-1} A_m e^{jk(m-\frac{N-1}{2})\, d\,(\nu - k_1/k)} \tag{93}$$

where A_o is the excitation coefficient of the element farthest to the left, or

$$S(\nu) = \sum_{m=\frac{N-1}{2}}^{\frac{N-1}{2}} A_m e^{jkmd(\nu - k_1/k)} \tag{94}$$

where A_o is the excitation coefficient of the central element,

5) For a discrete array with an even number of elements, N, centered at the origin, equation (92) becomes

$$S(\nu) = \sum_{m=0}^{N-1} A_m e^{jk(m-\frac{N-1}{2})\, d\,(\nu - k_1 k)} \tag{95}$$

where A_o is the excitation coefficient of the element farthest to the left, or

$$S(\nu) = \sum_{p=-N-1}^{N-1} A_p e^{j^2 pk \frac{d}{2}(\nu - k_1/k)} \quad \text{for p odd} \tag{96}$$

where $p = 2(m - \frac{N-1}{2})$ and A_{-1} and A_1 straddle the origin.

6) The space factor of an array with a continuous distribution centered at the origin is given by

$$S(\nu) = \int_{-a}^{a} A(x) e^{jkx(\nu - k_1/k)} \tag{97}$$

where A(x) is a complex number to which the currents at x are proportional, x is the displacement from the origin along the array, and 2a is the length of the aperture.

7) The power pattern $S(\nu)\, S^*(\nu)$, where $S^*(\nu)$ is the complex conjugate of $S(\nu)$, is not affected by the position of the array with respect to the origin. The phase of $S(\nu)$ is, however, dependent on the position of the origin.

8) It can be shown from equation (92) that

$$|S(\nu + q\lambda/d)| = |S(\nu)| \quad , q \text{ an integer} \tag{98}$$

In words, in a linear array of discrete equally spaced elements, $|S|$ is periodic in the variable ν and repeats itself at intervals of λ/d. Although $|S|$ has a period of λ/d, S may or may not be periodic with period λ/d. Thus, from equation (92) it can be shown that for $x_o = r \cdot d$ (r an integer)

$$S(\nu + q\lambda/d) = S(\nu), \quad q \text{ an integer} \tag{99}$$

That is, for an array with an odd number of elements, one of which is centered at the origin, $S(\nu)$ has a period λ/d. From equation (92) it can also be shown that

$$S(\nu + q2\lambda/d) = S(\nu), \quad q \text{ an integer} \tag{100}$$

That is, for an array with an even number of elements, one of which centered at the origin, $S(\nu)$ has a period $2\lambda/d$. (See Figure III-6.)

9) For a continuous array ($d \to 0$), $S(\nu)$ is not necessarily periodic. (The period is infinite.)

10) The physically significant portion of $S(\nu)$ is in the region $-1 \leq \nu \leq 1$, the so-called "visible" region or "real" space. Outside the visible region, θ takes on imaginary values and $S(\theta)$ cannot be measured physically. (See Figure III-7.)

11) If a linear array has a space factor $S(\nu)$, the same array with progressive phase shift will have a space factor $S_1(\nu)$, where

$$S_1(\nu) = S(\nu - k_1/k) \tag{101}$$

and k_1 is the progressive phase shift constant; that is, the pattern will be shifted in ν-space a distance $-k_1/k$.

12) In general, there is more than one aperture distribution which will produce a given $|S(\nu)|$. There is, however, only one aperture distribution that will produce a given $S(\nu)$, for the general case when $S(\nu)$ is complex: the field phase variations on the sphere centered at the origin are specified.

13) A number of investigators have shown that it is theoretically possible to design an array of given length to have any continuous single valued pattern whatever. The use of the proposed methods to produce highly directive antennas of small size is known as supergaining and has been widely discussed in the literature. (See References 8, 11, 57, 78, 91, 93, and 96.) It has been shown that high gain supergain antennas are physically unrealizable due to their extremely low efficiency, narrow bandwidth, and high tolerance requirements. The designer should not fall into the trap of using supergain techniques in order to get more directivity or shaping from a given aperture length than is practicable. On the other hand, mild forms of supergaining are quite useful, for example, the Hansen-Woodyard criterion[31] and the mild supergaining of short low gain arrays. Taylor[83] has devised a supergain index which will be helpful in determining if the degree of supergaining is prohibitive. For discrete arrays this index is

$$\gamma = \frac{2\pi \sum_{N=0}^{N-1} A_n^2}{\int_{-kd}^{kd} |S|^2 d\psi} = \frac{\int_{-\pi}^{\pi} |S|^2 d\psi}{\int_{-kd}^{kd} |S|^2 d\psi} \tag{102}$$

where $\psi = kd \cos \theta$; for continuous arrays the index is

$$\gamma = \frac{2\pi k \int_{-a}^{a} |g(x)|^2 dx}{\int_{-1}^{1} |S(\nu)|^2 d\nu} = \frac{\int_{-\infty}^{\infty} |S(\nu)|^2 d\nu}{\int_{-1}^{1} |S(\nu)|^2 d\nu} \tag{103}$$

where $\nu = \cos \theta$. For ordinary arrays, γ is very nearly unity; a slight amount of supergaining increases its value very rapidly, however, and should serve as a danger signal to the designer. A value of $\gamma = 10$ may be stated arbitrarily as the maximum allowable γ. It should be noted that when there are several different arrays which produce identical power patterns, the value of γ associated with each of these is the same.

14) In the synthesis problem, the complex field pattern, $S(\nu)$, the magnitude of the field, $|S(\nu)|$, or the power pattern, $S(\nu)\,S^*(\nu) = |S(\nu)|^2$ may be specified. If $|S(\nu)|$ is specified, a phase value may be assigned arbitrarily at each value of ν to obtain a satisfactory complex $S(\nu)$. The choice of the arbitrary phase values will, in general, affect the closeness of the synthesis approximation: there is an optimum set of

phase values for the field pattern, which allows the aperture to be used most efficiently. Thus, if a certain phase distribution in $S(\nu)$ is not required, it is not an efficient procedure to assign phase values arbitrarily to $|S(\nu)|$. There are, in fact, methods for synthesis which require only the specification of $|S(\nu)|$ in which the phase of $S(\nu)$ is allowed to take on the optimum values. From the standpoint of economical design, these latter methods are preferable to those which require an arbitrary statement of the complex field pattern $S(\nu)$.* On the other hand, the methods which require an arbitrary statement of the phase of $S(\nu)$ may be simpler and quite satisfactory. If $|S(\nu)|$ is given, one procedure is to assign a phase of zero to $S(\nu)$ and allow the magnitude of $S(\nu)$ to take on positive and negative values; that is, let $S(\nu)$ be positive on the main lobe, negative on the second lobe, positive on the third, and so on.

It will be found that all synthesis methods for slot arrays are dependent on equation (92). However, for long arrays (say more than 20 elements), the task of determining the A_m becomes arduous. For the sake of simplification, it is often assumed that a long array of discrete elements can be approximated by a continuous array. In other words, equation (97) is solved for A(x) and the values of A(x) at the x's corresponding to the element displacements from the origin are identified as the excitation coefficients for the corresponding elements. The validity of the approximation depends on how closely the $S(\nu)$ for the continuous array approaches the $S(\nu)$ for the discrete array in real space ($-1 \leq \nu \leq 1$). As can be seen from Figure III-7, the closeness of fit depends on the directivity (narrow beam and tapering sidelobes) of $S(\nu)$ and the ratio λ/d. Thus, for a directive $S(\nu)$, tapering sidelobes, and large λ/d the approximation is usually good. In a slot array the elements are generally spaced less than $d = \lambda$ to avoid two or more main lobes in real space,** and in many cases $d \approx \lambda/2$; further, the pattern of a long array is usually directive. Thus, for most practical arrays the approximation is a good one. Therefore, in the following discussions both discrete and continuous arrays will be treated.

3.3.2 Arrays of Few Elements: Discrete Array

The Dolph-Tchebyscheff Array

In many radar applications, it is desirable for the antenna to possess a power pattern, which, if the sidelobe level is specified, has a minimum beamwidth or, if the beamwidth is specified, has a minimum

---

*A striking example of the economy involved in the optimum phase design is presented in Appendix I.

**If the element factor is reasonably directive, the spacing may be greater than $d = \lambda$ and the pattern will not exhibit more than one main beam.

sidelobe level. A broadside array with $d \geq \lambda/2$ having such an optimum pattern together with methods for the calculation of the required amplitude distribution has been described by C. L. Dolph[17] and others. (References 5, 41, 56, 71.) The development of the method is based on the characteristics of the so-called Tchebyscheff polynomial,

$$\left.\begin{aligned} T_n(x) &= \cos(n \cdot \cos^{-1} x) \text{ for } |x| \leq 1 \\ T_n(x) &= \cosh(n \cdot \cosh^{-1} x) \text{ for } |x| \geq 1 \end{aligned}\right\} \tag{104}$$

which can also be written as a polynomial of degree n. The Tchebyscheff polynomial has the following properties:

a) It has n zeros all within the interval $-1 \leq x \leq 1$.
b) Its absolute value falls between 0 and 1 in the interval $-1 \leq x \leq 1$.
c) It approaches infinity as x^n in the interval $|x| > 1$.

Figure III-8 illustrates the shape of $T_4(x)$.

The space factor of an N element Dolph array is given by

$$S_N(\psi) = T_{N-1}(Z_o \cos \tfrac{\psi}{2}) \tag{105}$$

where $\psi = kd\nu$, $\nu = \cos\theta$, and Z_o is a constant which will be defined later. Equation (105) is illustrated by a graphical construction in Figure III-8 which depicts $T_4(Z_o \cos \psi/2)$ and shows how $S_5(\psi)$ can be found. Figure III-9 shows the space pattern of an 8-element optimum array. S_N is a real space factor which can be represented by a real polynomial; the excitation coefficients for the elements are real and symmetrical about the center of the array.

The most recent method for calculating the excitation coefficients has been suggested by van der Maas.[41] This method will be described below.

We define a quantity Z_o in terms of the required main beam-to-sidelobe voltage ratio, r, and the number of radiators N by

$$T_{N-1}(Z_o) = r \tag{106}$$

Z_o can be written explicitly as

$$Z_o = \frac{1}{2}\left[(r + \sqrt{r^2 - 1})^{\frac{1}{N-1}} + (r - \sqrt{r^2 - 1})^{\frac{1}{N-1}}\right] \tag{107}$$

or

$$Z_o = \cosh\left(\frac{1}{N-1} \operatorname{arc\,cosh} r\right) \tag{108}$$

If adequate tables of the hyperbolic cosine are available, equation (108) will be easier to calculate than equation (107). If we number the N radiators from left to right, 1, 2 ... K ... N, the series for the relative current in the Kth radiator, I_N^K, is given by

$$I_N^K = \frac{N-1}{N-K} \sum_{S=0} \begin{bmatrix} N-K \\ S+1 \end{bmatrix} \begin{bmatrix} K-2 \\ S \end{bmatrix} \alpha^{S+1} \quad \text{for } K \neq 1 \text{ and } K \neq N \tag{109}$$

$$I_N^K = 1 \quad \text{for } K=1 \text{ and } K=N \tag{110}$$

where

$$\begin{bmatrix} a \\ b \end{bmatrix} = \frac{a!}{b!\,(a-b)!}$$

The variable α is given by

$$\alpha = \frac{Z_o^2 - 1}{Z_o^2} = \tanh^2 \left[\frac{\ln \left[r + (r^2 - 1)^{1/2} \right]}{N - 1} \right] \tag{111}$$

The series terminates for $S = N - K - 1$ if $K \geq (N + 1)/2$ and for $S = K - 2$ if $K \leq (N + 1)/2$. It is interesting to note that the special case $1/r = 0$ (no sidelobes) gives the binomial distribution (excitation coefficient equal to the coefficients in the binomial expansion of $(c + d)^{N-1}$)or

$$I_N^K = \begin{bmatrix} N - 1 \\ K - 1 \end{bmatrix} \tag{112}$$

The special case $r = 1$ (no main beam) gives an array in which

$$I_N^1 = 1, \; I_N^N = 1 \text{ and } I_N^K = 0 \text{ for } K \neq 1 \text{ and } K \neq N \tag{113}$$

The procedure, then, for the design of a Dolph-Tchebyscheff array is as follows:

a) Having specified r, determine α from the second equation in (111) or by substituting for Z_o in the first equation in (111).

b) Determine the excitation coefficients I_N^K by summing the series (109).

(Dolph, Riblet, and Barbiere also indicate a method for finding I_N^K given the beamwidth to the first nulls rather than the sidelobe level. This method will

not be presented here. However, a useful curve[80] for the halfpower beamwidth versus the sidelobe ratio is given in Figure III-10.)

The excitation coefficients for a number of specific Tchebyscheff arrays have been tabulated by Dolph in his first article and others have been calculated and tabulated at the Hughes Aircraft Company. The latter tabulations are presented in Appendix B, complete with the Z_o and gain for each array.

There are two limitations on successful design: the main beam is broadside and $d \geq \lambda/2$. It is possible, by assigning the correct progressive phase shift with constant k_1 to the excitation coefficients, I_N^K, to aim the main beam in a direction $\overline{\theta}$ from end-fire according to the relation

$$\overline{\theta} = \arccos k_1/k \tag{114}$$

For $\overline{\theta}$ near 0°, the end-fire position, it is possible to obtain a narrower beamwidth than indicated by a Tchebyscheff analysis by instituting supergain tactics (for example, the Hansen-Woodyard criterion) so that the Dolph-Tchebyscheff array is no longer optimum. Similarly, if the spacing, d, is less than $\lambda/2$, it is possible to supergain the array in order to narrow the beam and/or lower the sidelobes; thus, the Dolph-Tchebyscheff array is not optimum for $d < \lambda/2$.

Shaped Beam: Field Strength Pattern Specified in Magnitude and Phase

Fourier Series Method (References 34b, 61, 94): By extending the limits and stationing the center of the array at the origin, equation (94) can be written for an odd number of elements as

$$S(\psi) = \sum_{M=-\infty}^{\infty} A_m e^{jm\psi} \tag{115}$$

in which

$$\psi = kd(\nu - k_1/k) \tag{116}$$

and $S(\psi)$ and A_m may be complex numbers. For an even number of elements, the equations are much the same with the exception that there is no A_o term, that is, no "d-c" term. Generally, however, there is no advantage in designing an array with an even number of elements rather than one with an odd number. If $S(\psi)$ is a well-behaved function and is periodic with period 2π, it can be expanded in a Fourier series, where the Fourier coefficients, A_m, are

$$A_m = \frac{1}{\pi} \int_{-\pi}^{\pi} S(\psi) e^{-jm\psi} \, dx \tag{117}$$

If

$$A_m = a_m + jb_m \tag{118}$$

and

$$A_m = A^*_{-m} \tag{119}$$

then $S(\psi)$ is real; if

$$A_m = -A^*_{-m} \tag{120}$$

then $S(\psi)$ is imaginary. Thus, equation (115) can be written

$$\mathrm{Re}S(\psi) = \sum_{m=-\infty}^{\infty} A'_m e^{jm\psi} \tag{121}$$

$$\mathrm{Im}S(\psi) = \sum_{m=-\infty}^{\infty} A''_m e^{jm\psi} \tag{122}$$

where A'_m obeys equation (119) and A''_m obeys equation (120), the relations (121) and (122) can be written in the more familiar form

$$\mathrm{Re}S(\psi) = 2\left\{\frac{a'_o}{2} + \sum_{m=1}^{\infty}\left[a'_m \cos m\psi + (-b'_m)\sin m\psi\right]\right\} \tag{123}$$

$$\mathrm{Im}S(\psi) = 2\left\{\frac{a''_o}{2} + \sum_{m=1}^{\infty}\left[a''_m \sin m\psi + b''_m \cos m\psi\right]\right\} \tag{124}$$

where $A'_m = a'_m + jb'_m$, $A''_m = a''_m + jb''_m$, $A'_o = \frac{a''_o}{2}$ and $A''_o = j\frac{b''_o}{2}$.

Equations (123) and (124) are Fourier series in which the a'_m's and $(-b'_m)$'s and the a''_m's and b''_m's are the Fourier coefficients which can be found by well known means.

The procedure, then, for synthesis by this method is:

1) Separate $S(\psi)$ into real and imaginary parts.
2) Find the Fourier coefficients for $\mathrm{Re}S(\psi)$ and for $\mathrm{Im}S(\psi)$ in (123) and (124).
3) Determine A'_m and A''_m from the coefficients found in step 2.
4) Determine A_m from $A_m = A'_m + A''_m$.

The pattern will be reproduced exactly only for an infinite number of elements. In the practical case, however, the number of elements is finite and the Fourier series, (123) and (124), will have only a finite number of terms.

The reader will notice from equation (116) that for $d < \lambda/2$ the range of ψ is less than 2π radians for $-1 \leq \nu \leq 1$ ($0 \leq \theta \leq \pi$); for $d = \lambda/2$ the range of ψ is 2π; and for $d > \lambda/2$ the range of ψ is greater than 2π. In fact, the range of ψ is

$$\bar{\psi} = 2kd \tag{125}$$

for $0 \leq \theta \leq \pi$. If the space factor, $S(\theta)$, is defined for $0 \leq \theta \leq \pi$ the space factor, $S(\psi)$, will be defined for

$$-kd(1 + k_1/k) \leq \psi \leq kd(1 - k_1/k) \tag{126}$$

that is, $S(\psi)$ will be periodic with period $\bar{\psi} = 2\,kd$ or $\bar{\nu} = \frac{\lambda}{d}$.* The rules associated with the Fourier series (123) and (124) require $S(\psi)$ to have a period of 2π radians. Thus, for $\bar{\psi} < 2\pi$ ($d < \lambda/2$), $S(\psi)$ is specified only over a portion of the required 2π radians and the function used to fill in the remainder of the interval can be chosen by the designer. It will be found that certain choices of "fill in" will be more satisfactory than others from the standpoint of the closeness-of-fit of the synthesized pattern to the required pattern and/or simplicity of the equations. A trial and error process is usually used to determine the best "fill in" function. If $\bar{\psi} = 2\pi$ ($d = \lambda/2$), the required interval will be filled by $S(\psi)$. If $\bar{\psi} > 2\pi$ ($d > \lambda/2$), $S(\psi)$ will not fit the 2π radian interval and this method cannot be used except in special cases,** for example, if $S(\theta)$ is specified over a limited range in θ (less than π radians).

Analog to Woodward's Method***: Another method which might be used in the present situation is an analog to Woodward's method which will be discussed with shaped beams (page 59). Application of Woodward's method to the present problem is not difficult. Figure III-11 gives a pictorial explanation of the method.

The important difference for the discrete case is that $S(\nu)$ is expressed as

---

*For an array with an even number of elements, $\bar{\psi} = 4kd$ and $\bar{\nu} = 2\lambda/d$ as noted in the Introduction. However, the symmetry of $S(\psi)$ in its period is such that the arguments to follow for an odd number of elements are not contradicted for an even number of elements.

**See Reference 94, page 639. Note use of $d_1 = 2k$.

***Suggested to the authors by T. T. Taylor.[1]

$$S(\nu) = \sum \frac{A_n \sin \frac{Nkd(\nu - \nu_o)}{2}}{N \sin \frac{kd(\nu - \nu_o)}{2}} \qquad (127)$$

Equation (127) is transformed to (140) (page 60), when $N \to \infty$ and $d \to 0$, that is, when the array becomes continuous.

Shaped Beam: Power Pattern Specified, Field Strength Phase Arbitrary

It is apparent that the methods for controlling the aperture illumination (section 3.2) can be made applicable in the present case by the simple expedient of assigning an arbitrary phase, say, zero, to the square root of the power pattern. Thus, the synthesized space factor,

$$S(\nu) = \sqrt{\Phi(\nu)} = |S(\nu)| \qquad (128)$$

where $\Phi(\nu)$ is the power pattern and is real. The methods to be described, however, are those which afford the optimum phase.

Circle Diagram Method (References 61 and 79): If the phase of the field pattern is not specified, it is uneconomical (design-wise) to use a synthesis method which limits the design to arbitrarily chosen field phase patterns, especially for arrays of few elements[79]. The circle diagram method provides an efficient means of synthesizing an array when the phase variation of the field pattern is not specified. The power pattern is approximated by the synthesis and the phase variation of the field pattern is allowed to take on any values necessary to reproduce the power pattern.

If the substitution

$$\psi = kd(\nu - k_1/k) \qquad (129)$$

is made, then equation (92) can be written

$$S(\psi) = e^{j \frac{x_o}{d} \psi} \sum_{m=0}^{N-1} A_m e^{jm\psi} \qquad (130)$$

If further substitution is made so that

$$Z = x + jy = re^{j\psi} \qquad (131)$$

where $r = 1$, then equation (130) can be written

$$S(Z) = Z^{\frac{x_o}{d}} \sum_{m=0}^{N-1} A_m Z^m \qquad (132)$$

By the fundamental theorem of algebra, the polynomial in (132) can be written in terms of its N-1 linear factors:

$$S(Z) = Z^{\frac{x_o}{d}} \cdot A_{N-1}(Z-Z_1)(Z-Z_2)\ldots(Z-Z_{N-1}) \qquad (133)$$

Thus, the equation $S(Z) = 0$ has N-1 roots given by $Z = Z_m$ and, in addition, a root of multiplicity $\frac{x_o}{d}$ at $Z = 0$. If these roots are plotted in the complex plane as shown in Figure III-12A, it is apparent that the value of S(Z) is proportional to the product of all the vectors which connect the point $Z = e^{j\Psi}$ to each of the roots. The locus of $e^{j\Psi}$ is the unit circle, as indicated. It is obvious that the magnitude of S(Z) is not affected by the presence of the root at the origin or its multiplicity; a root at infinity is also ineffective as far as producing changes in the magnitude of S(Z). Only roots near or upon the unit circle contribute changes in the magnitude of S(Z) to a significant degree.

Thus, the design procedure is:

1) Place a few roots judiciously in the complex plane and then determine $S_1(Z)$:

$$\left|S_1(Z)\right| = \left|A_{n-1}\right| \left|(Z-Z_1)\right| \cdot \left|(Z-Z_2)\ldots\right|\left|(Z-Z_{N-1})\right| \qquad (134)$$

(A scheme for simplifying the calculation in (134) is to take the logarithm of (134) and measure $\left|(Z-Z_n)\right|$ with a logarithmic scale.)

2) Relocate or add roots by trial and error until $\left|S_1(Z)\right| = \left|S(Z)\right| = \sqrt{\Phi(Z)}$.

3) Expand the product (134) obtaining the polynomial form (132) and the excitation coefficients A_m.

If the number of elements is not too large, the designer will, with some practice, be able to predict the effect of placing the roots at specific locations in the complex plane. Taylor and Whinnery, in their paper,[79] have listed a number of theorems which will help to give the designer an insight into the problem of placing the roots. A few simple rules will be stated here:

1) Roots at the origin or infinity are useless.

2) Roots on the unit circle have the greatest effect on S(Z); in fact, a root upon the unit circle will produce a zero in S(Z) as $e^{j\Psi}$ passes through it.

3) If any or several roots are moved to their respective image points, the relative variation of $\left|S(Z)\right|$ on the unit circle is unchanged. The image point of any complex number Z_n is defined by $1/Z_n^*$, which occurs at

the same polar angle as Z_n but has a magnitude which is the reciprocal of the magnitude of Z_n.

4) If all the roots of S(Z) lie on the unit circle, the solution to the array problem is unique; that is, there is only one disposition of the roots which will reproduce $|S(Z)|$. If, on the other hand, some (one or more) roots lie off the unit circle the solution is not unique; that is, some roots can be moved to their image positions thus changing the excitation coefficients but not affecting $|S(Z)|$.

As an example, in the circle diagram for an eight-element uniform array shown in Figure III-12, the seven roots are equally spaced around the periphery of the unit circle, with the exception of the point 1 + j0 at which no root occurs.

It has been pointed out previously that the range of ψ depends on the interelement spacing, d. It is possible, by using small values of $d(< \lambda/2)$ and strategic placement of zeros, to obtain surprisingly high values of gain. This technique of using a small value of d to obtain a visible range small in comparison with a period of $|S|$ and then adjusting $|S|$ by placement of the roots so that it exhibits considerably more directivity within this range than without it, is known as "supergaining" the array (see page 48).

For an array of more than 10 elements, the synthesis method described above is long and laborious. Taylor and Whinnery, however, have devised and built an analog device which operates on the principle of the circle diagram method. The roots are mechanically moved about on the complex plane and $|S(Z)|$ is observed directly on an oscilloscope. With this machine an experienced operator can synthesize a pattern in short order without excessive computation.

3.3.3 Arrays of Many Elements: Approximated by a Continuous Array

Narrow Beam and Low Sidelobes

The Dolph-Tchebyscheff Envelope: The Dolph-Tchebyscheff array for discrete elements has been described in the discussion of discrete arrays (section 3.3.2); the continuous case remains for consideration. It has been observed that, for a given sidelobe ratio, the normalized excitation coefficient values, when plotted with respect to the normalized displacements of the corresponding elements from the center of the array, tend to lie on the same smooth curve (called the envelope of the excitation coefficients) as N, the total number of elements, is increased. This phenomenon is illustrated in Figure III-13 in which the excitation coefficients for four 40-db arrays with 12, 24, 48 and 144 elements, respectively, are plotted. The excitation coefficients for the four arrays are normalized, in this case, to a value of unity at the center of the array, and the displacements of the elements are normalized so that the elements for each of the four arrays are equally spaced in the region $-1 \leq X \leq 1$ where X is the normalized displacement from the center of the array. With the envelope curve shown in the

illustration, the excitation coefficients can be found for any 40-db Dolph array having more than 24 elements. For an N-element 40-db array, the region $-1 \leq X \leq 1$ is divided into N-1 equal segments by N graduations. At each of these graduations, read from the curve the corresponding normalized (relative) excitation coefficient. Since the end elements do not appear to be related to the envelope (see Figure III-13), a different method is necessary to determine the coefficients for these elements.

A number of methods have been suggested for the determination of the envelope curve. Van der Maas[41] and Taylor[86] independently arrived at an analytical expression for the envelope curve:

$$g(p, A) = \frac{\pi A^2}{4} \cdot \frac{2 J_1\left[jA \sqrt{\pi^2 - p^2} \right]}{jA \sqrt{\pi^2 - p^2}} \tag{135}$$

where $\cosh \pi A = r$ = the voltage sidelobe ratio
$p = 2\pi s/\ell$, is a variable running from $-\pi$ to π
s = the physical distance from the center of the array
ℓ = the length of the array.

Here J_1 is a Bessel function of the first kind, the values of which have been tabulated for imaginary argument.* The envelope function, $g(p, A)$, for a 40-db sidelobe ratio has been plotted in Figure III-14, and calculated values of the excitation coefficients for a 24-element 40-db Dolph array are displayed on the graph for comparison. The excitation coefficients for the 24-element array were normalized so as to be equal to the envelope at the center of the array.

A method for approximating the envelope curve has been derived empirically by Bailin and others.[4] The approximation is

$$g(x) \approx \left[Ax^4 + Bx^2 + 1 \right]^2 \tag{136}$$

where

$$\left.\begin{aligned} A &= 0.0861 \cosh^{-1} r - 0.228 \\ -B &= 0.225 \cosh^{-1} r - 0.240 \end{aligned}\right\}$$

and x is the displacement from the center of the array normalized so that x varies from -1 to 1 for an array of length ℓ. In effect, equation (136)

*See Jahnke and Emde, Tables of Functions, Dover Publications, New York, 1943, pp. 227ff; British Association Mathematic Tables, Vols. VI and X, The University Press, Cambridge, 1952; National Bureau of Standards, Tables of $J_0(Z)$ and $J_1(Z)$ For Complex Argument, Columbia University Press, New York, 1943.

is a polynomial approximation for equation (135). It has been shown that the approximation is good (less than 5 percent error) for most practical arrays. The designer should be aware of the fact that the error in effecting a given aperture distribution for a slot array is in excess of 5 percent in most cases. It should also be noted that g in equation (135) or (136) need not be plotted to find the excitation coefficients of an array; the values of g can be computed only for values of p or x corresponding to element positions on the array.

The amplitude distribution for a Dolph array is discontinuous at the ends. For a very long array, the value of the amplitude at x = -1 and x = +1 becomes infinite with respect to the values at intermediate positions, but for all other values of x the amplitude is given by equations (135) and (136). In the case of a finite array, the excitation coefficients for the end elements are finite and can be found in terms of the next to last element by an exact analytical expression which is derivable from equation (108). The expression for an N-element array is

$$I_N^1 = I_N^N = I_N^{N-1} \frac{Z_o^2}{(N-1)(Z_o^2-1)} \tag{137}$$

where I_N^1 and I_N^N are the excitation coefficients for the end elements and Z_o is given by equations (107) and (108).

Taylor's Method (Reference 80): It is apparent from the preceding paragraph that a continuous Dolph antenna is not physically realizable due to the infinite discontinuity in the distribution at the ends of the aperture. Furthermore, a discrete Dolph array of very many elements may also be physically unrealizable because the excitation coefficients of the end elements will be very much higher than the coefficients of the intermediate elements. T. T. Taylor has suggested the use of a modified Dolph-Tchebyscheff pattern as the optimum in this situation. In the modification, the sidelobes are allowed to taper off at some arbitrary distance from the main beam.

Shaped Beam: Field Strength Pattern Specified in Magnitude and Phase

Woodward's Method (Reference 92): It is well known in antenna theory that the pattern of a uniform continuous array of half length $a(=\mathcal{L}/2)$ and aperture amplitude A is

$$S(\nu) = 2ka \cdot A \frac{\sin ka(\nu - \nu_o)}{ka(\nu - \nu_o)} \tag{138}$$

where $\nu_o = \cos \theta_o = k_1/k$ and θ_o is the position of the main beam from end-fire. $S(\nu)$ is shown in Figure III-15 with $\underline{a} = 2.5\lambda$. It is noticeable that the zeros are equally spaced except for those on either side of the main beam which occupy two "spaces." The width of one space is the reciprocal

of the aperture length in wavelengths, from which it follows that the beamwidth for a broadside uniform array at the first nulls is inversely proportional to the length of the aperture (B. W. = λ /2a). If we choose ν_o equal to an integral number of nominal beamwidths, that is, $\nu_o = n\lambda/2a$, then the inverse transform of equation (138) is

$$\left.\begin{aligned} g(x) &= Ae^{-jn\pi x/a} \qquad \text{for } -a \leq x \leq a \\ g(x) &= 0 \qquad\qquad\quad \text{for } a^2 > 1 \end{aligned}\right\} \tag{139}$$

in which A represents the uniform amplitude and the exponential represents the uniform progressive phase shift.

The Woodward method involves the expression of S as a finite sum of N + 1 component functions of the type (138):

$$S(\nu) = 2ka \sum_{n=-N/2}^{N/2} A_n \frac{\sin ka(\nu - n\lambda/2a)}{ka(\nu - n\lambda/2a)} \tag{140}$$

The summation in equation (140) may be regarded physically as the superposition of N + 1 uniform array patterns each with its characteristic direction given by $\nu_n = n\lambda/2a$. The relative spacing of the characteristic directions by integral multiples of $\lambda/2a$ (one "beamwidth") insures that the principal maximum of each component pattern coincides with the zero of all others (see Figure III-15). The pattern value at each characteristic direction is thus uniquely related to the corresponding A_n, and the A_n can be found by requiring that the total pattern have prescribed values at the characteristic directions. Thus, the aperture distribution can be written

$$\left.\begin{aligned} g(x) &= \sum_{n=-N/2}^{N/2} A_n e^{-jn\pi x/a} \qquad \text{for } x^2 \leq a^2 \\ g(x) &= 0 \qquad\qquad\qquad\qquad\quad \text{for } x^2 \geq a^2 \end{aligned}\right\} \tag{141}$$

where

$$A_n = \frac{1}{2ka} \left[S(\nu) \right]_{\nu = n\lambda/2a} \tag{142}$$

The design procedure is:

1) Determine the N + 1 values of $S(\nu)$ at $\nu = n\lambda/2a$ for $-1 \leq \nu \leq 1$.

2) Substitute the values found in step 1 into equation (142) to determine the A_n's (the factor 1/2 ka may be set equal to unity since the aperture distribution is a relative matter).

3) Substitute the A_n's into equation (141) to determine the aperture distribution. Notice that $S(\nu)$ in equation (140) may be complex, in which case A_n may also be complex, although we have tacitly assumed A_n to be real by referring to it as an amplitude.

We have pointed out previously that the synthesized pattern will coincide with the desired pattern at N + 1 points where $N/2 = 2a/\lambda$. In some situations, $S(\nu)$ will not be defined at one or more of the N + 1 points (see Figure III-16). In this case the designer can choose a value for $S(\nu)$ at the questionable points which makes the synthesized pattern approximate the desired pattern best. A trial and error process is used to determine the optimum value for $S(\nu)$ at the questionable points.

Fourier Transform Method: A Fourier series method has been described (page 52). The Fourier transform method is simply an extension of the discrete series summation to an integral for the continuous array.

The space factor for a continuous array is given by equation (97). If A(z) vanishes outside the aperture ($a^2 > 1$), then (97) can be written

$$S(\nu) = \int_{-\infty}^{\infty} A(z)\, e^{jkz(\nu - k_1/k)}\, dz \qquad (143)$$

The distribution function A(z) is the inverse transform of (143):

$$A(z) = \frac{1}{2\pi} \int_{-\infty}^{\infty} S(\nu) e^{-jkz(\nu - k_1/k)}\, d\nu \qquad (144)$$

The integral in equation (144) defines A(z) for <u>all</u> values of z; however, A(z) can be controlled only over the aperture ($-a \leq z \leq a$) and A(z) must be zero for $z^2 > a^2$. In other words, the major portion of A(z) must fall between z = -a and z = a for a good approximation to $S(\nu)$. In general, this situation is not the case. Thus, the designer should calculate the synthesized $S(\nu)$ produced by the portion of A(z) in the range $-a \leq z \leq a$ to determine whether the approximation is satisfactory.

R. C. Spencer discusses Fourier integral methods of pattern analysis and synthesis in two papers.[69, 70]

Shaped Beam: Power Pattern Specified, Field Strength Phase Arbitrary

Extension of Woodward's Method: Taylor[82] has extended Woodward's method so that any given single-valued continuous function can be approximated arbitrarily exactly rather than simply forcing the approximating function to coincide with the desired function at a set of points spaced by integers in the operating range. Further, the extension provides a method for approximating a real pattern $S_r(\omega)$ by $|S(\omega)|$, allowing the A_n

to become imaginary. It will be seen that this method parallels the circle diagram method of Taylor and Whinnery (page 55) and allows for the optimum phase.

The space factor is written as the product of a transcendental function, $Q_n(\omega)$, a polynomial, $P(\omega)$, and a constant:

$$\left| S(\omega) \right| = \frac{2ka}{\pi^N (\frac{N}{2}!)^2} \left| Q_N(\omega) \right| \left| P(\omega) \right| \tag{145}$$

where $\omega = \frac{2a}{\lambda}$. The transcendental function, $Q_N(\omega)$ is given by

$$Q_N(\omega) = \frac{(\frac{N}{2})^2}{(\frac{N}{2} + \omega)\,!\,(\frac{N}{2} - \omega)\,!} \tag{146}$$

or

$$Q_N(\omega) \approx e^{-\frac{2\omega^2}{N}} \quad \text{for N large} \tag{147}$$

It should be recognized that $Q_N(\omega)$ is defined continuously for all values of ω since the factorial is defined continuously in terms of the Γ-function. The method of synthesis consists in finding the polynomial $P(\omega)$, of degree not greater than N, such that the product $\left| Q_N(\omega) \right| \cdot \left| P(\omega) \right|$ approximates the desired pattern (here the constant factor has been set equal to unity for the sake of convenience). The number of the zeros of $P(\omega)$ may be less than, equal to, or greater than $4a/\lambda$ (the value prescribed in Woodward's original method). If $N/2 > 2a/\lambda$, it is possible to approximate any pattern or function arbitrarily exactly by concentrating these zeros in the operating region rather than by distributing them uniformly in the region $-N/2 \leq \omega \leq N/2$ which, for $N/2 > 2a/\lambda$, includes both real and imaginary space. This taking of zeros from imaginary space and concentrating them in real space is, of course, a supergain technique and is generally undesirable. To avoid supergaining, N should be chosen so that

$$\frac{N}{2} \leq 2a/\lambda \tag{148}$$

The real advantage of this method is that an optimum field phase can be found: the phase distribution in the field pattern which allows the aperture to be used most efficiently. This effect is accomplished by allowing the $P(\omega)$ to be complex and varying the positions of the zeros in the complex plane such that (145) is satisfied. A convenient method for finding $P(\omega)$ such that $\left| P(\omega) \right|$ approximates a given function is the potential analog method described by Taylor and Whinnery[79]. This method is similar to the method of placing zeros in the complex plane for the circle diagram method;

here, however, interest is in the profile on the real axis rather than on the unit circle. There are, of course, a great many methods for approximating a function by a polynomial, but there are no simple analytical methods for finding the best complex $P(\omega)$ which is required for the most efficient use of the aperture.

When $P(\omega)$ has been obtained, the calculation is completed by finding the A_n. These are given by:

$$A_n = \frac{1}{\pi^N \left(\frac{N}{2}!\right)^2} \left[Q_N(\omega) P(\omega) \right]_{\omega=n} \tag{149}$$

Finally, the aperture distribution, $g(x)$, may be calculated from equation (141).

This method, like the circle diagram method, is difficult to employ because of the trouble in finding the polynomial. The potential analyzer, however, simplifies the problem to a large extent and, in the case of shaped beams (versus directive beams), the use of this rather complicated technique may be warranted by the more efficient use of the available aperture length which it provides.

Geometrical Optics Method: Principle of Stationary Phase: An antenna with an aperture much larger than a wavelength and a phase distribution such that all of the energy in the aperture is radiated into real space (a nonsupergain antenna) can be analyzed by optical methods. In 1943, L. J. Chu[12] formulated design equations, based on optical considerations, which were used extensively to determine the shape of a cylindrical reflector and the primary feed pattern required to synthesize a shaped beam. A. S. Dunbar[19] extended this method to doubly-curved reflectors. More recently, Dunbar has taken a different approach to this problem, using the method of stationary phase, and has shown that the two results are equivalent.[20] Synthesis by this optical method requires the specification of the required power pattern, $P(\theta) = S(\theta)S^*(\theta)$, but does not allow for the optimum field phase. Nonetheless, Chu's method has been very successful with reflector-type antennas and is equally useful for linear arrays due to the simplicity of the mathematical manipulations involved.

The technique is to choose an arbitrary amplitude distribution, $A(x)$, usually a simple even function, and then apply the following design equations to determine the required phase along the aperture. The equations are:

$$\mu(x) = \cos \theta \tag{150}$$

and

$$\sin \theta P(\theta)\, d\theta = 2\pi f^2(\theta)\, A^2(x)\, dx \tag{151}$$

where $\mu(x) = \lambda/\lambda_g(x) = C/V(x)$; $\lambda_g(x)$ and $V(x)$ are the variable wavelength

and velocity respectively along the array; $P(\theta)$ is the power pattern for θ measured from endfire; $A(x)$ is the amplitude distribution; $f(\theta)$ is the element factor; and x is measured along the array from the center.

The wavelength, $\lambda_g(x)$, or velocity, $V(x)$, along the array can be controlled in a number of ways: by the use of ridge waveguide to feed the slots in the array or by curving the array from a straight datum line (the x-axis) along which $\lambda_g(x)$ or $V(x)$ is measured. This latter method is convenient for the design of linear arrays on curved surfaces.

3.4 PRACTICAL CONSIDERATIONS AND MEASUREMENTS

3.4.1 Effects of Manufacturing Tolerances

A finished array, although properly designed, may not meet design specifications due to inaccuracies in the mechanical construction. The designer has two alternatives in this situation: 1) he can over-design the array, or 2) he can insist on tighter shop tolerances. The first alternative leads to inefficient array design and the second results in high manufacturing costs. In order to make an intelligent compromise, the designer needs quantitative data on the effect of more stringent tolerance requirements on the probability of the antenna pattern meeting design specifications. This problem has been attacked for certain special cases (References 1, 42, and 60).

Bailin and Ehrlich describe a first-order statistical method for relating shop tolerances and pattern deterioration for a symmetrically excited broadside array for which there is no correlation among the radiations of the elements (that is, for which mutual coupling is negligible). As an example, a 24-element linear shunt slot array excited according to the Dolph-Tchebyscheff distribution was analyzed. The three actual array dimensions (slot length, ℓ; interelement spacing, d; and displacement from the centerline of the broad face, x) which affect the pattern were assumed to have values clustered about the design value (according to a normal distribution) for a large number of similar arrays. The standard deviation for the normal distribution is an indication of quality of workmanship (see Figure III-17A).

The results of similar calculations by O'Neill and Bailin are presented in Figure III-18 for a 12-element Tchebyscheff array and a 12-element cosine array. If the quality of workmanship corresponds to a standard deviation of 0.001 inch, the results indicate that, out of 100 arrays, only 16 will have sidelobes above the corresponding dashed curve.

It is general shop practice to reject work which does not fall within a specified region of precision. Thus, the distribution of actual dimensions will be limited by tolerance specifications and the normal distribution curve will be replaced by a truncated normal distribution as shown in Figure III-17B. This distribution represents a more realistic approach to the problem. Figure III-19 illustrates how the positions of the reference curves (the curves above which 16 percent of the arrays will have sidelobes) at certain points (θ) in the pattern vary with the prescribed tolerance. The σ_i represents the

standard deviation for the distribution and $a_i\sigma_i$ is the point at which the distribution is truncated.

Although the data presented here hold only for special arrays, they do give the designer a feeling for the problem and lead the way for further investigations.

3.4.2 Long Arrays

Beam Position for Nonresonant Arrays

Watson suggests that the interelement spacing for a nonresonant array be $4/9\lambda_g$ or $5/9\lambda_g$ for satisfactory input impedance and matched condition in the guide; another criterion is given by equation (61).

Still another criterion, which has proved experimentally sound, is to space the elements so that the main beam is at least one beamwidth off the broadside position. The input VSWR for this condition is of the order of 1.1 (see Figure III-2, page 153). Thus, if the array is long (that is, the beam is narrow), it is possible to have the main beam close to broadside without introducing serious reflections in the guide.

Lumped Array

For very long arrays (hundreds of elements), the radiators may be grouped together in batches of equal conductance (10 or 20 per group) in order to simplify the manufacturing process. The effect of lumping the elements will be small for long arrays since the slot conductances do not vary rapidly along the array.

Bending

Highly directive arrays are necessarily quite long; for example, a 400-element X-band array having a beamwidth of 1/4 degree is approximately 30 feet long. The designer, therefore, is faced with the problem of having to support the array in such a manner that it will not be distorted (thereby changing the relative displacements of the elements and distorting the pattern) when operating under various external loads or when supporting its own weight.

An elementary analysis of the effect of phase variations due to bending on the pattern of a uniform array has been made for three conditions:[2] 1) array rigidly supported at its ends, 2) array rigidly supported at 1/4 the array length from the ends, and 3) array rigidly supported at the ends and center (see Figure III-20). The array is assumed to execute simple harmonic motion under variable loads. However, for the purposes of this analysis, it is considered stationary at its maximum deflection, since the frequency of vibration is much less than the electrical frequency and since the array will be at or near its maximum deflection position for a relatively large portion of the period of vibration.

Figure III-21 illustrates the pattern distortion for a continuous uniform array for condition (1). A_θ is the amplitude of the vibration. Figure III-22 illustrates condition (2) and Figure III-23, condition (3).

Pulse Length

The resolving power of a radar depends in part on the transmitted pulse length; the shorter the pulse, the greater the range resolution. For a long, end-fed linear slot array, a pulse front can be considered as arriving at the feed end at t = 0, traveling down the guide, and arriving at the load end at $t = T_t$, the transit time. If the duration of the pulse, T_p, is less than T_t, the array is never completely illuminated, and consequently, the aperture of the antenna is not being utilized efficiently. This analysis is rather naive since 1) the pulse is distorted in the guide and the front is not defined, and 2) the individual slots have a transient build-up and decay time.

Bailin[2] gives an elementary solution to the pulse problem based on the assumptions of a traveling pulse and a frequency invariant slot equivalent circuit. Both assumptions are rather poor; nonetheless, the solution offers a picture of the manner in which an antenna pattern builds up (and decays) as the elements are progressively illuminated by the traveling pulse. Figure III-24 is a plot of the pattern build-up as a function of time. Here t_o is the time for the pulse front to travel between two adjacent slots at the phase velocity for the dominant frequency component of the pulse. Thus, it would take a pulse at least $2T_t(20\ t_o)$ long to approximate the steady-state pattern for an instant. Bailin suggests $3T_t$ as the minimum practical pulse length.

Manufacturing Tolerances

A somewhat questionable extrapolation of the data mentioned in the discussion of Effects of Manufacturing Tolerances, page 64, seems to indicate that tolerances become less critical for longer arrays. This result may be justified as follows: 1) the random errors in the slot parameters, which cause random radiation errors, are likely to average to a small value for very long arrays; and 2) since conductances, and slot parameters, vary slowly along the array for a long array, small random deviations from the slot design values are not likely to be critical.

3.4.3 Terminations

Nonresonant Array

Matched loads are usually used to terminate a nonresonant array. Watson, Fry and Goward, however, suggest the use of a group of resonantly spaced slots at the end of the array as a termination which would not waste power. These slots are separated from the main array by a length of waveguide of such length that the phase of the resonant section departs as little as possible from that which would be obtained were it nonresonant. This scheme is not very useful since the designer has little control over the

radiation from the load slots. They also suggest other arrangements, such as terminating the nonresonant array by a shorting plate, with or without making allowance for the mismatch it causes near the end. The latter technique assumes very low power at the load and can cause serious side-lobe deterioration in arrays designed for -20 db or lower due to the large mismatch at the termination.

Resonant Array

In a resonant shunt slot array, a short-circuit termination is usually placed $\lambda_g/4$ from the last slot; in a series slot array, a short circuit is usually placed $\lambda_g/2$ from the last slot. It is possible, however, in order to broadband the array, to place the shorting plate any odd multiple of $\lambda_g/4$ from the last slot in the first instance and any multiple of $\lambda_g/2$ in the second. The optimum short-to-last-slot displacement can be determined by a trial and error process. The extended short-circuit termination acts as a stub which, for the series case, becomes inductive as the frequency exceeds resonance; the parallel resonant circuit for the series slot becomes capacitive as the frequency exceeds resonance. Thus, a compensating action takes place which helps to improve the impedance bandwidth of the array. The length ($n\lambda_g/2$) of the stub determines the rate at which the stub reactance changes with frequency. Stub lengths slightly off $n\lambda_g/2$ or $m\lambda_g/4$ (m odd) may be used to match out some discontinuities in the guide, thereby improving the input impedance at the design frequency.

3.4.4 Feed Systems: Linear and Two-dimensional Arrays

Waveguide linear slot arrays, for the most part, are fed from one end as has been tacitly assumed throughout this report. Some investigators,[45] however, have suggested more elaborate feeding arrangements which serve to extend the impedance bandwidth of resonant arrays. The bandwidth of a resonant array decreases as its length increases. Thus, if a long array is divided into a number of equal smaller collinear arrays (sections), each fed separately, the sectioned array would have the bandwidth of one of its sections. A simple example of the sectioned array is a resonant array fed at its center. In this case, the two sections, one on each side of the feed, are practically independent arrays internally; the power flows in opposite directions in the respective sections, and each section is terminated by its own shorting plate. It should be apparent that the individual sections must be resonant arrays; if the sections were of the traveling wave type, the array would provide a split beam (the amount of split varying with frequency). The feed-array junction may be a simple tee, or a guide-to-guide coupling through a slot as described by Watson[87, 88]. The type of coupling, series or shunt, determines the relative orientation of slots in the sections: in the series case, the coupling slot or tee junction looks like a series generator in a transmission line and the fields on opposite sides of the generator are in opposed phase; in the shunt case, the fields on opposite sides of the equivalent generator are in phase.

For arrays of many sections, a branching or corporate structure[81] feeding system can be used. This arrangement may consist of a single waveguide input which leads directly to a tee or two-way junction, each arm of this junction leads to another junction, and so forth, the end result being 2^m outputs, where m is a positive integer. At each junction, the power may divide equally between the two output arms; hence, the power level at each of the final outputs would be equal. Since the path length from the original input to each of the outputs can be made the same, uniformity of phase can be preserved over a considerable range of operating frequencies. Figure III-25A illustrates a branching feed pictorially.

Actually, a corporate structure feeding system need have neither equal partition of power at each junction, nor be restricted to two-way junctions. For a given number of outputs, for example, it is possible to have a finite number of different power level combinations at the outputs. Figure III-25B shows the five possible arrangements for a six-output system which provide five different power level combinations. The path lengths can be made equal with little difficulty in all five arrangements. It is also possible to adjust the phases of the outputs by varying the path lengths slightly. If the path differences are small (less than $\lambda_g/2$), the broadband properties of the feed system will not be greatly impaired.

An alternative to the branching structure feed is provided by a series system. In this scheme, the power is fed to a linear slot array, resonant or nonresonant, in which each slot couples to an auxiliary waveguide. The slot couplings can be adjusted so that the outputs of the auxiliary guides have any desired relative levels. (Watson gives adequate design data for slot-coupled guides.) This arrangement offers more flexibility in the power outputs, but does not possess the broadband characteristic of the branching structure.

A limiting case of the sectioned array is obtained when each section contains only one radiator; for example, a horn, an open-ended waveguide, or a slot in the end of a waveguide. Such an array has the advantages that 1) for an equal path length branching feed, the array is broadband and the beam does not change direction with frequency, and 2) in certain cases, mutual coupling between adjacent radiators can be reduced. (See discussion of mutual coupling, section 3.4.7.)

Either the branching structure or the series system can be used to feed an array of arrays (a two-dimensional array). The series system is very convenient in this application. The linear arrays are cut in the auxiliary guides; all the linear arrays can be made identical, and the relative excitations of the individual linear arrays can be adjusted by the slot coupling from the main feed guide. (See Figure III-26.)

3.4.5 Suppression of Second-Order Beams and Cross Polarization

Second-Order Beams

If the element spacing in a linear array of isotropic radiators is greater than a wavelength, the radiation pattern will exhibit more than one main beam. Generally more than one beam is undesirable and beams other than the necessary or required beam are sometimes called second-order beams.

Another type of second-order beam is encountered in the design of longitudinal-displaced slot arrays. One usually designs such arrays on the assumption that all the slots are on the same straight line. This assumption, of course, is not quite correct since the array is, in fact, a two-dimensional array due to the staggering of the slots about the waveguide centerline. It is not surprising then that the three-dimensional pattern is not a figure of revolution about the array axis as with the linear array, but instead exhibits spurious lobes in planes containing the array axis (except for that plane which is normal to the plane containing the slots). The configuration of these second-order beams can be visualized by referring to the three-dimensional sketch in Figure III-27A. The intensity of the second-order beams is a function of the slot offset and, for practical arrays of medium length, may be 10 percent or more of the main beam field strength. Spurious lobes of this magnitude cannot be neglected in most applications.

Gruenberg[27] has made a thorough study of the second-order beam problem in longitudinal shunt slot arrays. In his paper, he analyzes the patterns of these arrays and also investigates methods of suppressing the second-order beams. One proposal involves the use of a special type of waveguide which allows the slots to be positioned in line as shown in Figure III-27B. This method, although successful, is rather uneconomical. A simpler technique is to fit the staggered slot array with a parallel plate section and flared horn as shown in Figure III-27C. If the width of the parallel plate region is less than a half wavelength, only the two lowest modes will be propagated. In this manner asymmetries in the field, caused by staggering of slots about the centerline, will not appear at the throat of the horn system. Thus, second-order beams resulting from slot offset will be effectively suppressed provided that the length of the parallel-plate region is of the order of a wavelength. The flared portion of the horn serves to match the parallel plate region to space and can also be used to increase directivity in the transverse plane.

The presence of the horn will affect the impedance characteristics[28] of the array and will tend to narrow the bandwidth due to reflections from the throat and the horn aperture. The use of horn systems with an exponential taper has been suggested as a solution.

Cross Polarization

The electric vectors across inclined slots are rotated with respect to the plane of principal polarization in such a manner that a quadrature component of polarization is present in the array pattern. This cross-polarized component can be detected by measuring a pattern with the

transmitter polarization rotated 90 degrees from the direction of principal polarization. The cross-polarized pattern for a linear array generally consists of two or more lobes straddling the position of the main beam. The intensity of the cross-polarized lobes depends on the magnitude of slot inclination and the position of these lobes is a function of slot spacing.

The device employed to suppress cross polarization is similar to that used for minimizing second-order beams, the parallel plate horn. In this case, the width of the parallel plate region must be small enough to suppress the propagation of the cross-polarized wave, that is, less than a half wavelength.

3.4.6 Array Parameters

The measurement of antenna parameters in general is adequately described elsewhere[64h]; there are, however, certain effects peculiar to the slot array which deserve special mention.

Pattern Measurements

Silver describes the manner in which the antenna pattern may be measured. Since a linear array has a wide beam in the plane normal to its axis and since the array is generally horizontal during a pattern measurement, care should be taken that the measured pattern is not distorted by spurious radiation or reflections at scattered elevation angles. If displaced slots are used in the array, patterns should be measured in the $\phi = 45^{\circ}$ planes to detect the second-order beams; and, if inclined slots are used, the polarization of the transmitting antenna should be rotated 90 degrees and a pattern measured to determine the amount of cross polarization present.

Gain Measurement and Calculation

The directive gain of a transmitting antenna referred to an ideal isotropic radiator is given by

$$\text{directive gain} = \frac{\text{peak power radiated/unit solid angle}}{\text{total power radiated}/4\pi} \tag{152}$$

Silver describes experimental methods for measuring this quantity.

The gain of a linear nonsupergain array of isotropic radiators with respect to the corresponding uniform array can be calculated from the following relations.

$$G = \frac{\left(\sum_{k=0}^{N-1} I_{k+1}\right)^2}{N\left(\sum_{k=0}^{N-1} I_{k+1}\right)^2} \qquad \text{for 2N elements} \tag{153}$$

and

$$G = \frac{\left(I_o + 2\sum_{k=1}^{N} I_k\right)^2}{2N+1\left(I_o^2 + 2\sum_{k=1}^{N} I_k^2\right)} \quad \text{for } 2N+1 \text{ elements} \tag{154}$$

where I_k is the relative excitation of the k^{th} element. The gain of the array, of course, is modified by the gain of the individual elements. If the array is short, it is difficult to take the element factor into account; if, however, the array is highly directive and broadside, the gain of the array can be shown to be proportional to the gain of the array with isotropic radiators.

The gain of an array of arrays in the xy-plane can be shown to be proportional to the product of the gain of an array in the x-direction and the gain of an array in the y-direction. It is assumed here that there is no mutual interaction among arrays.

Efficiency

The radiation efficiency of an antenna is the ratio of radiated power to input power. In a slot array, the power losses are due to the wall currents and, in the case of nonresonant arrays, power lost in the load.

The relative power into the load can be measured by the following scheme. Insert a slotted line between the array and the load (denoted by L) and feed the array through another slotted line (denoted by I). Measure the VSWR's in both lines (ρ_I and ρ_L) and the maximum and minimum voltages in both lines (E_{max_I}, E_{min_I} and E_{max_L}, E_{min_L}). Then

$$10 \log \frac{P_{net_L}}{P_{net_I}} = 20 \log \frac{E_{max_L}}{E_{max_I}} - 10 \log \frac{\rho_L}{\rho_I} \tag{155}$$

or

net power ratio (db) = maximum voltage ratio (db) - 1/2 VSWR ratio (db),

where

$$P_{net} = P_{incident} - P_{reflected} = K \cdot (E_{in}^2 - E_r^2) = K \cdot E_{max} E_{min} \tag{156}$$

However, there is no way to measure the wall current i^2R loss since this loss cannot be separated from the power radiated by the slots. It should be noted that the i^2R loss for the slotted guide is not the same as the loss for the guide before the slots are cut, since the slots have an effect on the wall currents.

Various schemes for measuring radiation efficiency[58] have been proposed but all are limited in their application and are rather inaccurate. The radiation efficiency is increased, however, when i^2R loss is decreased by increasing the wall conductance and, for nonresonant arrays, when the power into the load is decreased.

Another efficiency which can be defined for an antenna is the aperture efficiency. The array of equally spaced elements which affords the maximum gain is the uniform broadside array ($G_o = \frac{2Nd}{\lambda}$, where N = number of elements and d = interelement spacing). If the array has a gain less than G_o, the aperture is not being used as efficiently as it might be to provide gain. Thus, the ratio of the array gain and G_o is a measure of aperture efficiency. In practice, however, gain may be sacrificed to shape the beam or reduce sidelobes.

Input Impedance and VSWR

The input impedance of an array can be measured by slotted line techniques (section 2.2.2). The voltage minimum position is measured with a shorting plate terminating the slotted line and then the VSWR and minimum position are measured with the array terminating the slotted line.[44] Often design specifications require only the VSWR to be less than a certain value.

Power-Handling Capacity

The power-handling capacity of a waveguide slot array is generally limited by arcing in the slot and, for a nonresonant array, by power breakdown in the terminating load.

The "theoretical" power-handling capacity of a slot can be calculated as follows: The radiation admittance, Y_s, of a slot radiating on one side of an infinite ground plane is related to the radiation impedance, Z_w, of a wire dipole by Babinet's Principle[7] by

$$Y_s = G_s + jB_s = \frac{2Z_w}{\mu/\epsilon} = \frac{2Z_w}{(120\pi)^2} \tag{157}$$

The power radiated into half space is

$$P = \frac{V_m^2 G_s}{2} = \frac{V_m^2 R_w}{(120\pi)^2} \tag{158}$$

where V_m is the maximum voltage across the slot. If the field across the slot is uniform,

$$V_m = d \cdot E_m \tag{159}$$

where d is the slot width and E_m the peak field intensity in the slot. Assuming a breakdown strength of E_m = 30,000 volts/cm = 76,200 volts/inch and R = 73.2 ohms (References 32 and 48), the power-handling capacity of the slot is

$$P = \frac{(76,200)^2 \times 73.2\, d^2}{(120\,\pi)^2} = 2.98\, d^2 \text{ megawatts} \tag{160}$$

Thus, the slot width determines power breakdown.

The value of P given above probably cannot be obtained in practice. However, rounding and filleting sharp edges and corners will increase the power-handling capacity.

If all of space were replaced by a dielectric, Y_s would increase and P would also increase. On the other hand, if the slot is covered by a thin sheet of dielectric or if the slot is filled with dielectric, the breakdown power will decrease due to the leakage paths provided by the surface of the dielectric. The latter situation is the one that occurs in practice. Thus, a dielectric cover or load will generally decrease the power-handling capacity of a slot.

Bandwidth

The bandwidth of a slot array can be defined for one of a number of array parameters. For example, the pattern bandwidth is the region of frequencies for which the radiation pattern meets specifications. Methods of increasing bandwidth have been discussed.

3.4.7 Mutual Coupling in Linear and Planar Arrays

Throughout this report various aspects of the mutual coupling problem have been mentioned. Mutual coupling means the correlation between the excitation of a slot and the excitations of its neighbors due to fields in the space external to the guide. The following discussion purposes to integrate and expand the problem.

Empirical Techniques

In linear arrays employing essentially collinear elements (for example, longitudinally displaced or series inclined slots), it is general practice to neglect mutual coupling, or to assume the slot conductance for an element in the array is the same as the single slot conductance. And, in linear arrays employing essentially parallel side-by-side elements, (edge or transverse series slots), it is the general practice for long arrays to assume the slot conductance for an element in the array is equal to the average conductance of a large number of similar slots (the incremental conductance). To

reduce the mutual coupling among essentially parallel side-by-side slots, baffles (horns or auxiliary guides) are sometimes used to isolate the slots (see discussion of experimental and design data, section 2.3). In these arrangements mutual coupling is also neglected; that is, the conductance of the slot and baffle as an array element is assumed to be the same as the conductance of a single slot and baffle.

In planar arrays of similar slots, the slots in a row parallel to one dimension will all be essentially parallel side-by-side while slots in a row parallel to the other dimension will all be essentially collinear (assuming a rectangular array). The general practice in designing arrays of arrays using slots (actually there are few successful ones) is to construct a number of linear arrays which correspond to the rows for which the mutual coupling is strongest and then to array these linear arrays to form the two-dimensional array. The reason for this procedure is that schemes have been devised for designing linear arrays in the presence of mutual coupling and, if these linear arrays can be made to work, mutual coupling is neglected in constructing the array of arrays. This approach does not take into account the effect of echelon (or staggered parallel) slots. Baffle arrangements are sometimes erected between adjacent arrays to decrease the coupling. These baffles may take the form of parallel plate horns or of quarter-wave troughs in the ground plane which act as chokes.

Another technique, which is applicable to either linear or two-dimensional arrays with slightly tapered aperture distributions, is based on an argument similar to that for the use of incremental conductance. If the array is large compared with the wavelength (in both dimensions for a planar array), the interelement spacing is approximately $\lambda_g/2$, and the spacing between lumped elements on the equivalent transmission is approximately $\lambda_g/2$; then the array can be designed using only single slot conductances. The justification for this maneuver is that most of the elements (those near the center) will have the same environment and will therefore have their input impedances changed by the same factor. The few elements near the edges do not contribute much to the radiation pattern under the present assumptions. Since the radiation pattern is determined by the relative values of element excitation, the pattern will be a fairly good approximation to the required pattern. However, the array will be mismatched at its input. This mismatch can be cancelled out if the array is to be used for a narrow band of frequencies.

Although some of the schemes for coping with the mutual coupling problem are reasonably satisfactory in some instances, they are by no means exact or universal. For example, the reason for assuming negligible mutual coupling among collinear slots is that the far field pattern for an infinitely thin slot in an infinite ground plane has a zero in the collinear direction. In a practical array, however, adjacent slots are in the near field, the slot has a finite width, and ground plane is not infinite. Furthermore, the slots are not collinear; the longitudinal-displaced slots are staggered about the waveguide centerline and the inclined-series slots on the broad face are inclined to the centerline. However, an experimental investigation[22] has shown that neglecting mutual coupling in linear longitudinal shunt slot arrays is a valid

assumption in most cases. For an array of slots in which the conductances are less than 0.1, the ratio of the voltage across a slot in the presence of mutual coupling, V_s, to the voltage for no mutual coupling, V_o, is

$$\left| \frac{V_s}{V_o} \right| > 0.97 \tag{161}$$

when only one neighbor, $\lambda_g/2$ away, is taken into account, and

$$\left| \frac{V_s}{V_o} \right| > 0.96 \tag{162}$$

for both adjacent neighbors. However, for slot conductances of the order of 1.0, considering one neighbor,

$$\left| \frac{V_s}{V_o} \right| \approx 0.92 \tag{163}$$

In addition to the amplitude variations indicated, the mutual coupling produces phase variations which, in this case, are small. The above data are for slots in a waveguide without the benefit of an auxiliary ground plane. Because the slot spacing is approximately $\lambda_g/2$, the data hold for arrays near broadside only. Since, for reasonably large arrays, the slot conductances are generally less than 0.1 and inaccuracies in manufacture are of the same order as the effects of mutual coupling, neglecting mutual coupling in these arrays is probably a valid assumption. On the other hand, for arrays of very few slots in which each slot couples a large portion of the incident power, the mutual effects will probably distort the radiation pattern and corrections should be made for coupling by near neighbors. If the mutual coupling is not too serious, it may be possible to over-design the array to allow for sidelobe and beamwidth deterioration.

It should be emphasized here that most of the schemes for handling mutual coupling are applicable only for aperture distributions close to uniform and beam positions near broadside. For shaped beam antennas (which are usually near endfire), the possibility of using trapped wave antennas (corrugated surface, dielectric, and traveling wave slot antennas) should be investigated.

An Analysis of the Problem

In light of the difficulties encountered in designing waveguide-fed slot arrays in the presence of mutual coupling, it is interesting to note that corresponding dipole arrays can and have been designed in a straightforward manner. (See References 9, 35, and 38.) Examination of the differences between an array of dipoles fed from a transmission line and an array of slots coupled to a waveguide may resolve this apparent paradox.

In circuit theory, the mutual impedance of two coupled circuits is defined as the negative of the ratio of the emf V_{21} induced in circuit 2 by a current I_1 flowing in circuit 1 with circuit 2 open. This concept is essentially what is meant by the mutual impedance of two coupled antennas. The self-impedance Z_{11} of an antenna is the impedance seen at its terminals when no other antennas or reflecting surfaces are in the neighborhood. The impedance relations for an array of n-driven elements are

$$\left.\begin{aligned} V_1 &= I_1 Z_{11} + I_2 Z_{12} + I_3 Z_{13} + \ldots + I_n Z_{1n} \\ V_2 &= I_1 Z_{21} + I_2 Z_{22} + I_3 Z_{23} + \ldots + I_n Z_{2n} \\ V_3 &= I_1 Z_{31} + I_2 Z_{32} + I_3 Z_{33} + \ldots + I_n Z_{3n} \\ &\cdots\cdots\cdots\cdots \\ V_n &= I_1 Z_{n1} + I_2 Z_{n2} + I_3 Z_{n3} + \ldots + I_n Z_{nn} \end{aligned}\right\} \qquad (164)$$

where

V_n = terminal voltage of the n^{th} element

I_n = terminal current of the n^{th} element

Z_{1n} = mutual impedance between element 1 and the n^{th} element

Z_{nn} = self-impedance of the n^{th} element.

The driving point or terminal impedance of one of the elements, say element 1, is then

$$Z_1 = \frac{V_1}{I_1} = Z_{11} + \frac{I_2}{I_1} Z_{12} + \frac{I_3}{I_1} Z_{13} + \ldots + \frac{I_n}{I_1} Z_{1n} \qquad (165)$$

The number and spacing of the elements and their excitation currents are determined by the required pattern. If the elements are to be resonant, for example, their dimensions and self-impedances are determined. Theoretical equations and curves have been derived for the mutual impedances of the various types of dipole mutual coupling (collinear, parallel side-by-side and echelon) as a function of spacing. Thus, the driving point impedance, Z_n, for any element can be evaluated. If the terminals of the elements are now coupled to the feed transmission line through a transformer, the voltage across Z_n can be adjusted (independently of Z_n) to give the required I_n. Thus, the design procedure for the dipole array, though tedious for n large is not difficult.

For an array of slots fed directly from a waveguide, the problem is different. For the sake of the analogy, the self-impedance of the slot is said to be the value given by Babinet's Principle for the center-fed slot in an infinite plane (see page 4). The network which couples the slot to the guide is determined by the orientation of the slot in the guide. However, unlike the case of the dipole array, changing the value of the coupling network (or transformer) also changes the value of self-impedance and mutual impedance. The resonant length of a slot depends on its position in the guide, its impedance and radiation characteristics depend on the shape of the ground plane it sees, and the mutual impedance at a slot depends on its orientation with respect to its neighbors. In other words, the driving point impedance and the transformer coupling are not independent values. It is true that a waveguide-fed slot array might be designed and built using the single slot impedances (self-impedances), and then empirical corrections could be made. A probe might be used to measure the amplitude and phase distribution in the aperture and then the orientation and length of successive slots could be corrected. A correction in one slot, however, will change the excitation of most of the other slots, not only because of the mutual coupling external to the guide but also due to coupling within the guide. Unfortunately, as the process continues from slot to slot, there is no guarantee that it will be convergent. Still this technique might be feasible for arrays of less than five elements, although anyone who has tried it for longer arrays will attest to its futility.

The conclusion that one must reach is that an array of slots fed directly from a feed waveguide cannot be designed analytically if mutual coupling is present. This result is based on the uncertain or slow convergence of the iterative synthesis process and the lack of a solution for the internal-external coupling problem.

The above argument is based on a paper by Ehrlich and Curtis.[23] The solution which they suggest is the use of a waveguide and slot arrangement which will result in an equivalent circuit similar to that for the dipole array. The proposed array (which can be one- or two-dimensional) must have the following characteristics: 1) the slots terminate an equivalent two-wire line, 2) the transformer between the slot driving point impedance and the line is known, and 3) adjustment of the slot internal coupling does not alter the external array geometry. Such an array might consist of stub arms (auxiliary waveguides), series or shunt coupled by a slot to a main feed guide. The stubs are approximately one wavelength long and capped with an end plate containing a resonant slot. Each stub is equipped with a matching iris so that the coupling slot sees a match, and data for a slot feeding a matched guide can be used. This two-dimensional shunt-stub arm array is shown in Figure III-28.

Ehrlich and Curtis also present experimental data in their paper for mutual admittance between parallel side-by-side and echelon coupled slots. The data show that Babinet's Principle can be used to transform mutual impedance data for dipoles to equivalent data for slots. Thus, the design of the proposed slot array would be no more difficult than the design

of a similar dipole array. A comparison of the slot coupling data with the theoretical coupling for dipoles is presented in Figures III-29 through III-32. The discrepancies of the phase curves are attributed to the fact that the dipole data are for a half-wave dipole and the measured slots were resonant (slightly different than a half-wavelength long).

3.4.8 Some Constructed Arrays

The excitation coefficients of a 17-element linear array which would produce a power pattern proportional to $\csc^2 \theta \cos^{1/2} \theta$ from 3 degrees to 48 degrees were determined by a Fourier series method.[74] The voltage pattern was assumed real and symmetrical about the normal to the array, and therefore, the excitation coefficients were real and symmetrical about the center of the array. The array was designed for resonant spacing and used resonant longitudinal shunt slots. The measured input VSWR at the design frequency (9910 mc/s) was 1.0 (the design value) and the radiation pattern at the design frequency is shown in Figure III-33. There is less than 3-db deviation from the theoretical curve from 20 degrees to 55 degrees on both sides of the normal to the array. Machining tolerances are responsible in part for the departure of the radiation patterns from the theoretical curve because of the large (1870:1) range of radiated powers required from the elements.

The excitation coefficients of a 15-element linear array were determined by use of the Potential Analog Computer.[79] This array was designed to have an asymmetrical radiation pattern which was to follow the curve $\csc^2 \theta \cot^{1/2} \theta$ from 6 degrees to 60 degrees. The array used nonresonant longitudinal shunt slots with resonant spacing. The radiation pattern (Figure III-34) indicates a variation of less than 3 db from 1.5 degrees to 61 degrees. The sidelobes were found to be below 21 db and the measured input VSWR was 1.0 (the design value).

A 24-element linear nonresonant array of longitudinal shunt slots with a 22-inch aperture was designed for a -30 db sidelobe level and a beamwidth of 3.67 degrees. The design frequency was 9375 mc/s, at which frequency the beam position was chosen to be 2 degrees from the normal and tilted away from the input.

Tests of the linear array (shown in Figure III-35) were very satisfactory. The sidelobe level measured in a plane through the axis of the array and perpendicular to the waveguide face containing the slots is -28 db at the design frequency, and is lower than -26 db over the 15-percent band included between 8500 and 10,000 mc/s (Figure III-36). Sidelobes of -19 to -22 db exist outside the principal planes of the array. These lobes were found at ± 45 degrees in planes passing through the axis of the array and tilted approximately ± 30 degrees from broadside. These lobes are caused by the slot staggering about the centerline of the broad face of the waveguide (see discussion of second-order beams, section 3.4.5). Restrictive vanes placed on the guide reduced these lobes with little effect on the rest of the pattern. However, if the array is to be used as a primary feed for a reflector, the vanes

are not necessary because the gain of the reflector reduces the magnitude of the off-axis lobes to below the level of the rest of the sidelobes. The beamwidth of the array varies from 4.5 degrees to 3.4 degrees over the band because the antenna aperture, measured in wavelengths, increases with frequency. The measured beamwidth at the design frequency was 3.70 degrees. The pattern of the array at the design frequency is shown in Figure III-36. The beam position of the array as a function of frequency is given by equation (60). The measured input VSWR is plotted in Figure III-37 on which the cross gives the calculated VSWR at the design frequency. The low values of VSWR extend well beyond the limits of the graph. The efficiency of the array is greater than 70 percent from 9210 to 9730 mc/s and is nearly 80 percent at the design frequency. Most of this lost power is dissipated in the matched termination. Since fulfillment of theoretical pattern requirements of this array was more important than efficiency, the conductance of the last slot was chosen to be 0.05. If the array had been designed with a conductance of 0.10 for the last slot, the conductances of all the succeeding slots would have been increased and the antenna would have had an efficiency close to 90 percent with only a slight effect upon the pattern.

A 24-element longitudinal shunt slot linear array designed for a sidelobe level of -40 db was designed and built. The measured sidelobe level of the array was below -34 db at 9375 mc/s (the design frequency). The observed beamwidth was 4.3 degrees as compared with the theoretical value of 4.07. The efficiency of this array was somewhat higher than that of the previous 24-element array because the array was designed with higher slot conductances.

The results of measurements on three 144-element longitudinal shunt slot linear arrays designed for -40 db sidelobe level show that the beamwidth is the same as the design value (0.71 degree). The maximum sidelobe level is -29 db exclusive of the secondary lobes produced by the slot offset from the waveguide centerline. Restrictive horns caused a reduction of the secondary beams and a rise in some of the other sidelobes to about -28 db.

A 66-element nonresonant edge slot array with a flared parallel plate horn was designed using incremental conductances. The excitation coefficients were calculated by Taylor's method[80] for narrow beam and low sidelobe patterns. A Dolph-Tchebyscheff distribution was not used because it was felt that the strong excitation at the ends of the array would lead to spurious sidelobes due to diffraction effects at the end of the horn. The design beamwidth was 1.6 degrees and the design sidelobe level -25 db. The main beam position was 1.5 degrees. The measured pattern showed a sidelobe level of -22 db and a beamwidth of approximately 1.6 degrees.

A 204-element nonresonant edge slot array at X-band was designed with Taylor's narrow beam and low sidelobe level distribution. The calculation of the excitation coefficients was made for n = 5 and proved to be a relatively simple calculation. The value of n was chosen to be 5 because it

was found that larger values would change the excitation coefficients by amounts so small that they would exceed the manufacturing tolerances. The design beamwidth was 0.4 degree and the design sidelobe level was -25 db. The main beam was 2 degrees off broadside. Measured patterns showed a sidelobe level of -24 db and beamwidth of 0.4 degree. The pattern was very close to the calculated pattern. Figure III-38 is a pattern of a 30-element test array designed with the same distribution as the 204-element array. The slot conductances were determined by the incremental conductance method. One of the major difficulties encountered was the matter of supporting the array since it was some 16 feet long.

A 64-element, 3000-mc sectioned array is described in a French journal.[45] Edge slots were used and their conductances measured by an incremental conductance technique. The aim was to build a wide band broadside array to feed a cylindrical reflector. A two- and a four-section array were built. The sections were fed by a corporate structure feed system.

A linear array of series slots in the broad face has been built with a horn for suppression of cross polarization and increased directivity in the transverse plane[37]. A Dolph distribution was employed to obtain a design sidelobe level of -32 db. The measured pattern indicated a sidelobe level of about -31 db. The array was centerfed by a resonant slot-coupled series-T junction. The slots were measured at X-band and the dimensions scaled to L-band for the array shown in Figure III-39. (Several of the slots in the picture are covered by masking tape.)

A 16-element linear array of inclined dumbbell slots in the broad face of a rectangular outer, circular inner conductor TEM line[77] is shown in Figure III-40. The array was designed with a -30 db Tchebyscheff distribution, and the beam position was chosen to be 10 degrees off broadside at the design frequency of 3000 mc. The measured input VSWR at 3000 mc was 1.37 and the measured sidelobe level -22 db. The sidelobe error is attributed to the effects of machining tolerances and the possibility of insufficiently accurate slot data.

An array of 13 transverse slots on a circular cylinder of finite length[90] is shown in Figure III-41. Each slot is fed by a separate rectangular X-band waveguide. The 13 guides are slot coupled to a main feed guide in the shape of a circular arc. The slots are cut in the narrow face of the guide and are dumbbell loaded. Since the slots as shown will not radiate, a metal rod was inserted in the vicinity of the slots to excite them. The cylinder is 12 wavelengths in circumference and 4 feet long. A comparison of measured and calculated patterns is shown in Figure III-42. The poor sidelobe correlation is due to the extreme sensitivity of the rod excited slots to mechanical deformation, and to the finite cylinder length to a lesser degree.

A two-dimensional array of series inclined slots designed by L. A. Kurtz is pictured in Figure III-26. Mutual coupling effects were purposely neglected in the design. Each linear array is fed by a series inclined slot in the traveling wave feed guide. The linear arrays as well as the feed array

were designed to give a uniform distribution. The measured E-plane and H-plane patterns indicate excellent correlation with the sin u/u pattern. The pattern in the direction of strongest mutual coupling suffered from some deterioration in the remote sidelobes although the maximum (first) sidelobe was about 13 db down from the peak of the main beam.

APPENDIX A

AN EXAMPLE OF THE ECONOMY INVOLVED IN USING OPTIMUM PHASE DESIGN FOR ARRAY SYNTHESIS.*

Let the amplitude variation of the required pattern, $S(\psi)$ where $\psi = kd \cos\theta$, be that sketched in Figure A1-1. The circle diagram representing $S(\psi)$ is also shown in the figure. Then the analytic expression $S(\psi)$ is

$$S(\psi) = r + e^{j\psi} \tag{166}$$

and the power pattern is

$$SS^*(\psi) = r^2 + 2r\cos\psi + 1 \tag{167}$$

From equation (166) it can be seen that the required pattern will be produced exactly by two elements, A_o and A_1, having excitations r and 1, respectively. On the other hand, if the power pattern (167) were given and $S(\psi)$ were assumed real, that is, if

$$S(\psi) = \sqrt{1 + r^2 + 2r\cos\psi} = \sum_{n=0}^{N-1} A_n \cos n\psi \tag{168}$$

then,

$$A_n = \frac{1}{\pi}\int_o^{2\pi} S\cos n\psi \; d\psi$$

$$= \frac{\sqrt{1+r^2}}{\pi}\int_o^{2\pi}\sqrt{1 + \frac{2r}{1+r^2}\cos\psi}\cdot\cos n\psi \; d\psi \tag{169}$$

The radical in the integrand of equation (169) can be expanded in an infinite Fourier cosine series:

$$\sqrt{1 + \frac{2r}{1+r^2}\cos\psi} = a_o + a_1\cos\psi + a_2\cos 2\psi + a_3\cos 3\psi + \ldots \tag{170}$$

The facts that the expansion of the radical includes a $\cos n\psi$ term for all n and that the radical is multiplied by $\cos n\psi$ in the integrand of (169) indicate that A_n exists for all n. In other words, assumption of real $S(\psi)$ forces the use of an array with an infinite number of elements to produce exactly a pattern which can be produced exactly by an array of only two elements by allowing the phase of $S(\psi)$ to take on the optimum value given by equation (166).

*This example was suggested to the authors by T. T. Taylor.

APPENDIX B

JI NT VALUES FOR DOLPH-TSCHEBYSCHEFF ARRAYS

TABLE OF CONTENTS

Number of Elements	Sidelobe Level (decibels down)
4	20
6	30
7	20
8	28, 30, 32
10	25
12	20, 30, 40
16	32, 36
18	25
24	20, 30, 40
33	25
38	30
40	36
48	20, 30, 40
66	35
144	40

4 Elements

20 db

k		I_k
1		6.34467
2		3.65532
Z_o	=	1.54043
r	=	10
ψ	=	0.93255

6 Elements

30 db

k		I_k
1		15.97290
2		10.92129
3		4.72224
Z_o	=	1.364048
r	=	31.62278
ψ	=	0.83991

7 Elements

20 db

k		I_k
0		3.76820
1		3.45054
2		2.61588
3		2.04944
Z_o	=	1.12704
r	=	10
ψ	=	0.95082

8 Elements

k		28 db I_k	30 db I_k	32 db I_k
1		9.411472	12.19580	15.76045
2		7.753466	9.90250	12.61676
3		5.116790	6.32654	7.809191
4		2.837067	3.19794	3.624265
Z_o	=	1.160635	1.1806586	1.201956
r	=	25.11887	31.62278	39.81072
$\mathscr{D}$	=	0.862324	0.841612	0.822562

10 Elements

25 db

k		I_k
1		5.0500
2		4.54167
3		3.64306
4		2.55344
5		1.99461
Z_o	=	1.07973575
r	=	17.782794
$\mathscr{D}$	=	0.904804

12 Elements

k		20 db I_k	30 db I_k	40 db I_k
1		2.09821	8.12761	29.29670
2		1.98542	7.43902	25.95992
3		1.77354	6.20007	20.21841
4		1.48752	4.64892	13.57260
5		1.16013	3.06107	7.53420
6		I.49518	2.14609	3.41817
Z_o	=	1.03725	1.07190	1.11826
r	=	10	31.62278	100
$\mathscr{D}$	=	0.96428	0.85284	0.75976

16 Elements

k		32 db I_k	36 db I_k
1		7.81	13.19830
2		7.50	12.43593
3		6.73	11.01836
4		5.70	9.13899
5		4.55	7.04060
6		3.37	4.97075
7		2.28	3.13961
8		1.86	2.15322
Z_o	=	1.042880	1.0524605
r	=	39.81072	63.09574
$\mathscr{G}$	=	0.840	0.799355

18 Elements

k		25 db I_k
1		2.74792
2		2.66535
3		2.50596
4		2.28072
5		2.00480
6		1.69616
7		1.37397
8		1.05695
9		1.45099
Z_o	=	1.02213846
r	=	17.782794
$\mathscr{G}$	=	0.921175

24 Elements

k		20 db I_k	30 db I_k	40 db I_k
1		1.01822	3.9901	14.5769
2		1.00528	3.9080	14.1372
3		0.97977	3.7478	13.3433
4		0.94242	3.5173	12.2159
5		0.89428	3.2274	10.8317
6		0.83671	2.8918	9.2731
7		0.77128	2.5256	7.62242
8		0.699775	2.1444	6.07028
9		0.62406	1.7643	4.58229
10		0.54608	1.3991	3.26402
11		0.46775	1.0614	2.15811
12		1.21436	1.4504	1.83112
Z_o	=	1.0084801	1.016298	1.026655
r	=	10	31.62278	100
$\mathscr{D}$	=	0.94044	0.87134	0.77191

33 Elements

25 db

k	I_k
0	1.4730106
1	1.4666424
2	1.4476607
3	1.4164483
4	1.3736270
5	1.3200464
6	1.2567533
7	1.1849740
8	1.1060732
9	1.0215286
10	0.9328810
11	0.8417027
12	0.7495607
13	0.6579695
14	0.5683664
15	0.4820701
16	1.2199843
Z_o =	1.0062314
r =	17.782794
$\mathscr{D}$ =	0.919856

38 Elements		40 Elements	
30 db		36 db	
k	I_k	k	I_k
1	2.49199	1	5.182363
2	2.47178	2	5.135927
3	2.43221	3	5.044040
4	2.37382	4	4.908665
5	2.29722	5	4.732775
6	2.20441	6	4.520148
7	2.09746	7	4.275316
8	1.97766	8	4.003356
9	1.84679	9	3.709761
10	1.70799	10	3.400315
11	1.56401	11	3.080970
12	1.41622	12	2.757645
13	1.26664	13	2.436042
14	1.11879	14	2.121467
15	0.97510	15	1.818732
16	0.83613	16	1.532093
17	0.70359	17	1.265176
18	0.57550	18	1.020841
19	1.26063	19	0.801212
		20	1.348897
Z_o =	1.0062895	Z_o =	1.00770345
r =	31.62278	r =	63.09574
$\mathscr{L}$ =	0.87665	$\mathscr{L}$ =	0.81739

48 Elements

k	20 db I_k	30 db I_k	40 db I_k
1	0.49995	1.96412	7.19977
2	0.49842	1.95430	7.14943
3	0.49536	1.93479	7.04964
4	0.49080	1.90581	6.90211
5	0.48478	1.86770	6.70939
6	0.47732	1.82092	6.47475
7	0.46849	1.76601	6.20216
8	0.45834	1.70361	5.89614
9	0.44694	1.63444	5.56169
10	0.43437	1.55927	5.20417
11	0.42071	I.47895	4.82916
12	0.40606	1.39437	4.44232
13	0.39051	1.30643	4.04933
14	0.37416	1.21606	3.65569
15	0.35712	1.12418	3.26668
16	0.33949	1.03173	2.88717
17	0.32139	0.93958	2.52162
18	0.30293	0.84859	2.17395
19	0.28423	0.75957	1.84749
20	0.26538	0.67325	1.54493
21	0.24651	0.59032	1.26832
22	0.22772	0.51138	1.01905
23	0.20911	0.43693	0.79787
24	1.09993	1.20045	1.34718
Z_o =	1.002029	1.003895	1.006361
r =	10	31.62278	100
$\mathscr{Y}$ =	0.85821	0.87718	0.78280

66 Elements

35 db

k	I_k
1	2.73787
2	2.72927
3	2.71214
4	2.68661
5	2.65286
6	2.61117
7	2.56184
8	2.50525
9	2.44182
10	2.38875
11	2.29635
12	2.21538
13	2.12967
14	2.03985
15	1.94653
16	1.85035
17	1.75197
18	1.65202
19	1.55115
20	1.45000
21	1.34917
22	1.24926
23	1.15083
24	1.07115
25	0.96050
26	0.86955
27	0.78198
28	0.69815
29	0.61837
30	0.54293
31	0.47203
32	0.40585
33	1.18698

Z_o = 1.00264

r_{ℓ} = 56.23413

ℓ = 0.83149

144 Elements

40 db

k	I_k	k	I_k
1	2.3727	39	1.3103
2	2.3709	40	1.2676
3	2.3673	41	1.2249
4	2.3619	42	1.1824
5	2.3548	43	1.1400
6	2.3458	44	1.0989
7	2.3351	45	1.0562
8	2.3226	46	1.0148
9	2.3085	47	0.97385
10	2.2927	48	0.93336
11	2.2752	49	0.89339
12	2.2561	50	0.85398
13	2.2355	51	0.81518
14	2.2132	52	0.77704
15	2.1895	53	0.73959
16	2.1643	54	0.70288
17	2.1377	55	0.66694
18	2.1097	56	0.63180
19	2.0804	57	0.59749
20	2.0499	58	0.56405
21	2.0181	59	0.53150
22	1.9852	60	0.49987
23	1.9512	61	0.46918
24	1.9161	62	0.43943
25	1.8801	63	0.41065
26	1.8432	64	0.38285
27	1.8055	65	0.35605
28	1.7669	66	0.33024
29	1.7276	67	0.30544
30	1.6877	68	0.28165
31	1.6472	69	0.25886
32	1.6062	70	0.23708
33	1.5647	71	0.21631
34	1.5229	72	1.1031
35	1.4807	Z_o =	1.000687
36	1.4383	r =	100
37	1.3957	$\mathcal{Y}$ =	0.78938
38	1.3531		

BIBLIOGRAPHY

1. Bailin, L. L. and Ehrlich, M. J., "Factors Affecting the Performance of Linear Arrays," Proc. IRE 41 (1953) pp 235-241.
2. Bailin, L. L., "Fundamental Limitations of Long Arrays," Hughes Aircraft Company TM-330, October 1953.
3. Bailin, L. L., "The Radiation Field Produced by a Slot in Large Circular Cylinders," Hughes Aircraft Company TM-309, June 1953.
4. Bailin, L. L., Wehner, R. S. and Kaminow, I. P., "Empirical Approximations to the Current Values for Large Dolph-Tchebyscheff Arrays," IRE Convention Record, Part 2, 1954.
5. Barbiere, D., "A Method for Calculating the Current Distribution of Tchebyscheff Arrays," Proc. IRE 40 (1952) pp 78-82.
6. Bethe, H. A., "Theory of Diffraction by Small Holes," Phys. Rev., (2) 66 (1944) pp 163-182.
7. Booker, H. G., "Slot Aerials and Their Relation to Complementary Wire Dipoles (Babinet's Principle)," J. Instn. Electr. Engr., (IIIA) 93 (1946) pp 620-626.
8. Bouwkamp, C. J. and De Bruijn, N. G., "The Problem of Optimum Antenna Current Distribution," Philips Research Rpts. 1 (1946) p 135.
9. Carter, P. S., Hansell, C. W. and Lindenblad, N. E., "Development of Directive Transmitting Antennas by RCA Communications, Inc.," Proc. IRE 19 (1931) p 1773.
10. Carter, P. S. and others, "Slot Antennas in Elliptic Cylinders and Airplane Vertical Stabilizer," RCA Labs, Rocky Point, Rpt. No. CM-45-15, April 1948.
11. Chu, L. J., "Physical Limitations of Omnidirectional Antennas," J. A. P. 19 (1948) p 1163.
12. Chu, L. J., "Microwave Beam-Shaping Antennas," Res. Lab. of Electr., MIT, 1947, T.R. 40. See also Silver (op. cit.), Chap. 13.
13. Clapp, R. E., "Probe-Fed Slots as Radiating Elements in Linear Arrays," R. L., MIT, Rpt. No. 455, January 1944.
14. Copson, E. T., "An Integral Equation Method of Solving Plane Diffraction Problems," Roy. Soc. of London (Proc) (A) 186 (1946) pp 100-118.
15. Cullen, A. L. and Goward, F. K., "The Design of a Waveguide-Fed Array of Slots to Give a Specified Radiation Pattern," J. Instn. Electr. Engrs. (IIIA) 93 (1946) p 683.
16. Cullen, A. L., "Laterally-Displaced Slot in Rectangular Waveguide," Wireless Engineer, January 1949, pp 3-10.
17. Dolph, C. L., "A Current for Broadside Arrays which Optimizes the Relationship between Beamwidth and Sidelobe Level," Proc. IRE 34 (1946) pp 335-348.
18. DuHamel, R. H., "Pattern Synthesis for Antenna Arrays on Circular, Elliptic, and Spherical Surfaces," U. of Illinois, T.R. 16 ATI, May 1952, pp 166-395.
19. Dunbar, A. S., "Calculation of Doubly Curved Reflectors for Shaped Beams," Proc. IRE 36 (1948) pp 1289-1296.
20. Dunbar, A. S., "On the Theory of Beam Shaping," J. A. P. 23 (1952) p 847.

21. Ehrlich, M. J., Reed, R. H. and Short, J., "Broad Band Slot Studies," Hughes Aircraft Company Status Rpt. Pt. I-B (484A-08-F), January 1952.
22. Ehrlich, M. J. and Short, J., "Mutual Coupling Considerations in Linear Slot Array Design," Hughes Aircraft Company TM-303, April 1953.
23. Ehrlich, M. J. and Curtis, C. W., "Mutual Coupling in a Two-Dimensional Planar Slot Array," Hughes Aircraft Company TM-319, October 1953.
24. Feiker, C. E. and Clark, Jr., S. C., "Properties of Longitudinal Slots in Circular Waveguides," Tele-Tech 10 (March 1951) pp 42-44.
25. Felsen, L. B. and Oliner, A. A., "Determination of Equivalent Circuit Parameters for Dissipative Microwave Structures," Proc. IRE 42 (1954) pp 477-483.
26. Fry, D. W. and Goward, F. K., "Aerials for Centimeter Wave-Lengths," Cambridge Univ. Press, London, 1950; a) p 119, b) p 121, c) p 115, d) pp 117-125.
27. Gruenberg, H., "Second Order Beams of Slotted Waveguide Arrays," Can. J. Physics 31 (1953) pp 55-69.
28. Gruenberg, H., "Theory of Waveguide-Fed Slots Radiating into Parallel Plate Regions," J.A.P. 23 (1952) p 733.
29. Gullemin, E. A., "Communication Networks," Vol II, John Wiley and Sons, New York, 1935, p 439.
30. Guptill, E. W. and Watson, W. H., "Directive Antenna for Microwaves," U.S. Pat. No. 2596480.
31. Hansen, W. W. and Woodyard, J. R., "New Principle in Directional Antenna Design," Proc. IRE 26 (1938) p 333. See also Silver (op. cit.) p 278.
32. Herlin, M. A. and Brown, S. C., "Breakdown of a Gas at Microwave Frequencies," Phys. Rev. 74 (1948) pp 291-296.
33. Hines, J. N., Rumsey, V. H. and Tice, T. E., "On the Design of Arrays," Ohio State Univ. Res. Found. Rpt. 486-15, November 1953.
34. Jordan, E. C., "Electromagnetic Waves and Radiating Systems," Prentice-Hall, Inc., New York, 1951; a) p 455 et seq., b) pp 433-440.
35. Kraus, J. D., "Antennas," McGraw-Hill Book Co., New York, 1950, Chapters 10 and 11.
36. Kurtz, L. A. and Strumwasser, E., "Design Application of Edge Slots," Hughes Aircraft Company TM-266, January 1952.
37. Kurtz, L. A., "Design Application of Series Slot," Hughes Aircraft Company TM-273, December 1951.
38. La Port, E. A., "Radio Antenna Engineering," McGraw-Hill Book Co., Inc., New York, 1952, pp 290-300.
39. Lucke, W. S., "Mutual Admittance of Slots in Cylinders," Stanford Res. Inst. TR-36, Proj. 591.
40. Lewin, L., "Advanced Theory of Waveguides," Iliffe and Sons, London, 1951, pp 121-128.
41. van der Maas, G. J., "A Simplified Calculation for Dolph-Tchebyscheff Arrays," J.A.P. 25 (1954) pp 121-124.
42. O'Neill, H. and Ballin, L. L., "Further Effects of Manufacturing Tolerances on the Performance of Linear Shunt Slot Arrays," Hughes Aircraft Company TM-293, February 1953.

43. Oliner, A. A., "Equivalent Circuits for Slots in Rectangular Waveguide," Proc. IRE 42 (1954) p 477.
44. Oliner, A. A. and others, "Instruction Manual on Equivalent Circuit Measurements of Waveguide Structures," Poly. Inst. of Brooklyn, R-284-52, PIB-223, March 1953.
45. Ortusi, J. and Boissinot, G., "Slotted Waveguides and Their Application as Aerials: Experimental" (in French), Ann. Radioelect. 5 (1950) pp 308-320.
46. Papas, C. H., "Currents on the Surface of an Infinite Cylinder Excited by an Axial Slot," Q.A.M. 7 (1949) pp 175-182.
47. Papas, C. H., "Radiation from a Transverse Slot in an Infinite Cylinder," J. Math. Phys. 28 (1950) pp 227-236.
48. Pim, J. A., "The Electrical Breakdown Strength of Air at Ultra High Frequencies," J. Instn. Electr. Engrs. (III) 96 (1949) p 117.
49. Pistolkors, A. A., "Radiation from a Transverse Slit on the Surface of a Circular Cylinder" (in Russian), J. Tech. Phys. USSR, 17 (1947) pp 377-388.
50. Pistolkors, A. A., "Radiation from Longitudinal Slits in a Circular Cylinder," Comptes Rendus (Dolclady) de l'Academic des Sciences de l'URSS 52 (1946) pp 127-130.
51. Ragan, G. L., "Microwave Transmission Circuits," Vol. 9 MIT Rad. Lab Series, McGraw-Hill Book Co., New York, 1948, pp 481-483.
52. Rayleigh, Lord, "On the Passage of Electric Waves through Tubes or the Vibrations of a Dielectric Cylinder," Phil. Mag. (5) 43 (1897) pp 125-132. See also Scientific Papers, Lord Rayleigh, Vol. 4, pp 1892-1901.
53. Rayleigh, Lord, "On the Passage of Waves through Apertures in Plane Screens and Allied Problems," Phil. Mag. (5) 43 (1897) pp 259-272.
54. Rayleigh, Lord, "On the Incidence of Aerial and Electric Waves upon Small Obstacles in the Form of Ellipsoids or Elliptic Cylinders and on the Passage of Electric Waves through a Circular Aperture in a Conducting Screen," Phil. Mag. (5) 44 (1897) pp 28-52.
55. Reich, H. J. and others, "Very High Frequency Techniques," Vol. I, R.R.L. Staff, McGraw-Hill Book Co., New York, 1947, Chap. 7
56. Riblet, H. J., "Discussion on 'A Current Distribution...'," Proc. IRE 35 (1947) p 489.
57. Riblet, H. J., "Note on Maximum Directivity of an Antenna," Proc. IRE 36 (1948) pp 620-623.
58. Rumsey, V. H. and others, "Analysis and Measurement of Antenna Parameters," Ohio State Univ. Final Engr. Rpt. 478-24, November 1953.
59. Rumsey, V. H., "Traveling Wave Slot Antennas," Ohio State Univ. Rpt. 400-11, December 1951 (Confidential).
60. Ruze, J., "Effect of Aperture Distribution Errors on the Radiation Pattern," Air Force Cambridge Research Center, January 1952.
61. Schelkunoff, S. A., "A Mathematical Theory of Linear Arrays," Bell Syst. Tech. J. 22 (1943) pp 80-107.
62. Sensiper, S., "Cylindrical Radio Waves," Hughes Aircraft Co. TM-310, June 1953.
63. Sensiper, S., Sterns, W. G., Taylor, T. T., "A Further Study of the Patterns of Single Slots on Circular Conducting Cylinders," Trans. IRE PGAP-3, August 1952, pp 240-250.

64. Silver, S. and others, "Microwave Antenna Theory and Design," Vol. 12, Rad. Lab. Series, McGraw-Hill Book Co., New York, 1949; a) p 98, b) p 291, c) p 313, eqs. 66 and 67, d) p 373, e) p 299 f) pp 306, 310, 325-328, g) p 325, h) Chap. 15.
65. Silver, S., and Saunders, W. K., "The External Field Produced by a Slot in an Infinite Circular Cylinder," J.A.P. 21 (1950) pp 153-158.
66. Silver, S. and Saunders, W. K., "The Radiation from a Transverse Slot in a Circular Cylinder," J.A.P. 21 (1950) pp 745-749.
67. Sinclair, G., "The Patterns of Slotted Cylinder Antennas," Proc. IRE 36 (1948) p 1487.
68. Sinclair, G., "The Patterns of Antennas Located near Cylinders of Elliptical Cross Section," Proc. IRE 39 (1951) pp 660-668.
69. Spencer, R. C., "Fourier Integral Methods of Pattern Analysis," MIT R.L. Rpt. No. 762-1, January 1946.
70. Spencer, R. C., and Austin, P. H., "Tables and Methods of Calculation for Line Sources," MIT R.L. Rpt. No. 762-2, March 1946.
71. Stegen, R. J., "Excitation Coefficients and Beamwidths of Tchebyscheff Arrays," Proc. IRE 41 (1953) pp 1671-1764.
72. Stegen, R. J., "Longitudinal Shunt Slot Characteristics," Hughes Aircraft Co. TM-261, November 1951.
73. Stegen, R. J., "Waveguide Slot Measurement Techniques," Hughes Aircraft Co. TM-262, December 1951.
74. Stegen, R. J., "Design Techniques for Waveguide Slot Arrays," Hughes Aircraft Co. TM-264, December 1951.
75. Stevenson, A. F., "Theory of Slots in Rectangular Waveguides," J.A.P. 19 (1948) pp 24-38.
76. Stratton, J. A., "Electromagnetic Theory," McGraw-Hill Book Co., New York, 1941.
77. Strumwasser, E., Short, J., Stegen, R. J. and Miller, J. R., "Slot Studies in Rectangular TEM Transmission Line," Hughes Aircraft Co. TM-265, January 1952.
78. Taylor, T. T., Letter to the Editor, Proc. IRE 36 (1948) p 1135.
79. Taylor, T. T. and Whinnery, J. R., "Applications of Potential Theory to the Design of Linear Arrays," J.A.P. 22 (1951) pp 19-29.
80. Taylor, T. T., "Design of Line Sources for Narrow Beamwidth and Low Sidelobes," Hughes Aircraft Co. TM-316, 31 July 1953.
81. Taylor, T. T., "Corporate Structure Feeding Systems for Antenna Arrays," Hughes Aircraft Co. TM-202, September 1948.
82. Taylor, T. T., "Antenna Pattern Synthesis Method with Discussion of Energy Storage Considerations," Hughes Aircraft Co., R and D Labs., 11 April 1951.
83. Taylor, T. T., "Antenna Pattern Synthesis Methods for Arrays and Aperture Distributions," Hughes Aircraft Co. Rpt. M-55, August 1952.
84. Taylor, T. T., "Design of Circular and Cylindrical Antennas," Hughes Aircraft Co. TM-280, January 1952.
85. Taylor, T. T., "Radiation from Field Distributions on Elliptic Cylinders," Hughes Aircraft Co. TM-304, March 1953.
86. Taylor, T. T., "Dolph Arrays of Many Elements," Hughes Aircraft Co. TM-320, August 1953.
87. Watson, W. H., "The Physical Principles of Waveguide Transmission and Antenna Systems," Clarendon Press, Oxford, 1947, p 131.

88. Watson, W. H., "Resonant Slots," J. Instn. Electr. Engrs. (IIIA) 93, pp 747-777; a) p 755.
89. Watson, W. H. and Guptill, E. W., "Directive Antenna for Micro-Waves," U. S. Pat. 2573746.
90. Williams, I. K., "Circumferential Slot Array on a Circular Cylinder," Hughes Aircraft Co. TM-318, September 1953.
91. Wilmotte, R. M., "Letter to the Editor," Proc. IRE 36 (1948) p 878.
92. Woodward, P. M., "A Method of Calculating the Field over a Plane Aperture Required to Produce a Given Polar Diagram," J. Instn. Electr. Engrs. (IIIA) 93 (1946) p 1554.
93. Woodward, P. M. and Lawson, J. P., "The Theoretical Precision with which an Arbitrary Radiation Pattern May be Obtained from a Source of Finite Size," J. Instn. Electr. Engrs. (III) 95 (1948) pp 263-370.
94. Wolff, I., "Determination of the Radiating System which Produces a Specified Directional Pattern," Proc. IRE 25 (1937) p 630.
95. Wong, J. Y., "Radiation Conductance of Axial and Transverse Slots in Cylinders of Elliptic Cross Section," Proc. IRE 41 (1953) p 1172.
96. Yaru, N., "Note on Super Gain Antenna Arrays," Proc. IRE 39, September 1951.

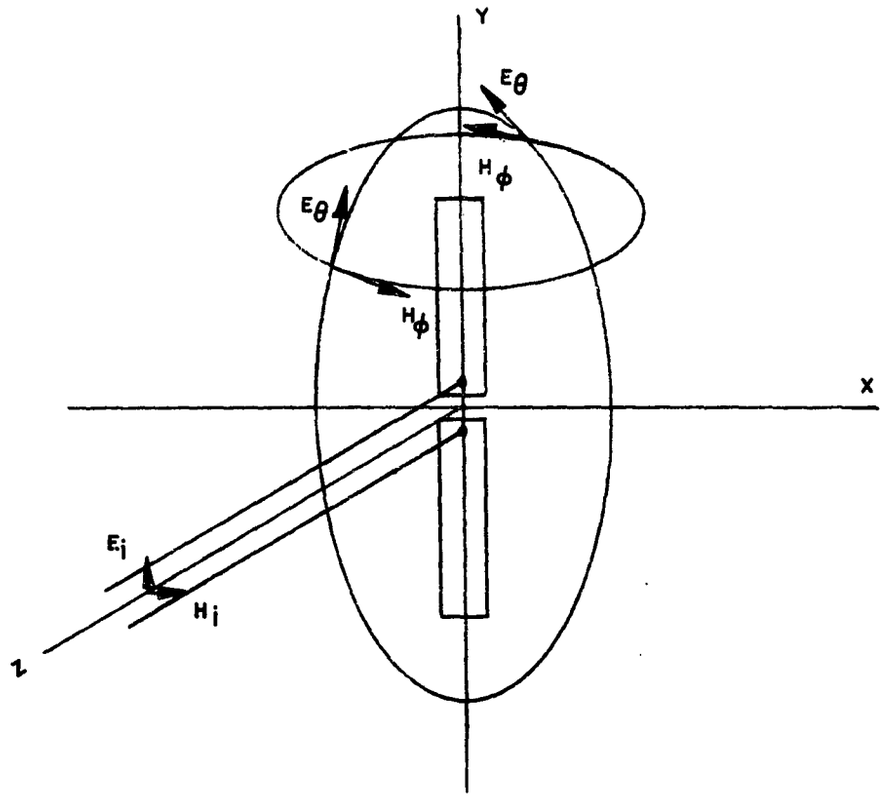

A)

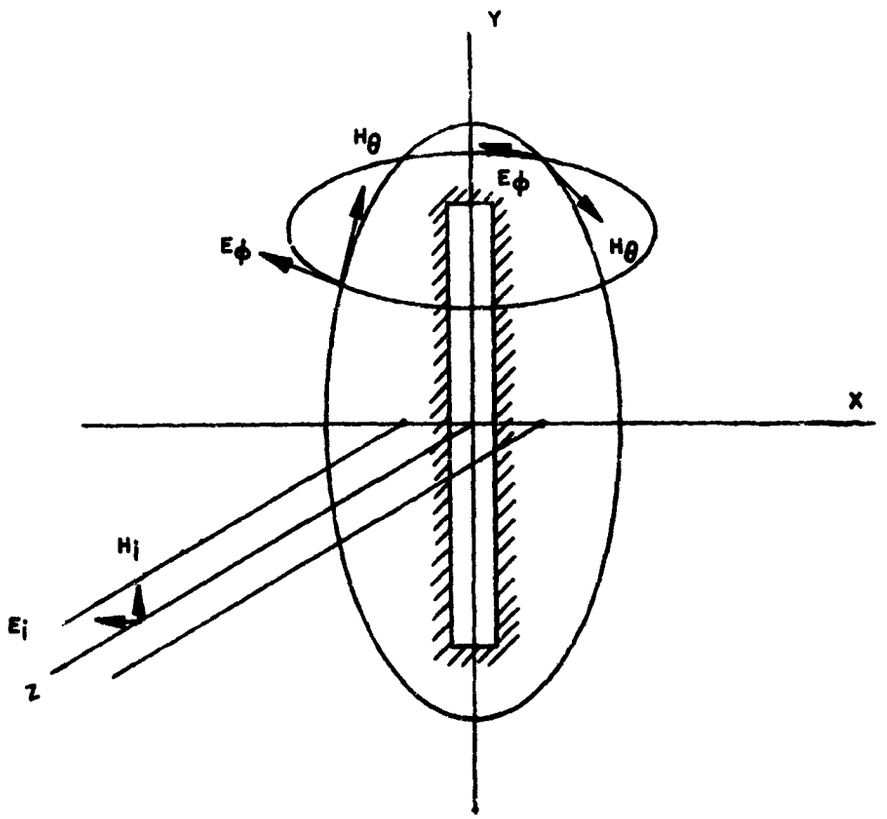

B)

Figure II-1. Application of Babinet's Principle.

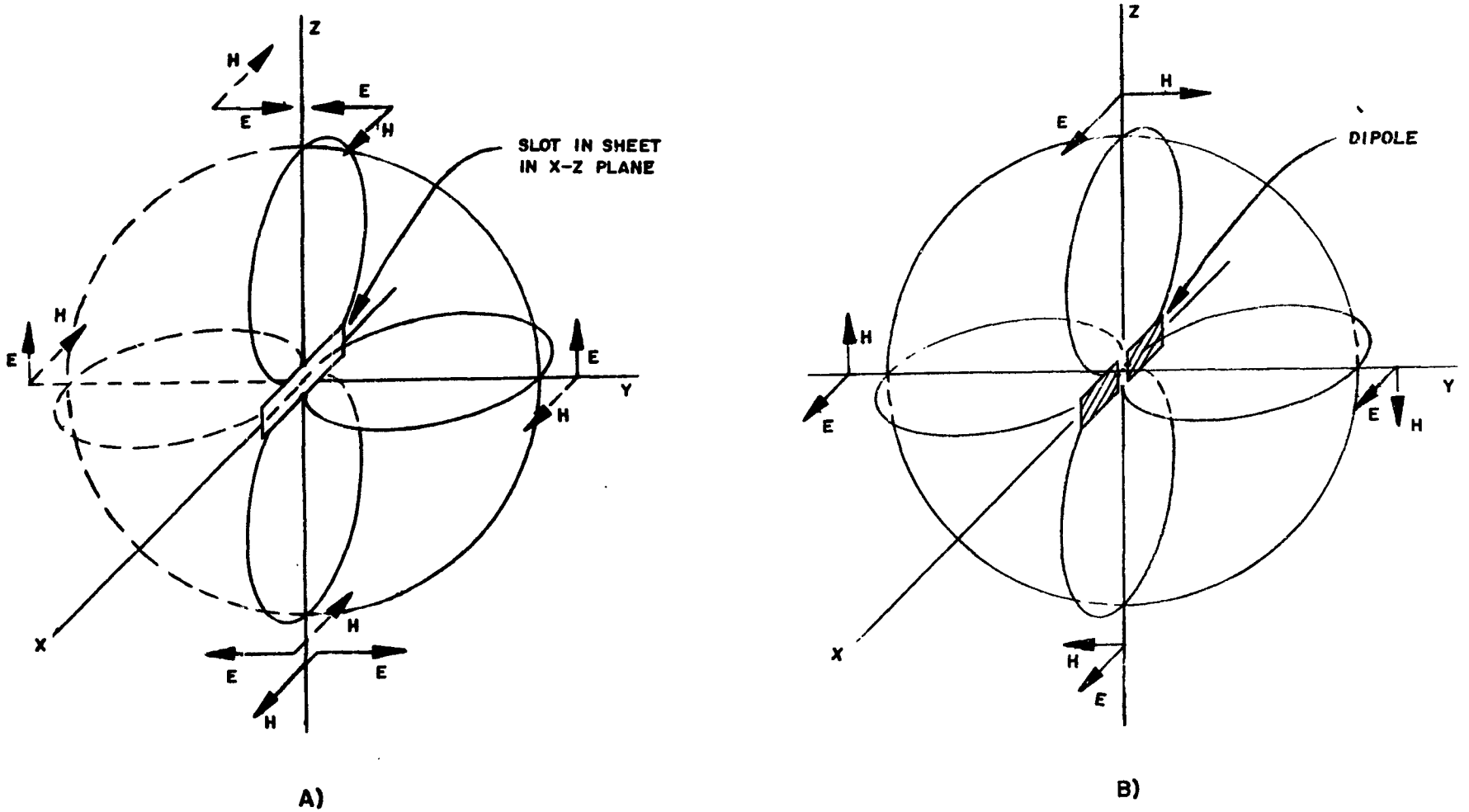

Figure II-2. Radiation Patterns for Half-Wave Slot and Complementary Dipole

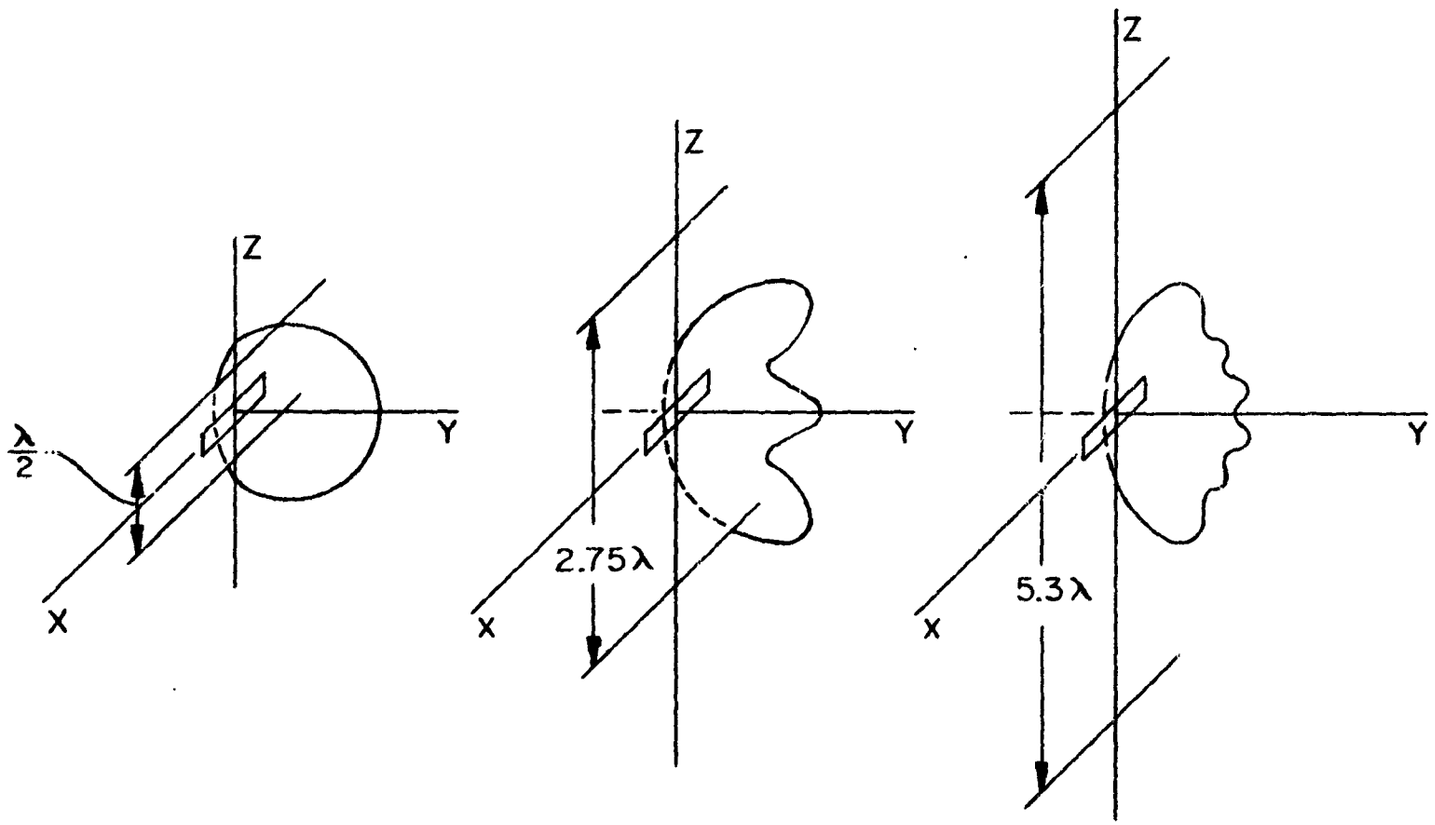

Figure II-3. E-Plane Patterns for Slots Radiating into Ground Planes of Variable Length

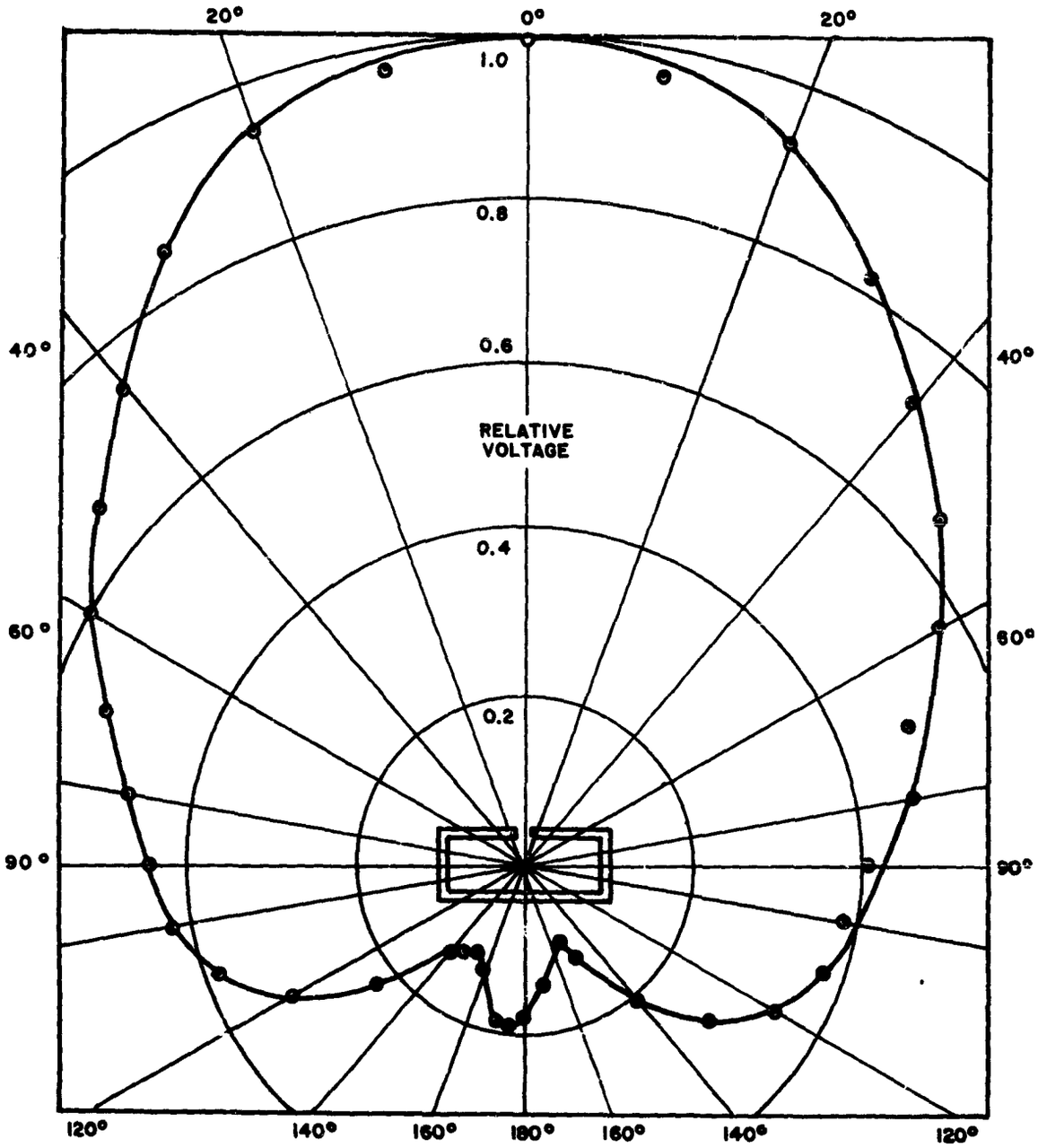

Figure II-4. E-Plane Radiation Pattern of Low Conductance Longitudinal Shunt Slot

f = 9200 mcps
conductance = 0.022
waveguide = 1.0 by 0.5 inch

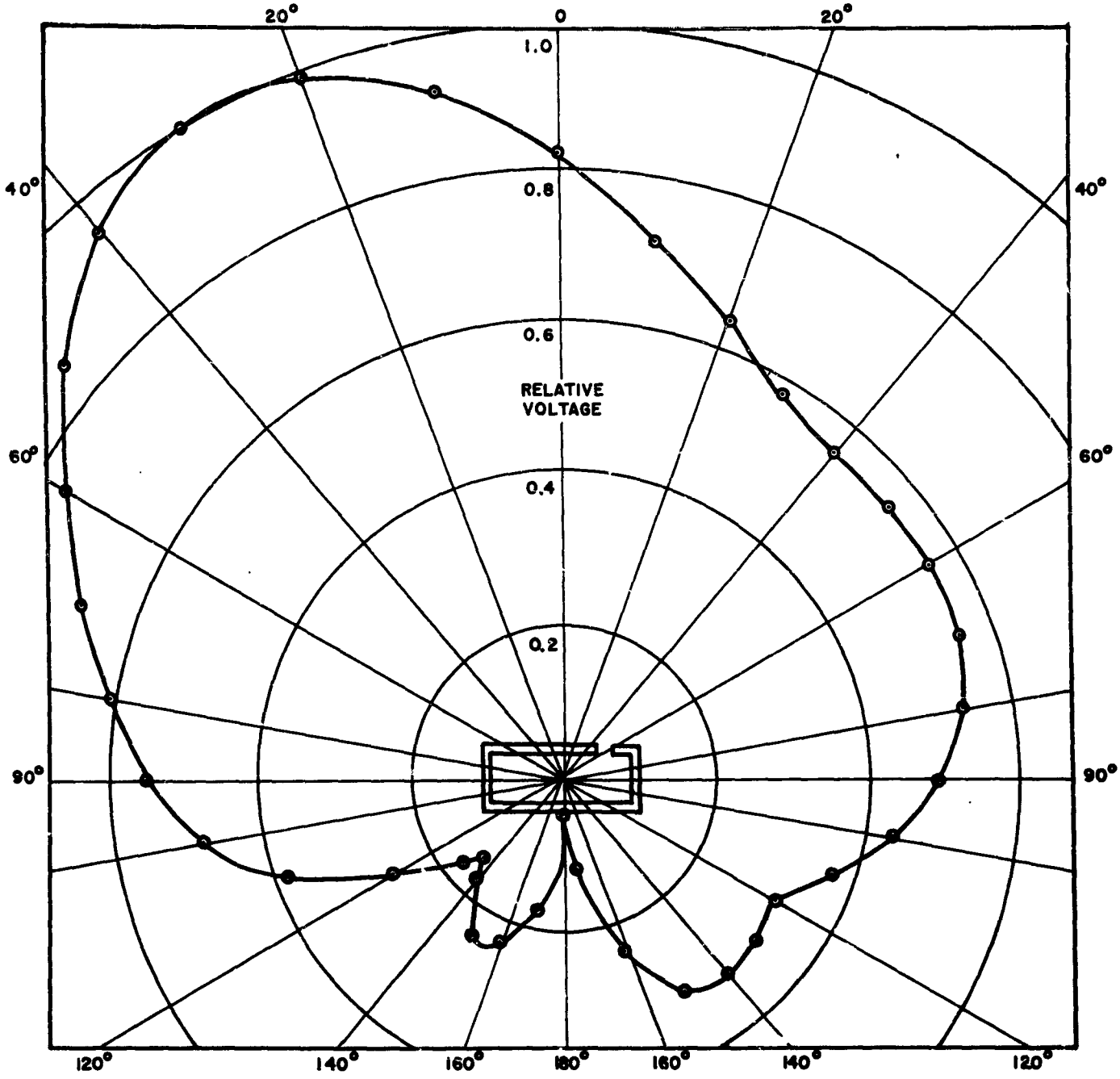

Figure II-5. E-Plane Radiation Pattern of High Conductance Longitudinal Shunt Slot

f = 9200 mcps
conductance = 0.558
waveguide = 1.0 by 0.5 inch

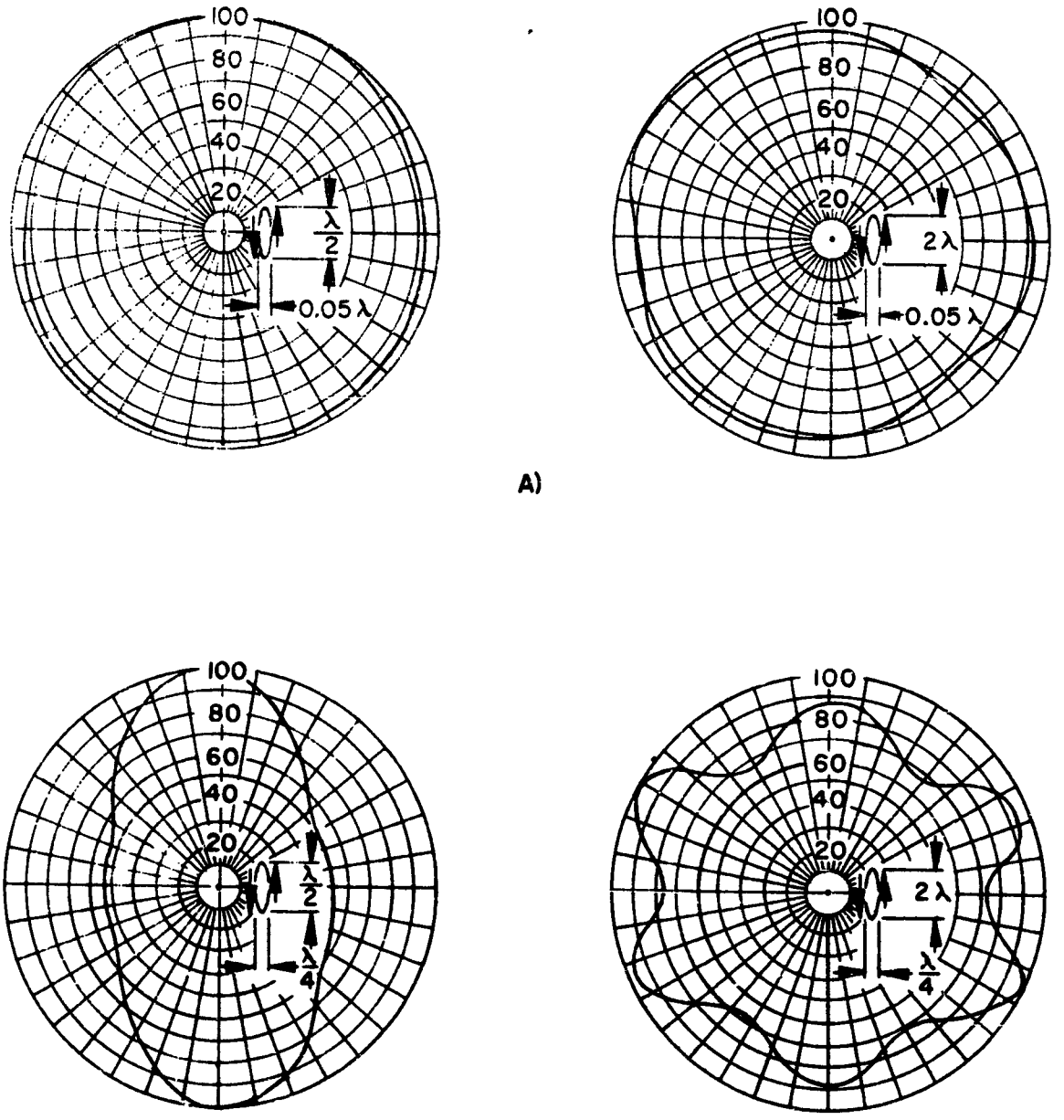

Figure II-6. E-Plane Patterns for In-Phase Slot Pairs on Elliptic Cylinders

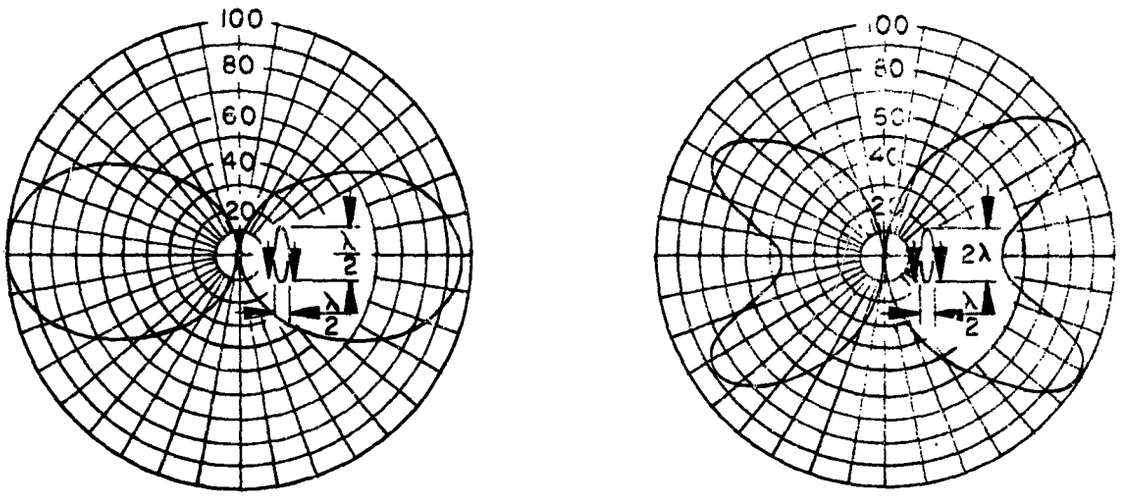

A) THIN CYLINDER

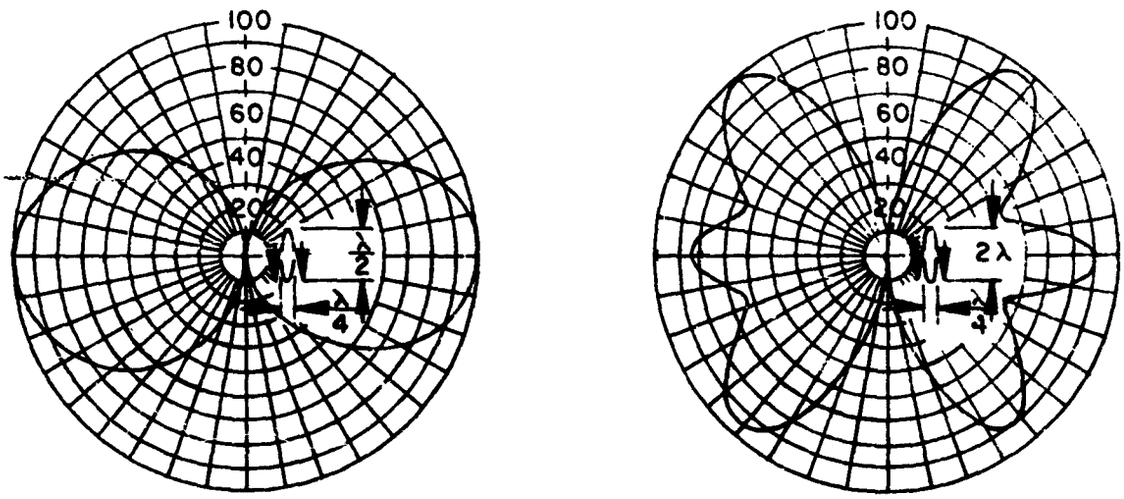

B) THICK CYLINDER

Figure II-7. E-Plane Patterns for Slot Pairs in Phase Opposition

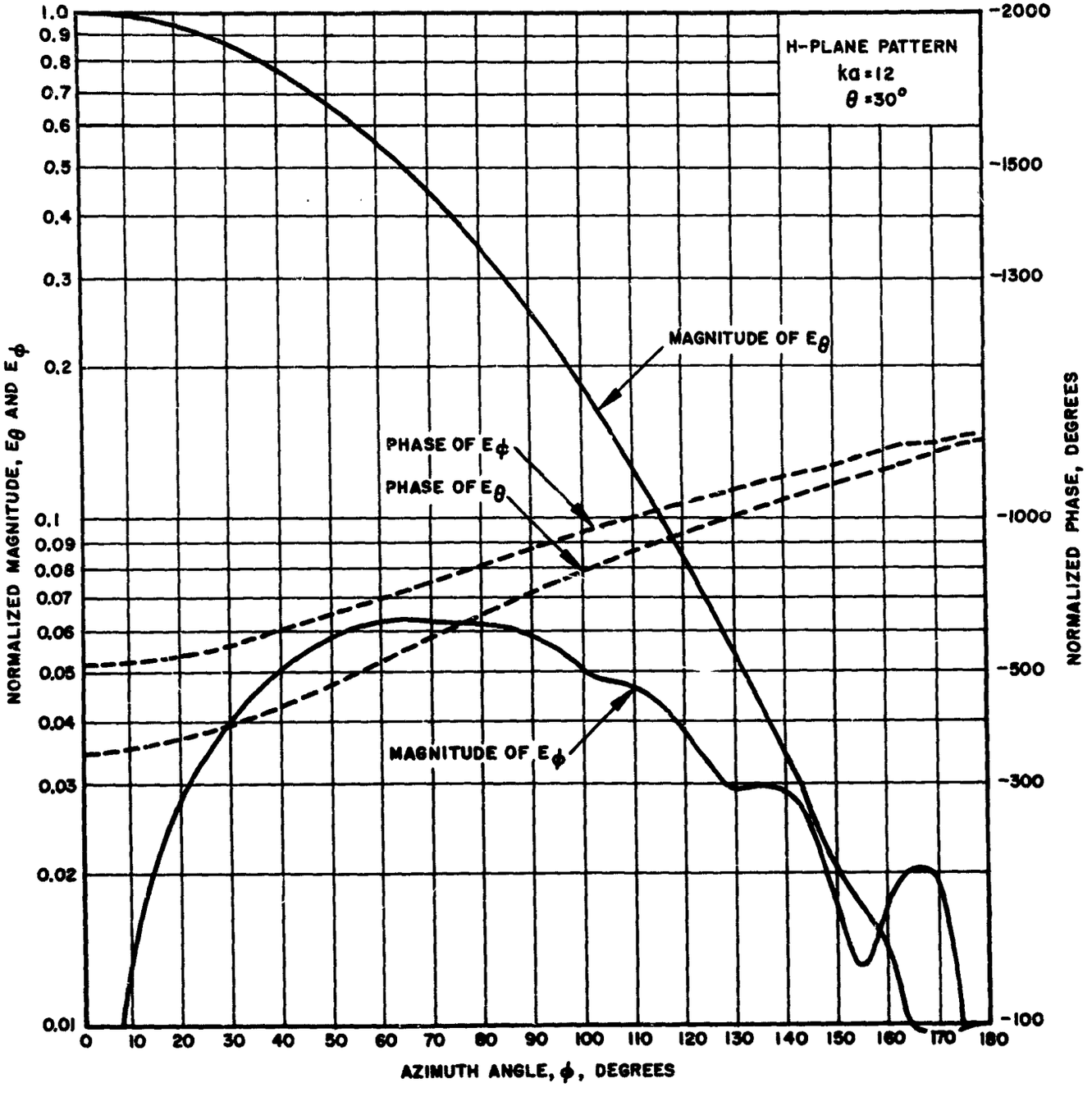

Figure II-8. H-Plane Pattern of Circumferential Half-Wave Length Slot

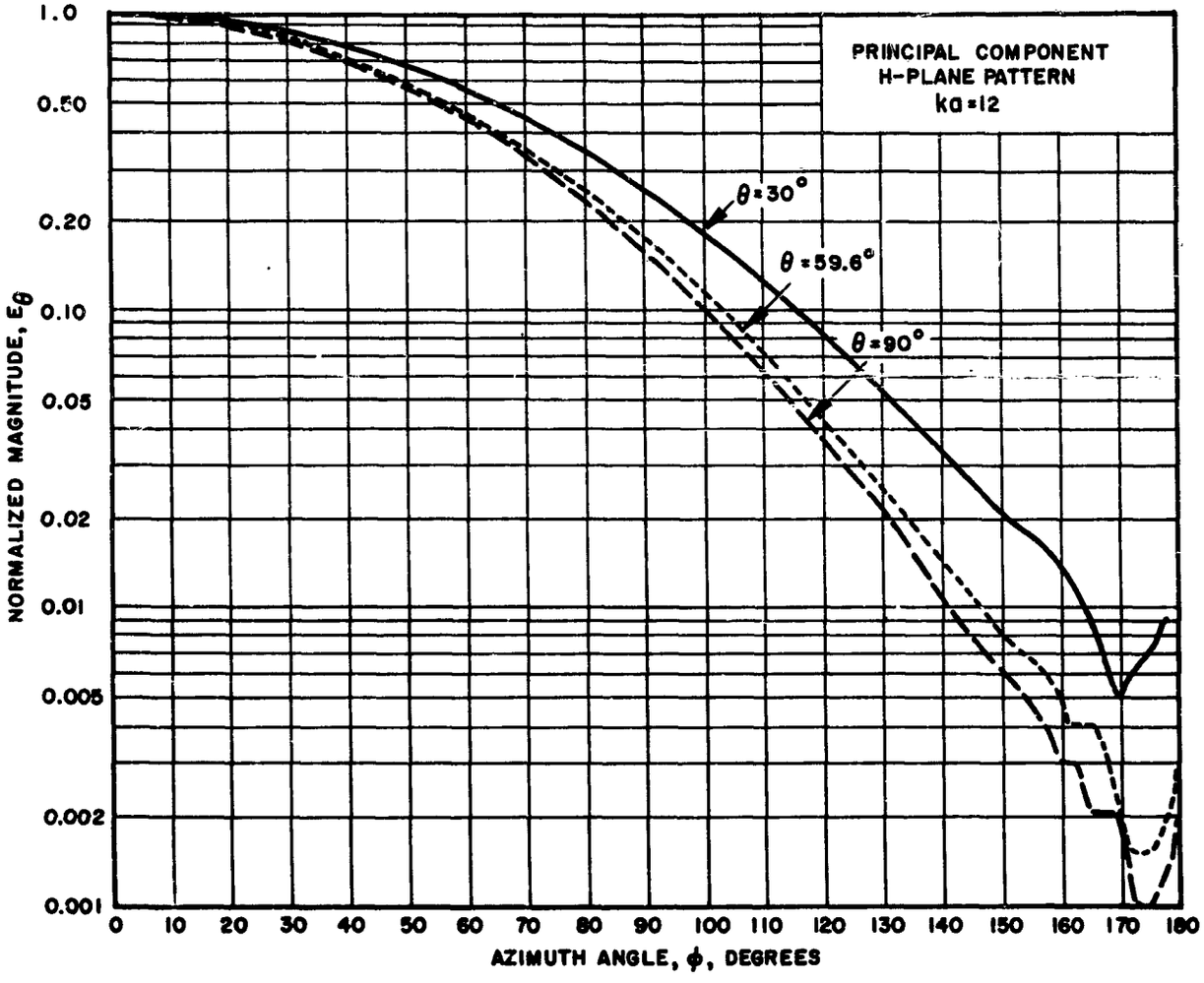

Figure II-9. Principal Component of H-Plane Pattern for Circumferential Half-Wave Length Slot

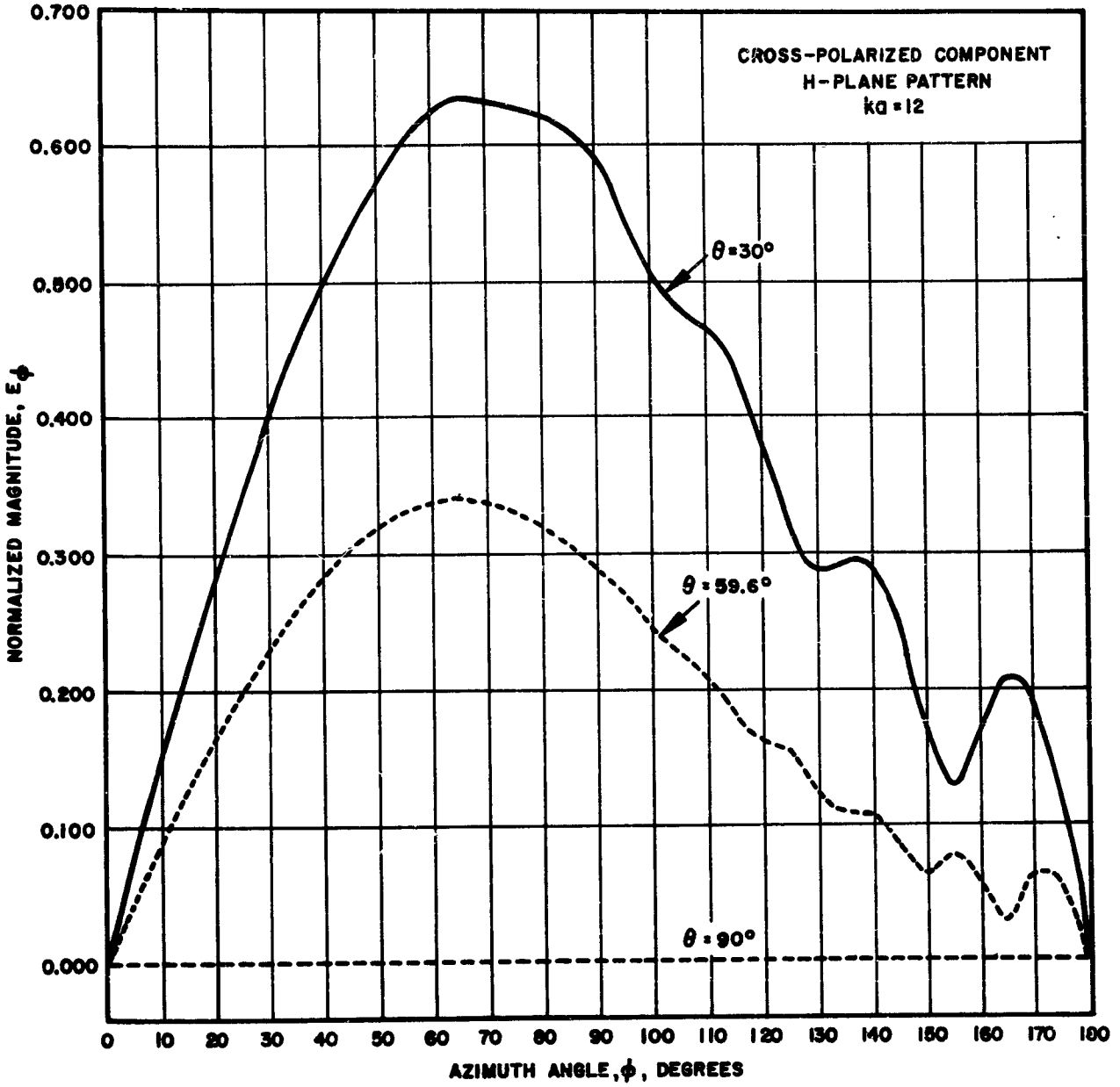

Figure II-10. Cross-Polarized Component of H-Plane Pattern for Circumferential Half-Wave Length Slot

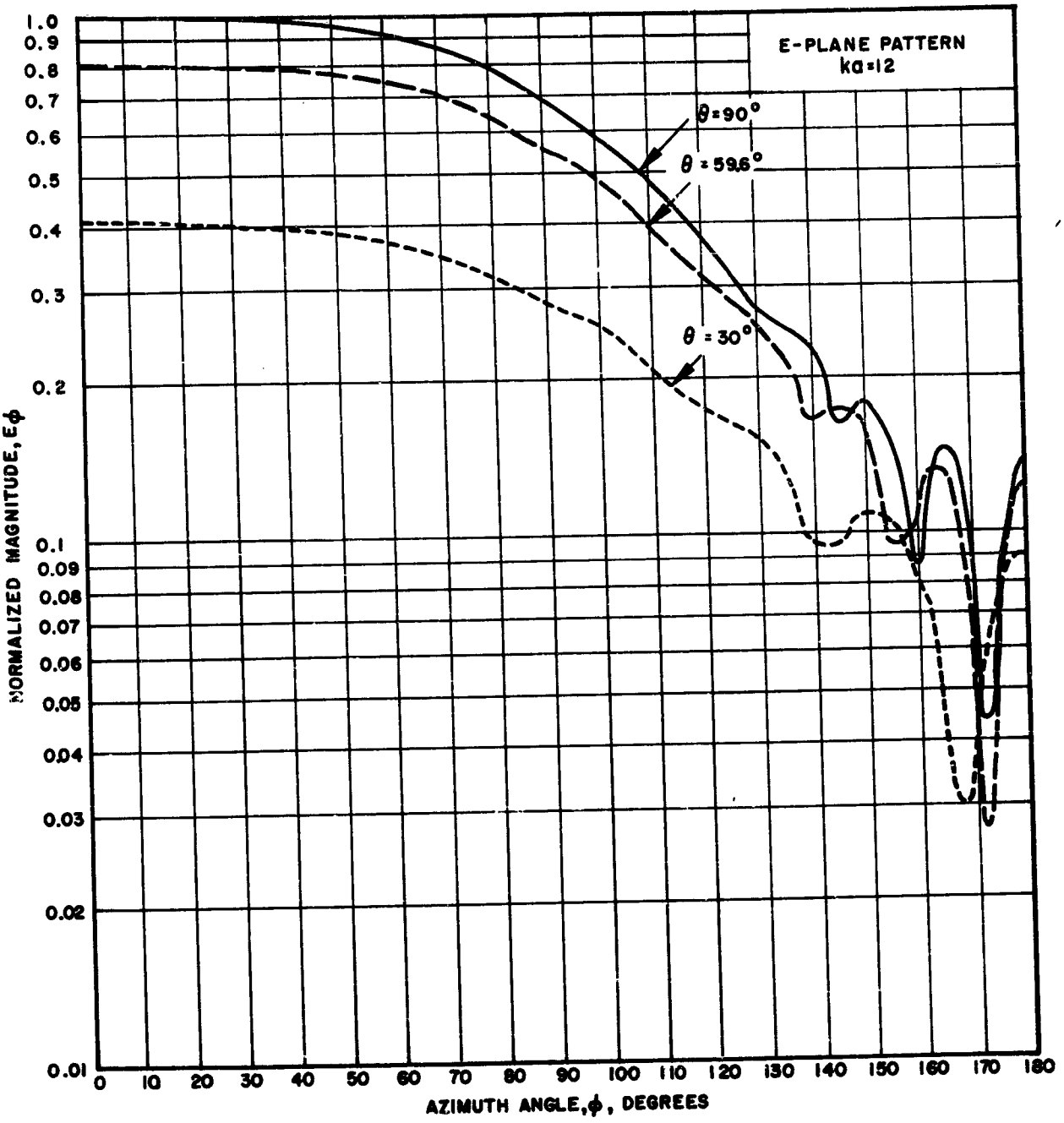

Figure II-11. E-Plane Pattern of Axial Half-Wave Length Slot

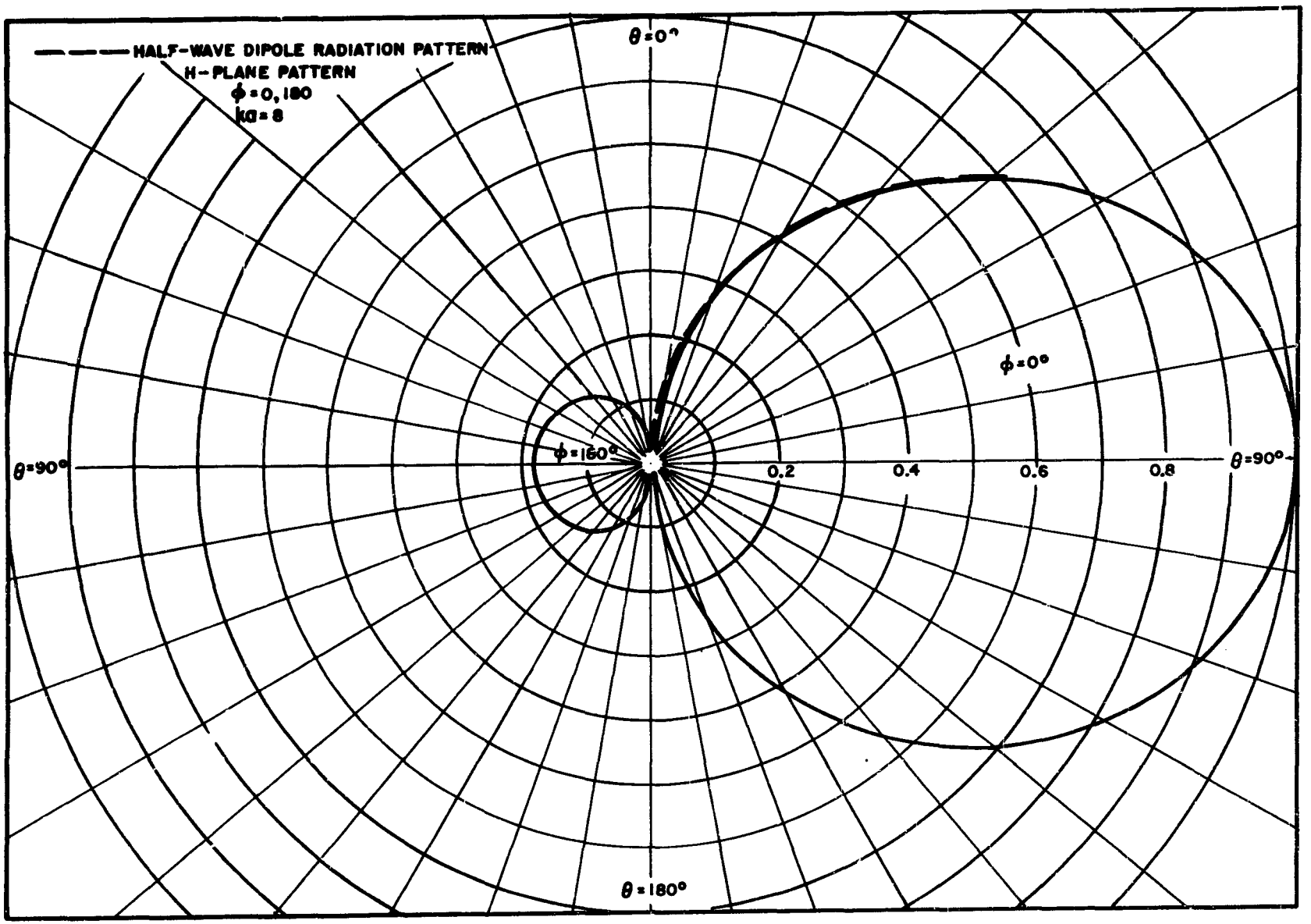

Figure II-12. H-Plane Pattern of Axial Half-Wave Length Slot

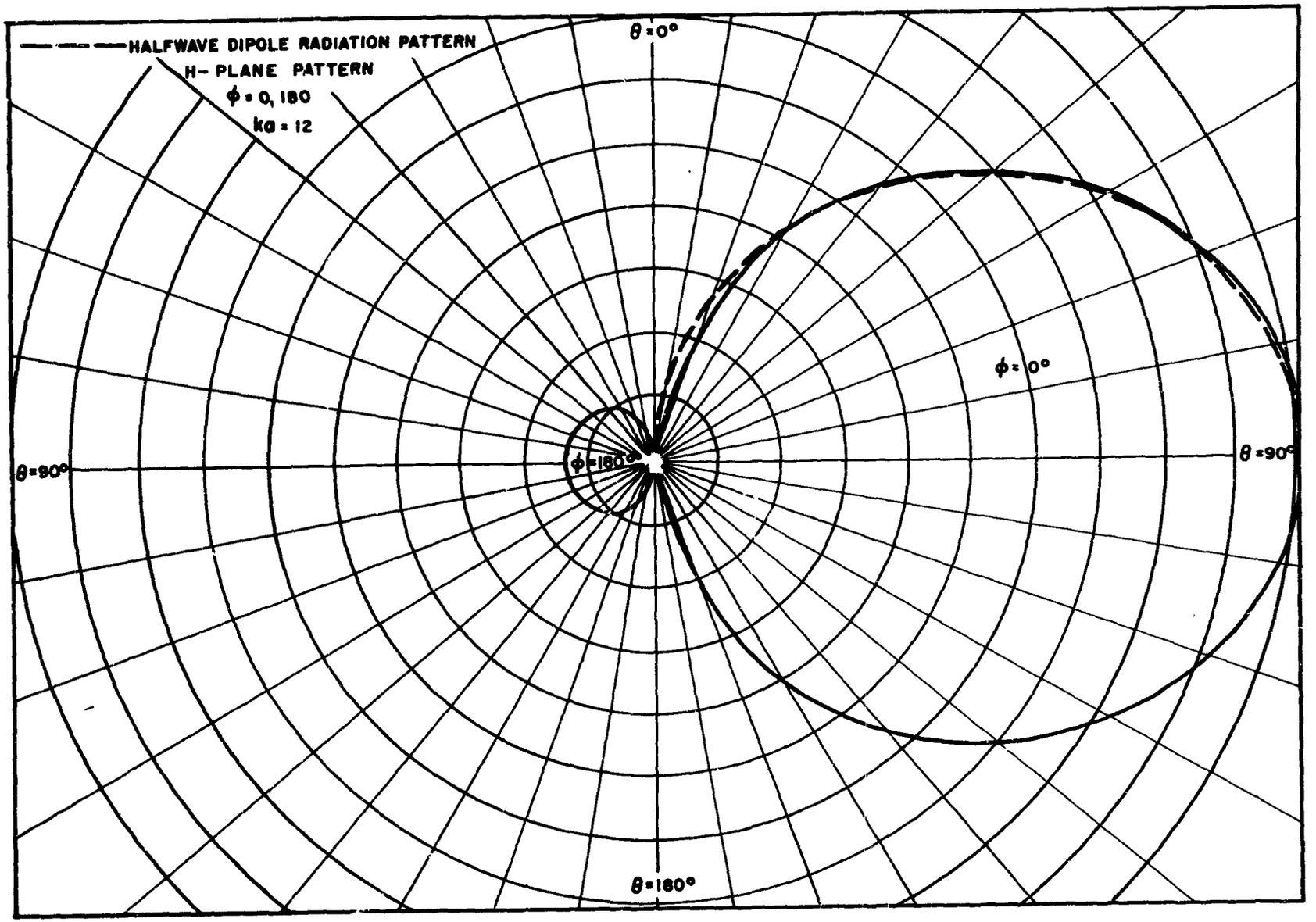

Figure II-13. H-Plane Pattern of Axial Half-Wave Length Slot

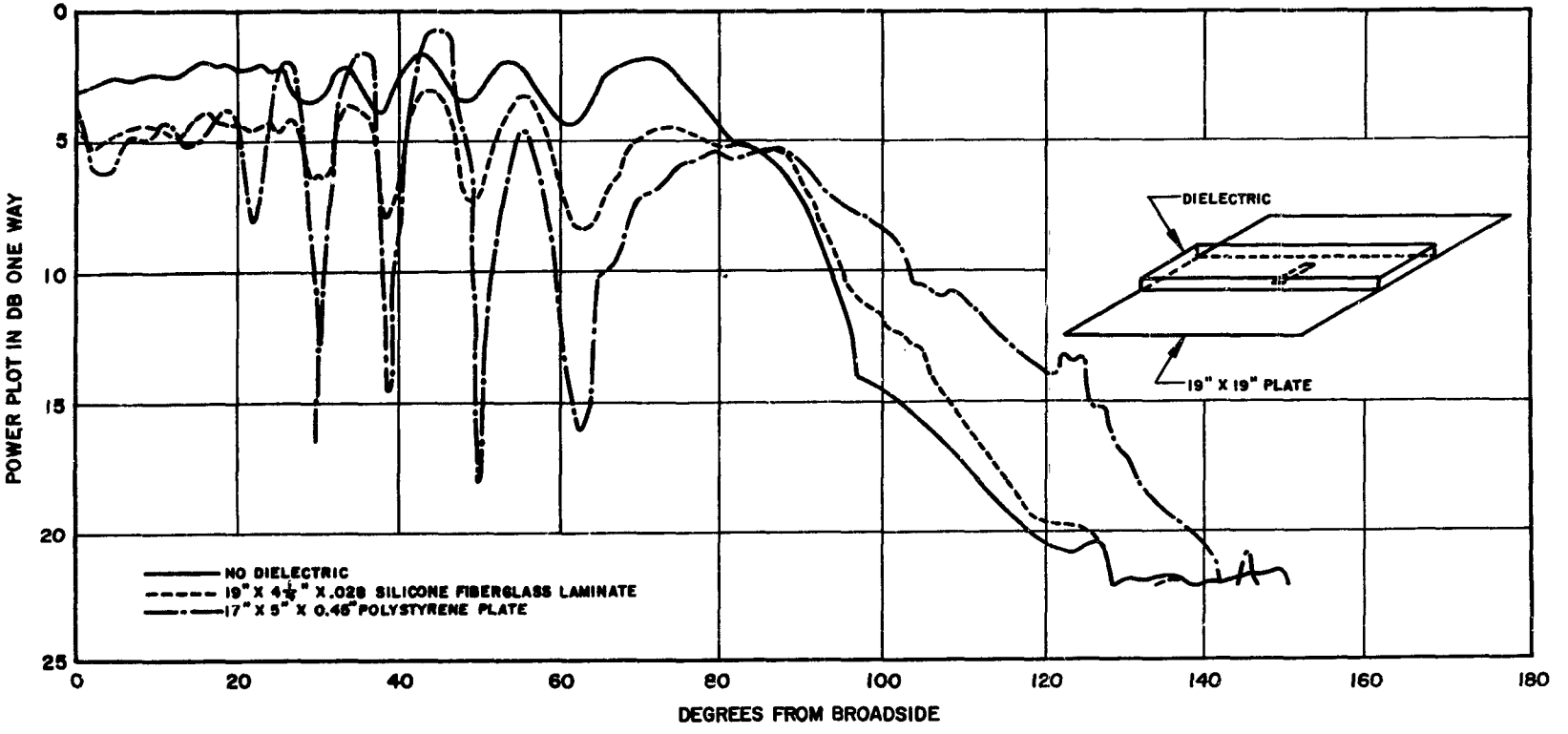

Figure II-14. *Effect of Dielectric Covers*
f = 9000 megacycles

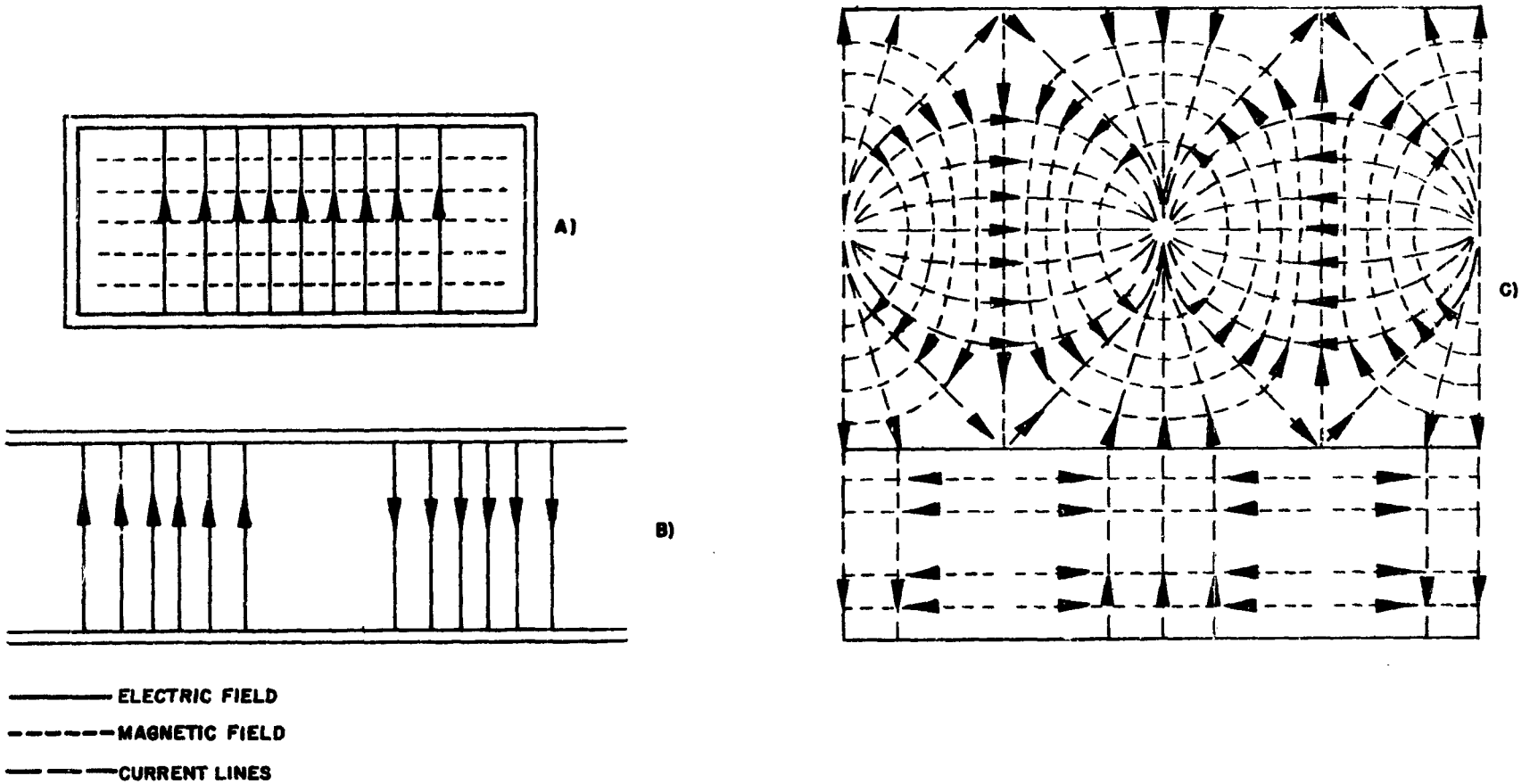

Figure II-15. Wall Current Distribution for Rectangular Waveguide Propagating TE_{01} Mode

A) Cross Sectional View
B) Longitudinal View
C) Surface View

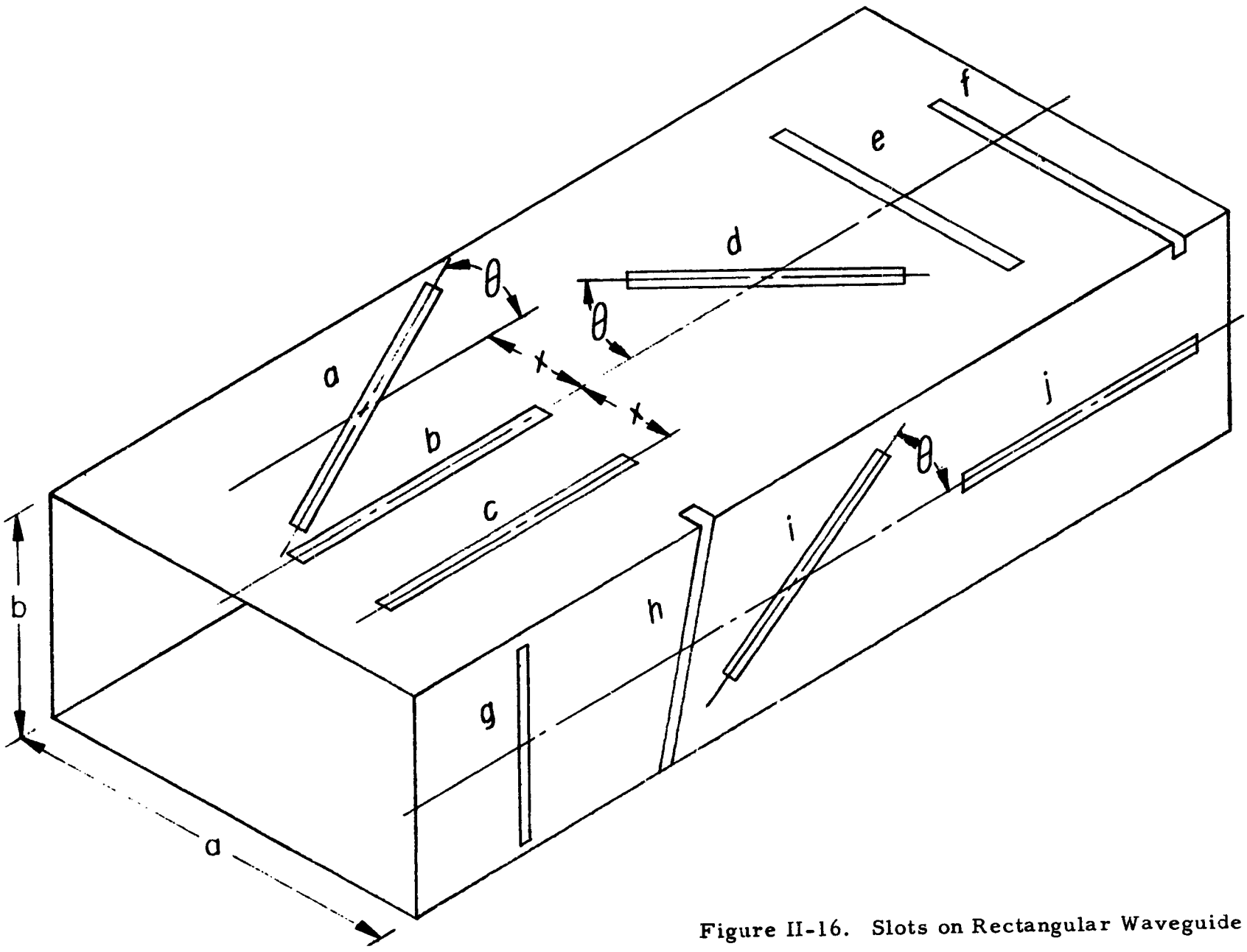

Figure II-16. Slots on Rectangular Waveguide

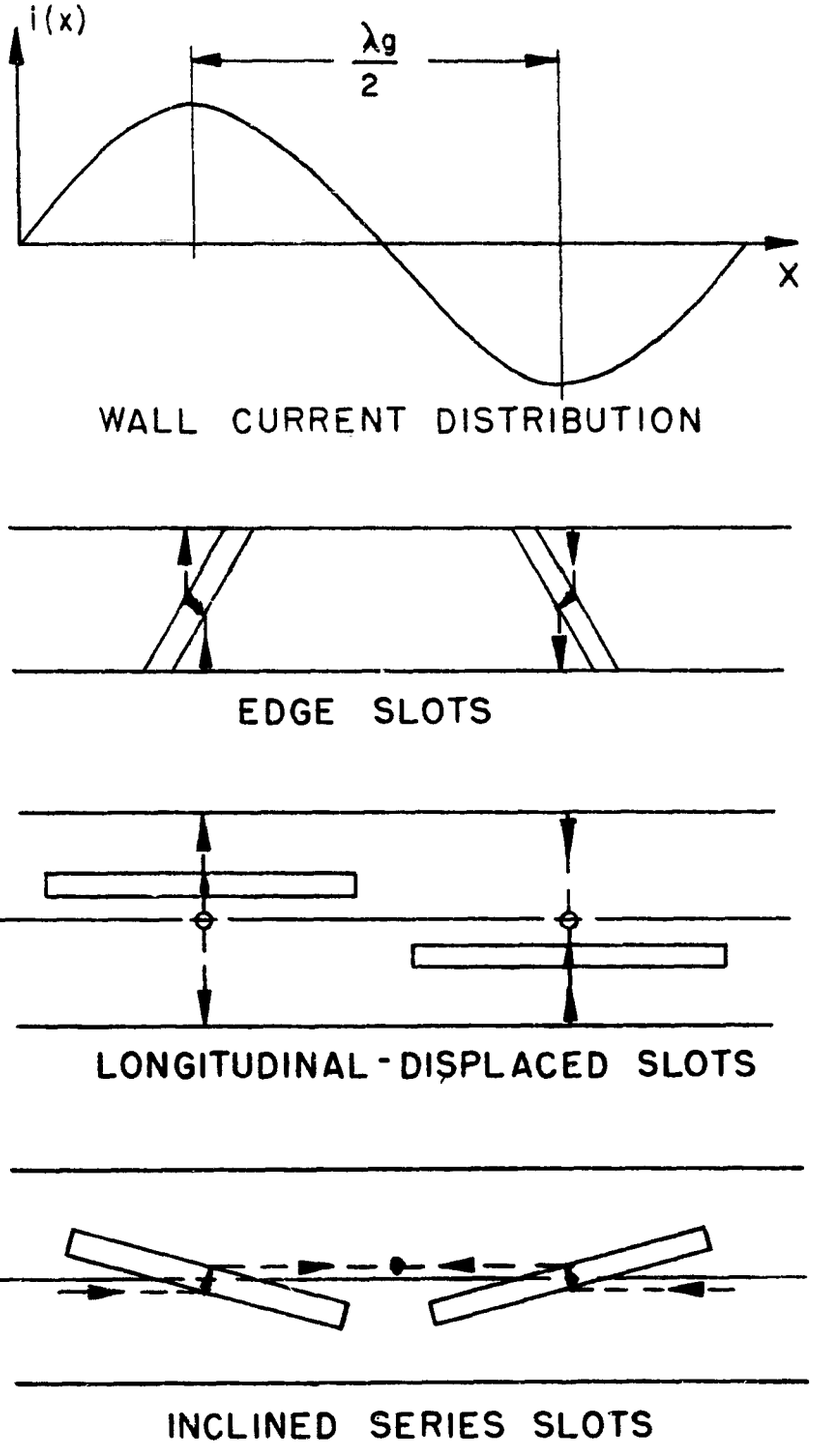

Figure II-17. Phase Reversal in Adjacent Slots

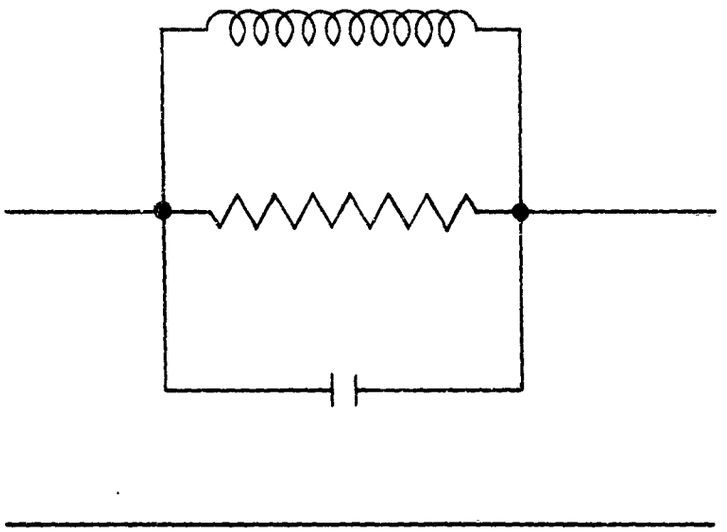

SERIES SLOT

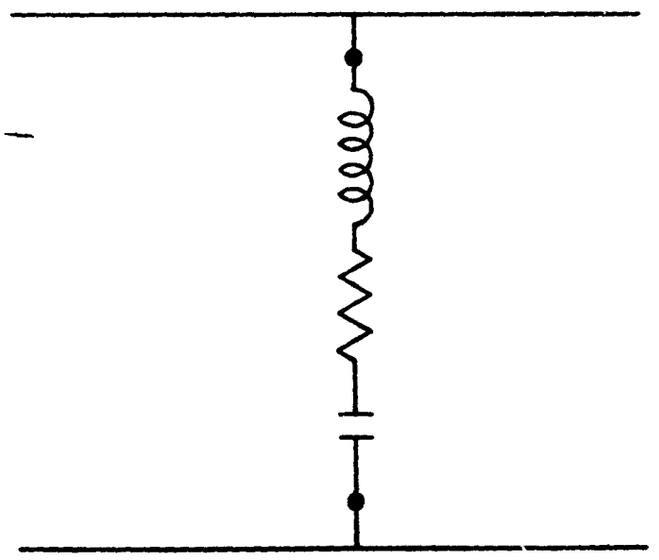

SHUNT SLOT

Figure II-18. Slot Equivalent Circuits Near First Resonance

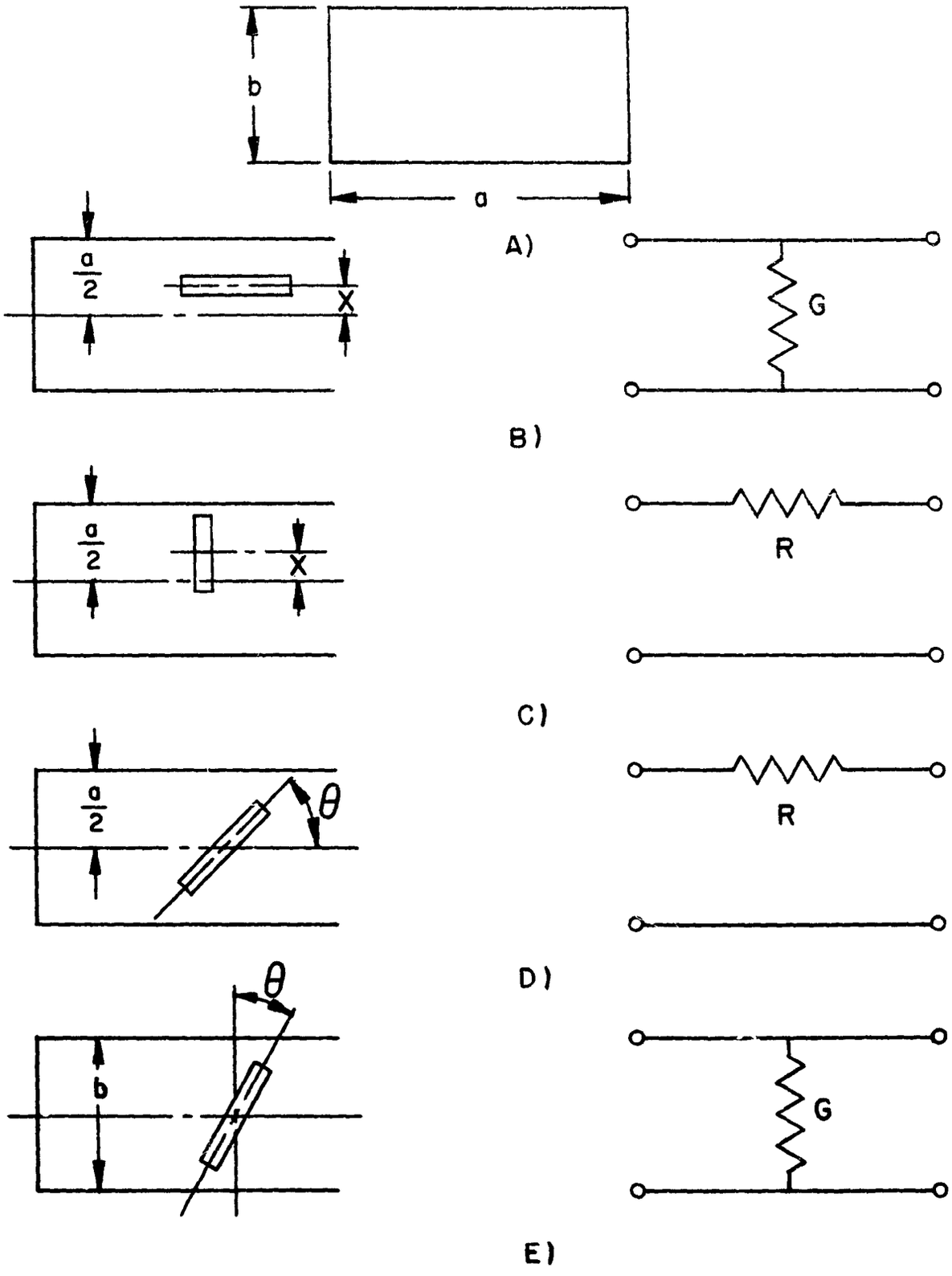

Figure II-19. Stevenson's Equivalent Circuit Representations

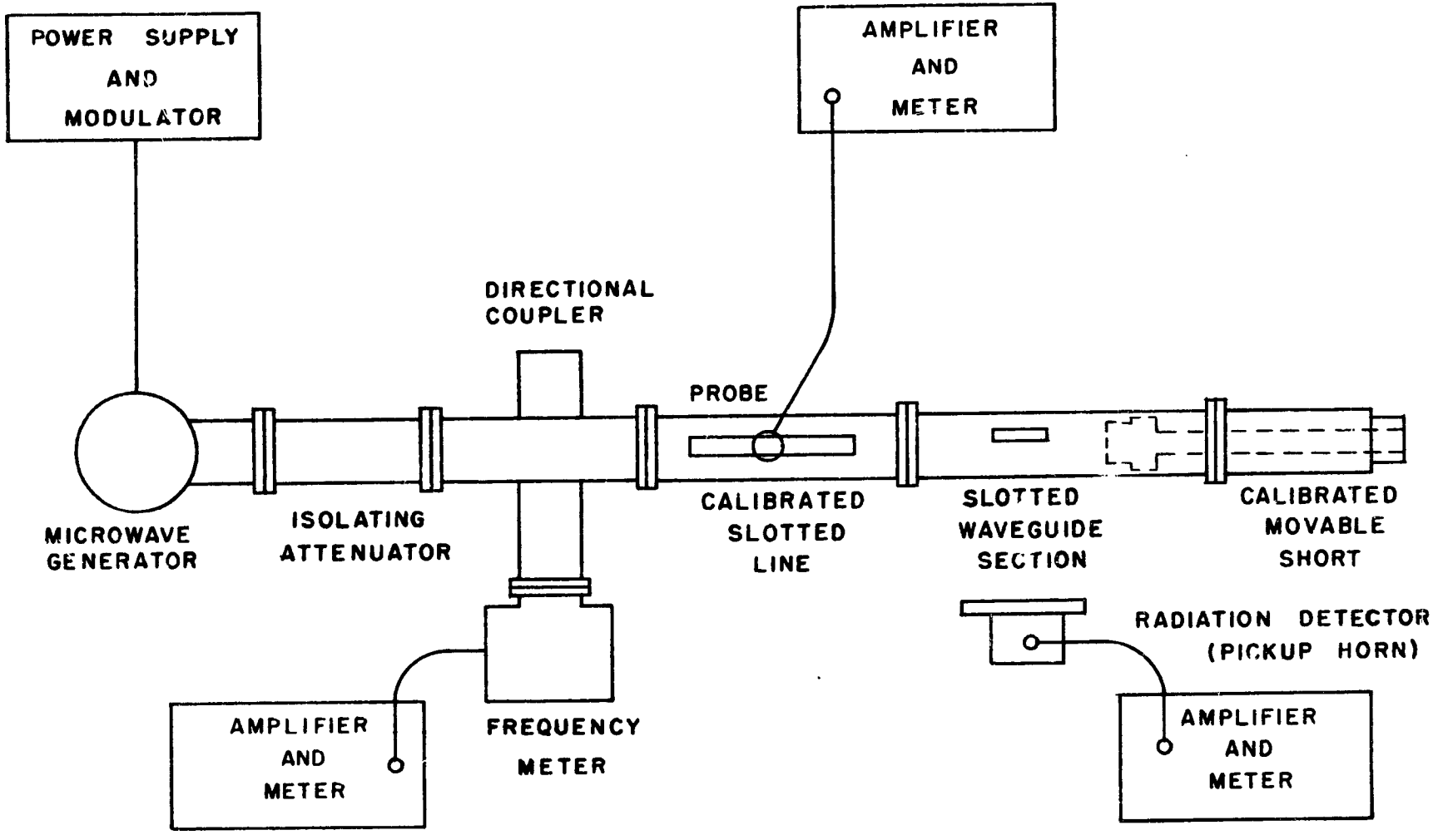

Figure II-20. Typical Slot Impedance Measurement

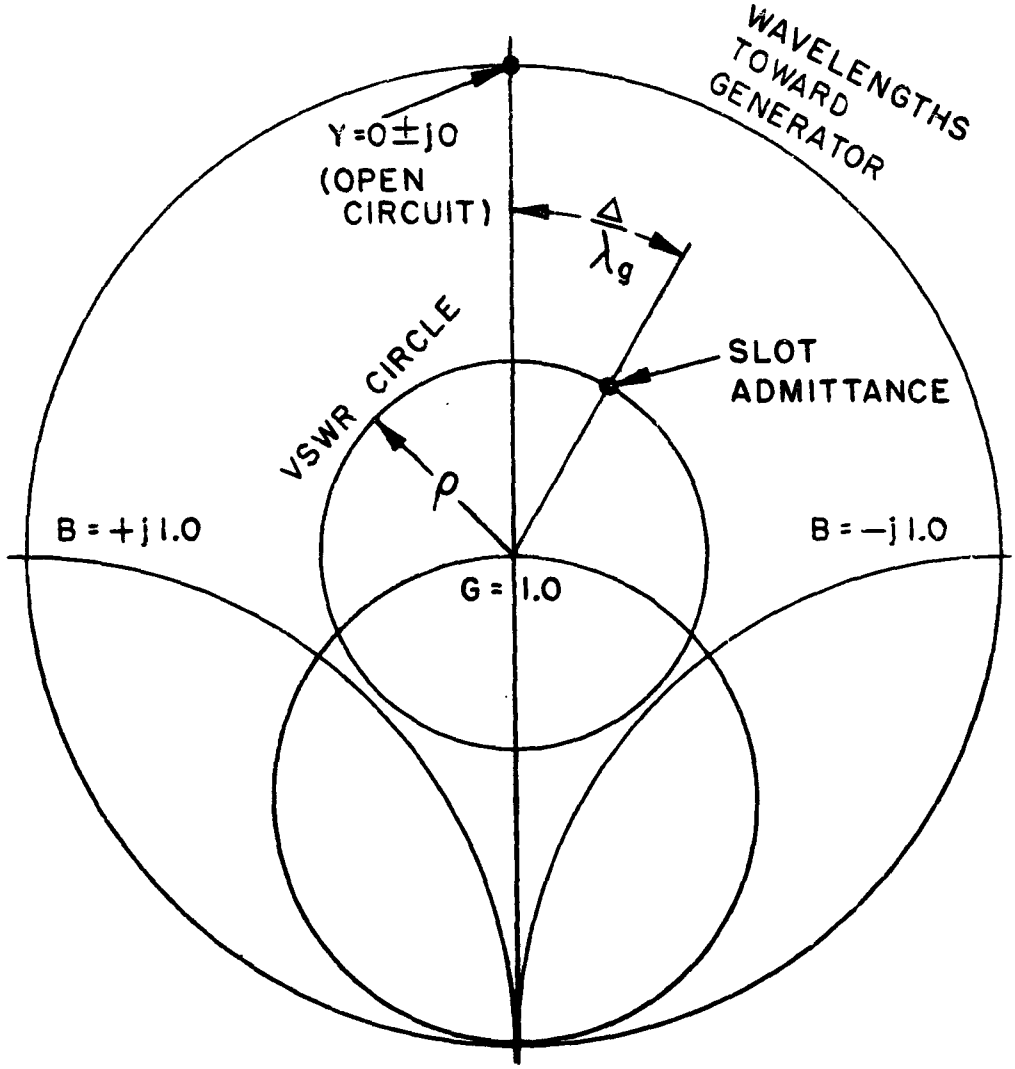

Figure II-21. Calculation of Slot Admittance on Smith Admittance Chart

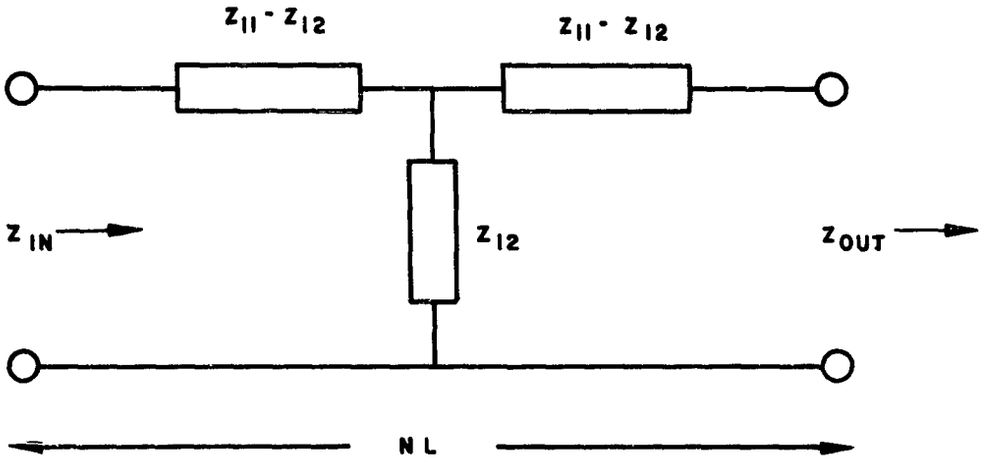

A) SERIES AND SHUNT ELEMENTS OF EQUIVALENT T

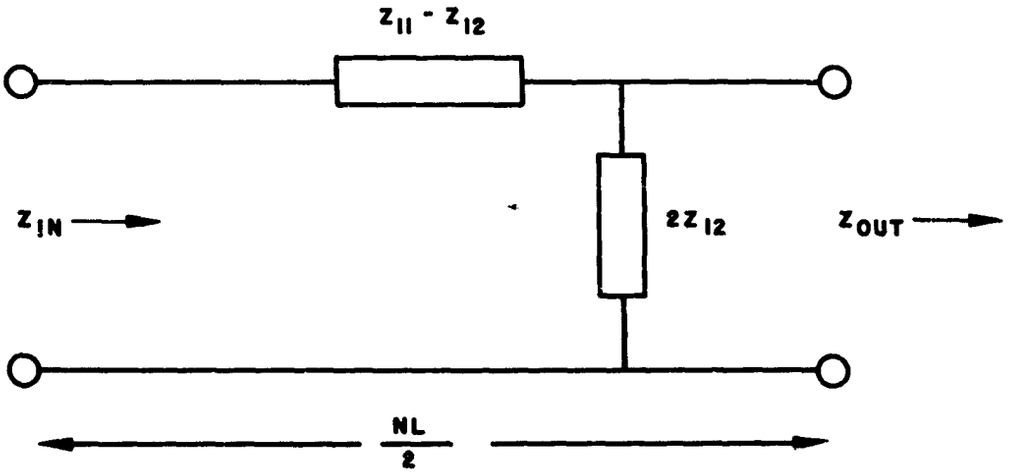

B) OPEN- AND SHORT- CIRCUIT IMPEDANCE OF HALF THE NETWORK

Figure II-22. Equivalent Networks

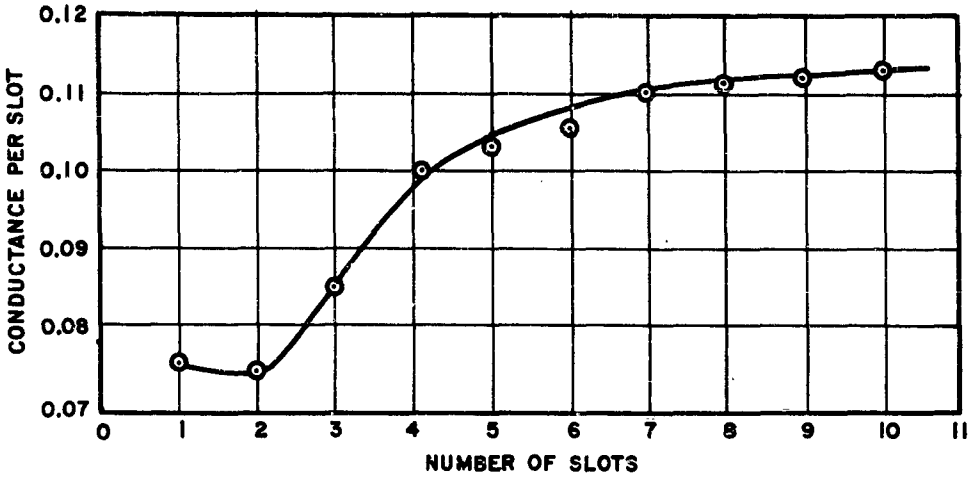

A)

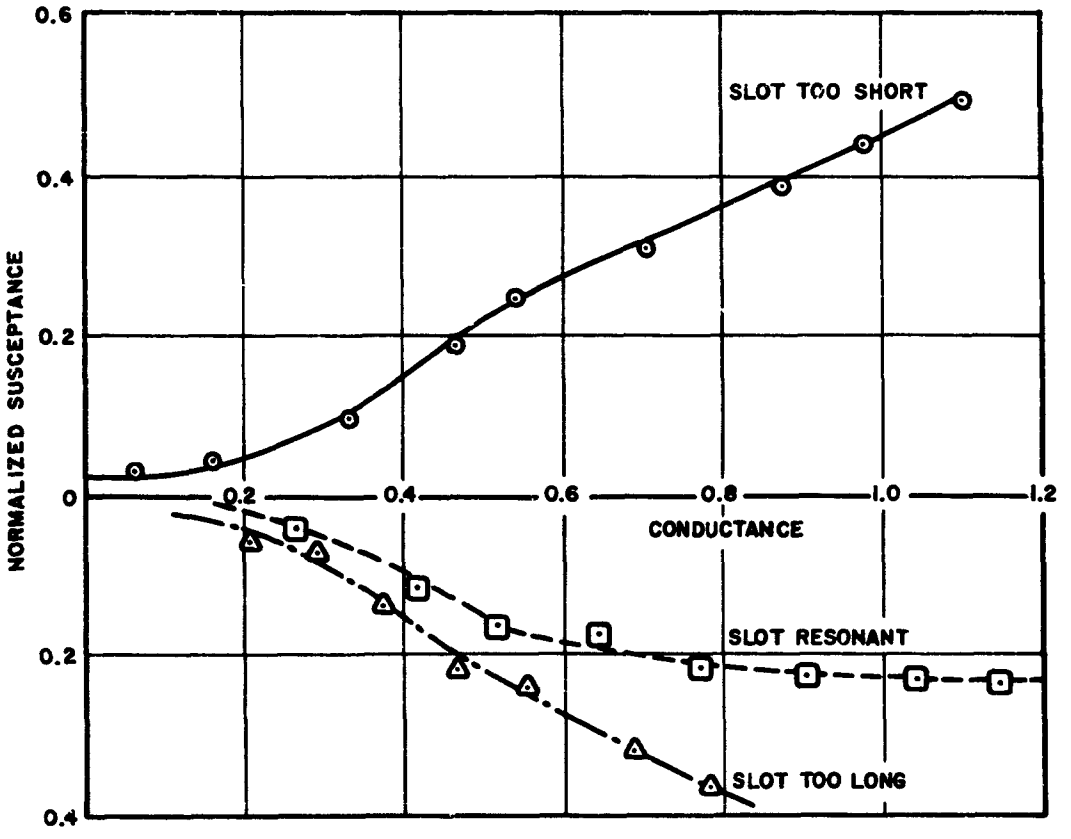

B)

Figure II-23. Incremental Conductance

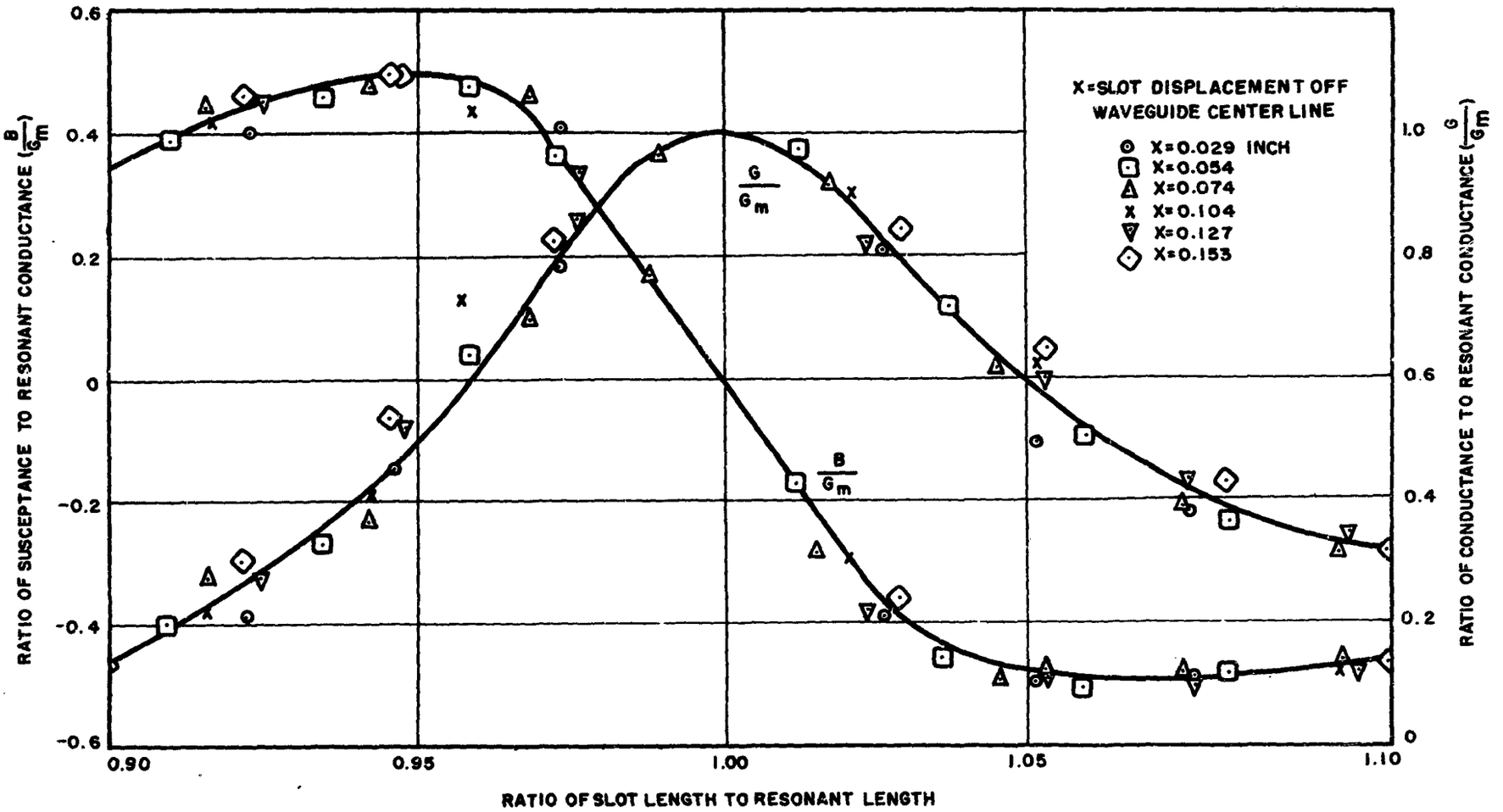

Figure II-24. Variation of Components of Admittance of Longitudinal Shunt Slot

f = 9375 mcps
slot width = 0.0625 inch
waveguide = 1.0 by 0.5 inch

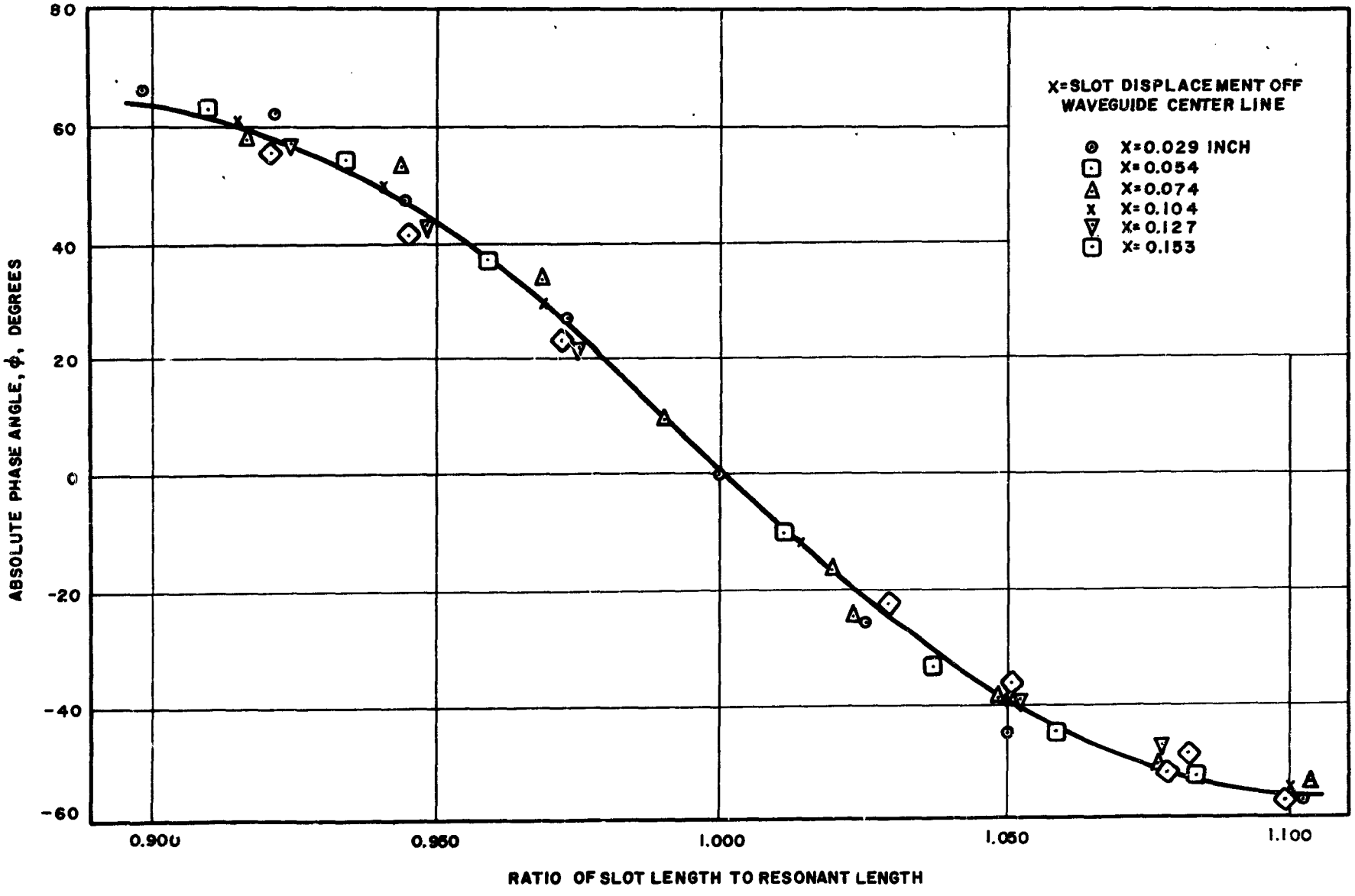

Figure II-25. Absolute Phase Angle of Slot Radiation versus Ratio of Length to Resonant Length

f = 9375 mcps
slot width = 0.0625 inch
waveguide = 1.0 by 0.5 inch

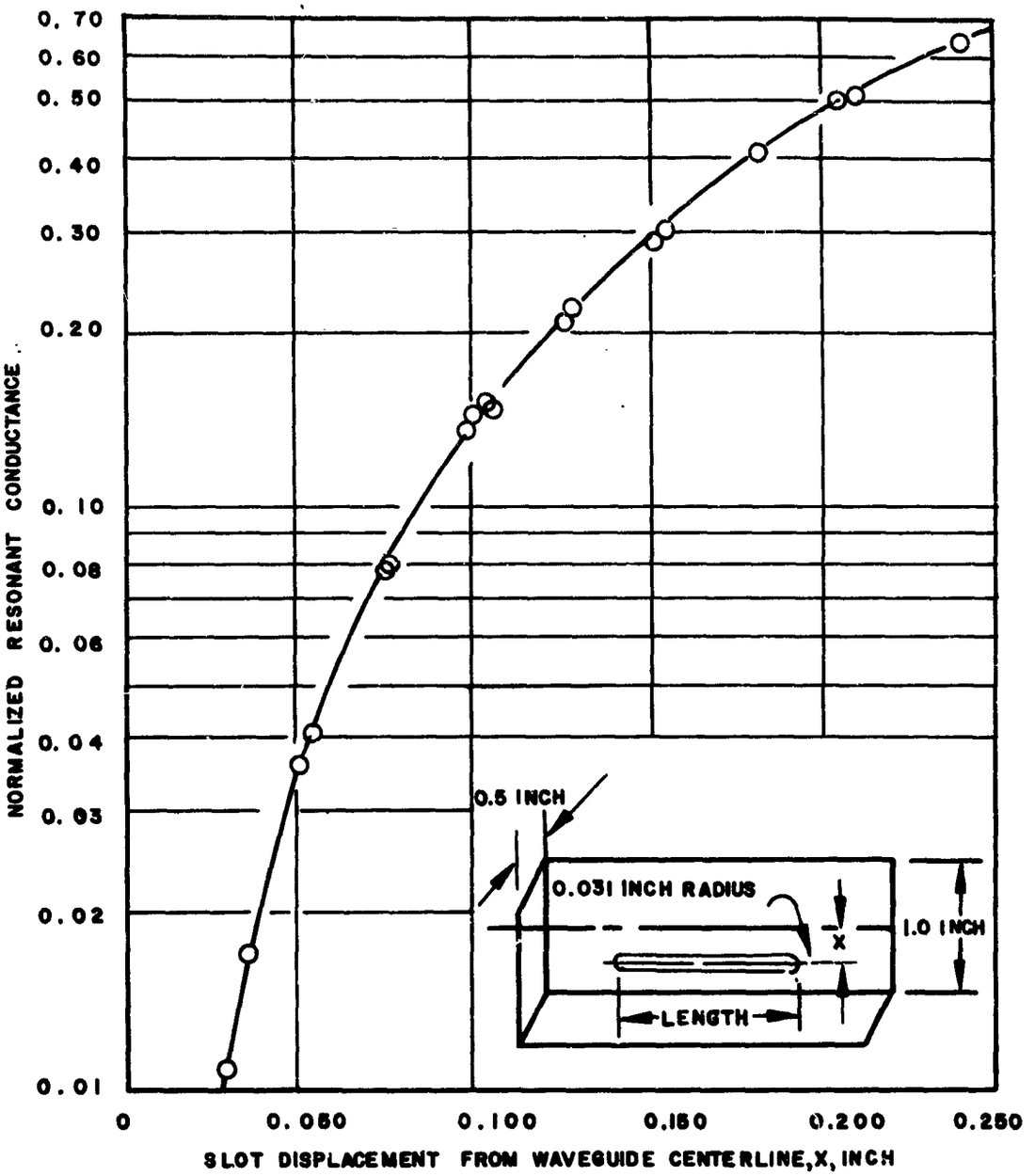

Figure II-26. Resonant Conductance of Longitudinal Shunt Slot versus Slot Displacement
(All points are measured; curve is semi-empirical)

f = 9375 mc/s
waveguide = 1.0 by 0.5 inch
slot width = 0.0625 inch

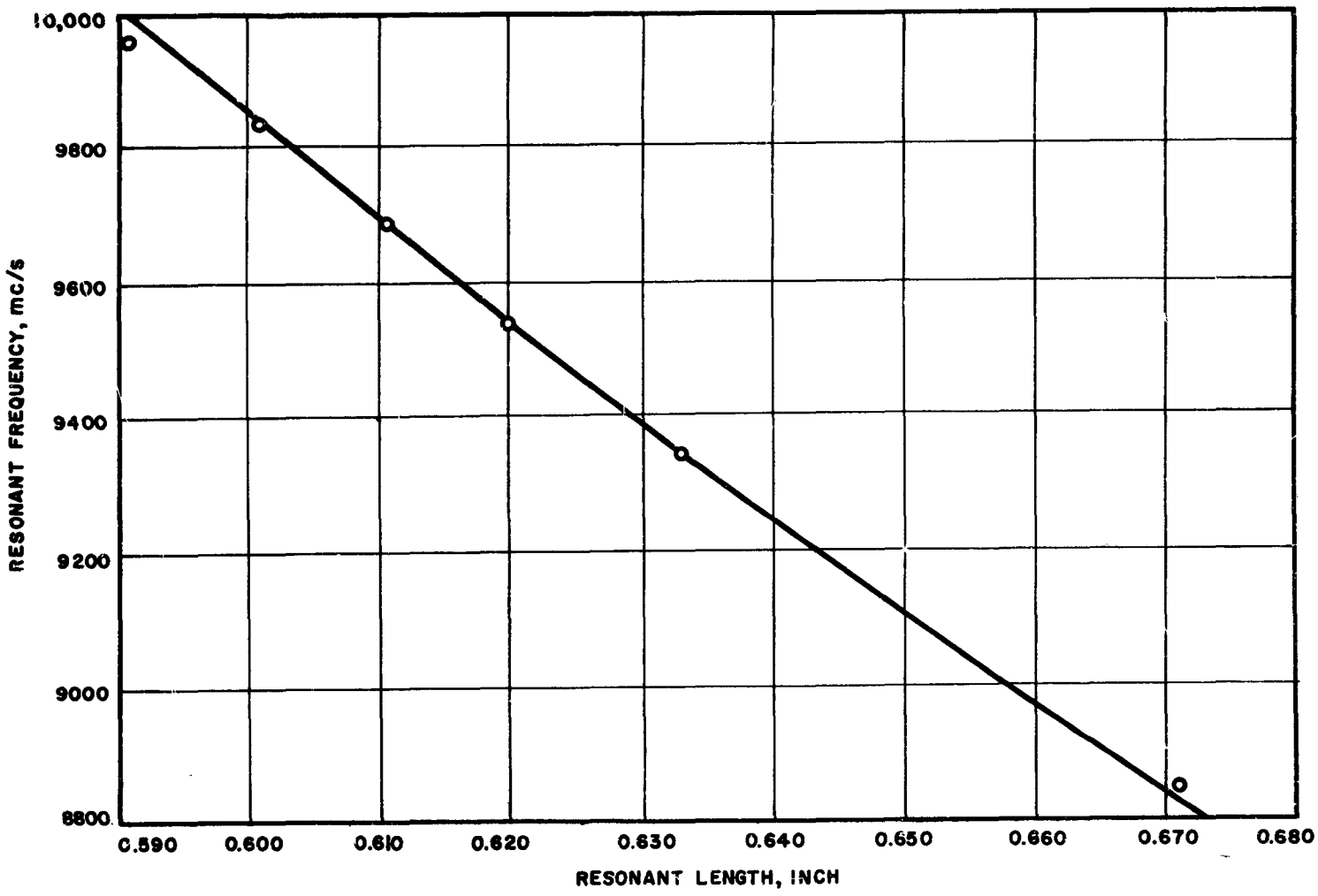

Figure II-27. Shunt Slot Resonant Frequency versus Length
(Points are measured; curve is semi-empirical)

slot width = 0.0625 inch
waveguide = 1.0 by 0.5 inch
slot displacement, X = 0.2040 inch

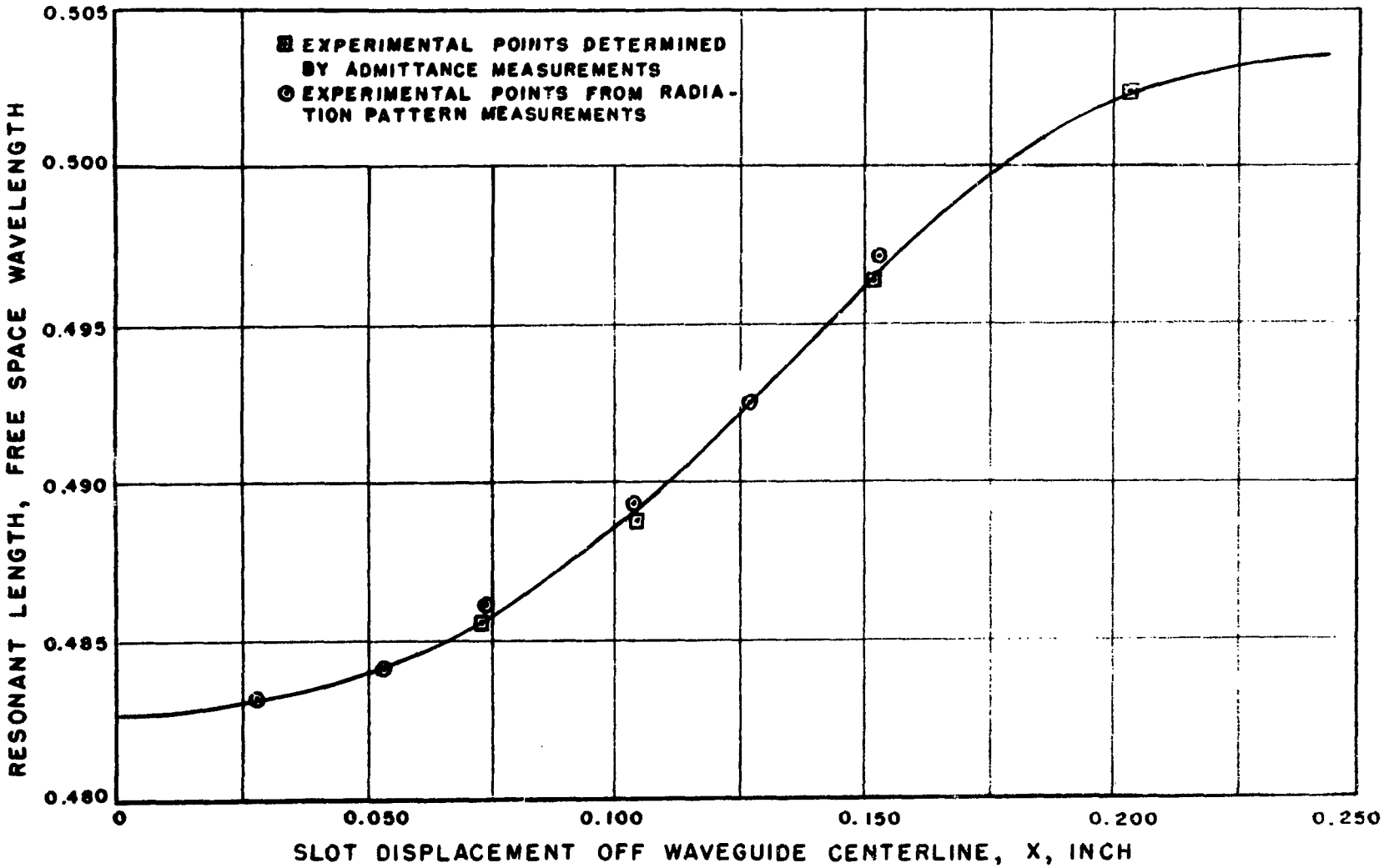

Figure II-28. Shunt Slot Resonant Frequency versus Displacement Off Waveguide Centerline

slot width = 0.0625 inch
waveguide = 1.0 by 0.5 inch

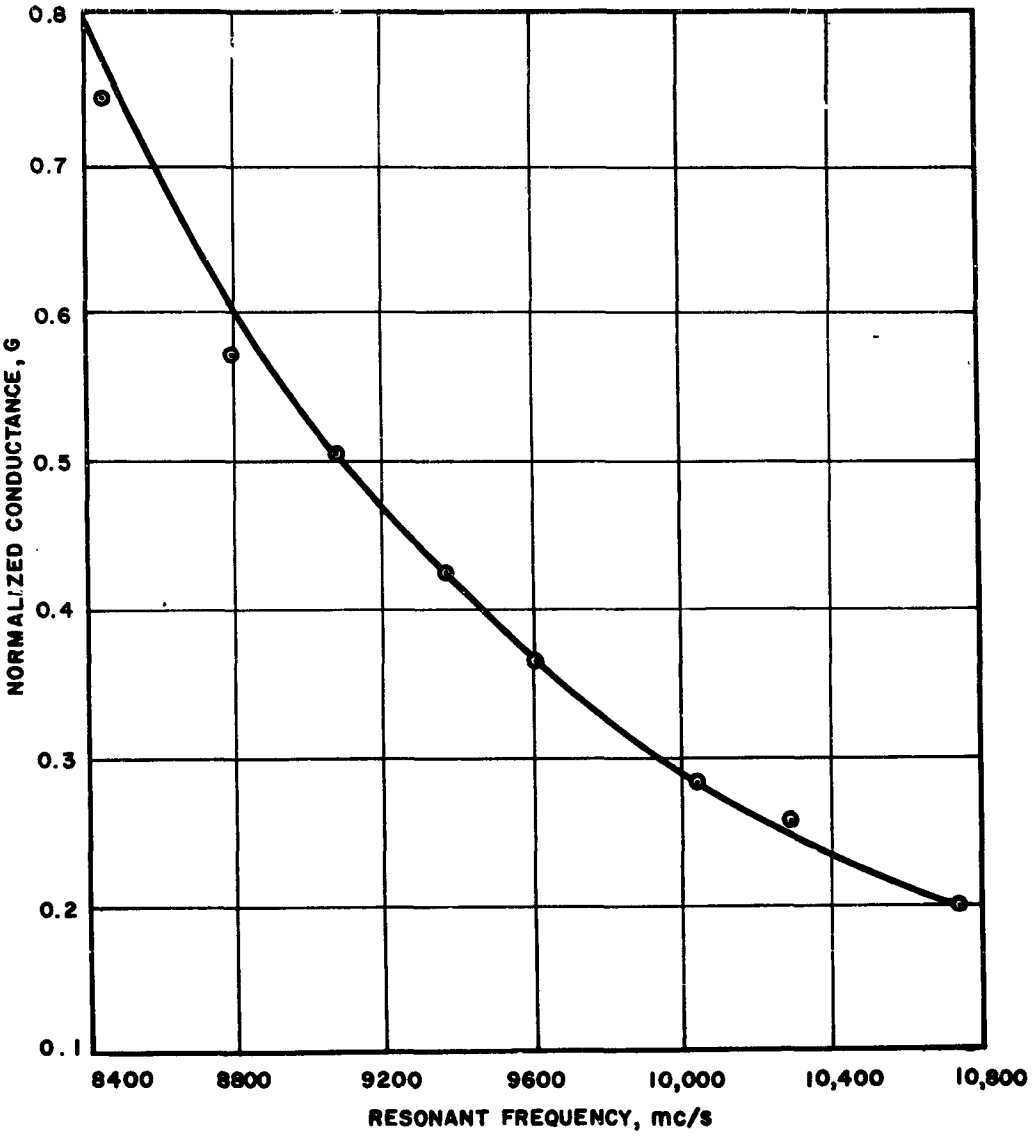

Figure II-29. Resonant Conductance of Longitudinal Shunt Slot
(Points are measured; curve is semi-empirical)

slot width = 0.0625 inch
waveguide = 1.0 by 0.5 inch
slot displacement, X = 0.1833 inch

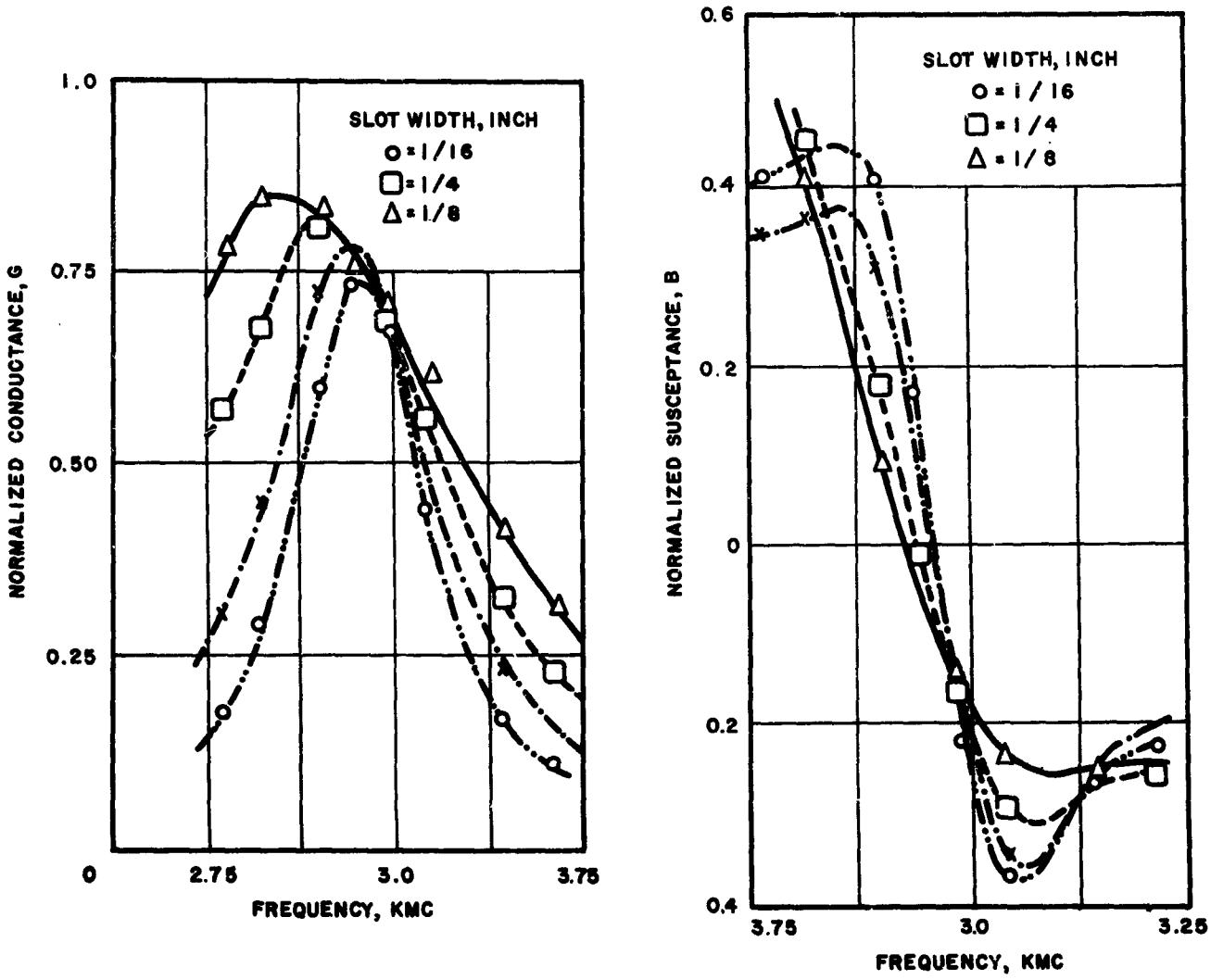

Figure II-30. Shunt Slot Admittance Characteristics

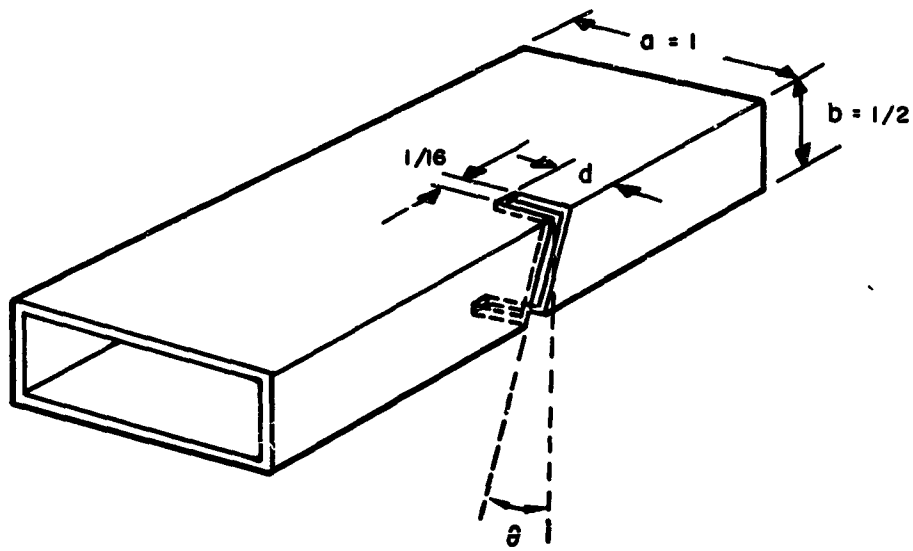

Figure II-31. Edge Slot in Rectangular Waveguide (All dimensions are in inches)

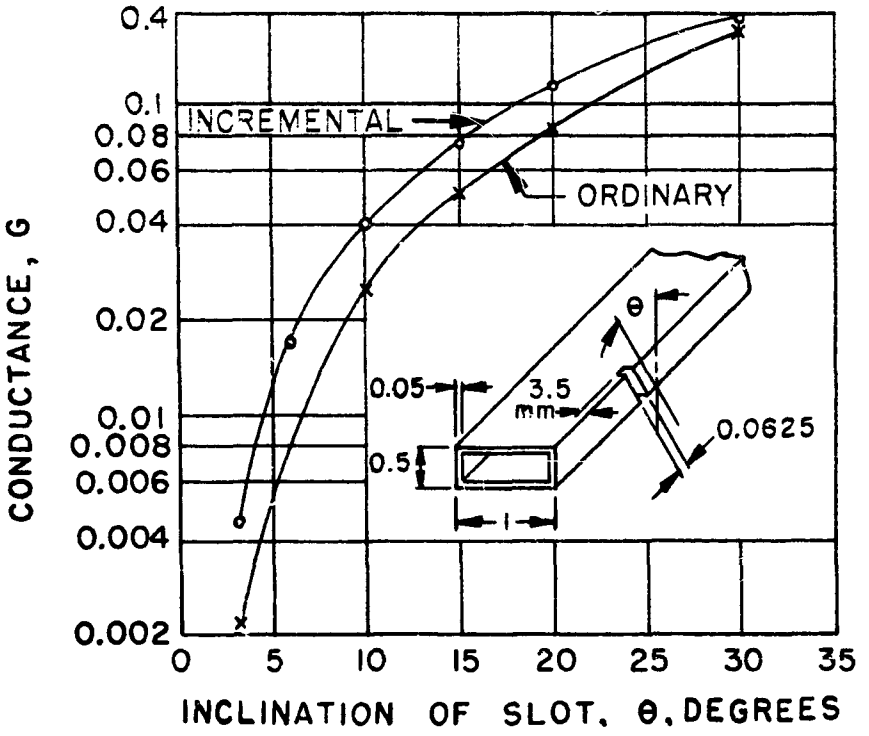

Figure II-32. Incremental and Single Slot Conductance
(Unmarked dimensions of waveguide section are in inches)
λ = 3.20 centimeters

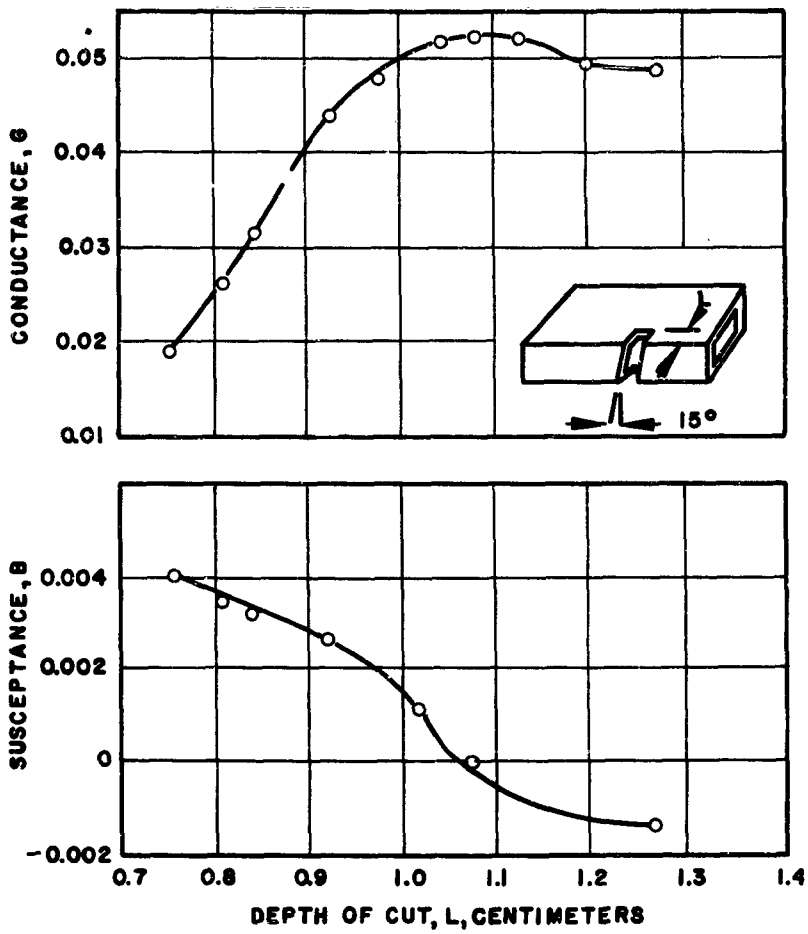

Figure II-33. Variation of Slot Admittance with Depth of Cut

waveguide = 1-3/8 by 2-7/8 inches
λ = 10.7 centimeters

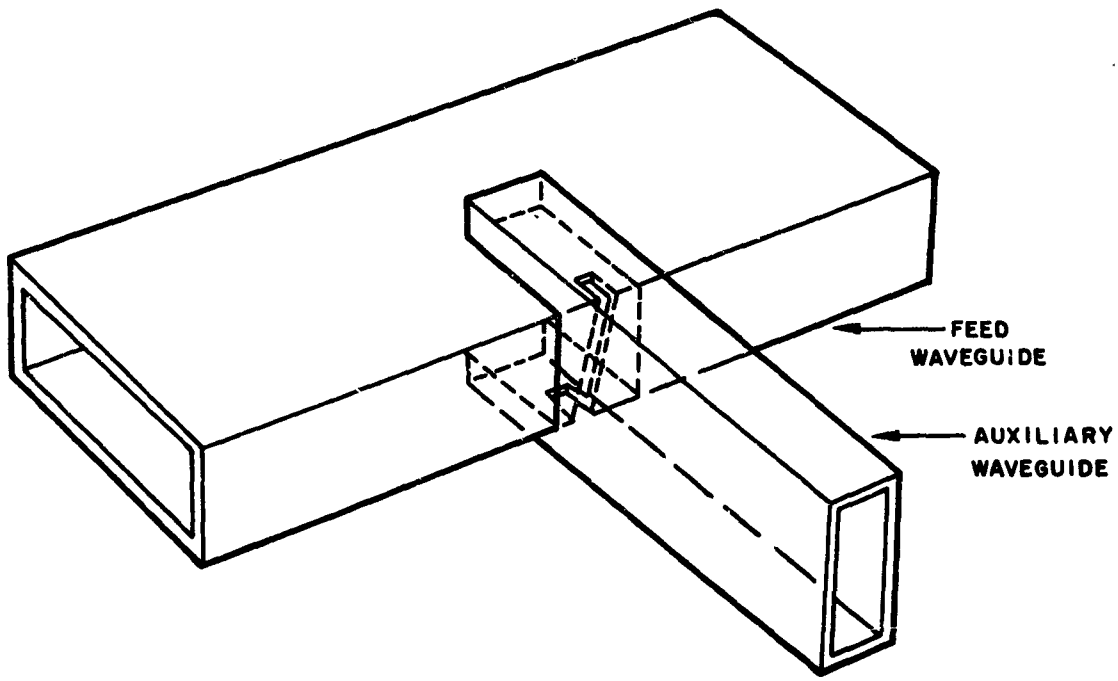

Figure II-34. Edge-Slot Coupling to Auxiliary Waveguide

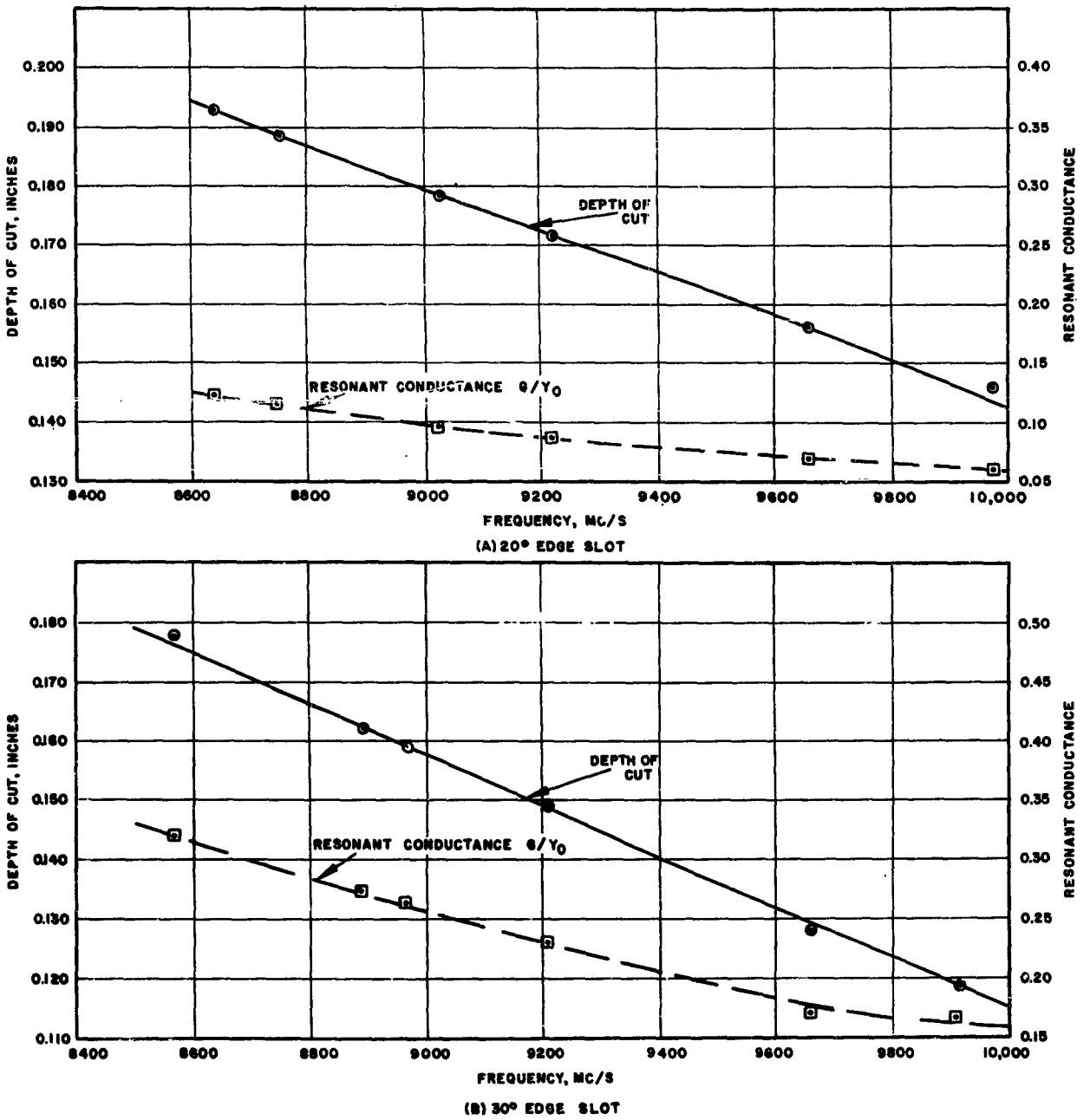

Figure II-35. Conductance and Depth of Cut versus Resonant Frequency for Edge Slots
(Shunt-series coupling between waveguides)

Auxiliary guide terminated by Z_o
waveguide = 0.400 by 0.900 inch
wall thickness = 0.050 inch

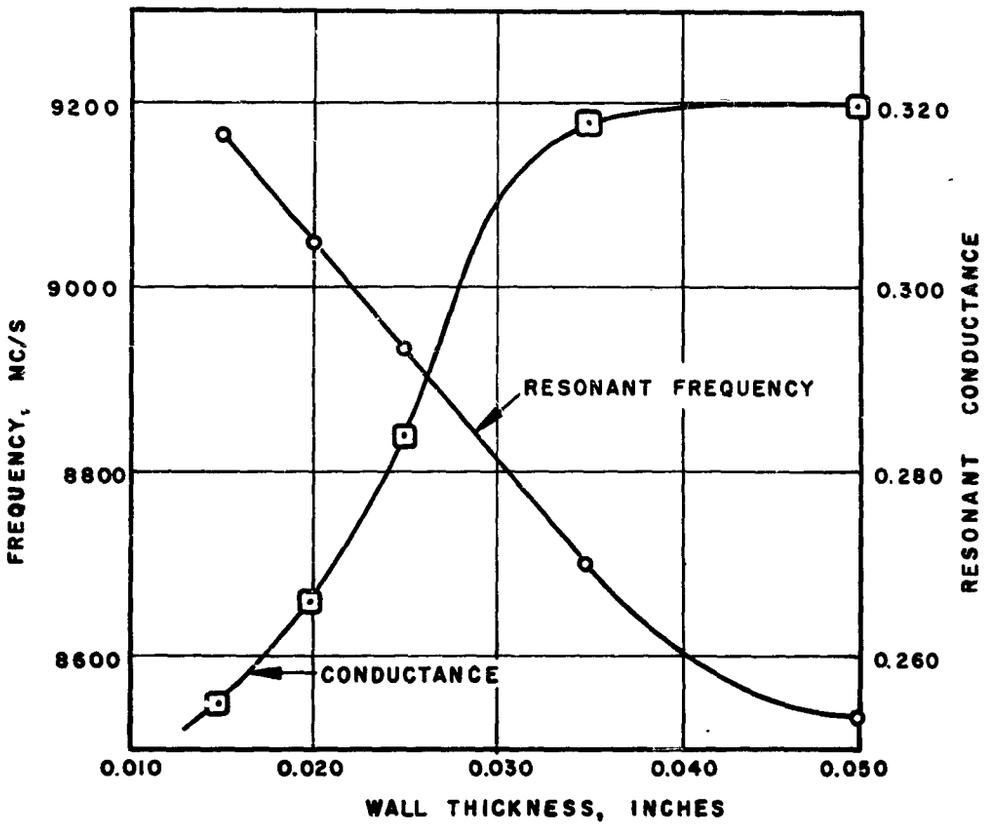

Figure II-36. Conductance and Resonant Frequency versus Wall Thickness for a 30° Edge Slot

waveguide = 1 by 0.5 by 0.05 inch
slot width = 0.064 inch

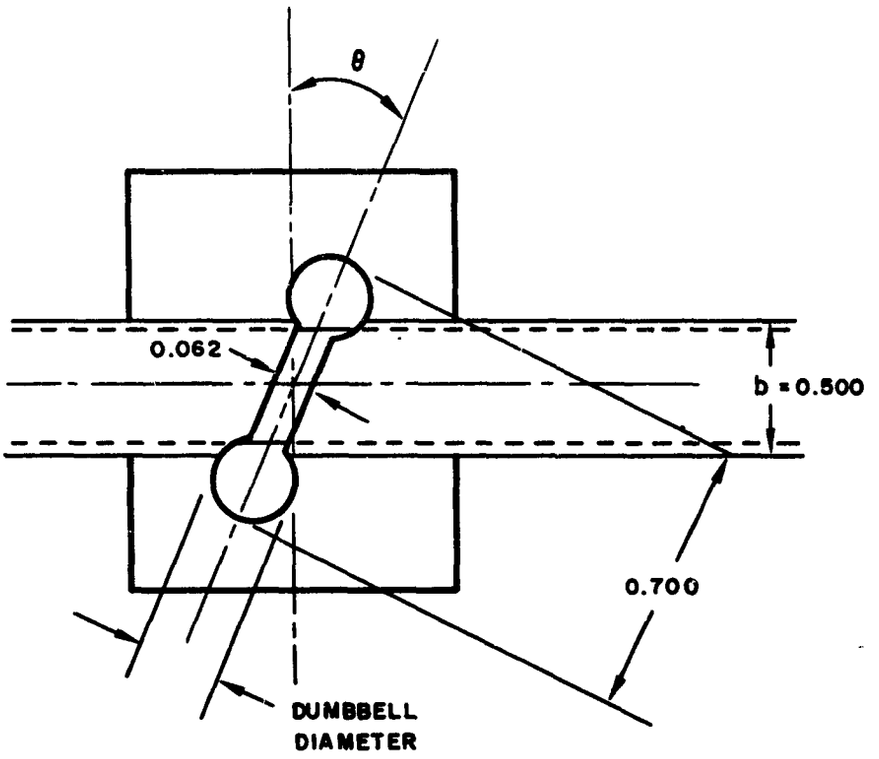

Figure II-37. Dumbbell Slot in Narrow Face of Waveguide (Dimensions in inches)

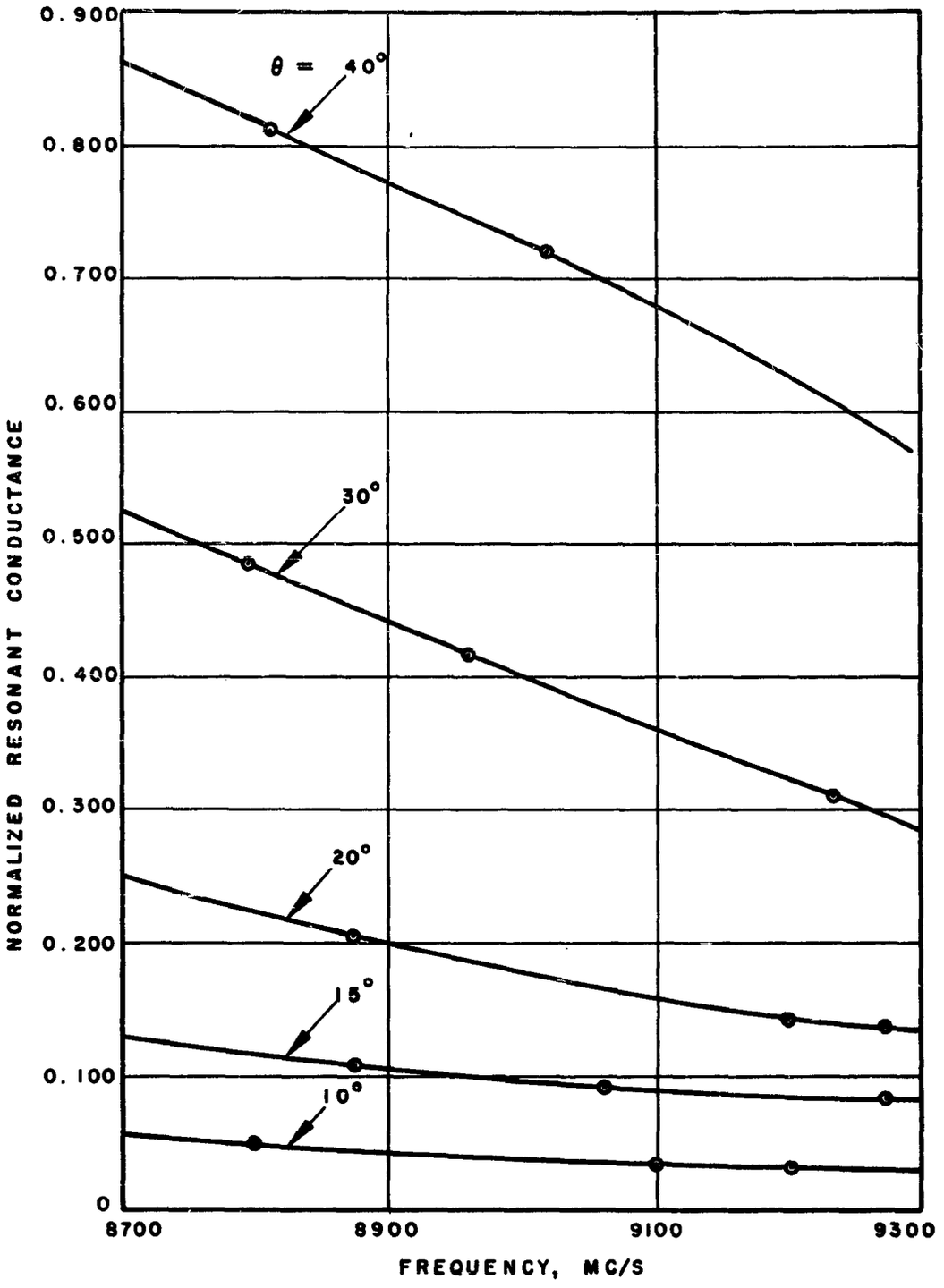

Figure II-38. Resonant Conductances of Dumbbell Slots as Function of Inclination, θ

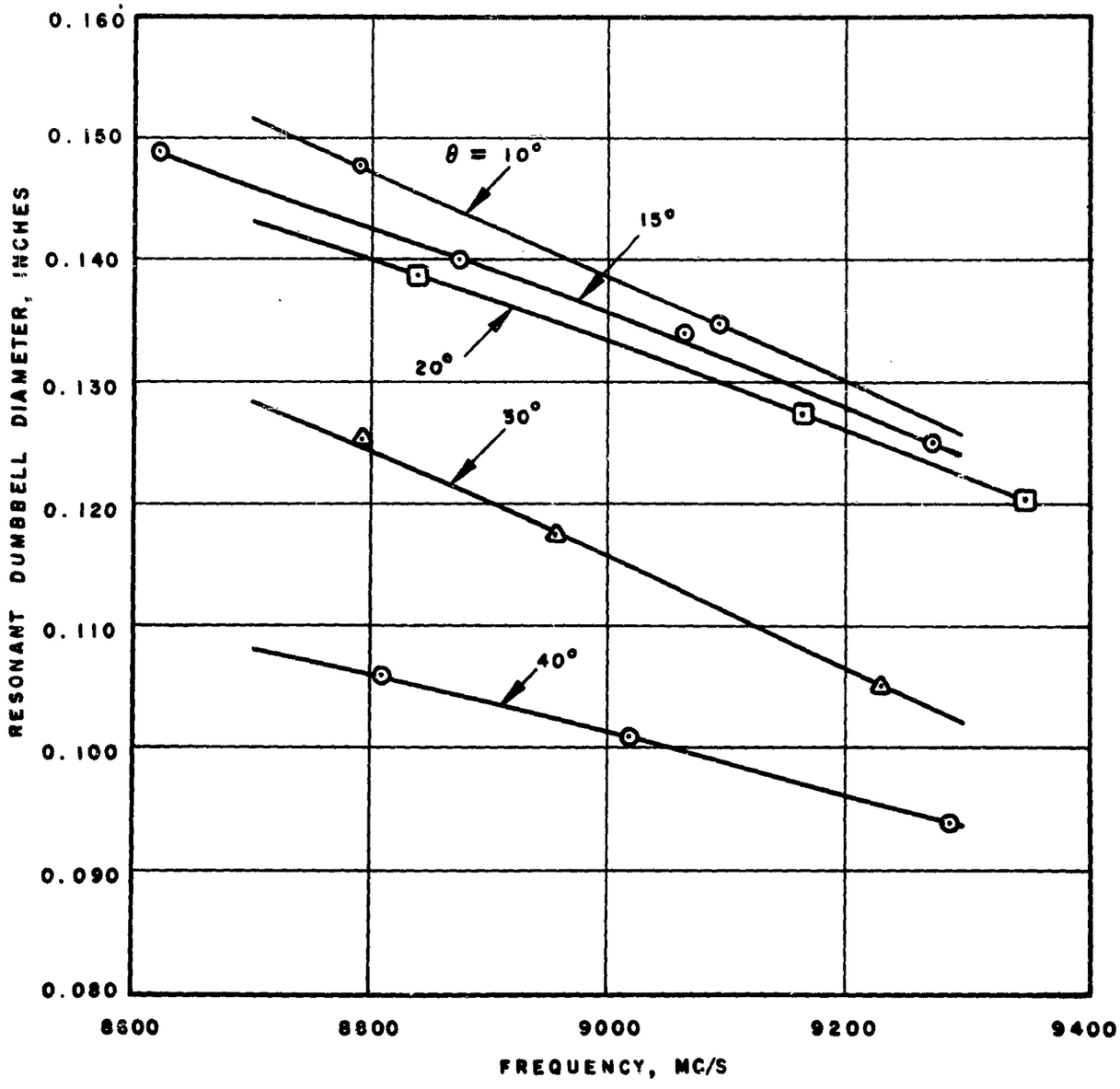

Figure II-39. Resonant Dumbbell Diameters as Function of Slot Inclination, θ

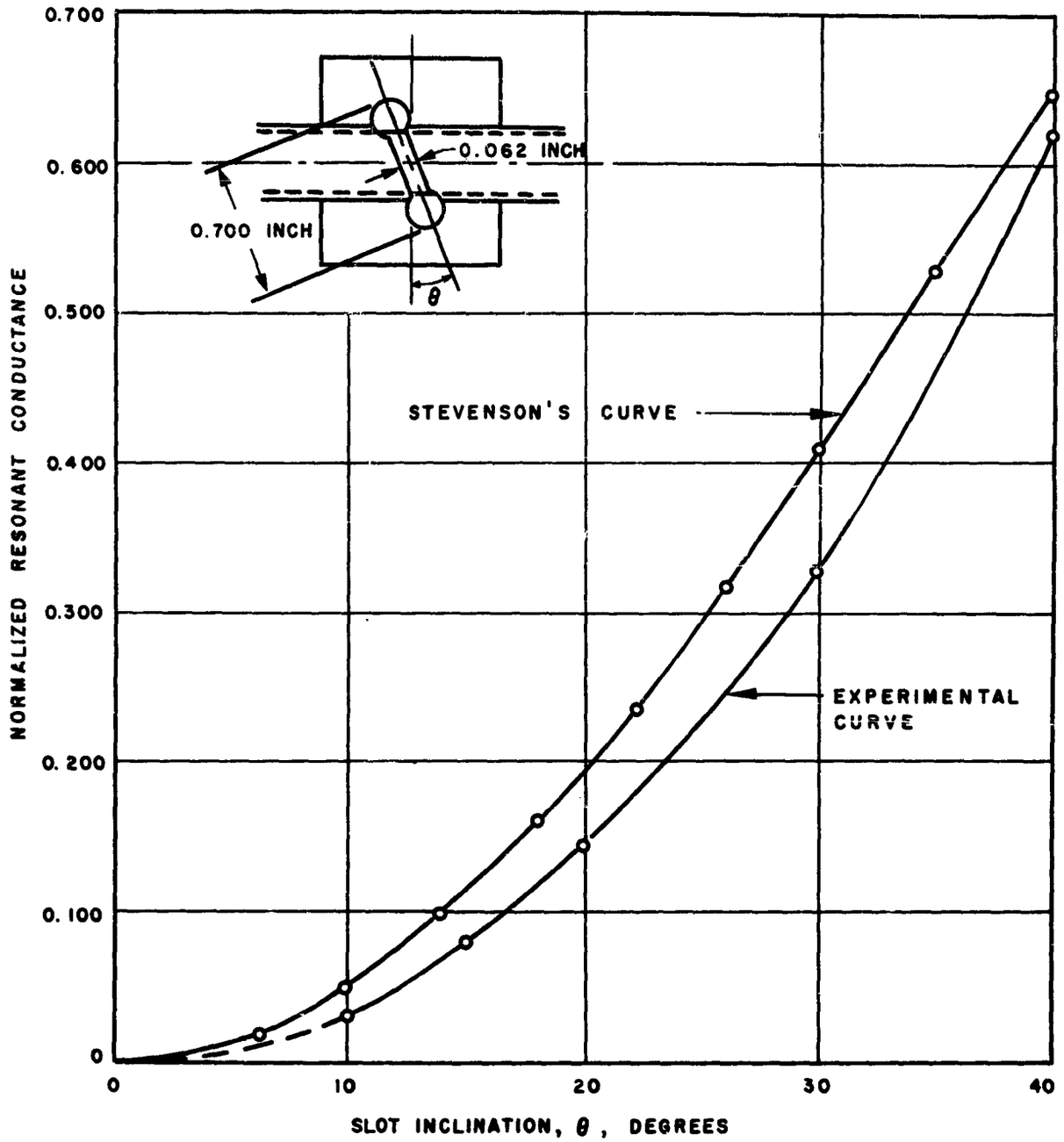

Figure II-40. Resonant Conductance of Dumbbell Slot as Function of Inclination at 9200 mcps

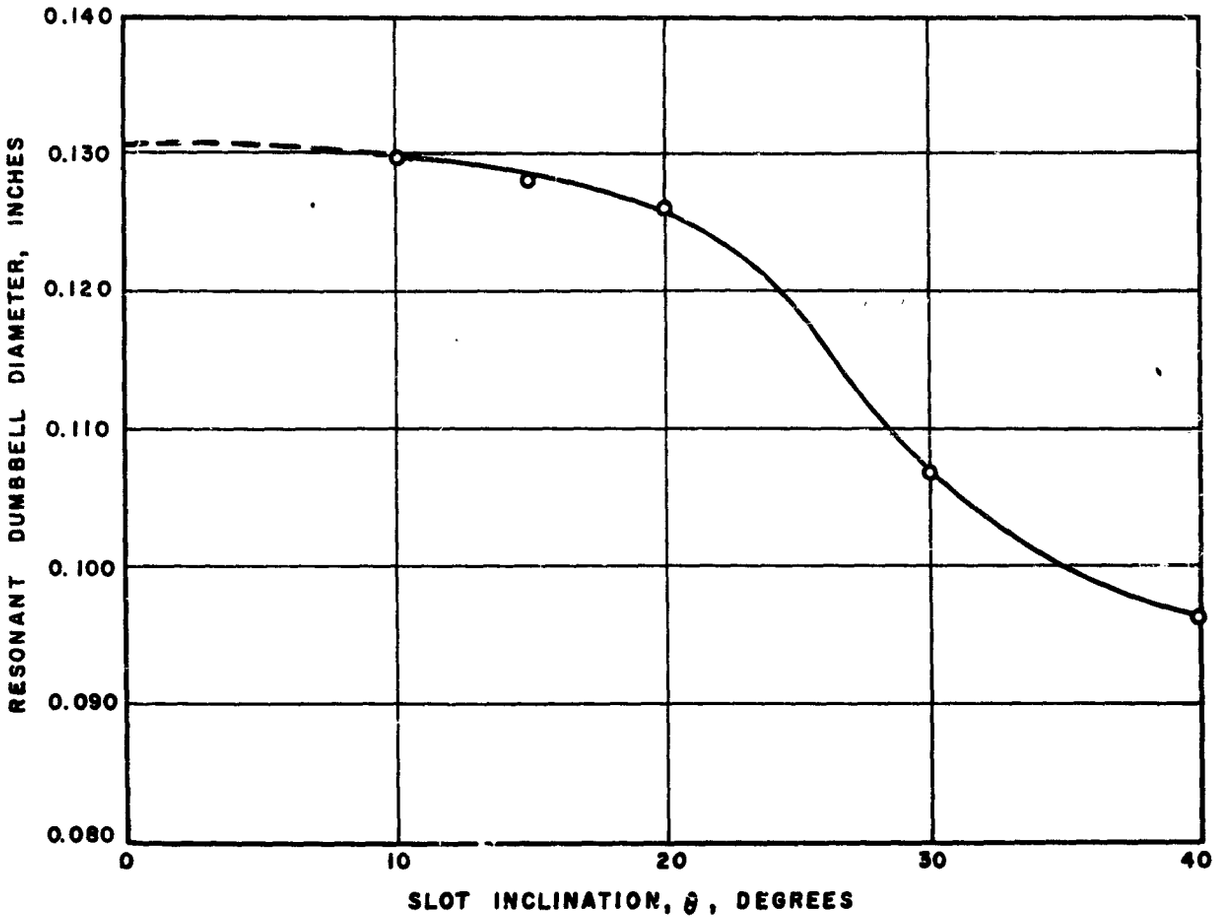

Figure II-41. Resonant Dumbbell Diameter as Function of Slot Inclination at 9200 mcps

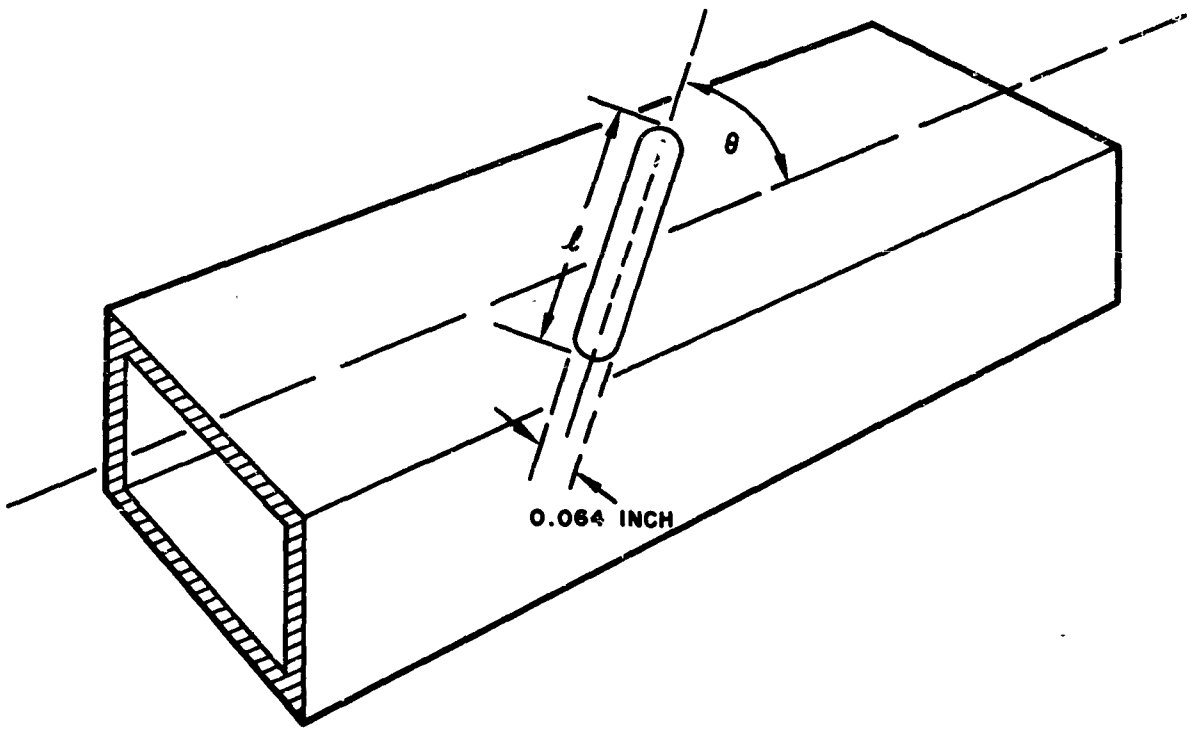

Figure II-42. Series Slot in Rectangular Guide

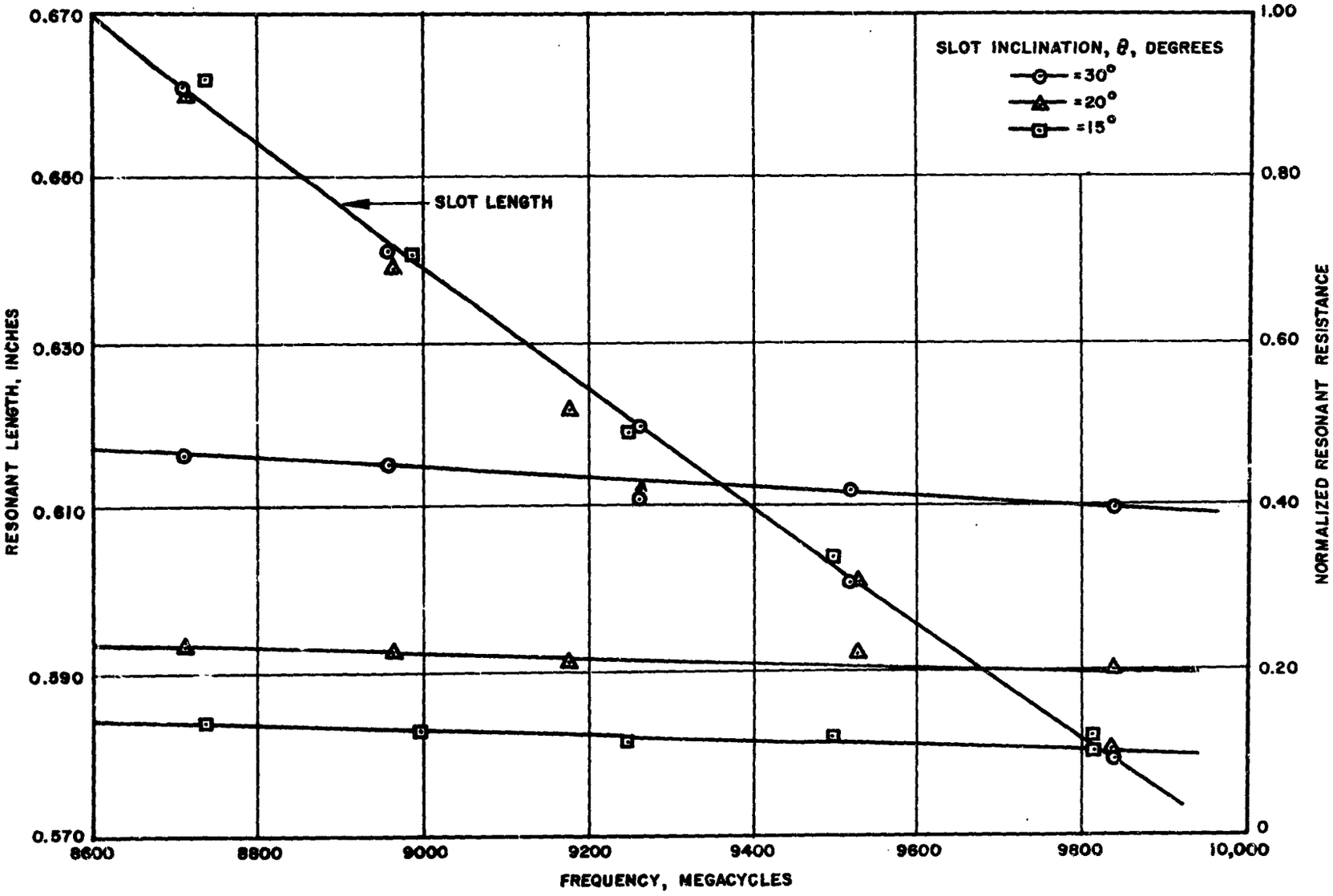

Figure II-.3. Resonant Length and Normalized Resistance versus Frequency for Series Inclined Slot on Centerline of Waveguide

waveguide = 0.400 by 0.900 inch

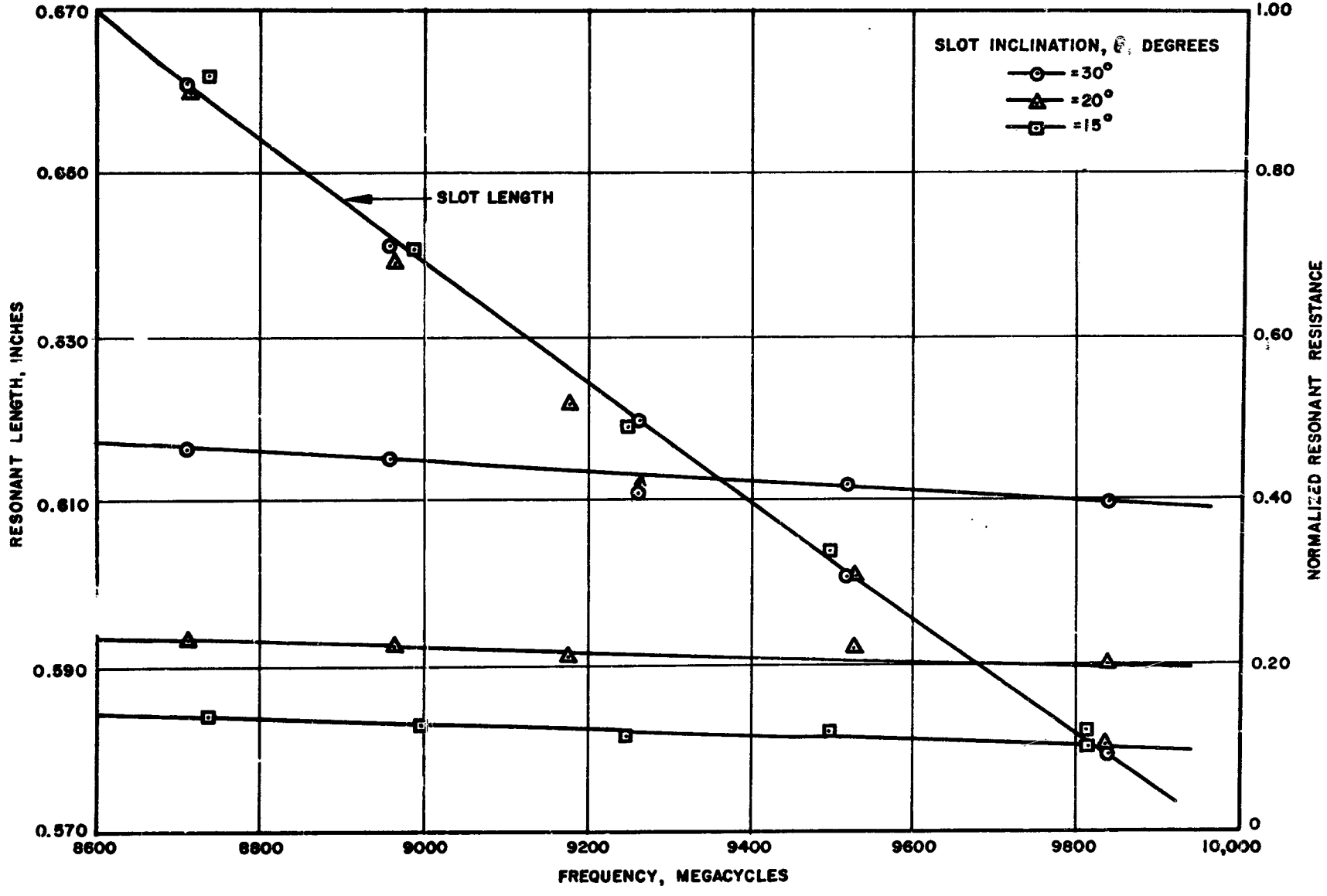

Figure II-43. Resonant Length and Normalized Resistance versus Frequency for Series Inclined Slot on Centerline of Waveguide

waveguide = 0.400 by 0.900 inch

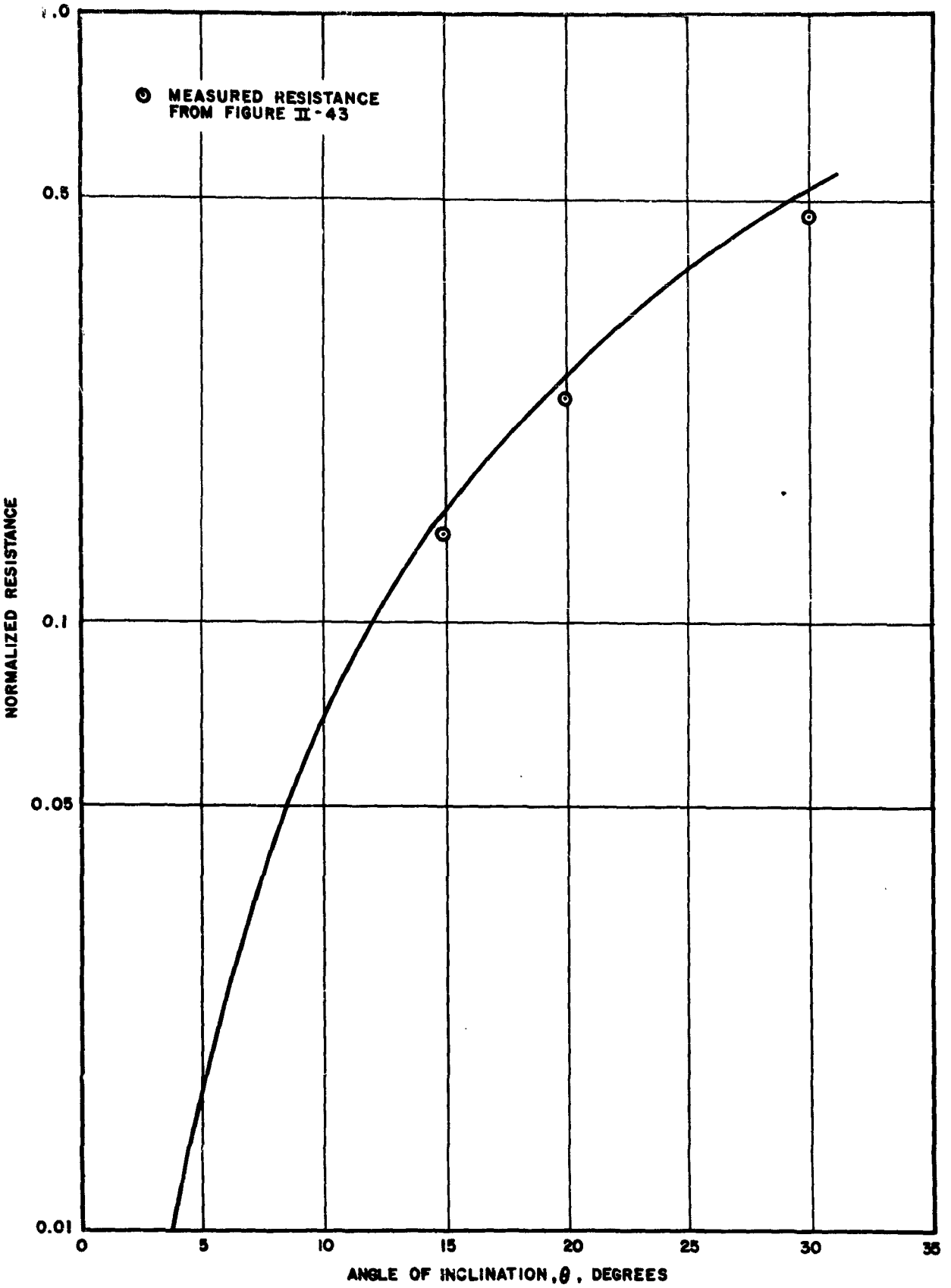

Figure II-44. Comparison of Measured Resistance with Theoretical Curve Calculated from Stevenson's Equation

f = 8700 megacycles

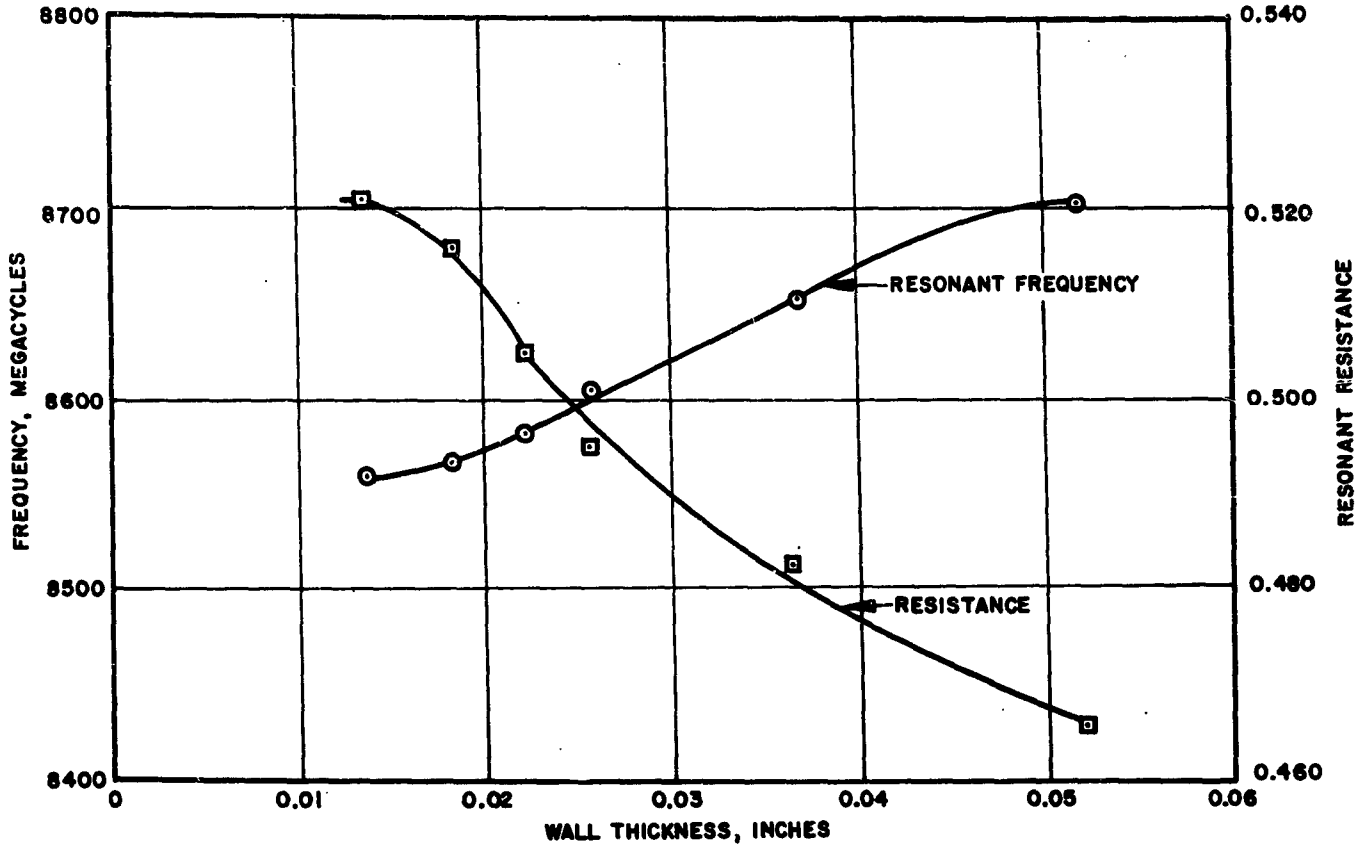

Figure II-45. Resistance and Resonant Frequency versus Wall Thickness for Series Slot

slot inclination = 30°
slot length = 0.661 inch
slot width = 0.064 inch
waveguide = 1 by 0.5 by 0.05 inch

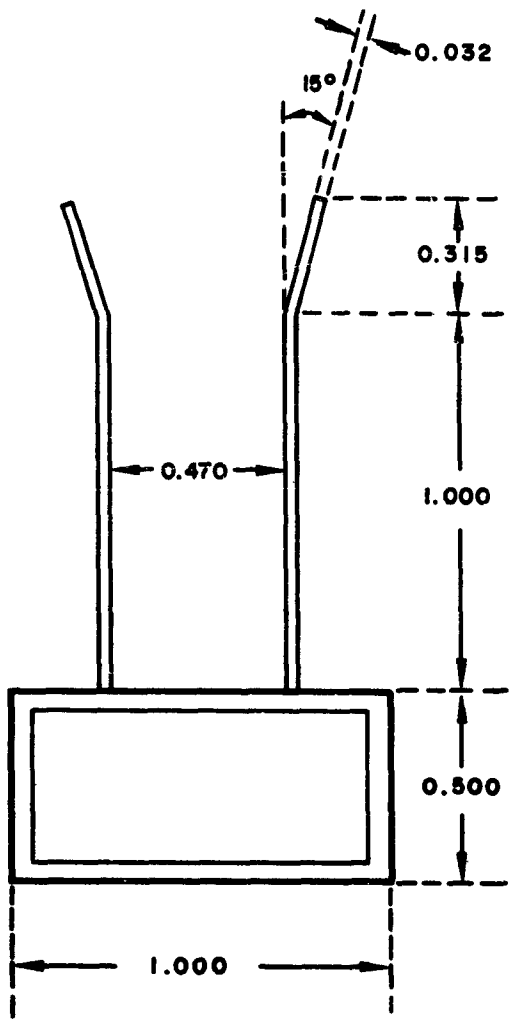

Figure II-46. Flared Parallel-Plate Horn
(All unmarked dimensions in inches)

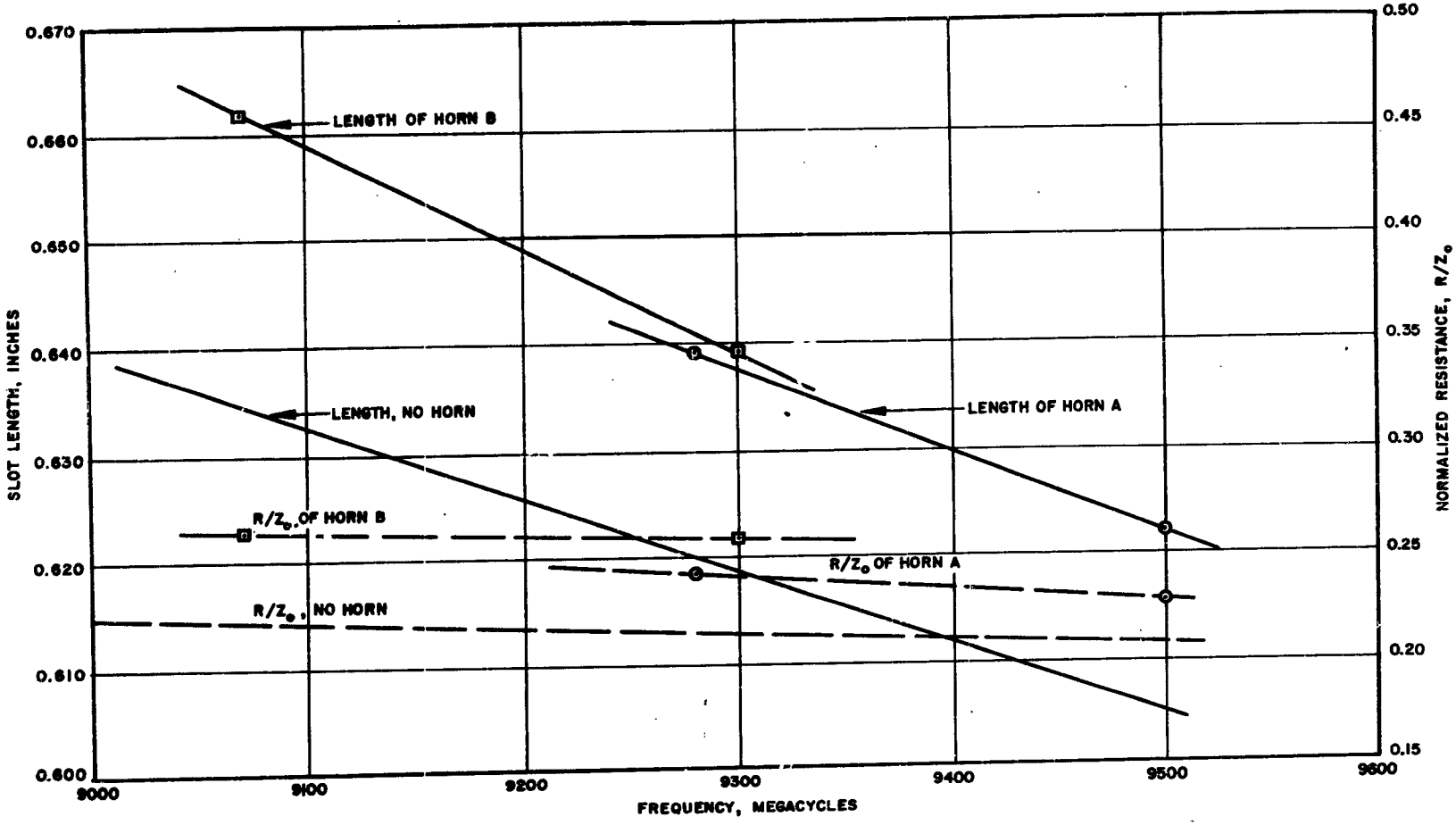

Figure II-47. Resonant Lengths and Resistances versus Frequency for 20° Slot with Two Different Horns

slot width = 0.625 inch
waveguide = 0.5 by 1 inch
horn A = see Figure II-46
horn B = flare length 2.2
flare angle 40°
no horn = see Figure II-43

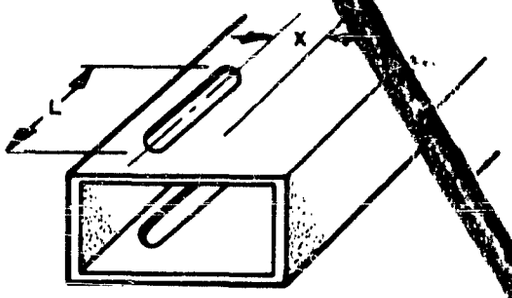

Figure II-48 Arrangement of Slots on Waveguide

slot width = 0.0625 inch
waveguide = 1 by 0.5 by 0.050 inch

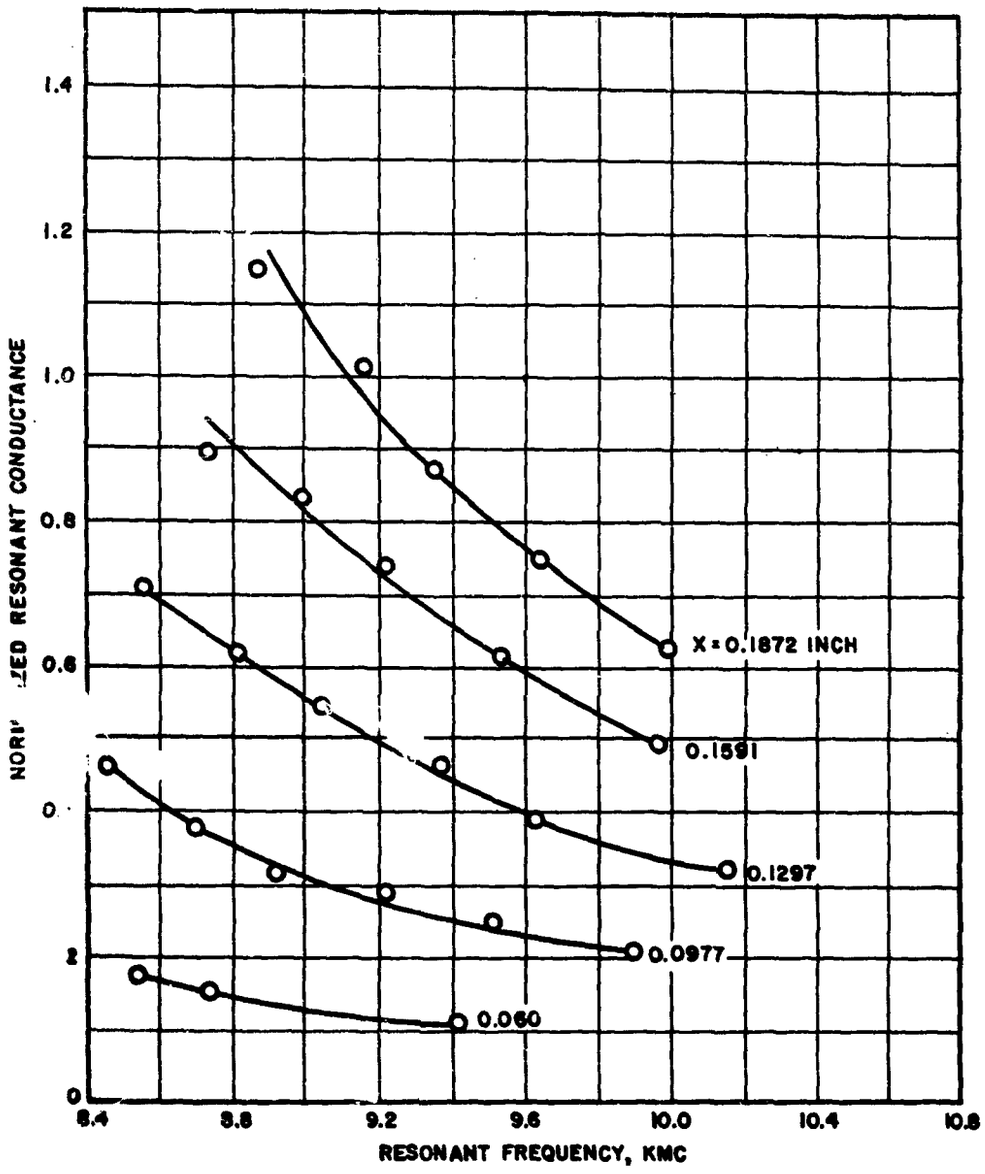

A) Curves of Resonant Conductance versus Resonant Frequency

Figure II-49. In-Phase Shunt Slot Pair Characteristics

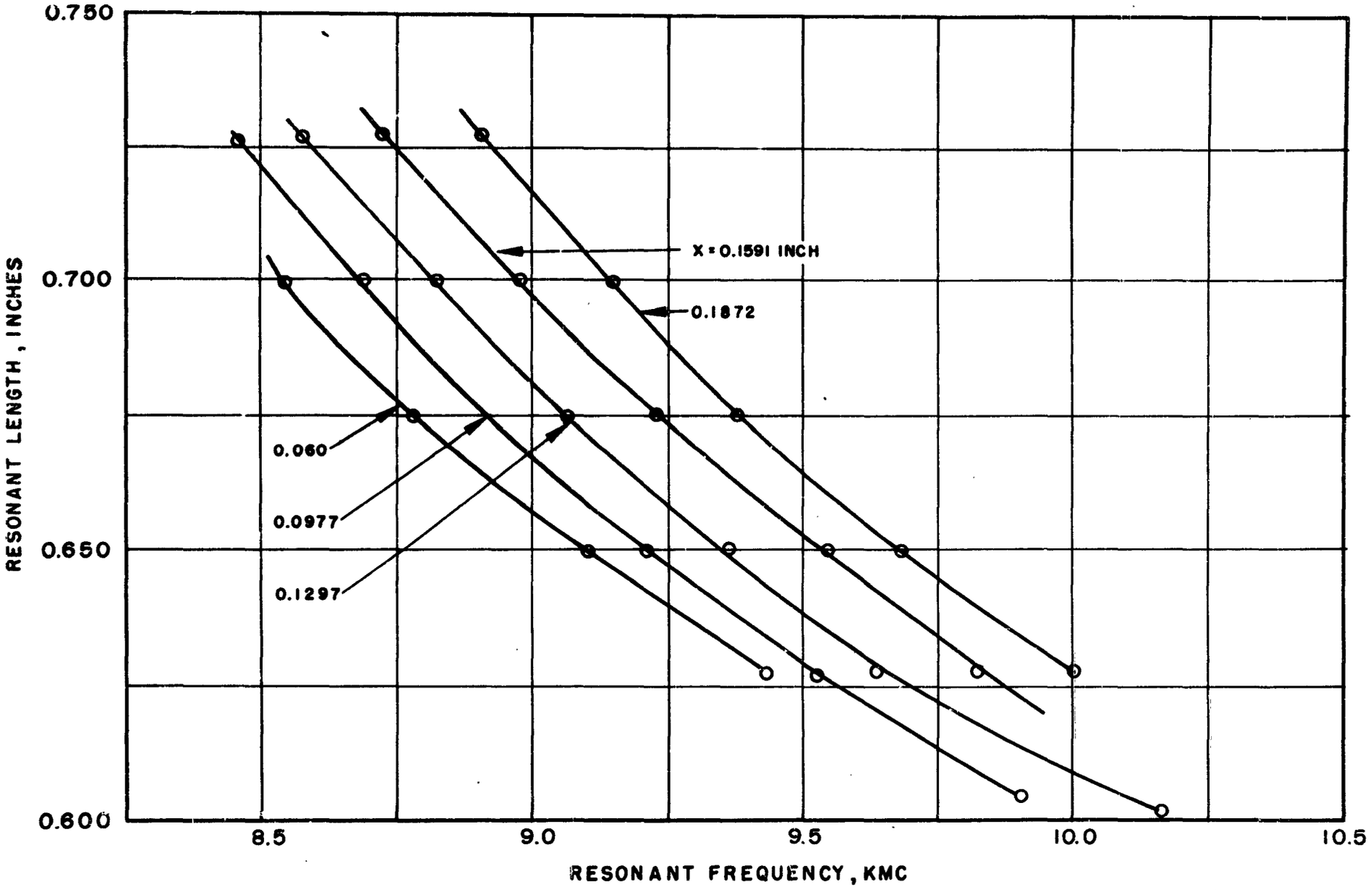

B) Curves of Resonant Length versus Resonant Frequency

Figure II-49. In-Phase Shunt Slot Pair Characteristics

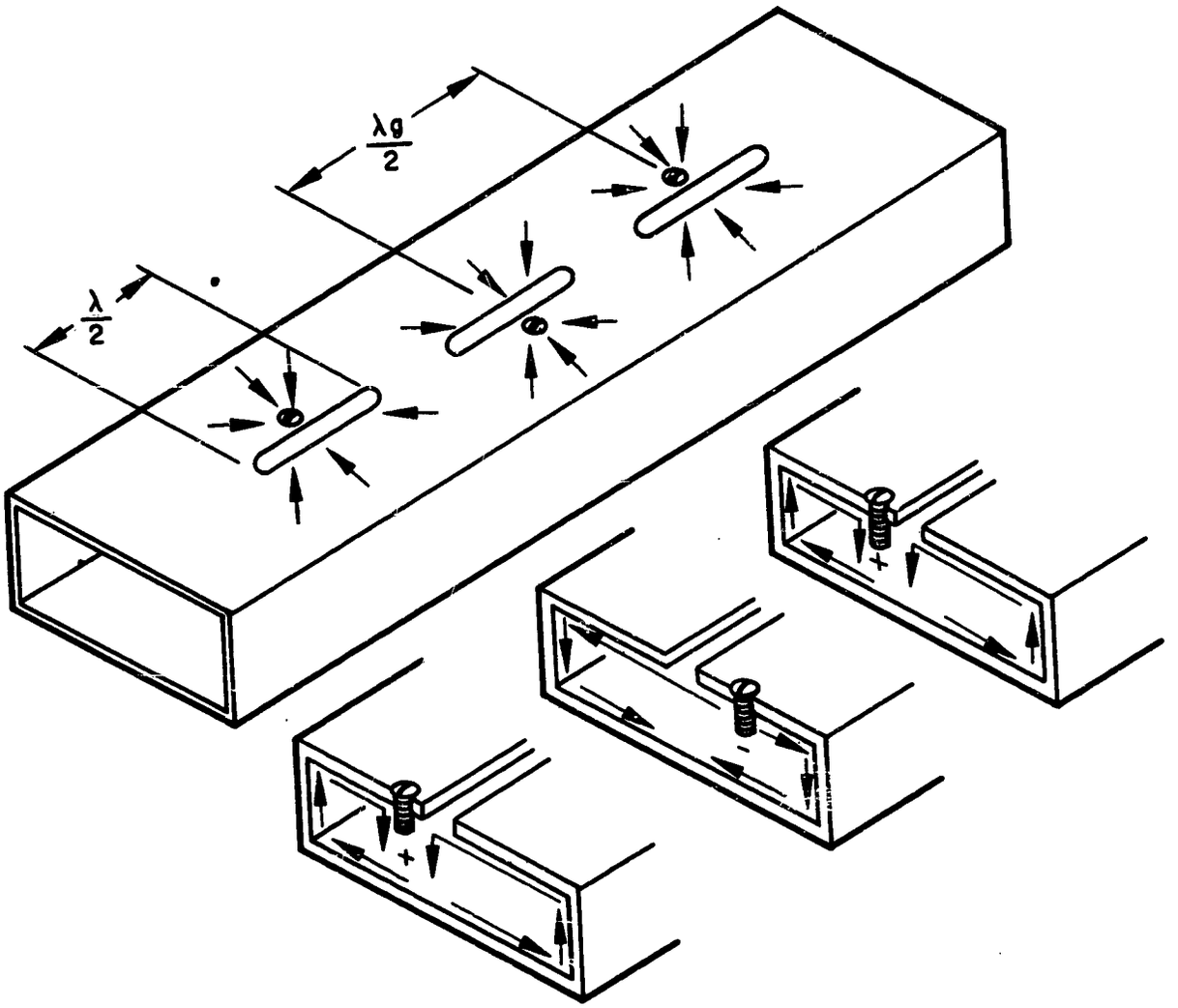

Figure II-50. Probe-Excited Slots

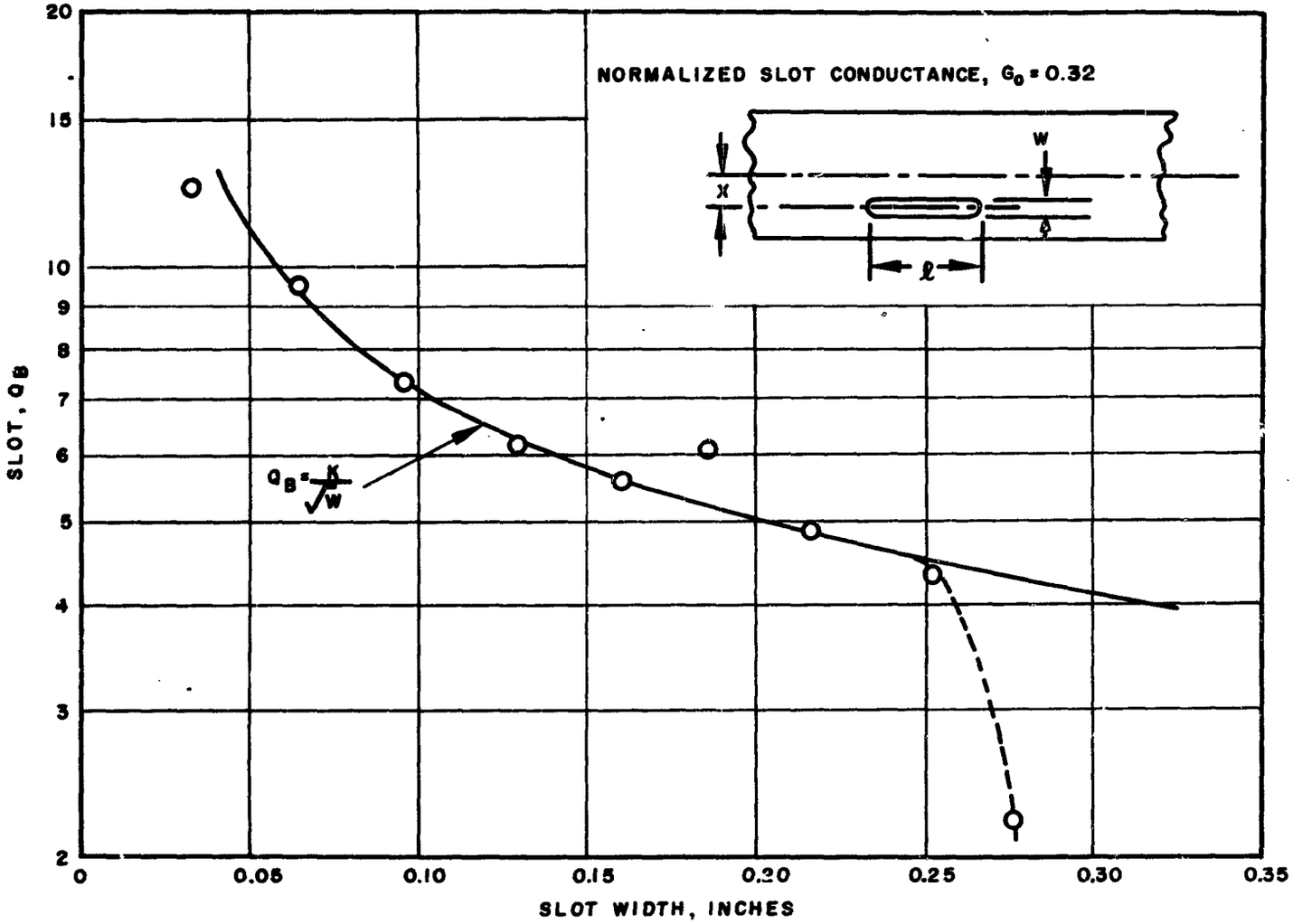

Figure II-51. Slot Q as Function of Width

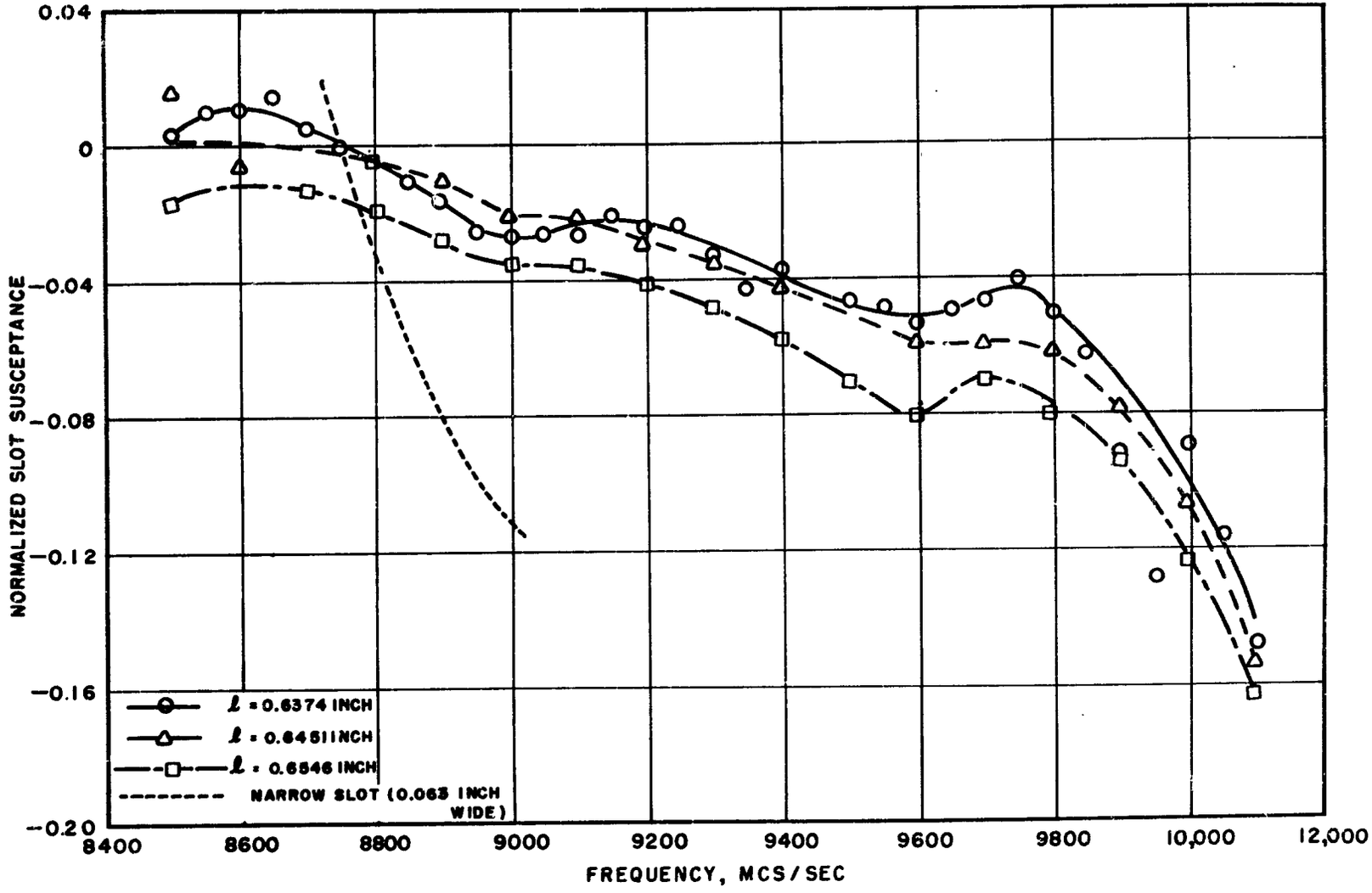

Figure II-52. Susceptance of Wide Longitudinal Shunt Slot
(normalized to f = 8750 mcps)

slot width = 0.316 inch
centerline displacement = 0.137 inch

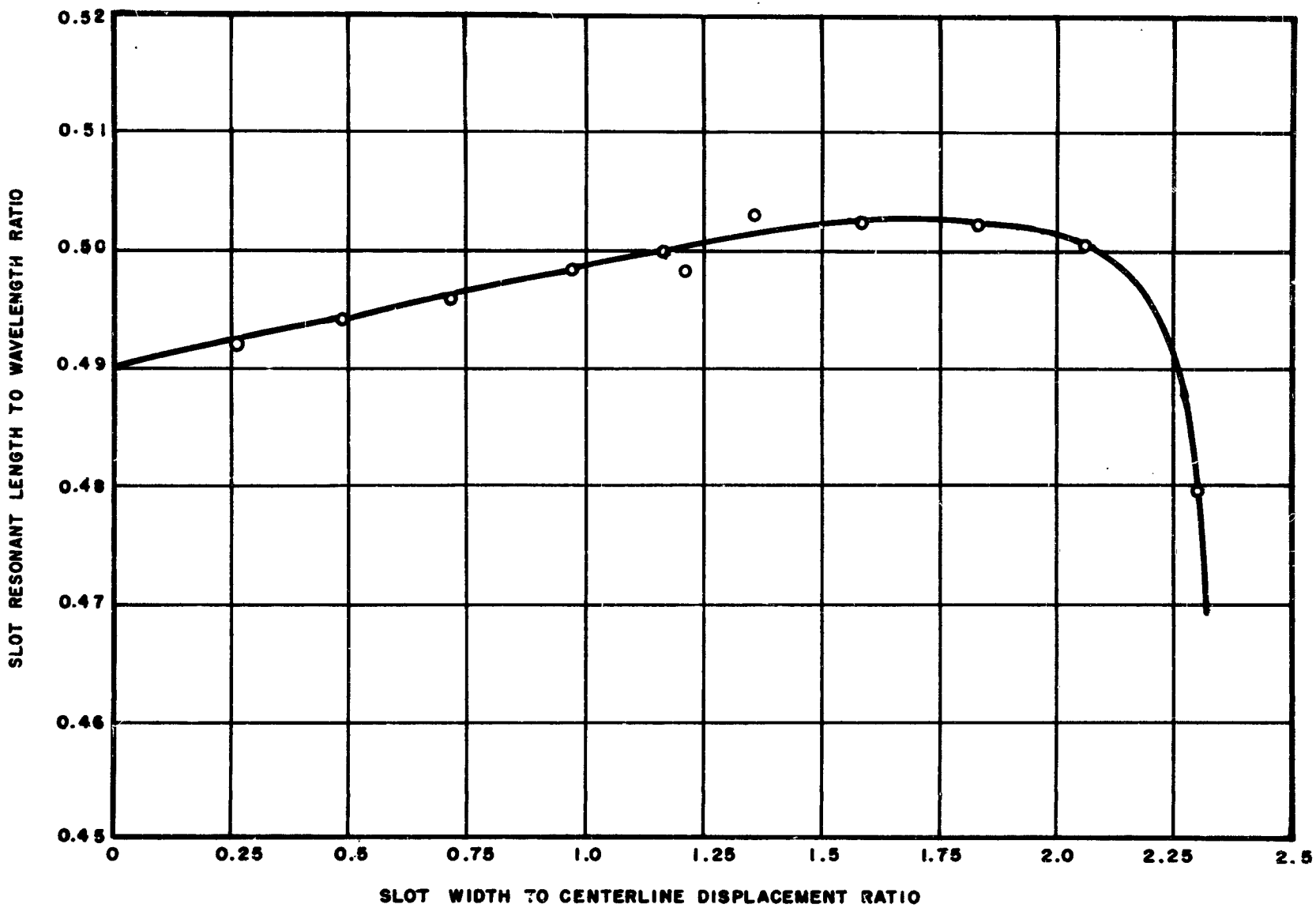

Figure II-53. Effect of Slot Width on Resonant Length

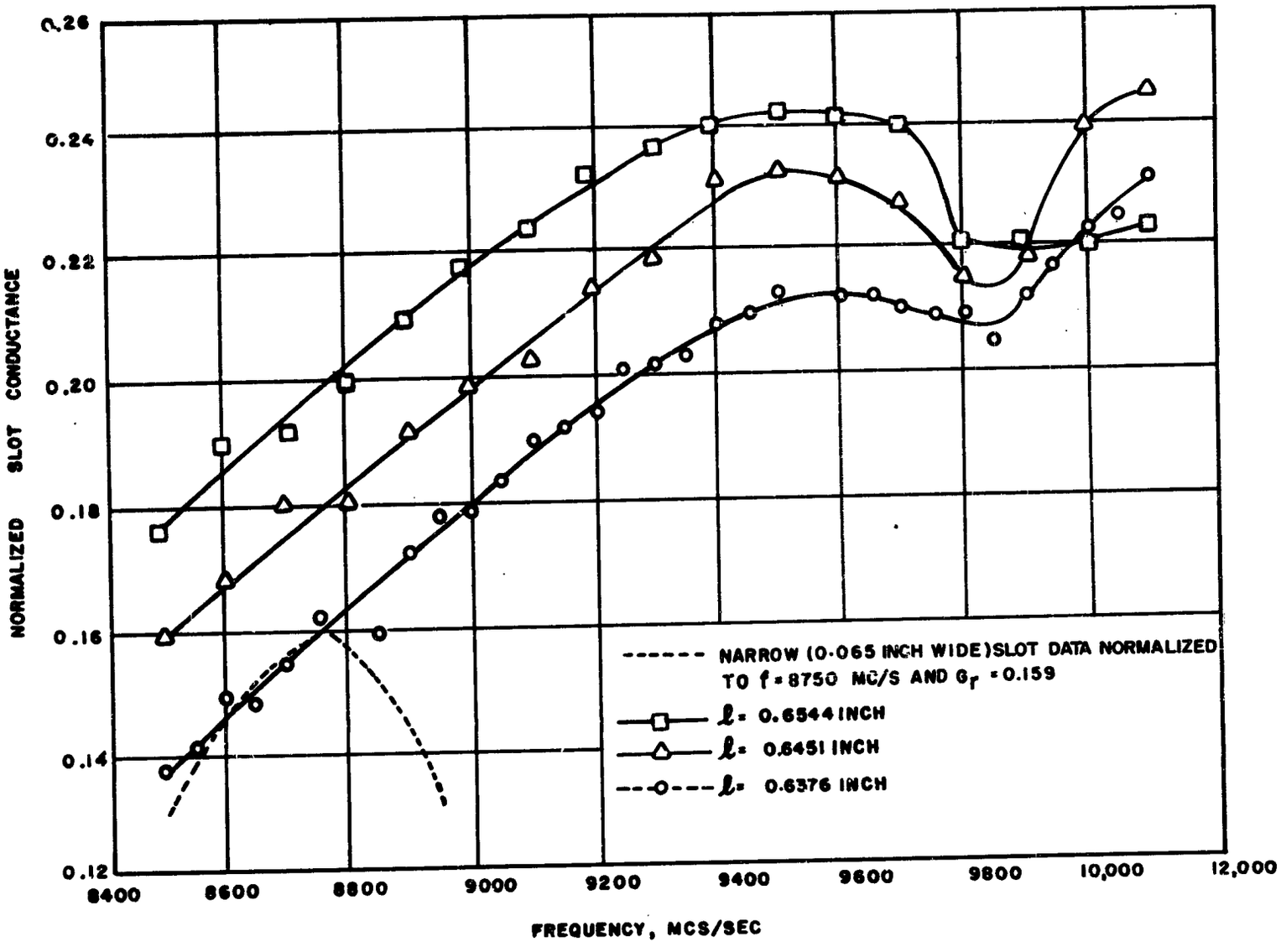

Figure II-54. Conductance of Wide Longitudinal Shunt Slot

f = approximate resonant frequency of 0.637-inch long slot
slot width = 0.316 inch
centerline displacement = 0.137 inch

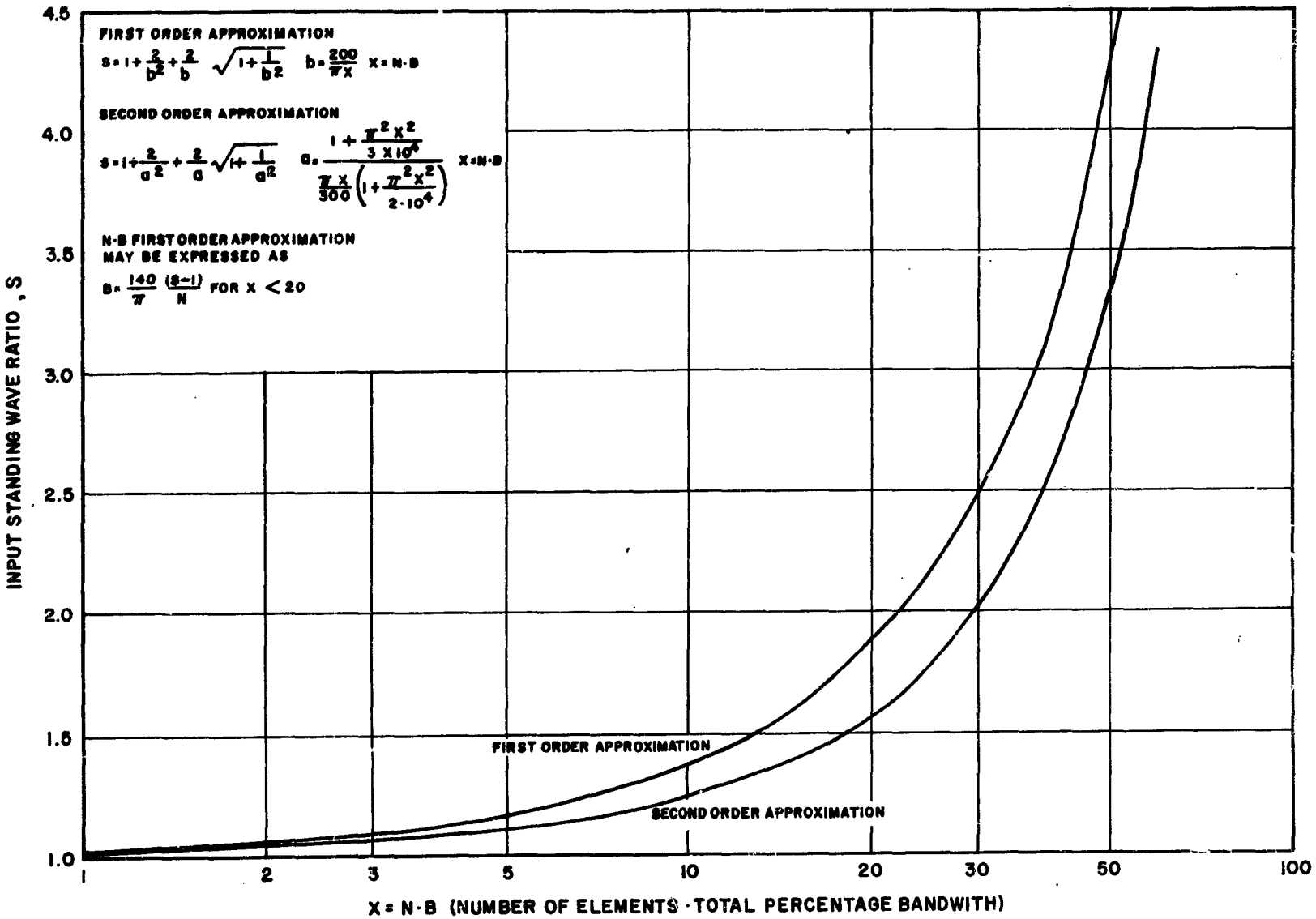

Figure III-1. Bandwidth of Resonant Arrays

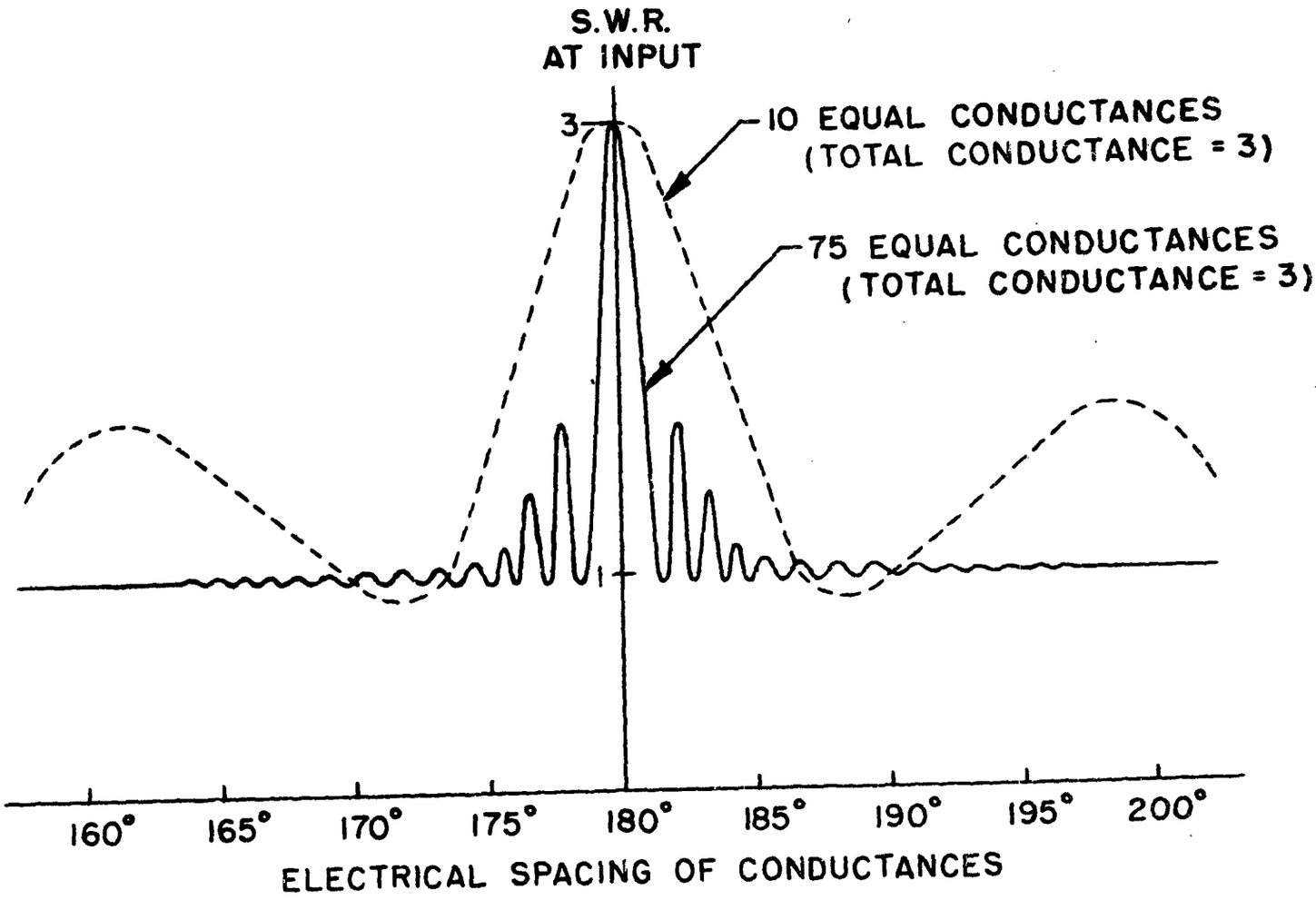

Figure III-2. Array Input SWR as Function of Interelement Spacing

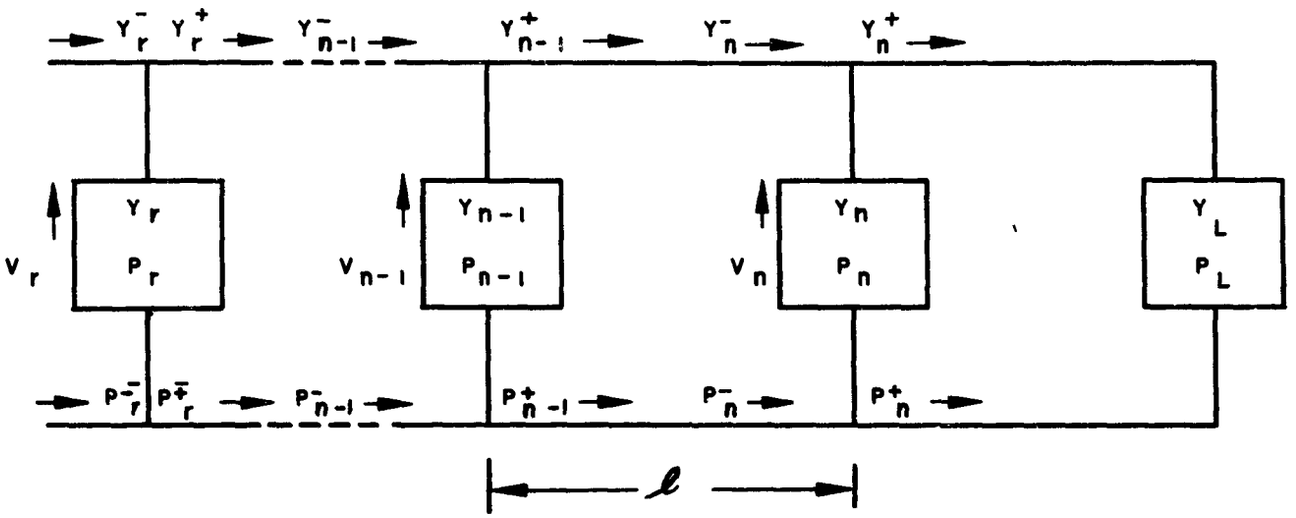

Figure III-3. Equivalent Circuit of Array of Shunt Elements

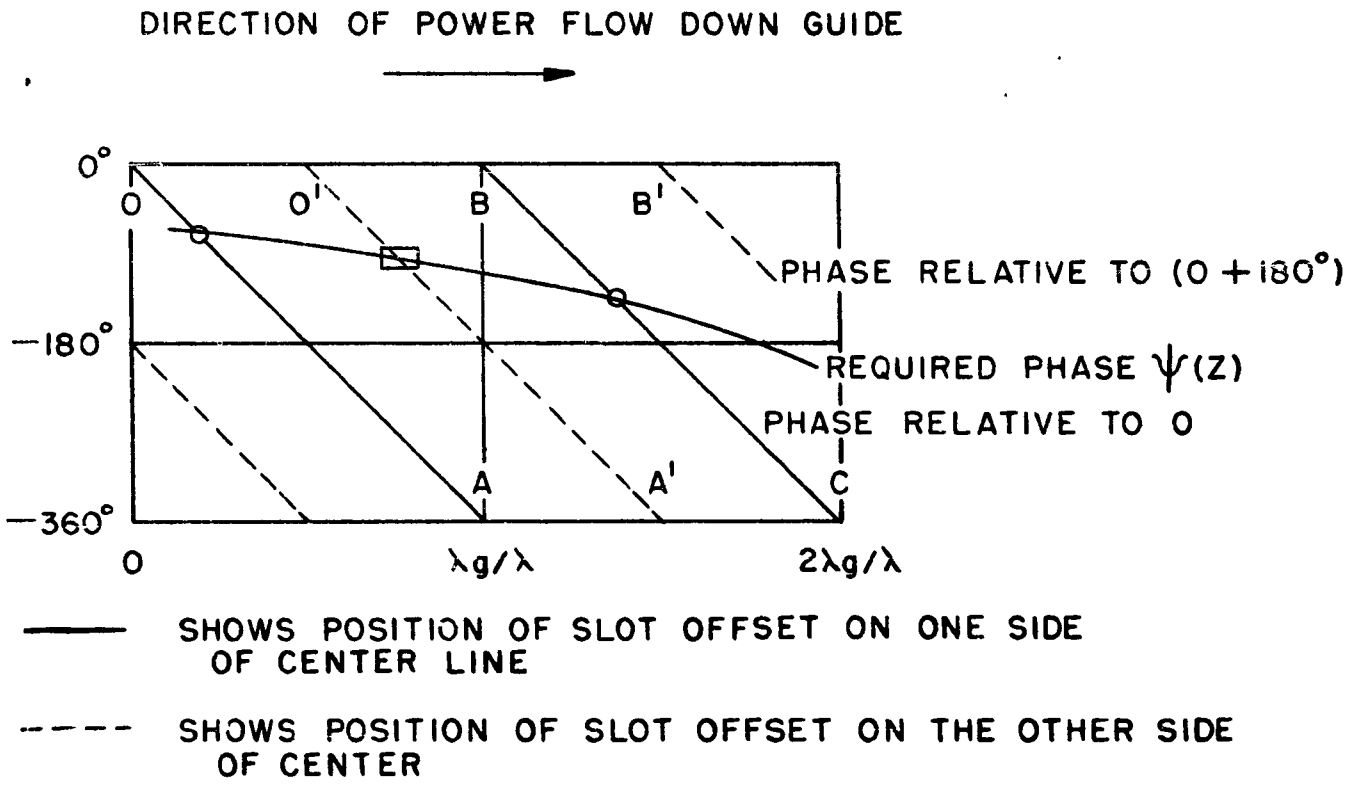

Figure III-4. Graphical Method for Determining Slot Spacing

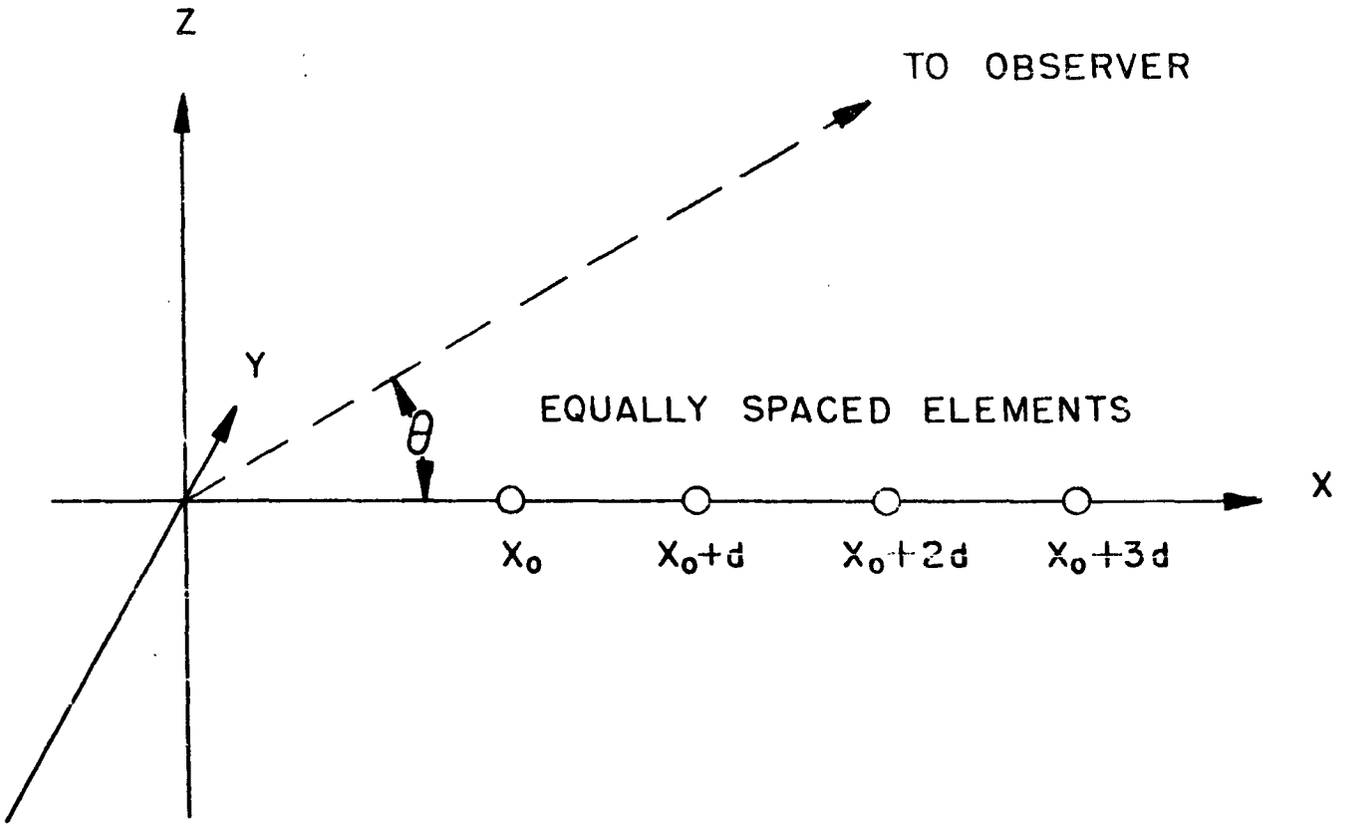

Figure III-5. Linear Discrete Array

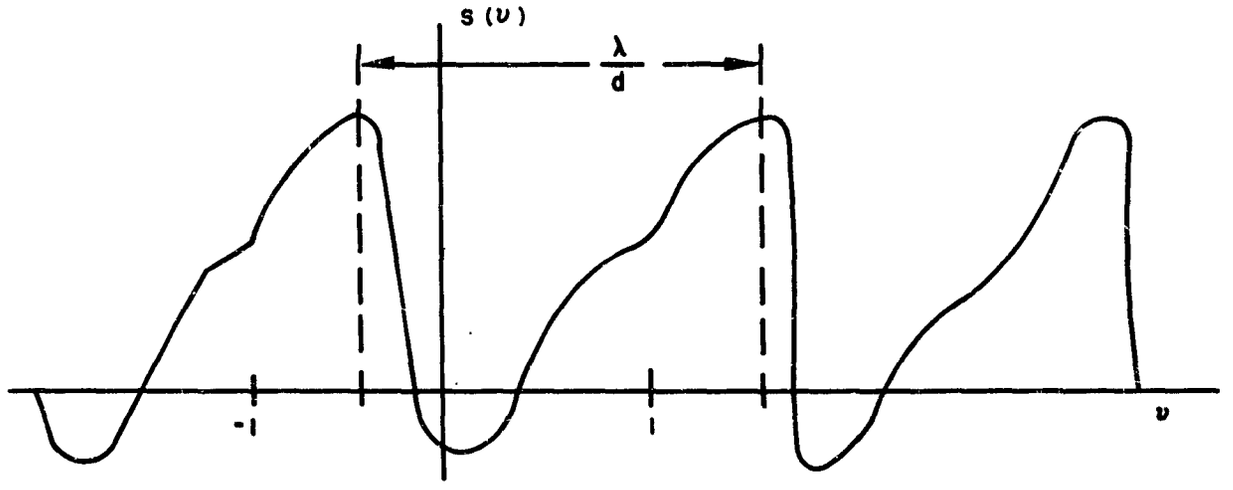

A) Odd Number of Elements

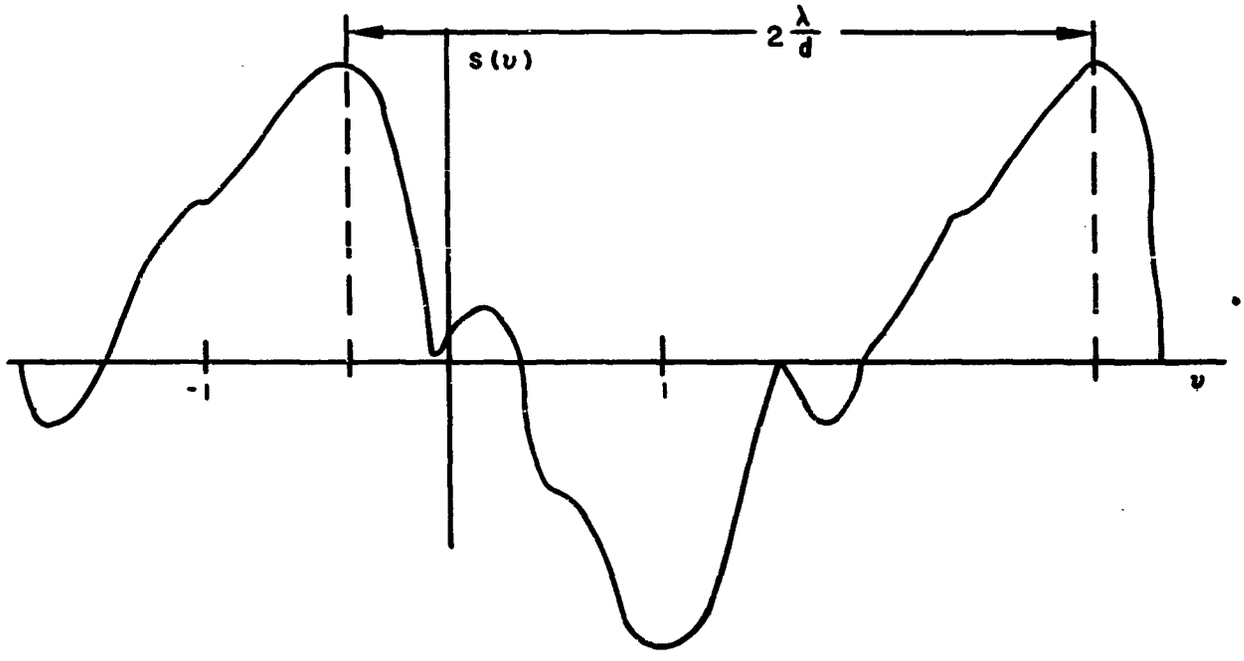

B) Even Number

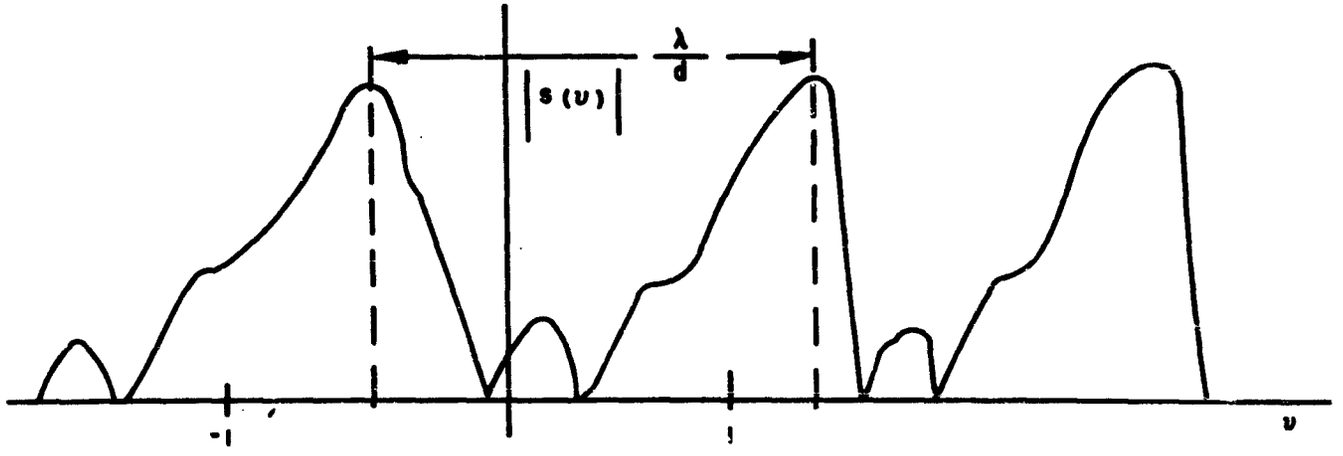

C) Odd or Even Number

Figure III-6. Array Patterns

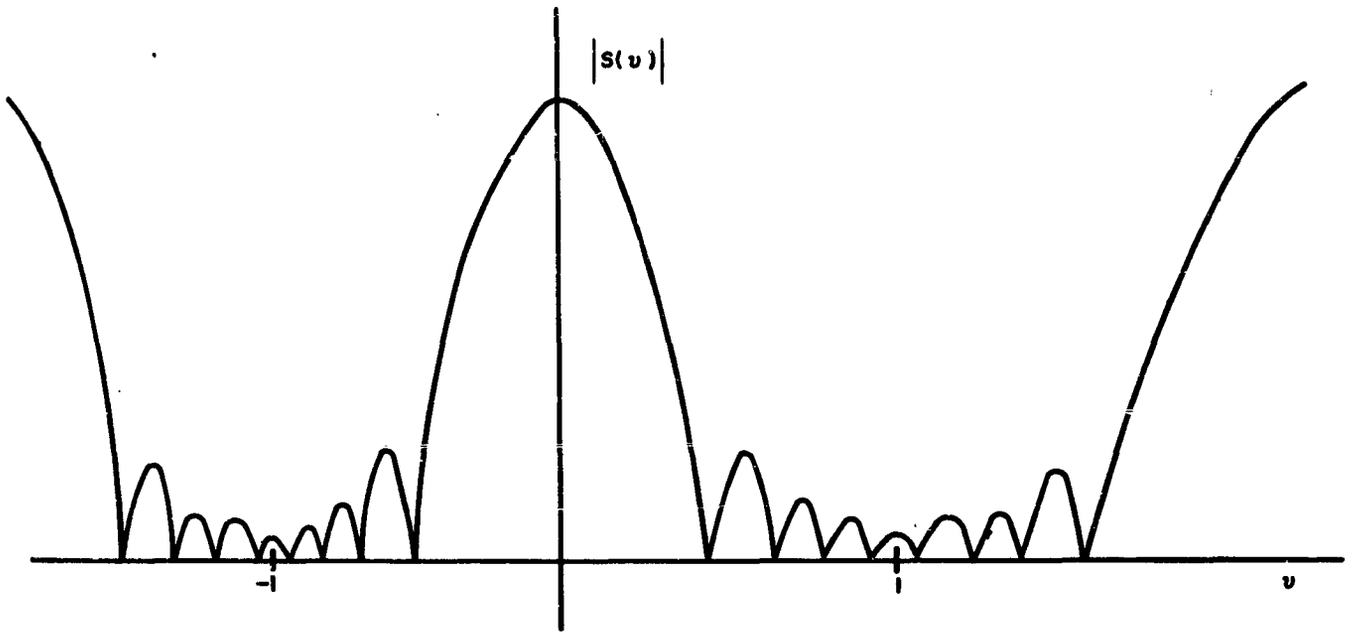

A) Discrete Array

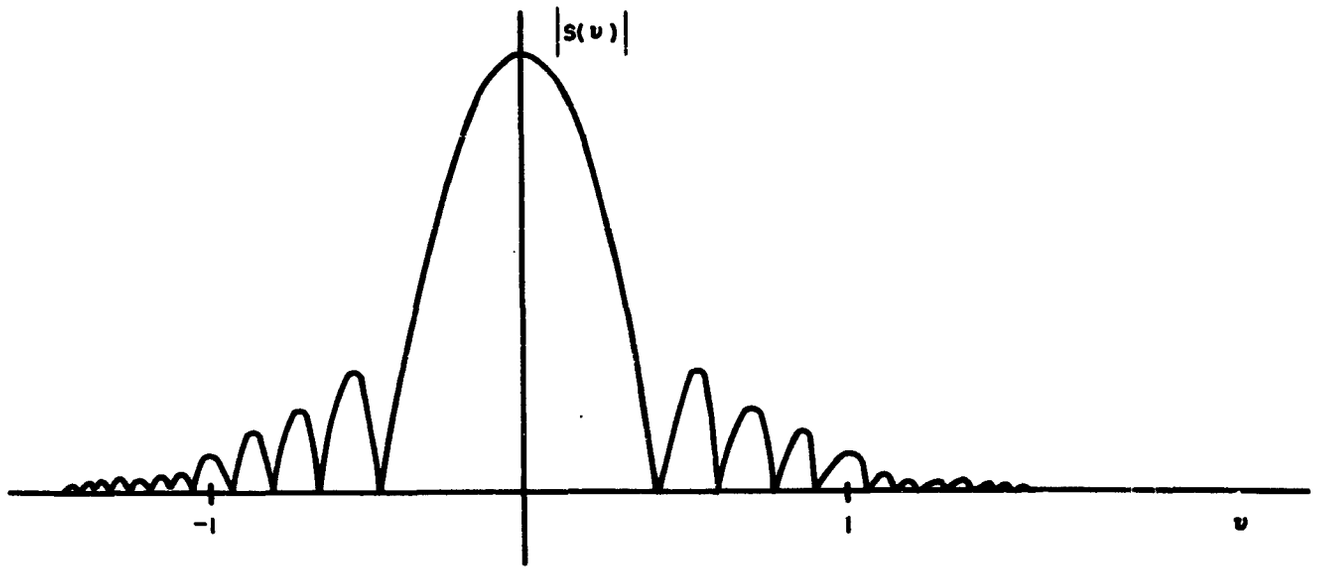

B) Continuous Array

Figure III-7. Similar Patterns in "Real Space" for Discrete and Continuous Array

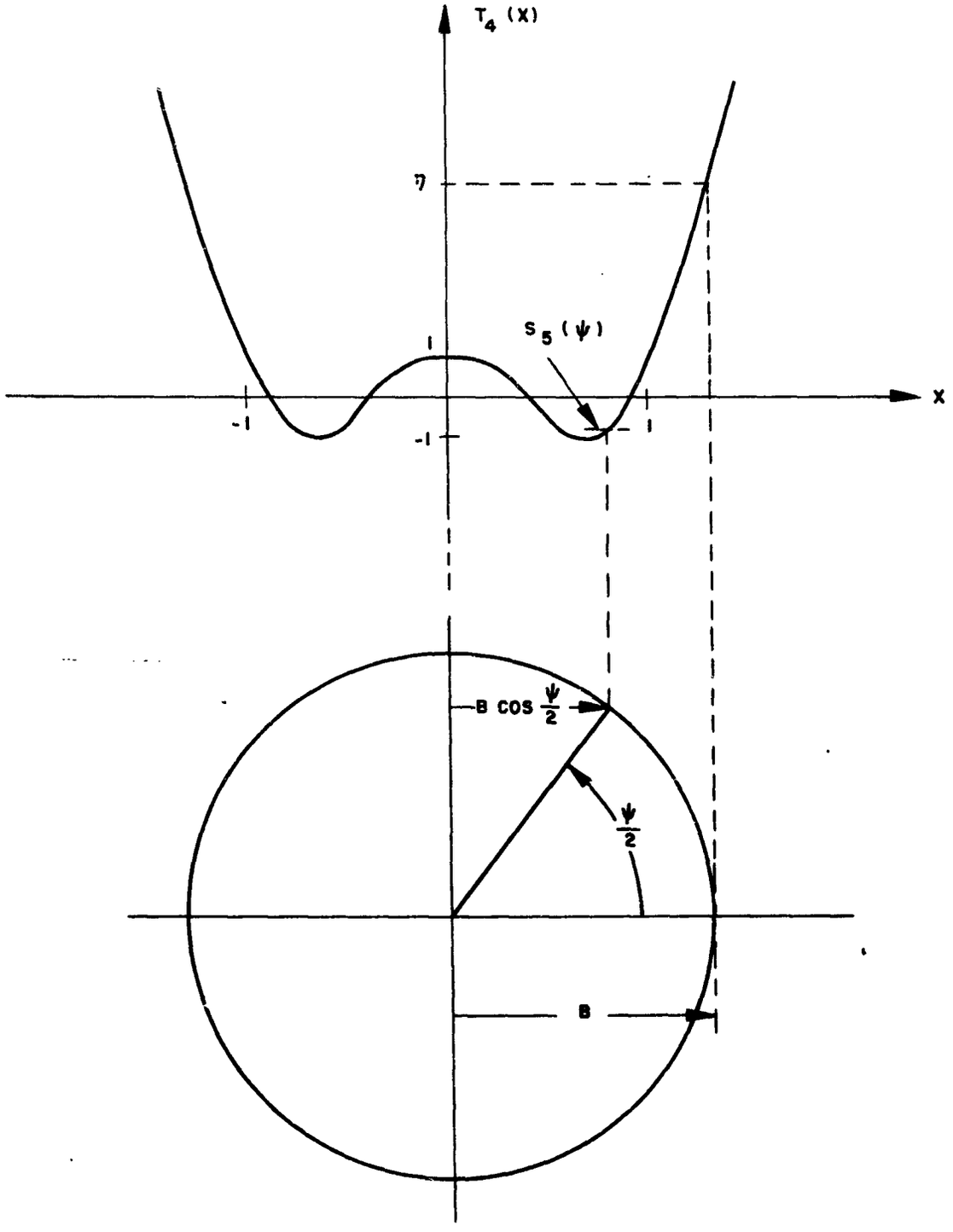

Figure III-8. Tchebyscheff Polynomial and Graphical Method for Determining Field Pattern

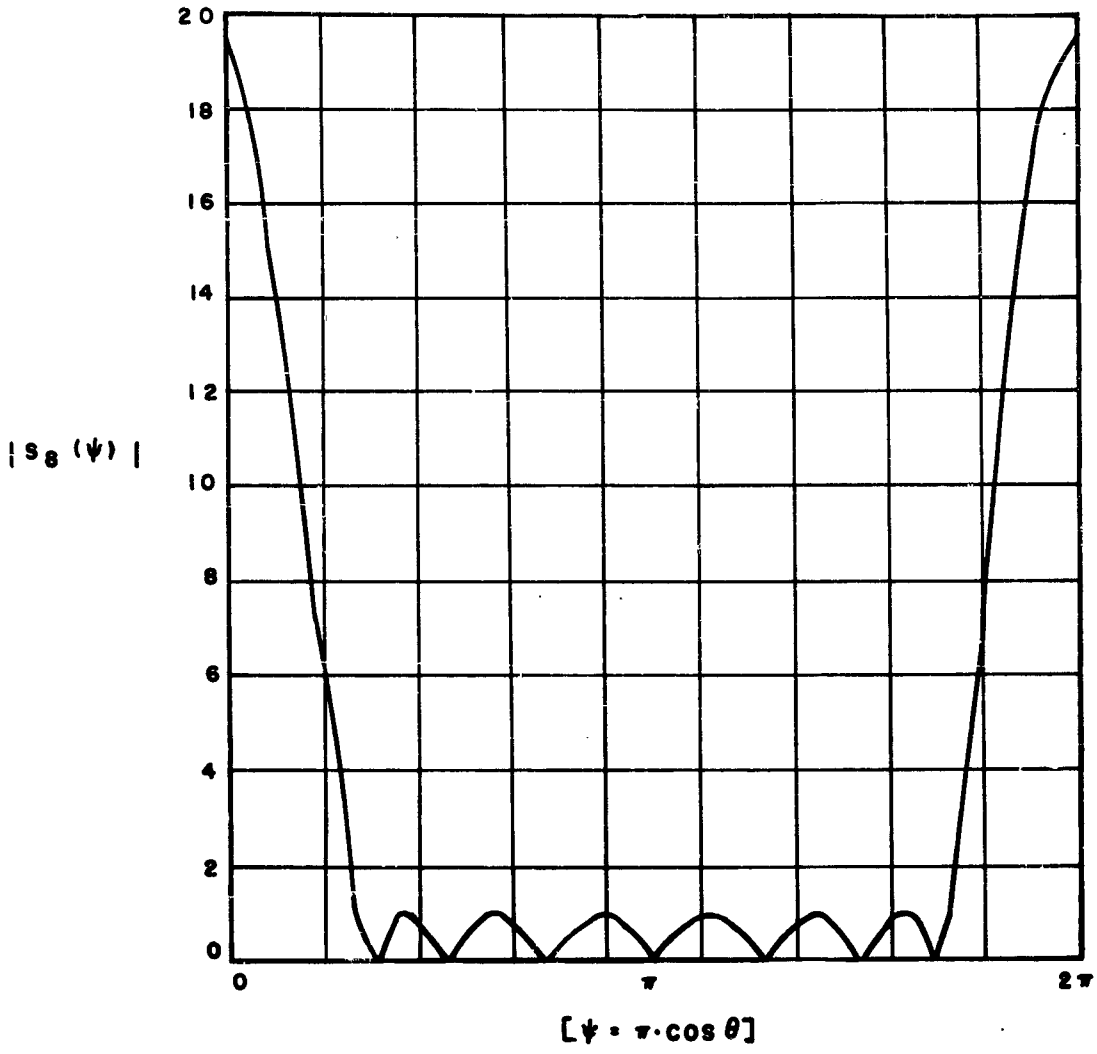

Figure III-9. Optimum Pattern for 8-Element Broadside Array with 25.8-db Sidelobe Level

$$\left|S_8(\psi)\right| = \left|T_7(Z_o \cos \frac{\psi}{2})\right|$$

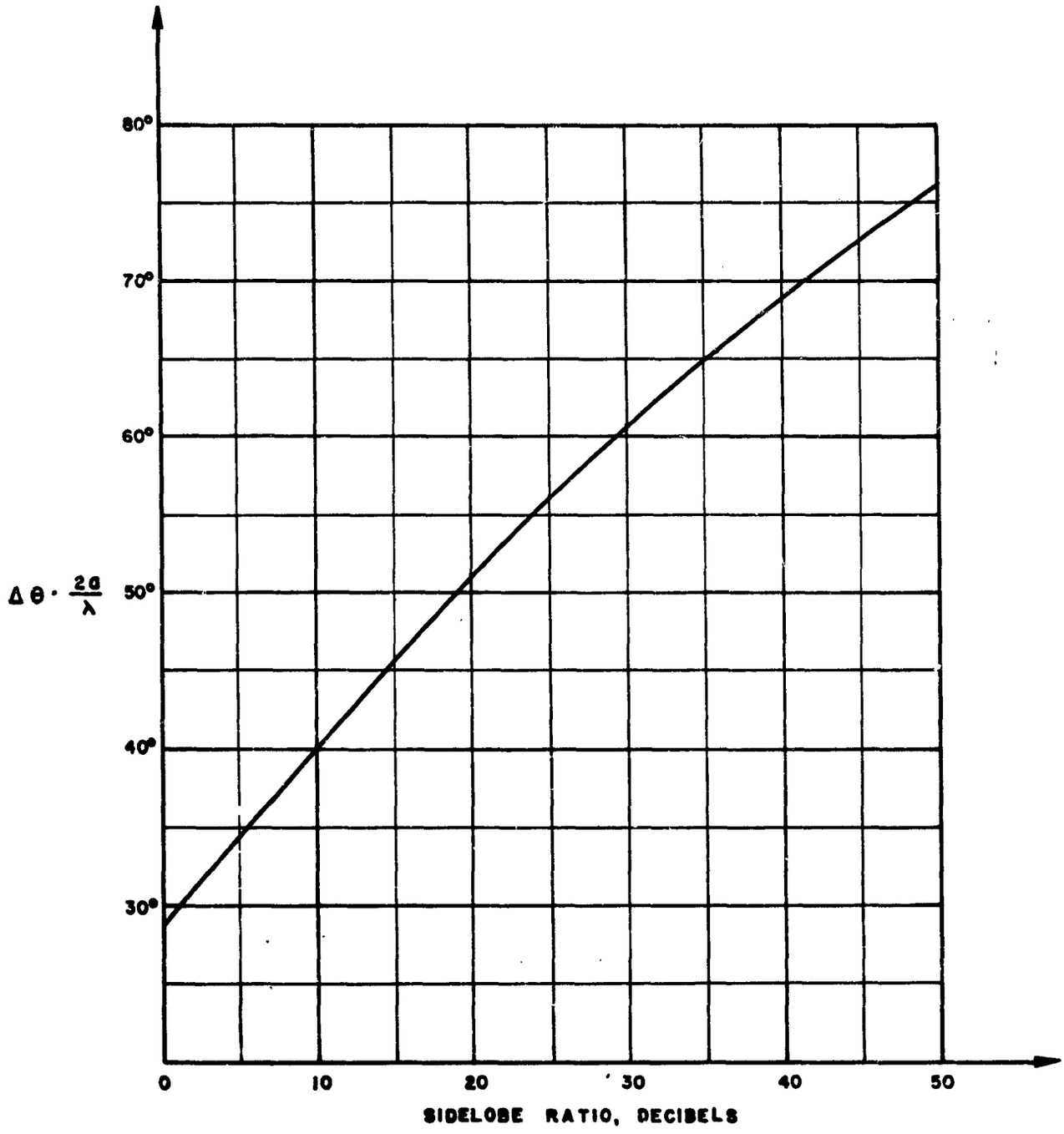

Figure III-10. Beamwidth versus Sidelobe Ratio for Ideal Space Factor

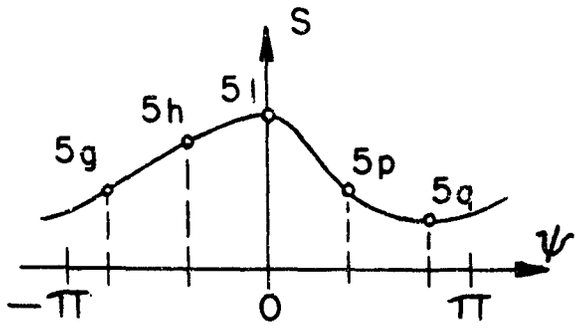

A_{-2}	A_{-1}	A_0	A_1	A_2
-2δ	$-\delta$	0	δ	2δ
$ge^{-i4\delta}$	$ge^{-i2\delta}$	g	$ge^{i2\delta}$	$ge^{i4\delta}$
$he^{-i2\delta}$	$he^{-i\delta}$	h	$he^{i\delta}$	$he^{i2\delta}$
ℓ	ℓ	ℓ	ℓ	ℓ
$pe^{i2\delta}$	$pe^{i\delta}$	p	$pe^{-i\delta}$	$pe^{-i2\delta}$
$qe^{i4\delta}$	$qe^{i2\delta}$	q	$qe^{-i2\delta}$	$qe^{-i4\delta}$

$$A_{-2} = ge^{-i4\delta} + he^{-i2\delta} + \ell + pe^{i2\delta} + qe^{i4\delta}$$

etc.

$$\delta = \frac{2\pi}{N}$$

Figure III-11. Woodward's Method for Discrete Elements

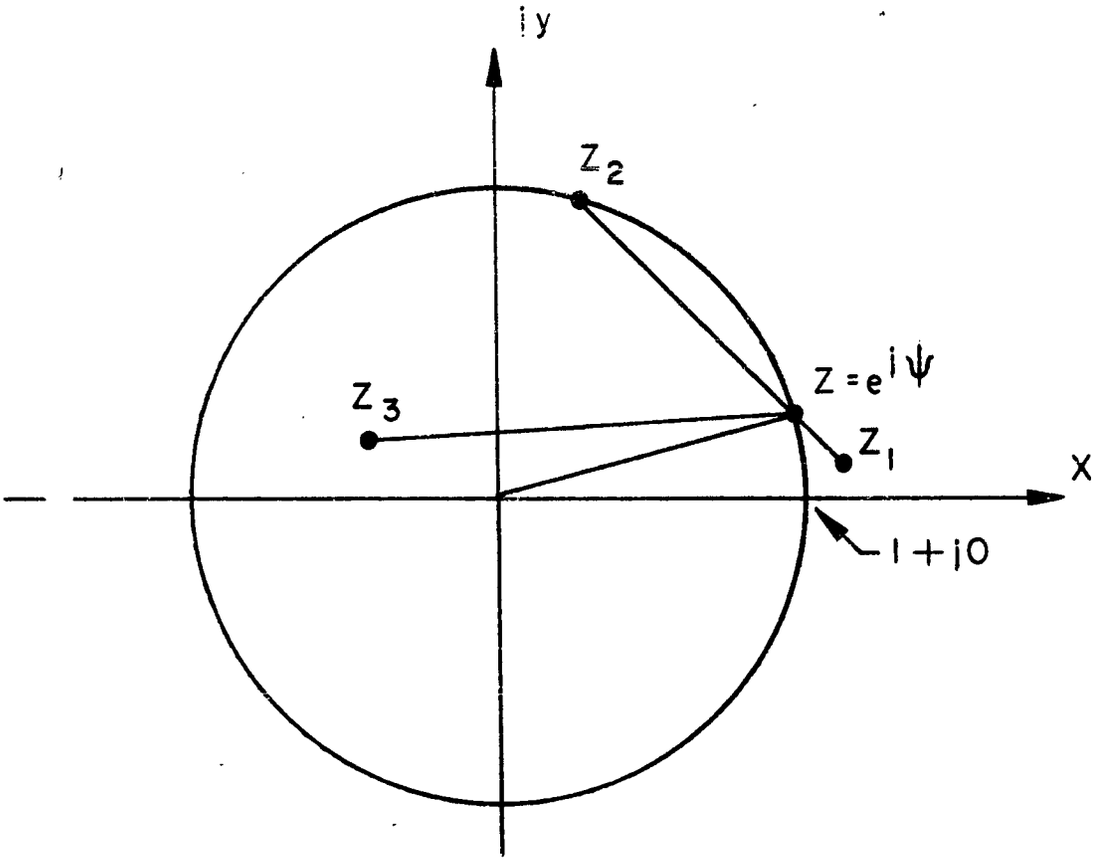

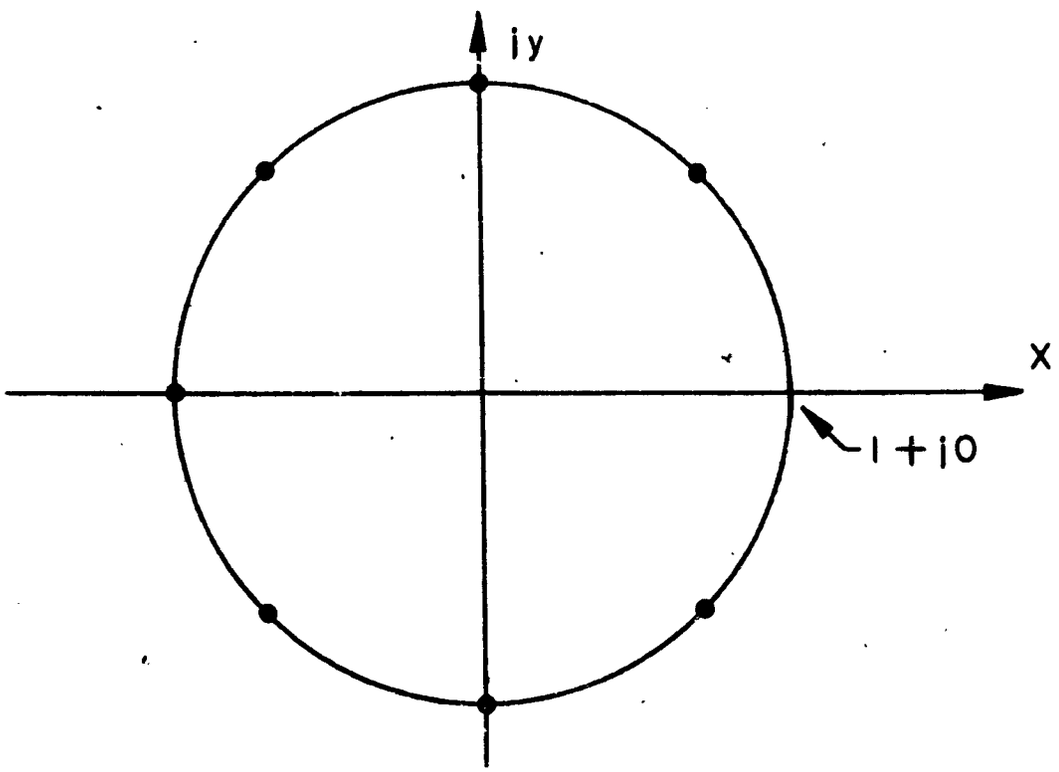

Figure III-12. Circle Diagram Method

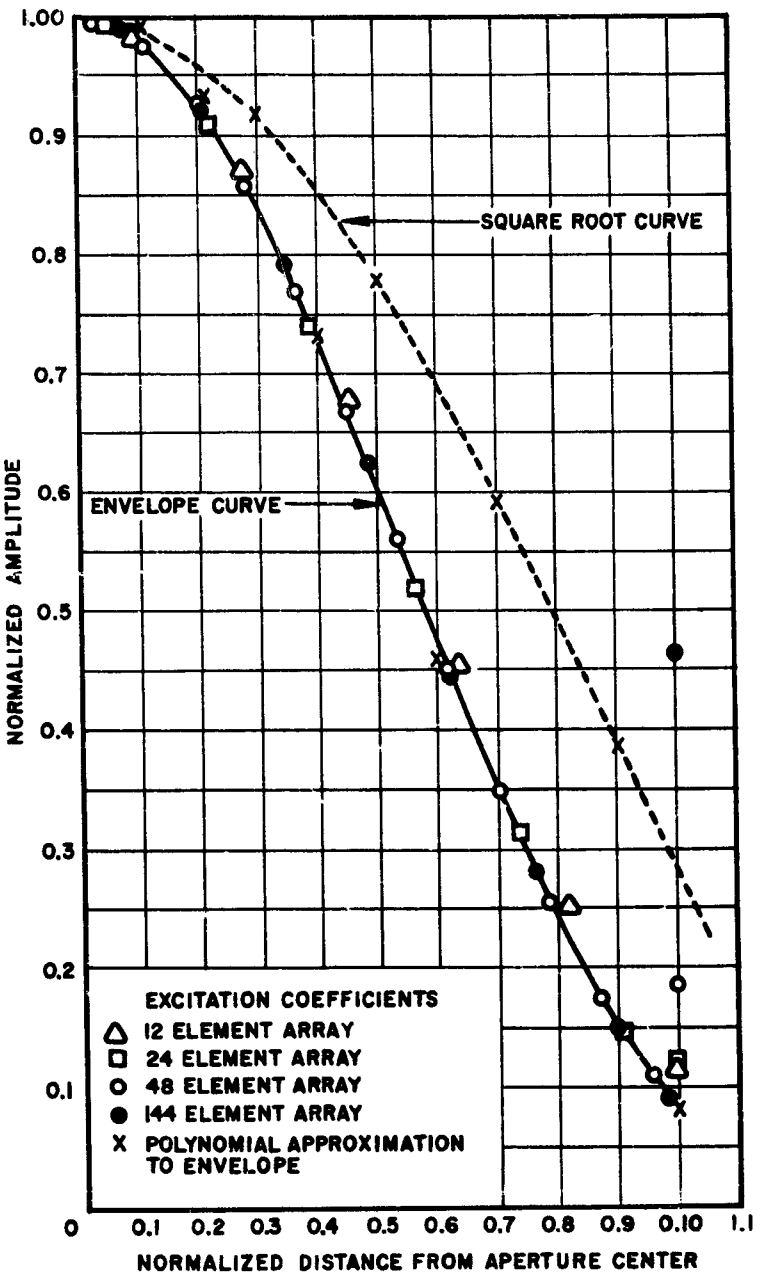

Figure III-13. Amplitude Distribution for 40-db Tchebyscheff Arrays

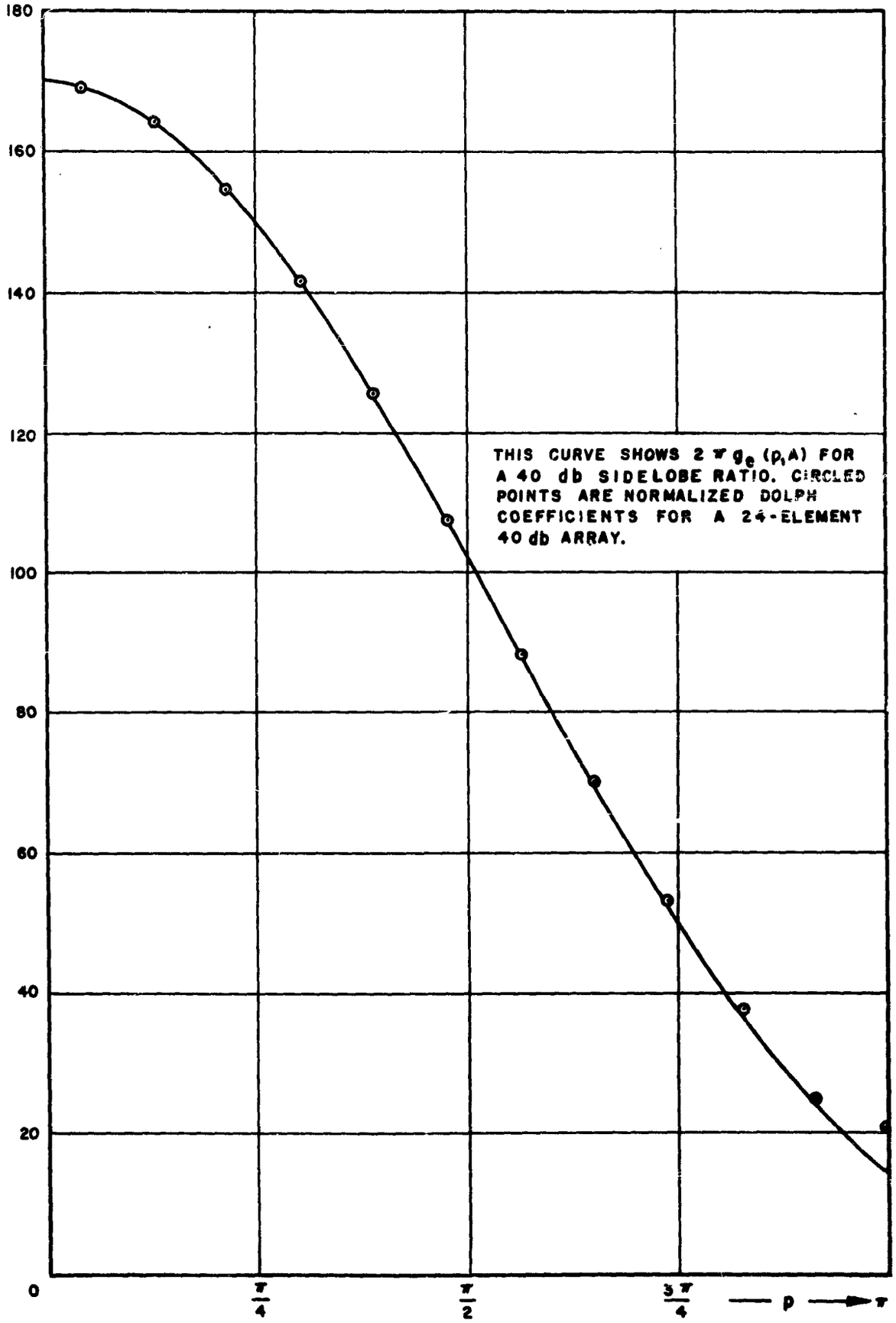

Figure III-14. Envelope Function, g(p, A), for 40-db Sidelobe Ratio

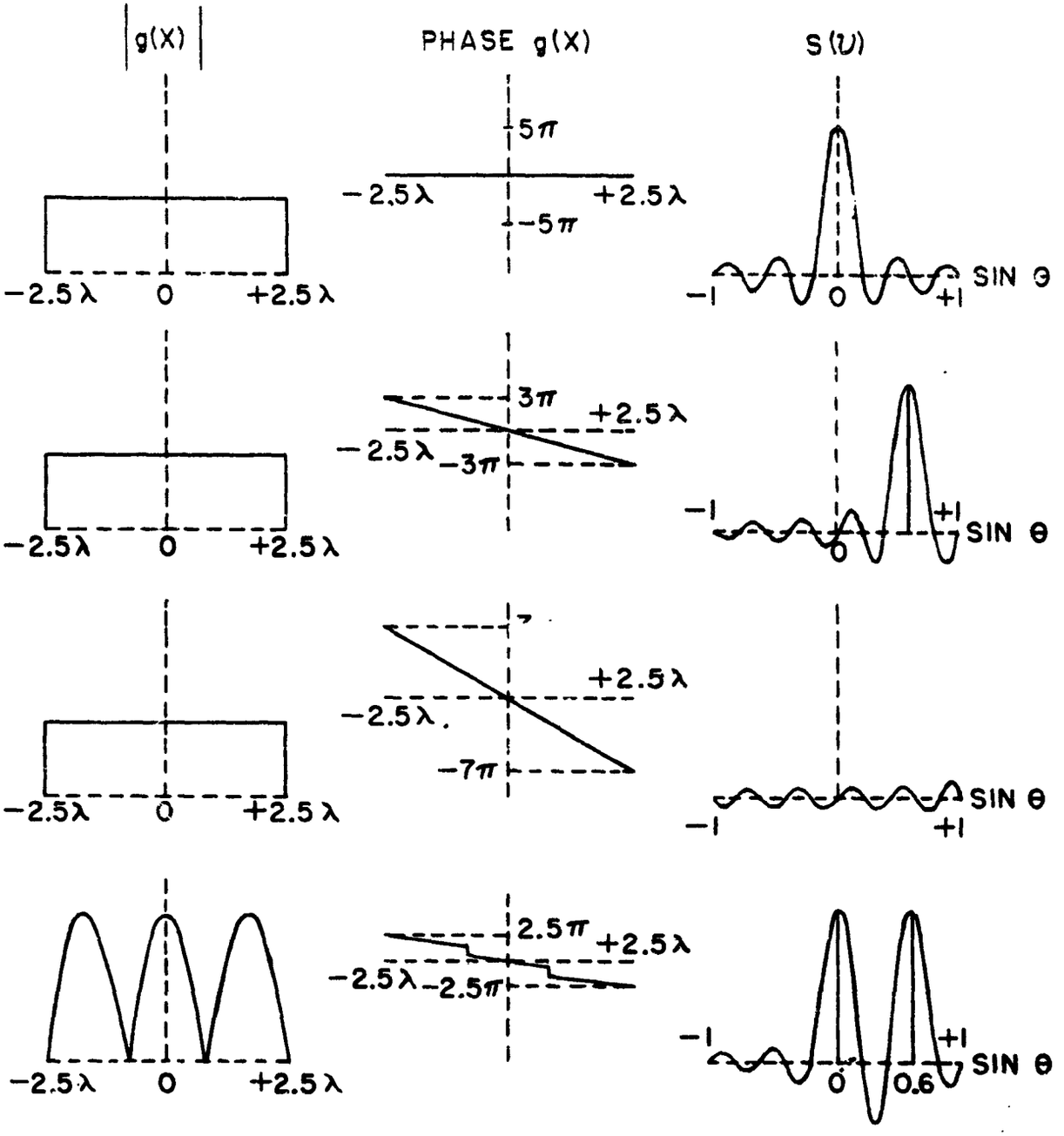

Figure III-15. Woodward's Method

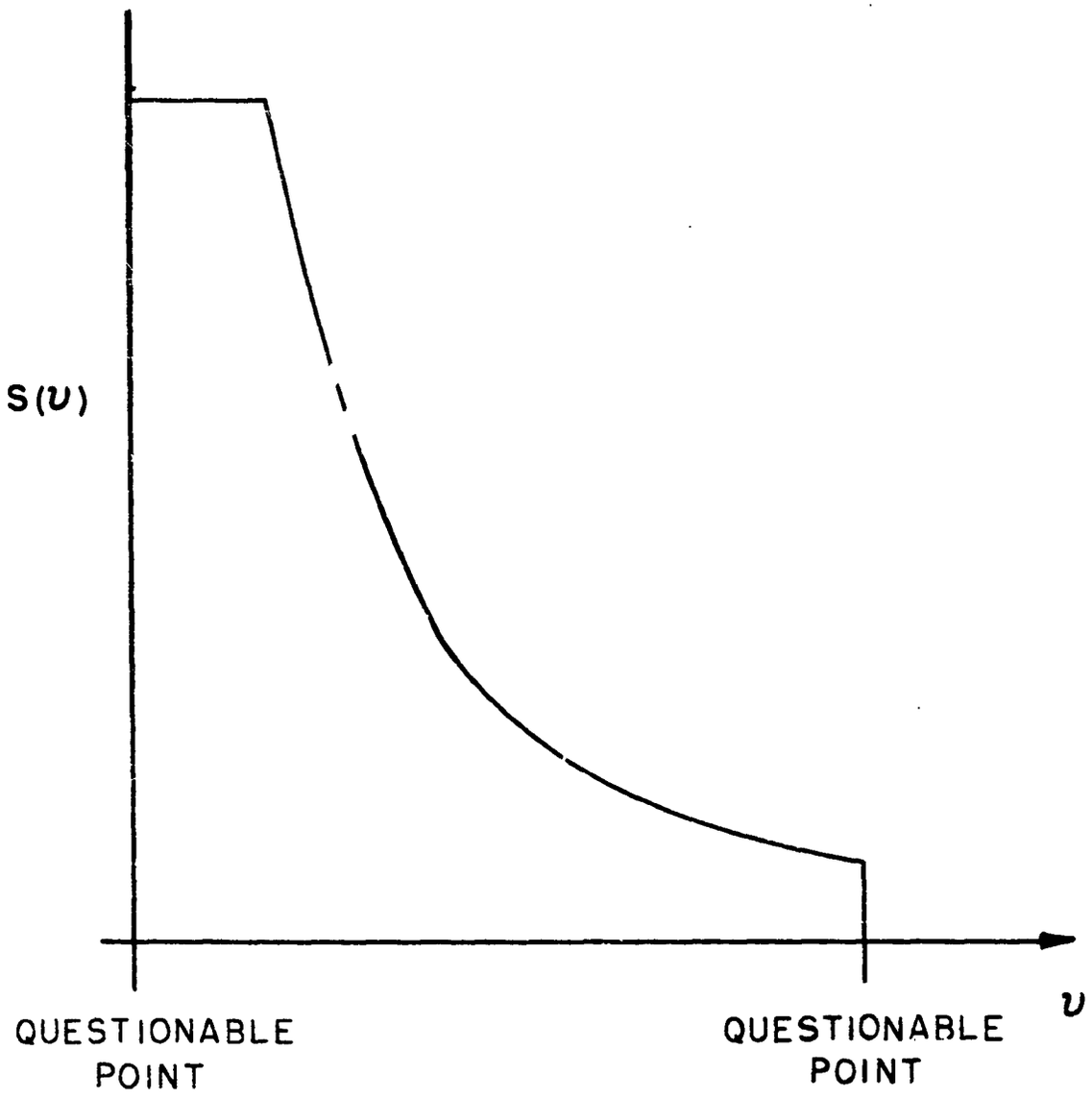

Figure III-16. Pattern to be Synthesized by Woodward's Method Showing Questionable Points

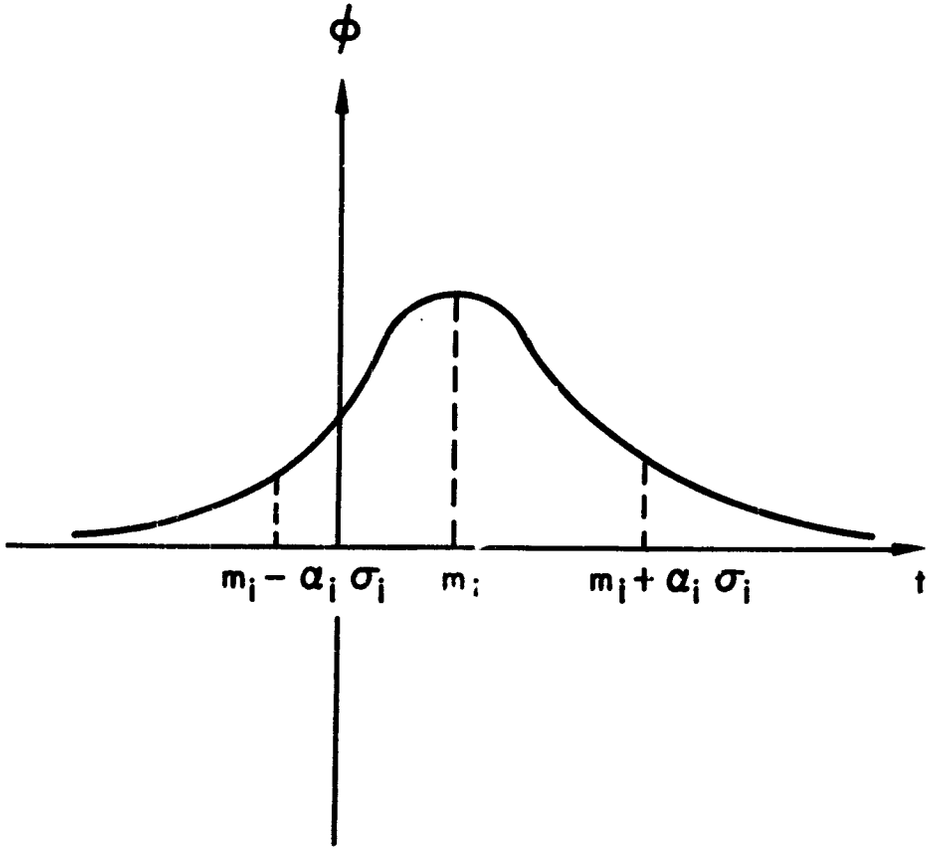

A) COMPLETE NORMAL DISTRIBUTION

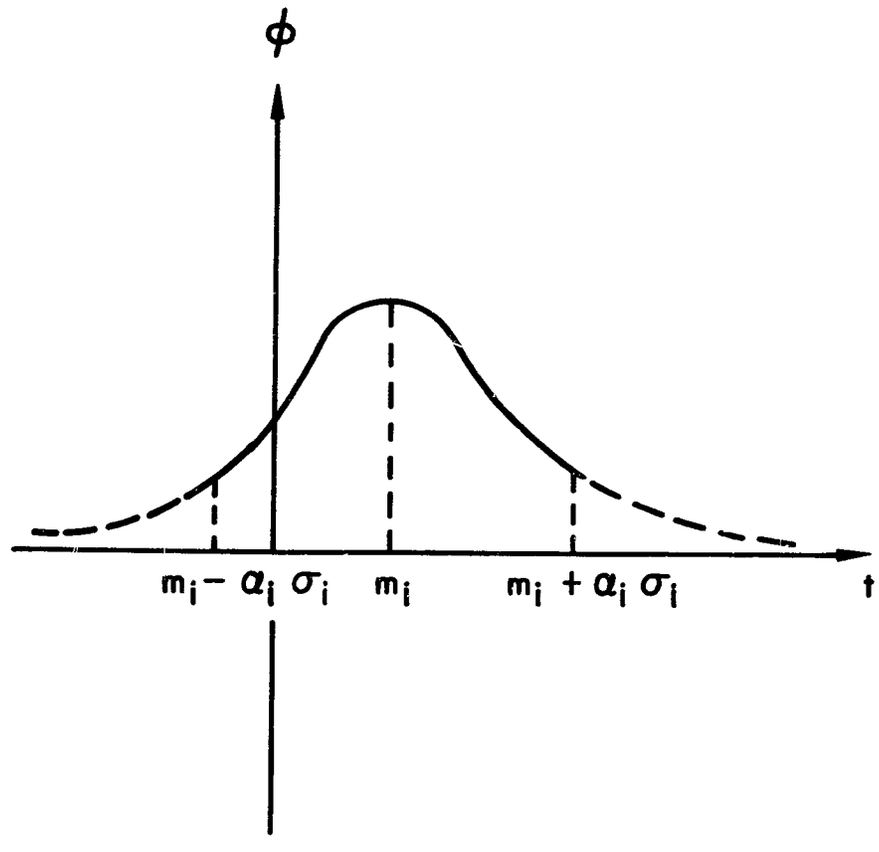

B) TRUNCATED NORMAL DISTRIBUTION

Figure III-17. Machining Accuracy

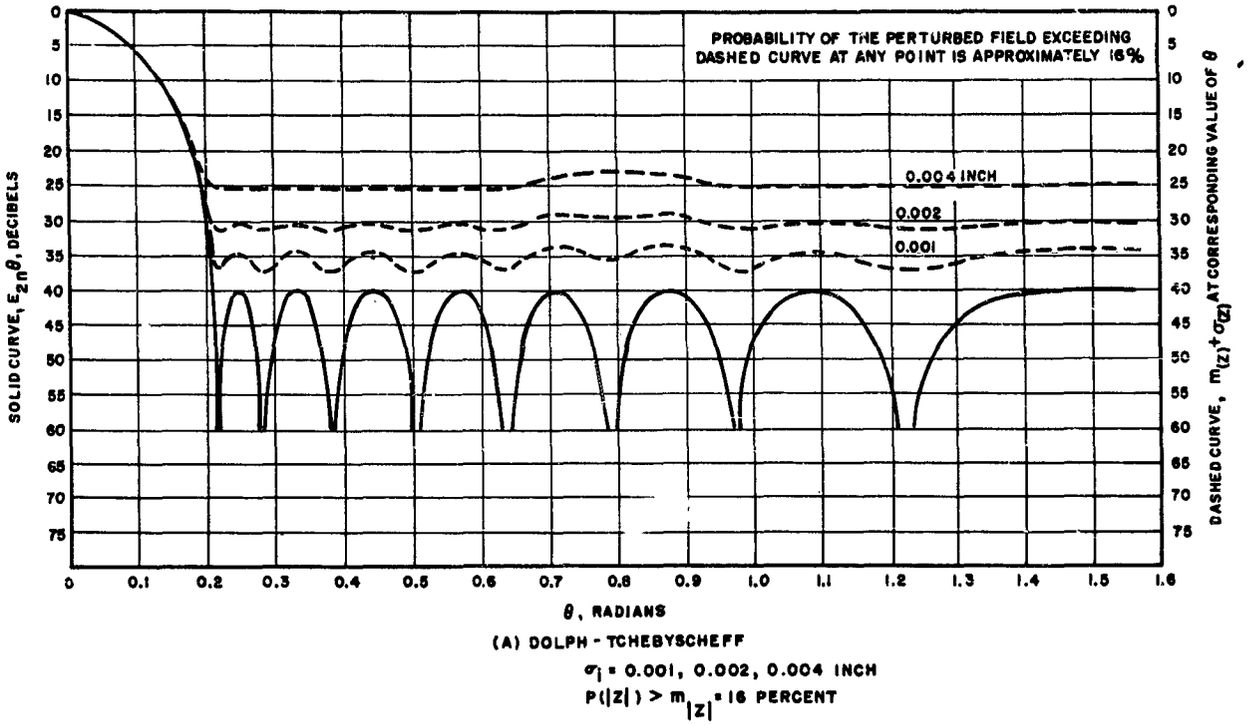

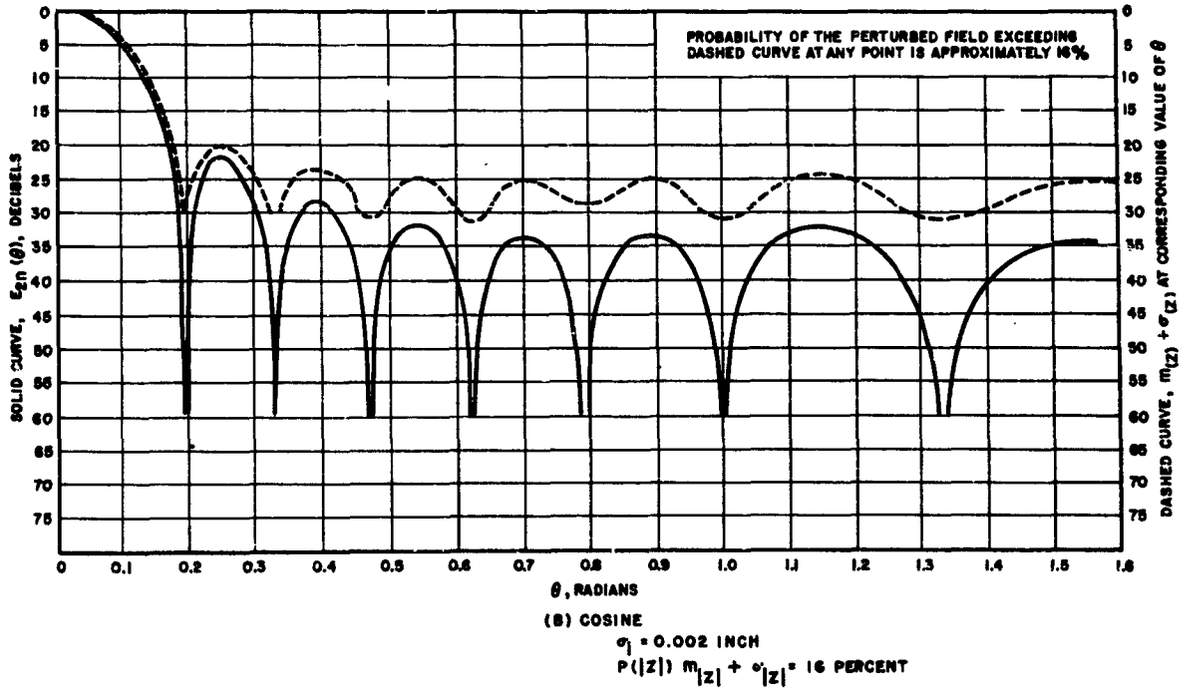

Figure III-18. Distributions

Parameters d, ℓ, x taken as normally distributed variables with standard deviations. Possibility of perturbed field exceeding dashed curves at any point is approximately 16 percent.

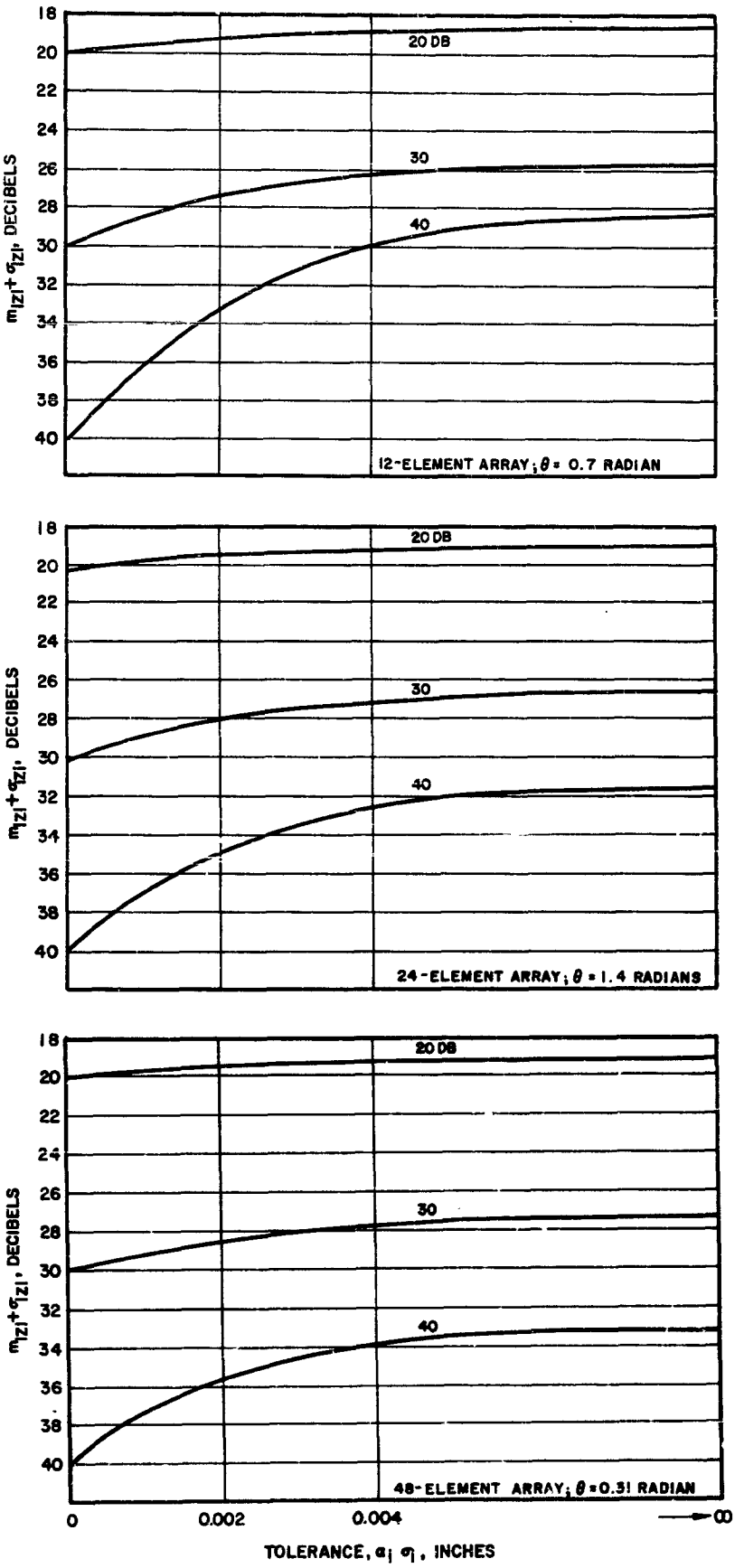

Figure III-19. Sidelobe Level as Function of Tolerance
Dolph-Tchebyscheff Distributions
σ_i = 0.002 inch

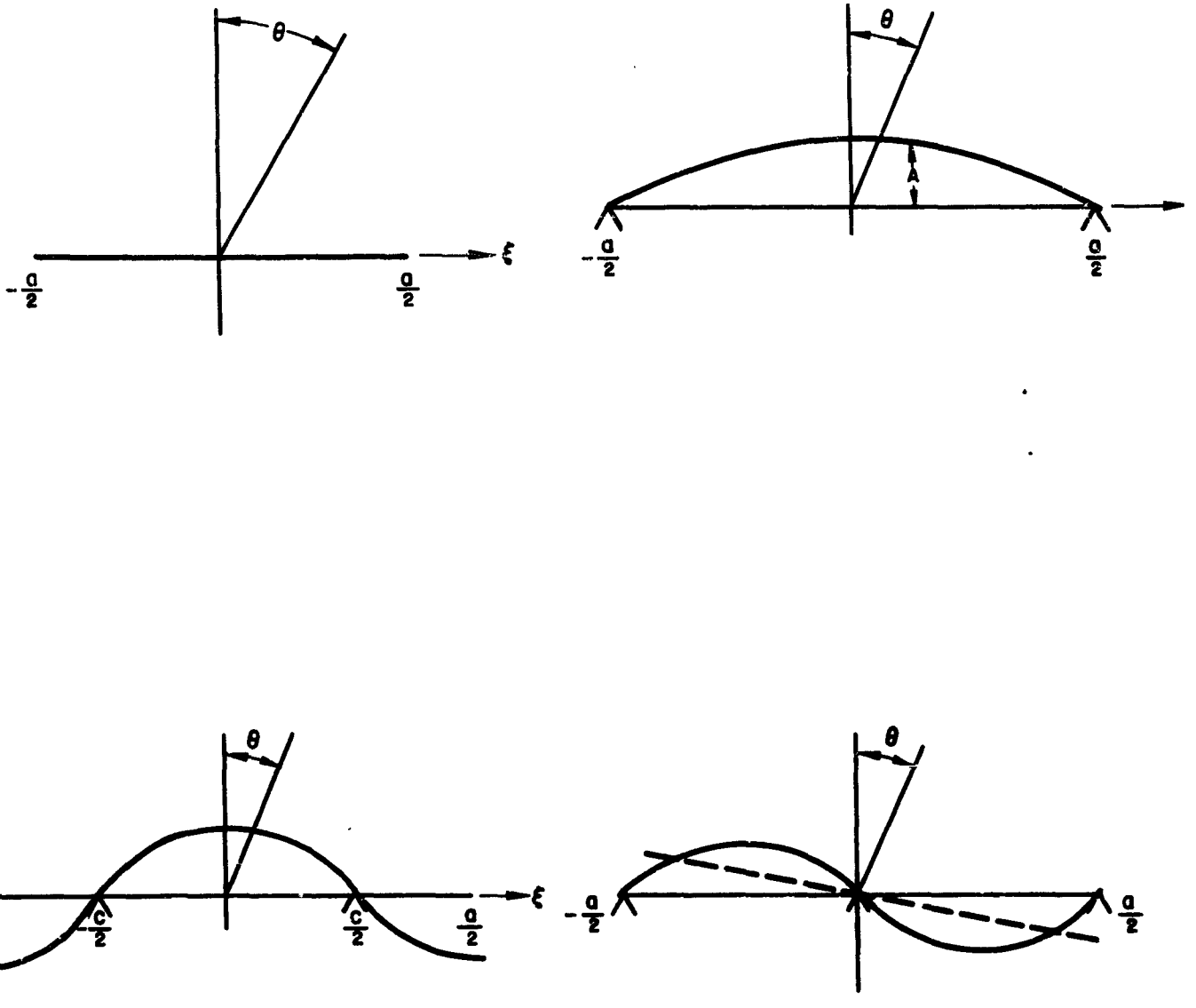

Figure III-20. Array Bending

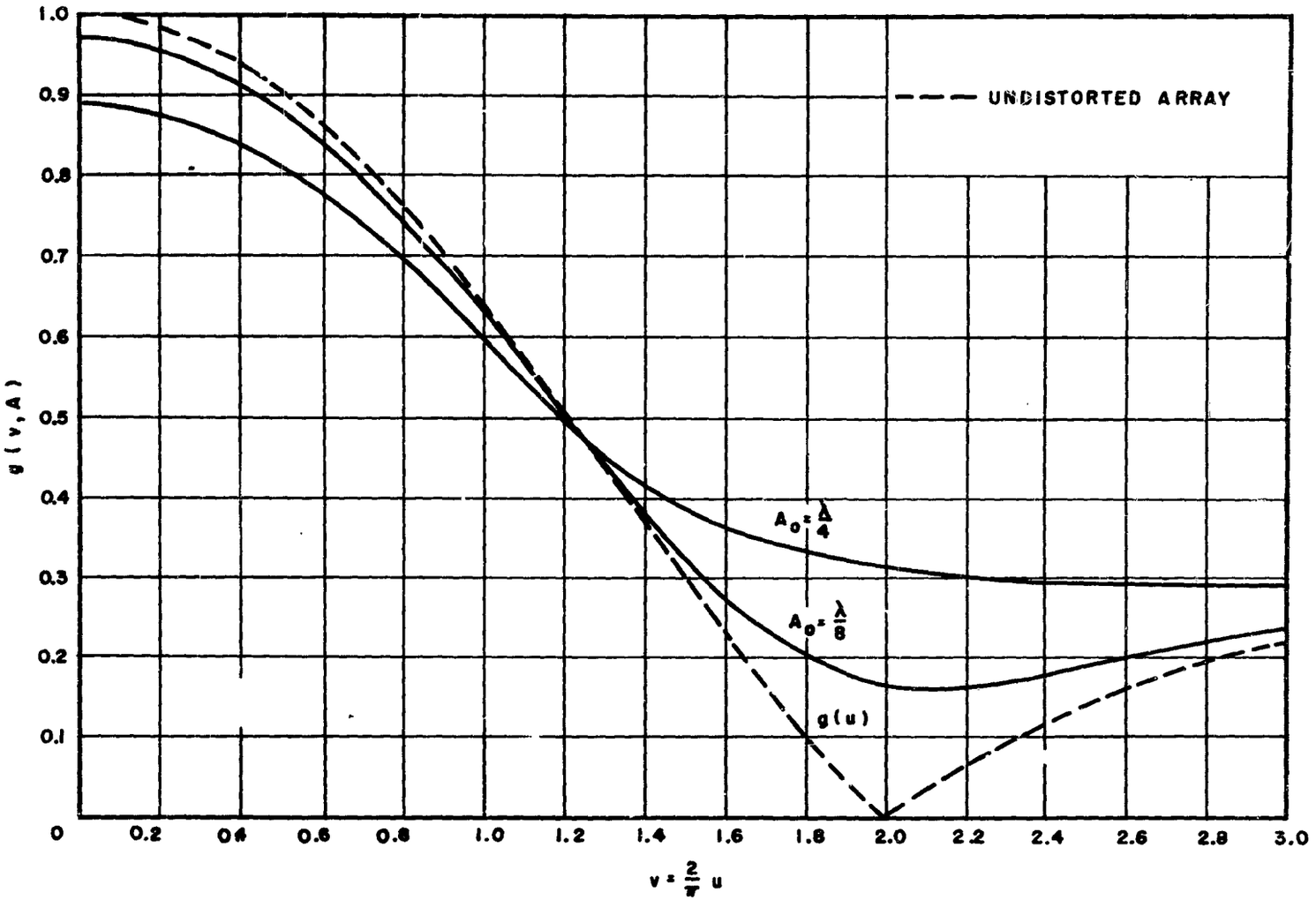

Figure III-21. Radiation Pattern for Bending Array Supported at End Points

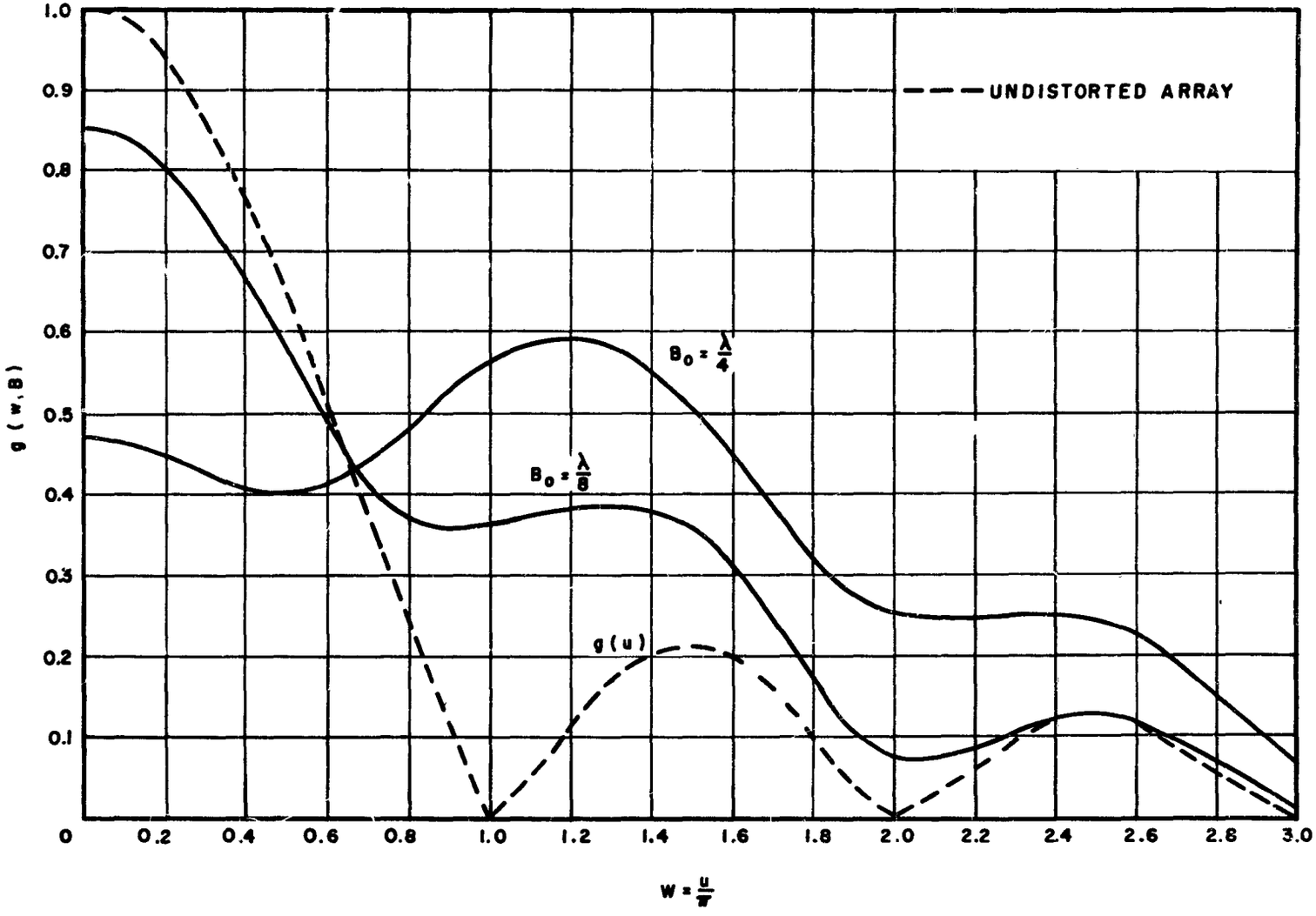

Figure III-22. Radiation Pattern for Bending Array Supported One-Fourth of Array Length from Each End

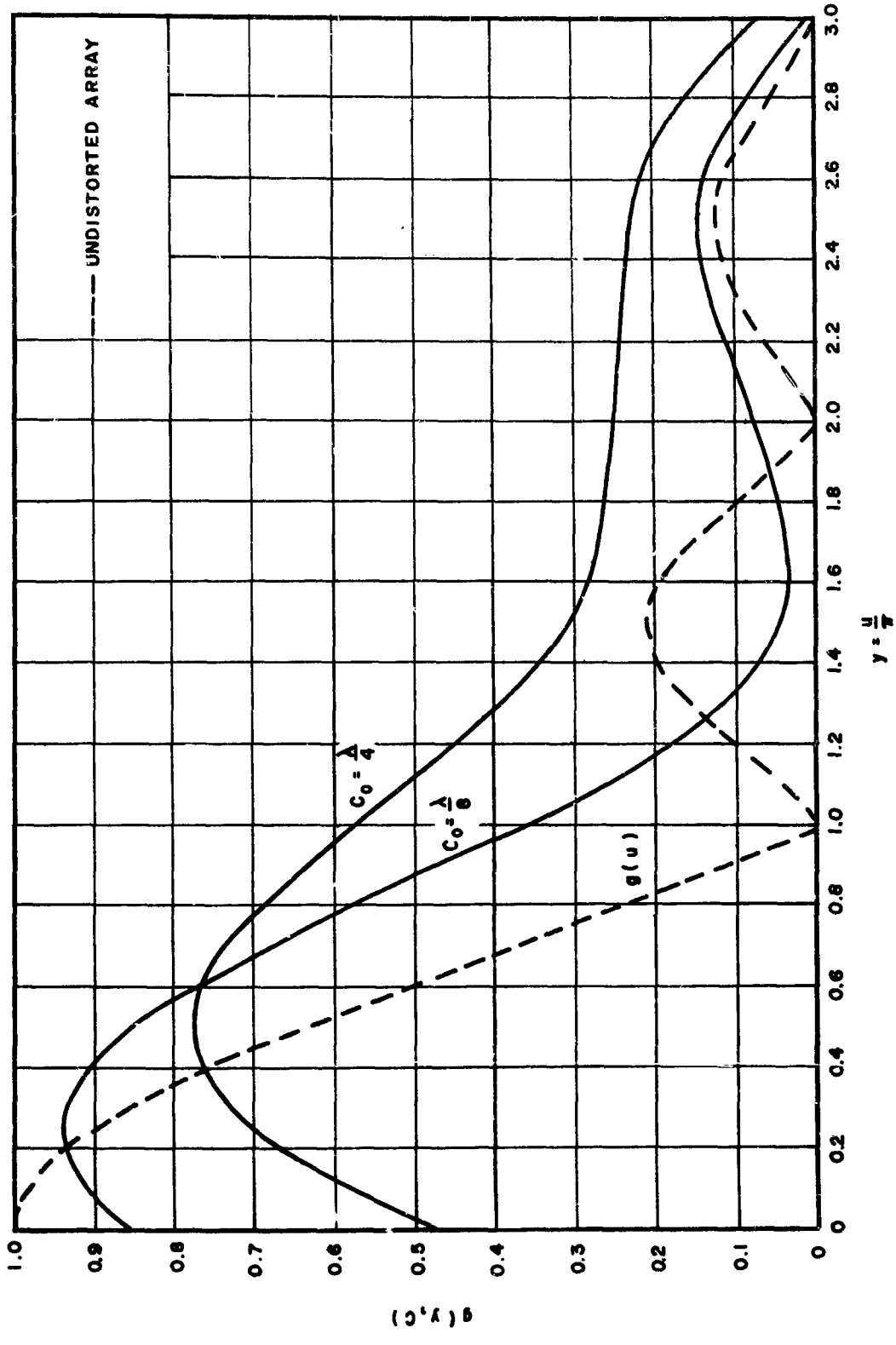

Figure III-23. Radiation Pattern for Bending Array Supported at Center and at Ends

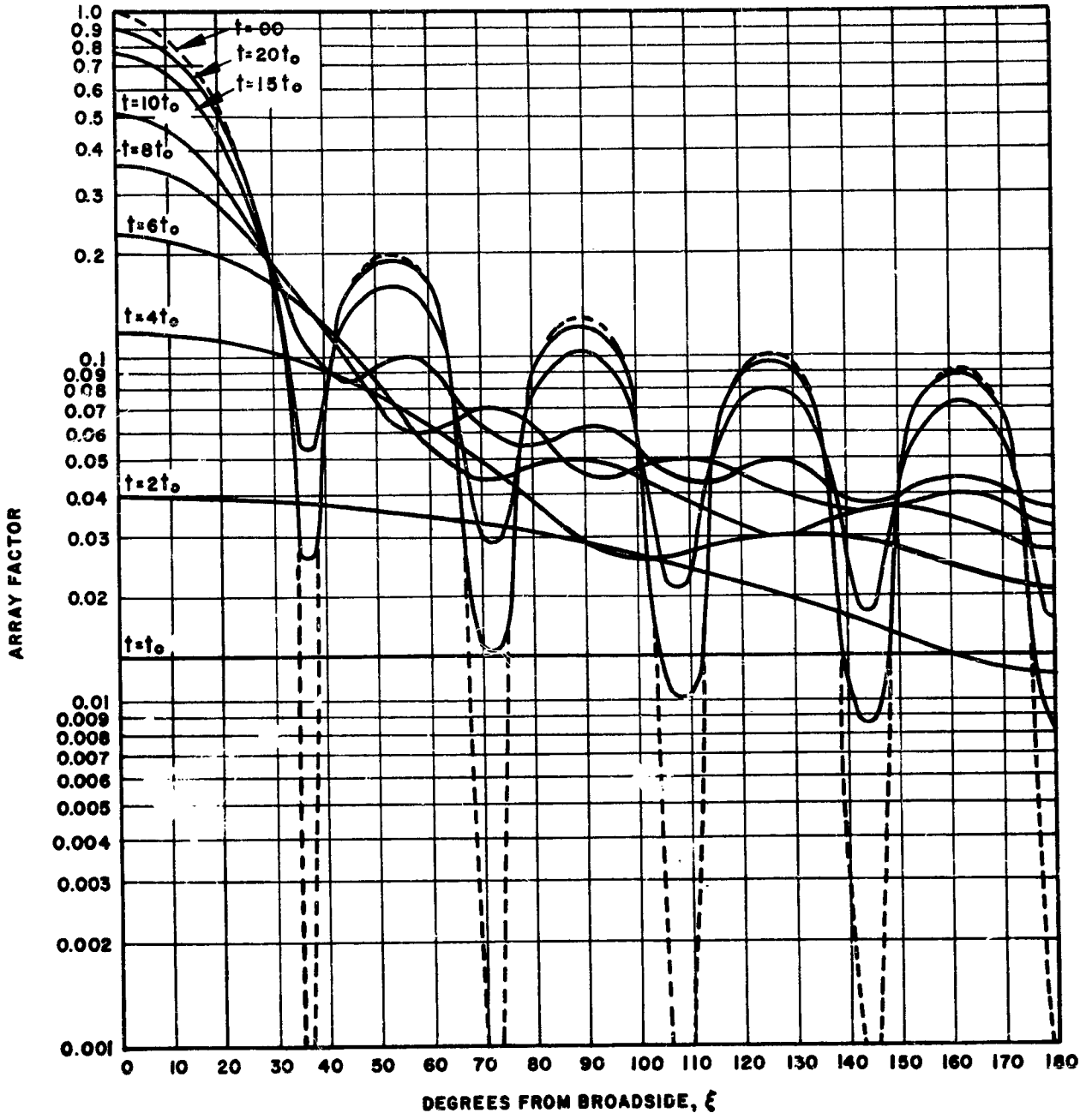

Figure III-24. Pattern Build-Up as Function of Time
N = 10
t_o = time for pulse front to travel between 2 adjacent slots

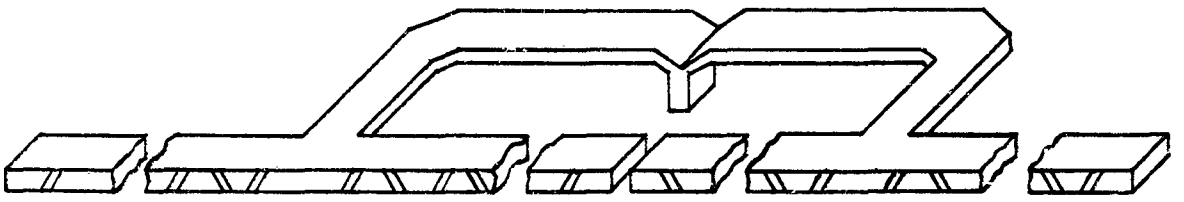

A) Branching Feed System for Sectioned Edge Slot Array

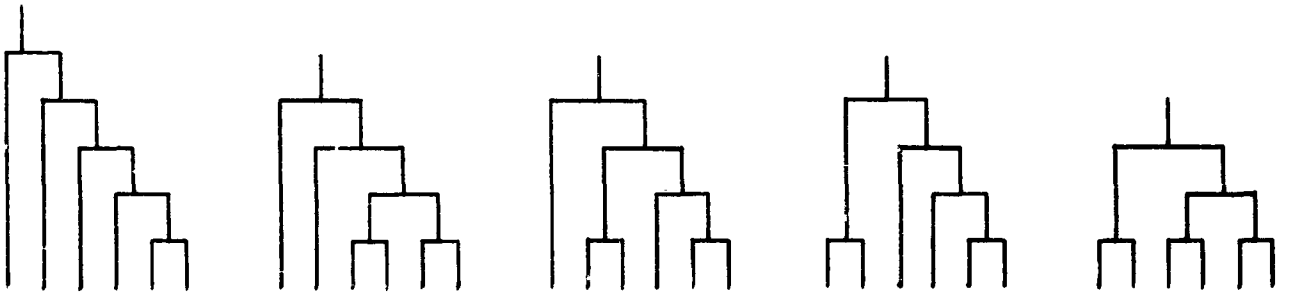

B) Five Possible Arrangements for Six Output System

Figure III-25. Branching Feeds

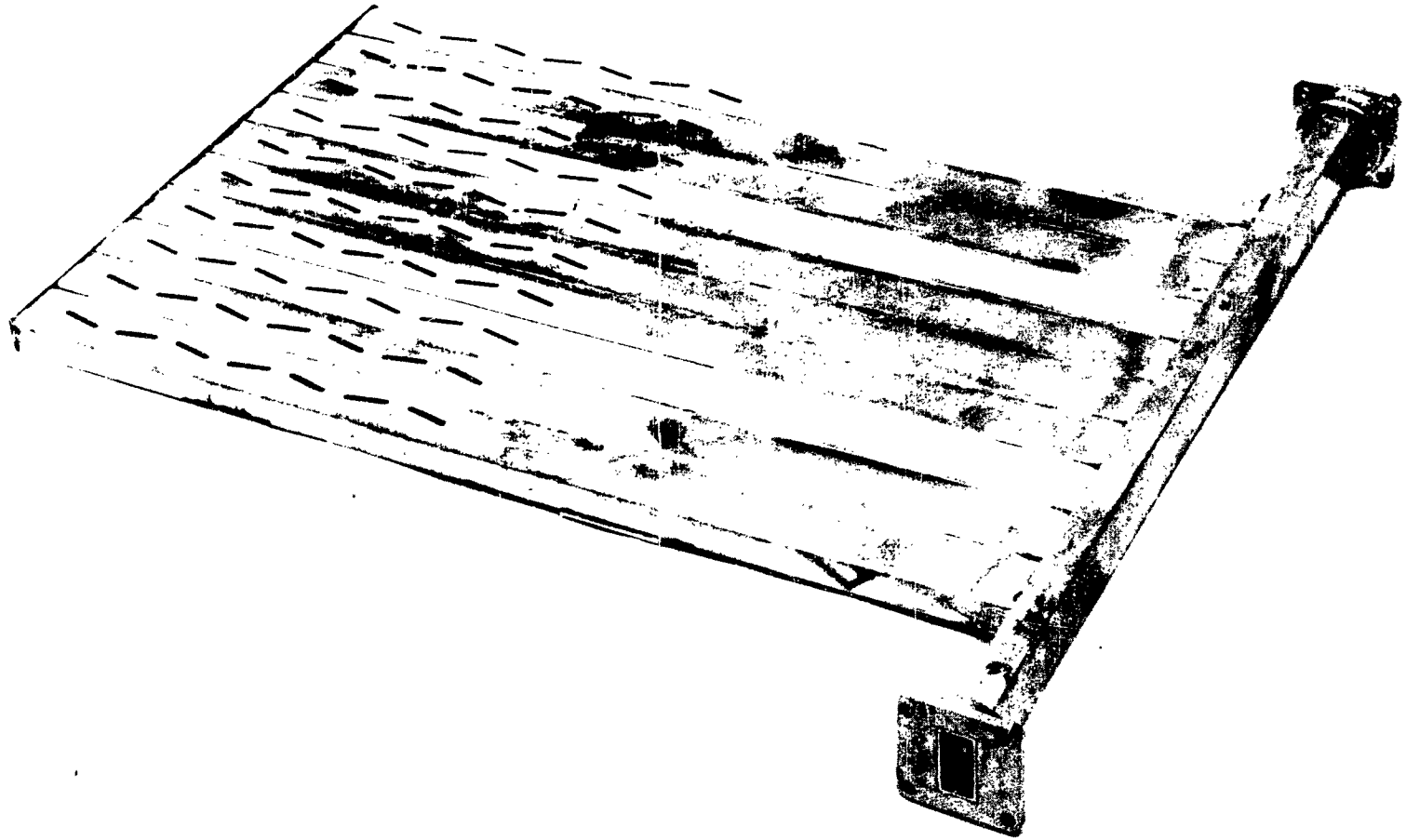

Figure III-26. Two-Dimensional Slot Array

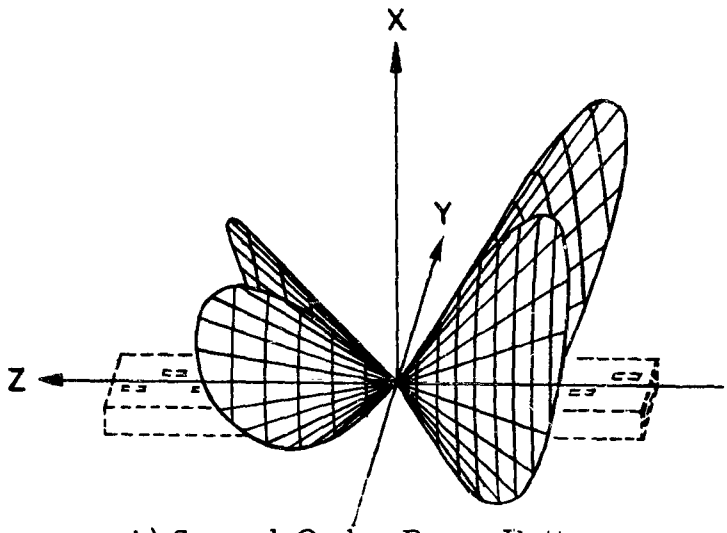

A) Second-Order Beam Pattern

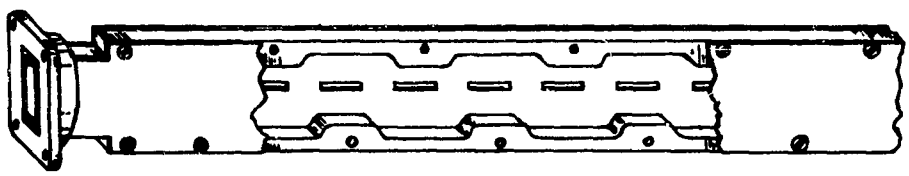

B) In-Line Shunt Slot Array

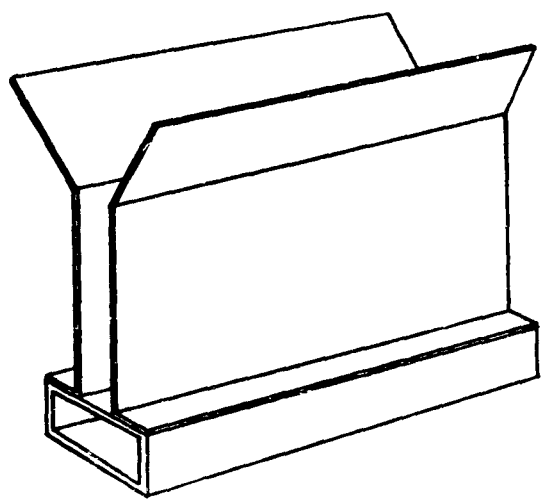

C) Parallel Plate Horn

Figure III-27. Suppression of Second-Order Beams

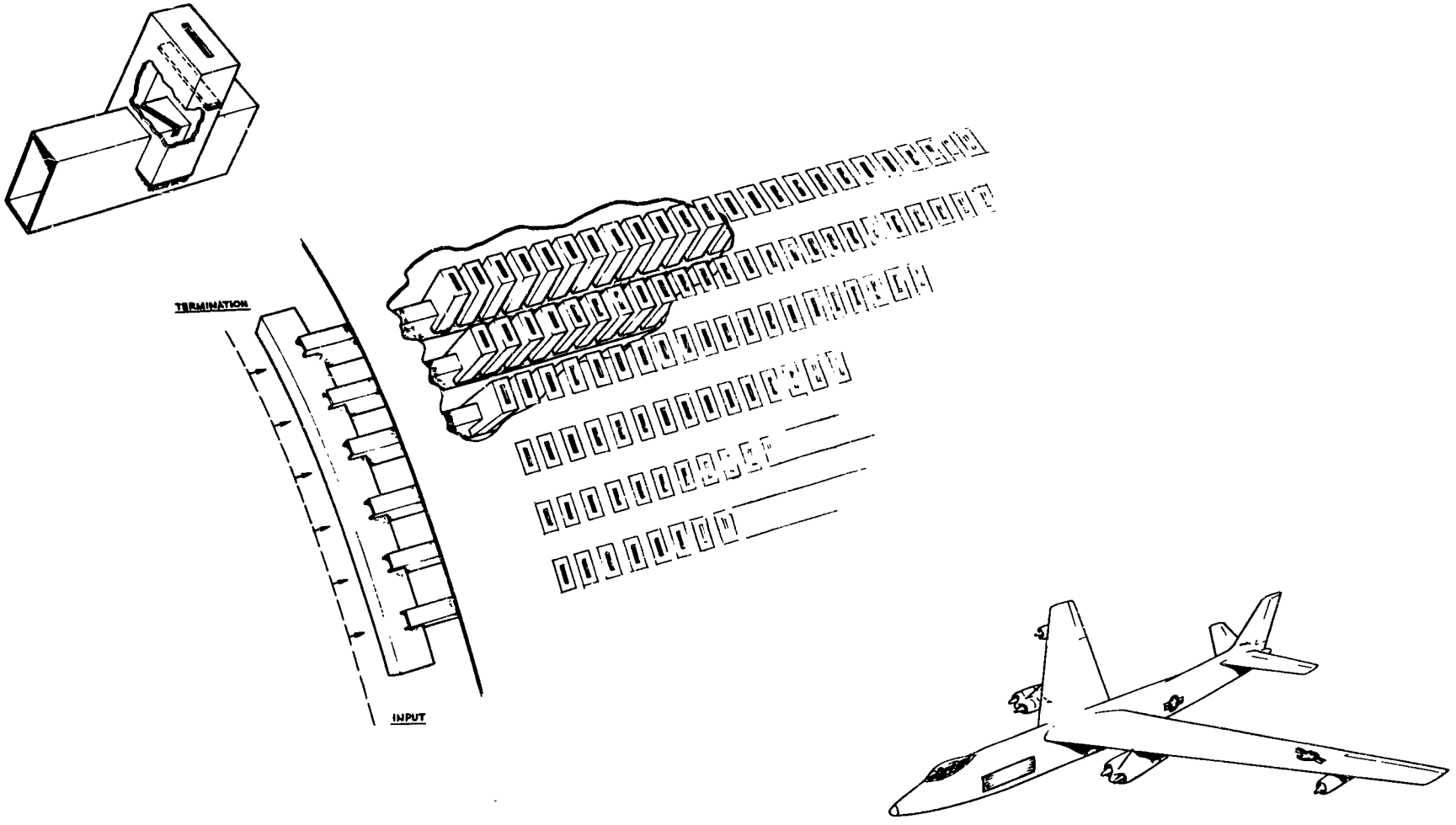

Figure III-28. Two-Dimensional Slot Array in Which Each Slot Is Fed from Individual Four-Terminal Network

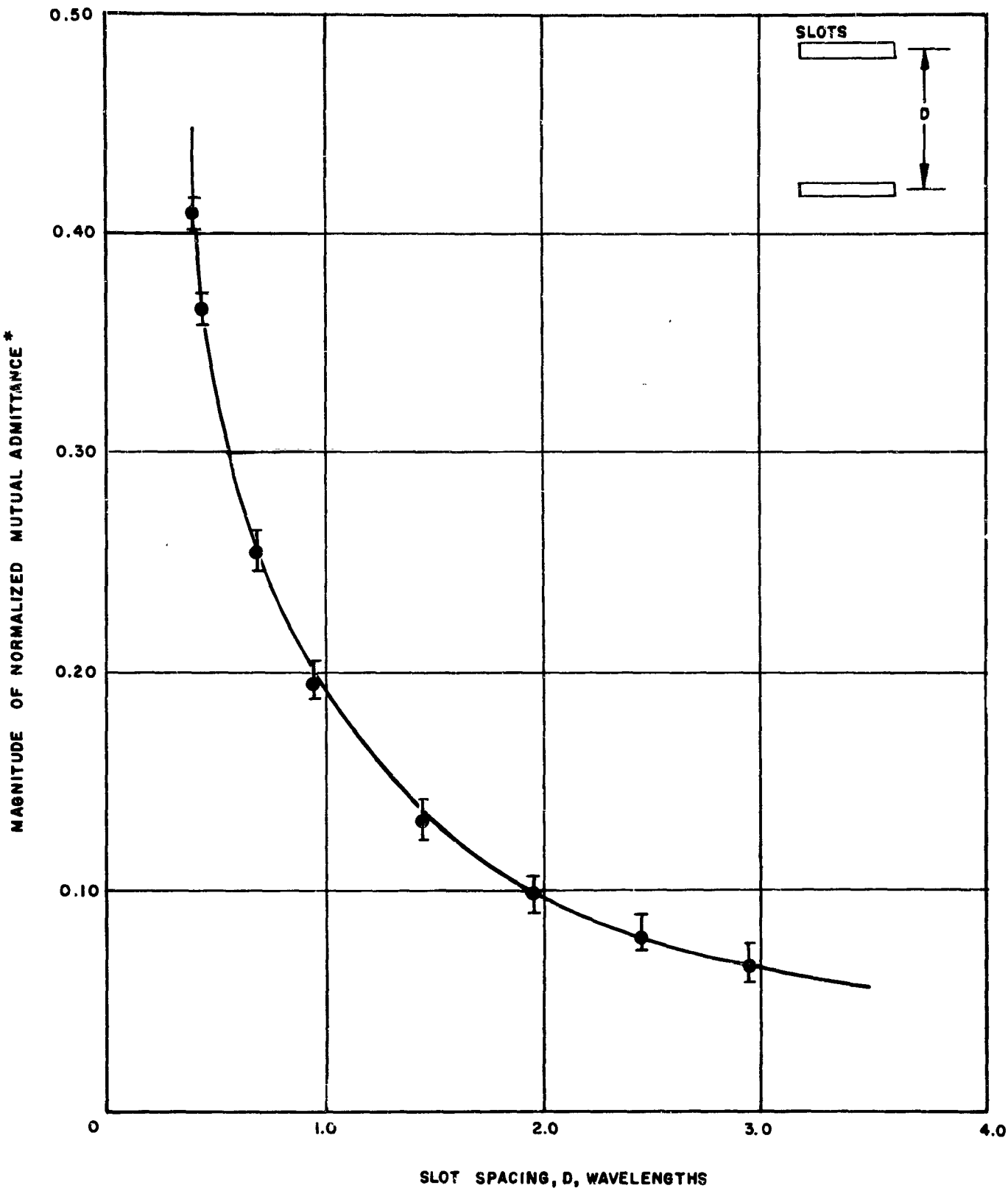

Figure III-29. Magnitude of Normalized Mutual Admittance Between Parallel Slots in Waveguide
(Curve is theoretical; points are measured)

*Mutual admittance is normalized to waveguide characteristic admittance

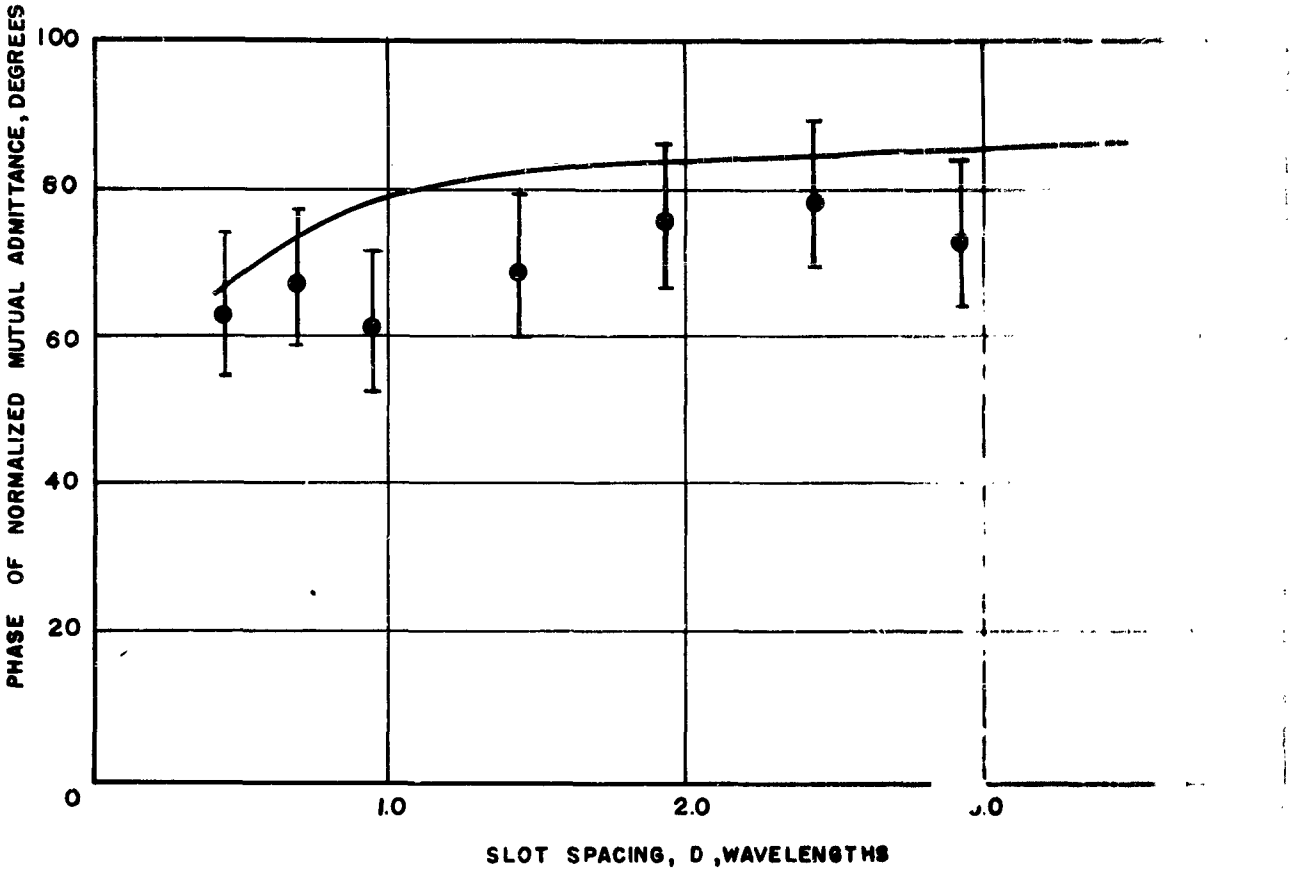

Figure III-30. Phase of Mutual Admittance of Para[illegible] Slots in Wa[illegible]
(Curve is theoretical; points a[illegible] experimental.

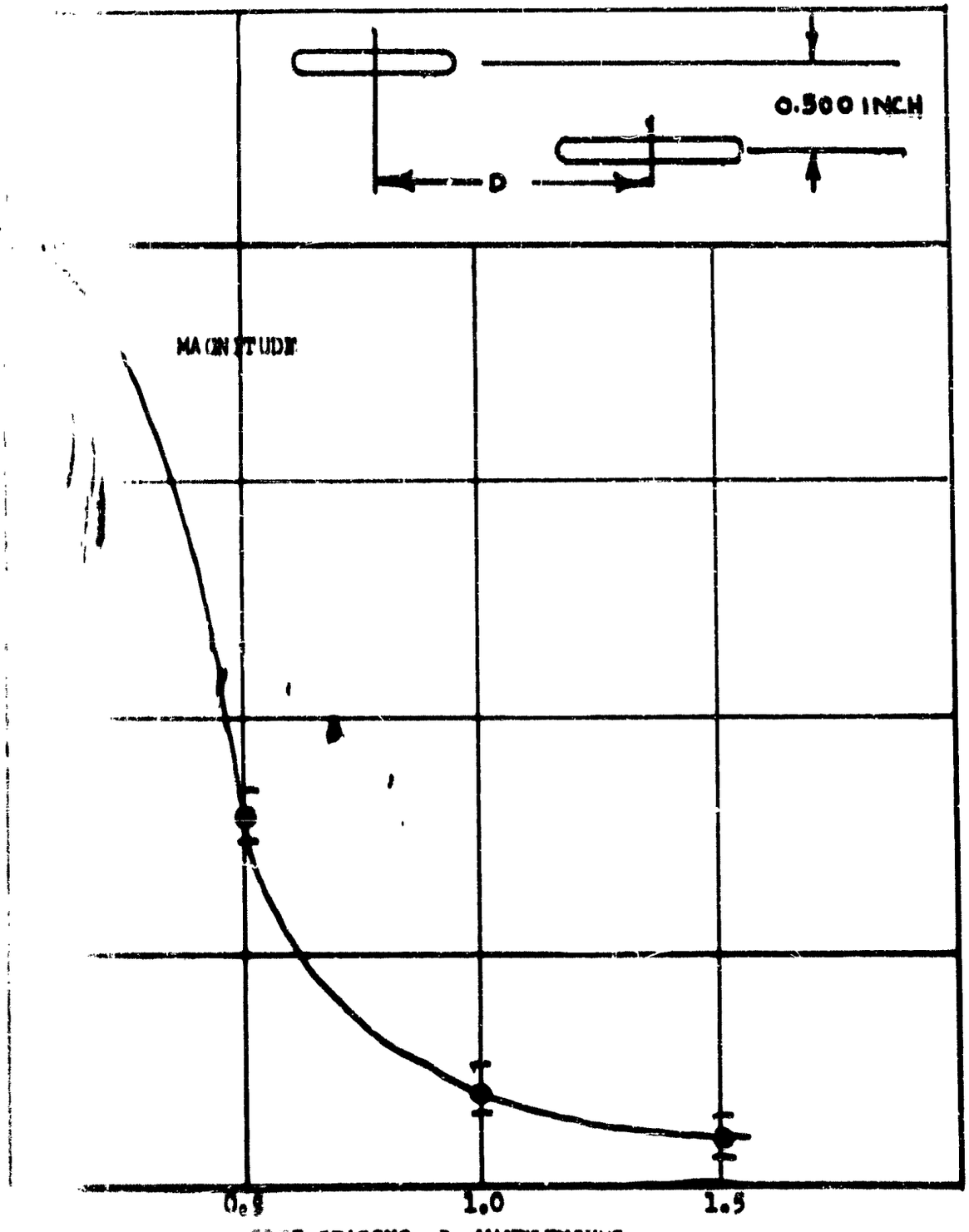

Fig. III-11. Magnitude of Normalized Mutual Admittance Between Parallel Staggered Slots in Waveguide
(Curve is theoretical; points are experimental
*Admittance is normalized to waveguide characteristic admittance

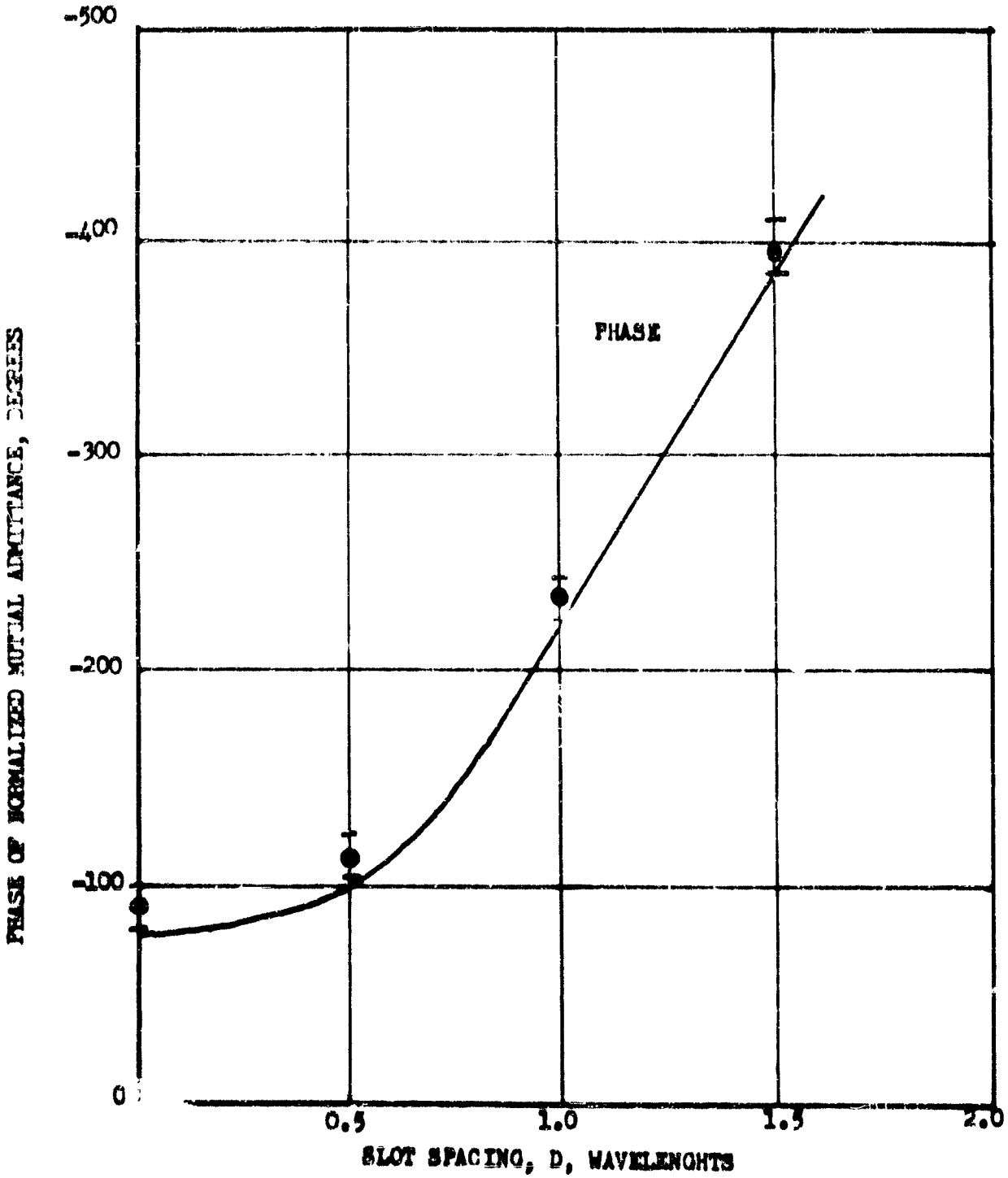

Figure III-32. Phase of Mutual Admittance Between Parallel-Staggered Slots in Waveguide
(Curve is theoretical; points are experimental)

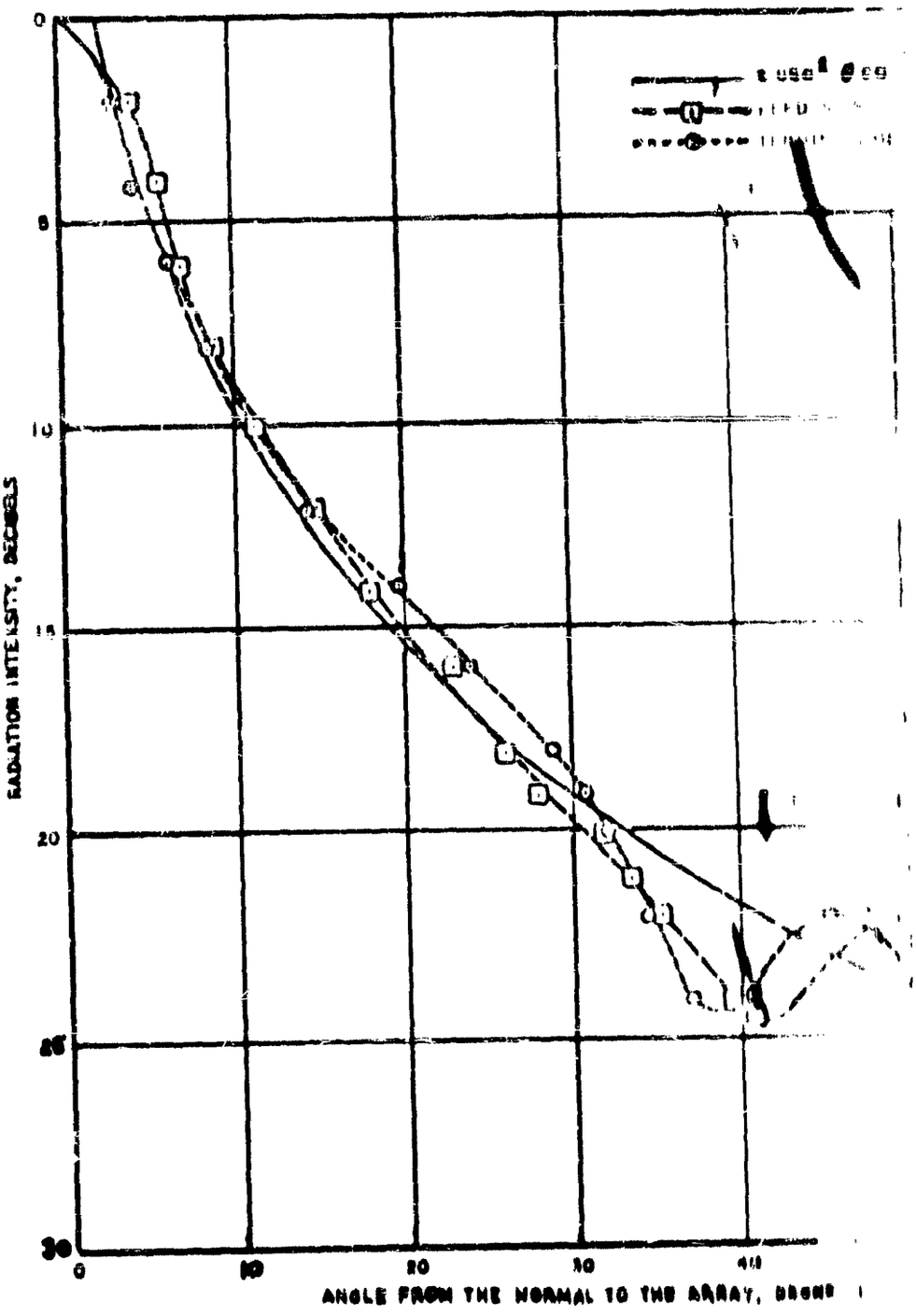

Figure III 38. Radiation Pattern of 17-Element A
Longitudinal Shunt Slot

f 9910 mcps
slot width 0.0645 inch
waveguide 1 0 by 0 5 i

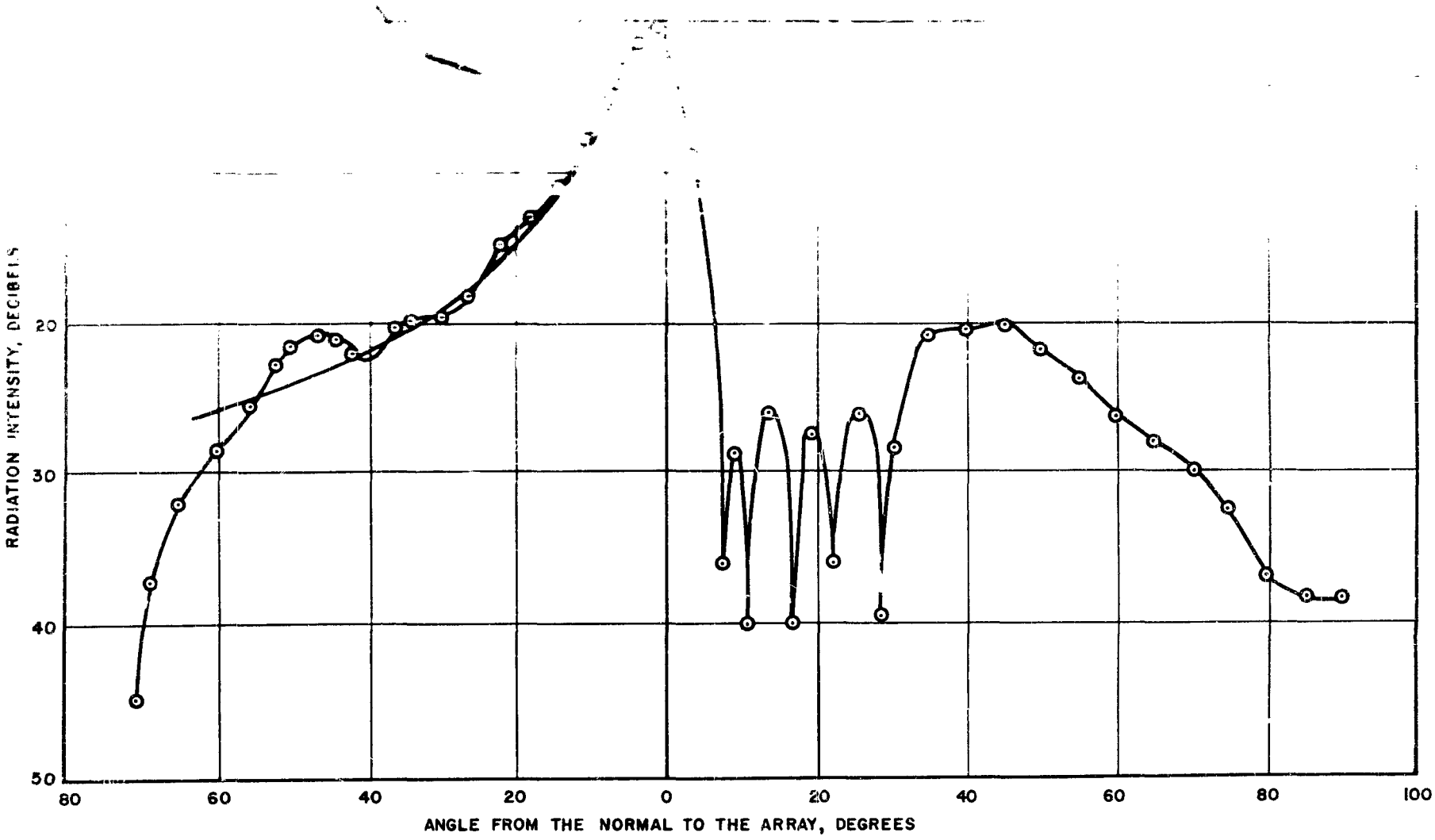

Figure III-34. Radiation Pattern of 15-Element Array of Nonresonant Longitudinal Shunt Slots

f = 9375 mcps
slot width = 0.0625 inch
waveguide = 1.0 by 0.5 inch

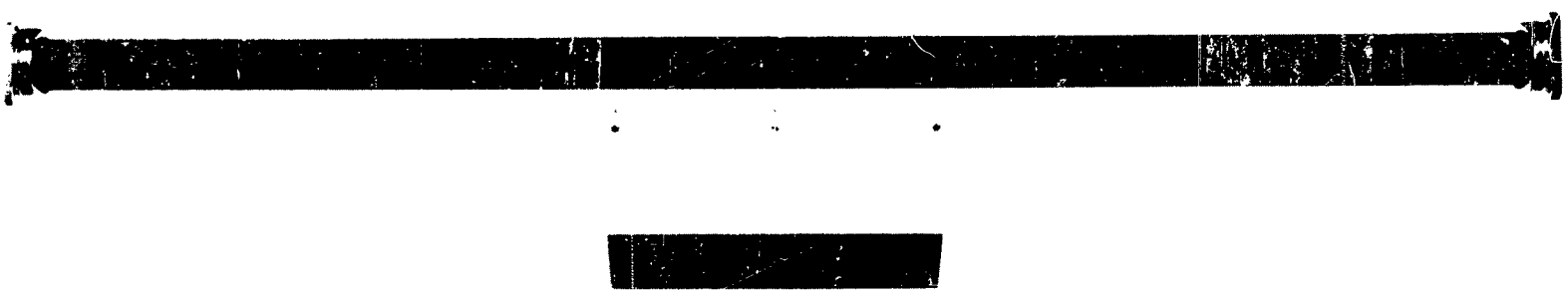

Figure III-35. 24-Element Linear Slot Array

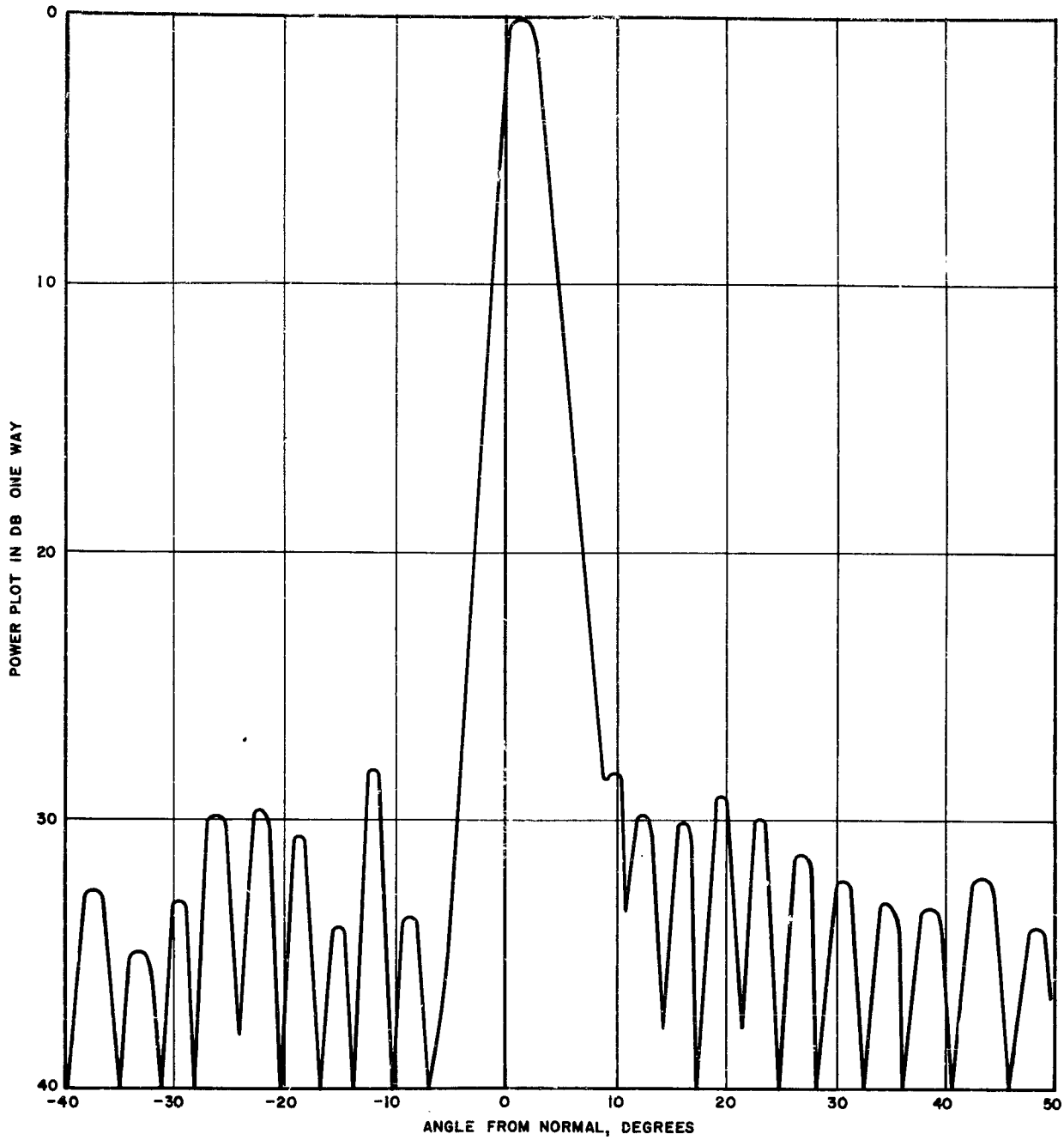

Figure III-36. Radiation Pattern at 9375 mcps of 24-Element Array 30-db sidelobe level design

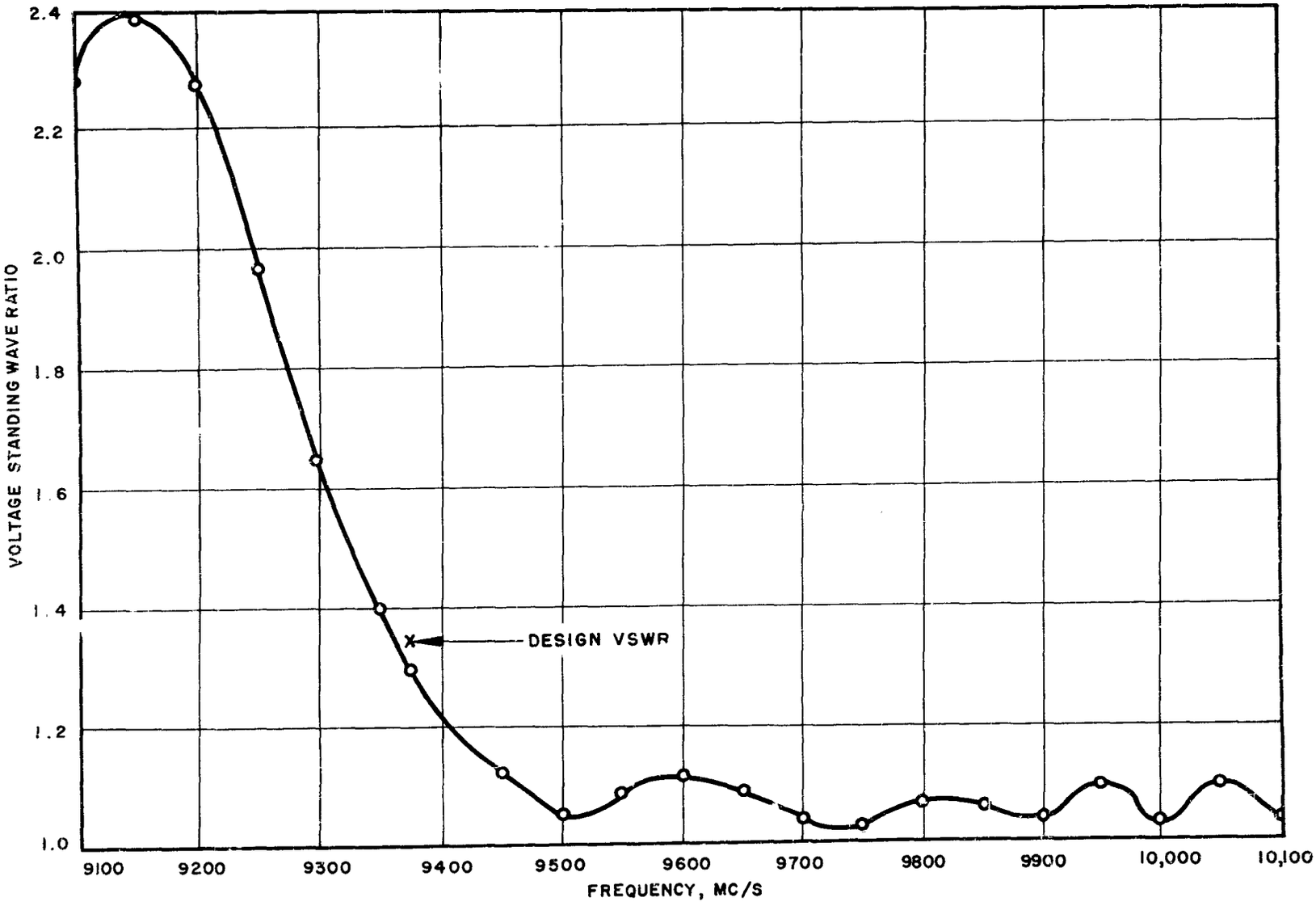

Figure III-37. Input VSWR of 24-Element Array of Resonant Longitudinal Shunt Slots

slot width = 0.0625 inch
waveguide = 1.0 by 0.5 inch

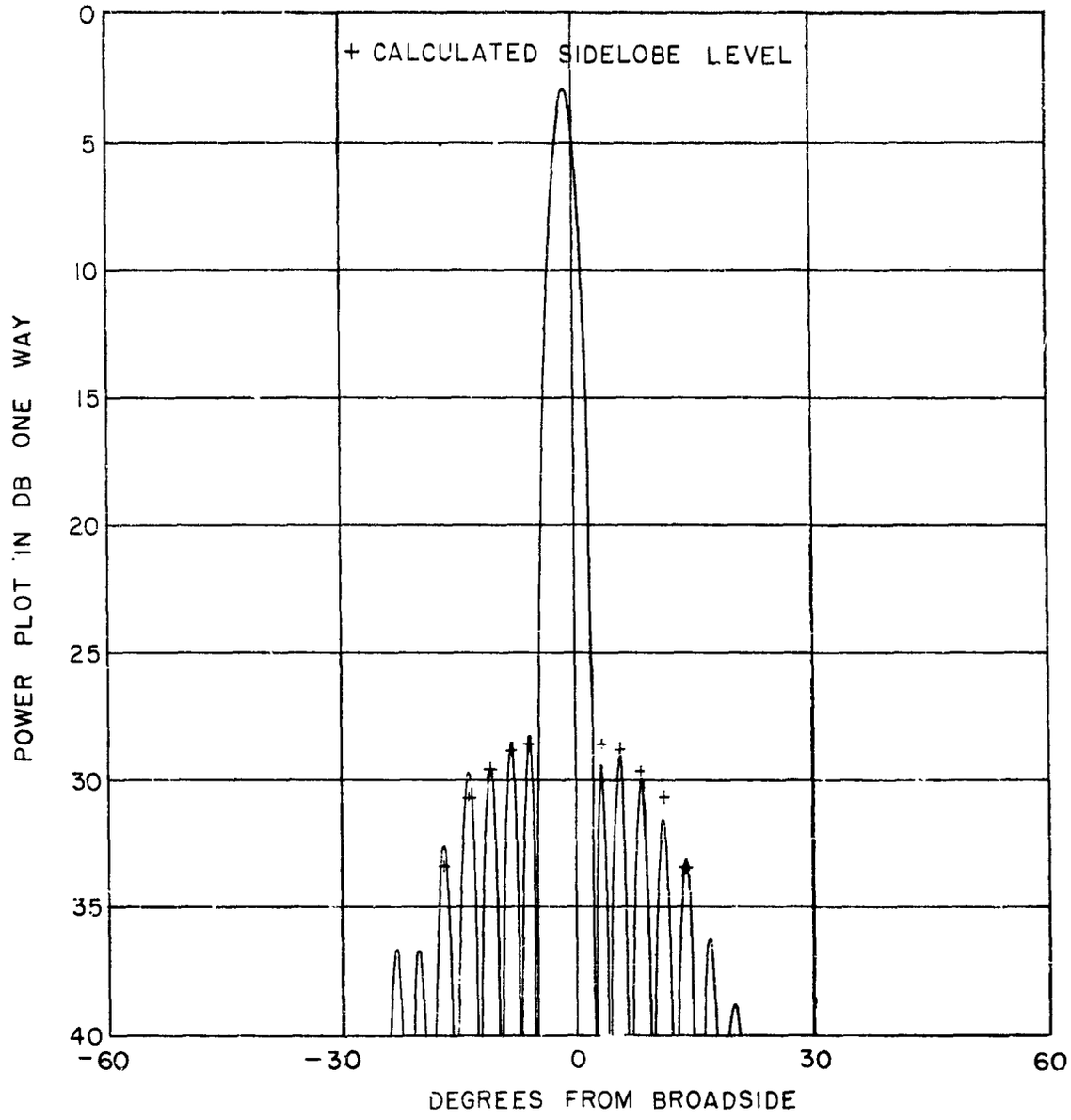

Figure III-38. 30-Element Test Array Designed by Taylor Distribution
f = 9375 mc

Figure III-39. Array of Inclined Series Slots with Flared Horn

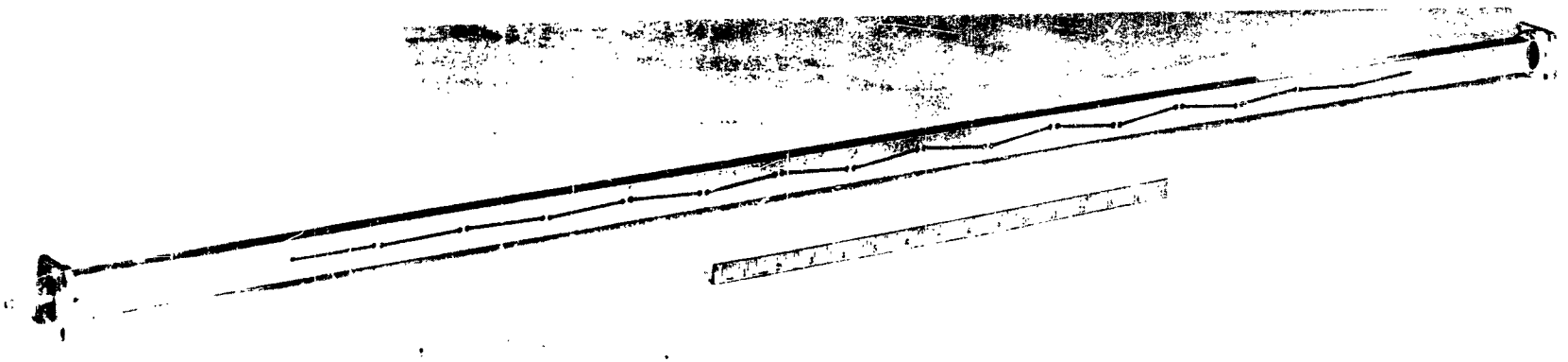

Figure III-40. Sixteen-Element TEM Array

Figure III-41. Array of Slots on Circular Cylinder

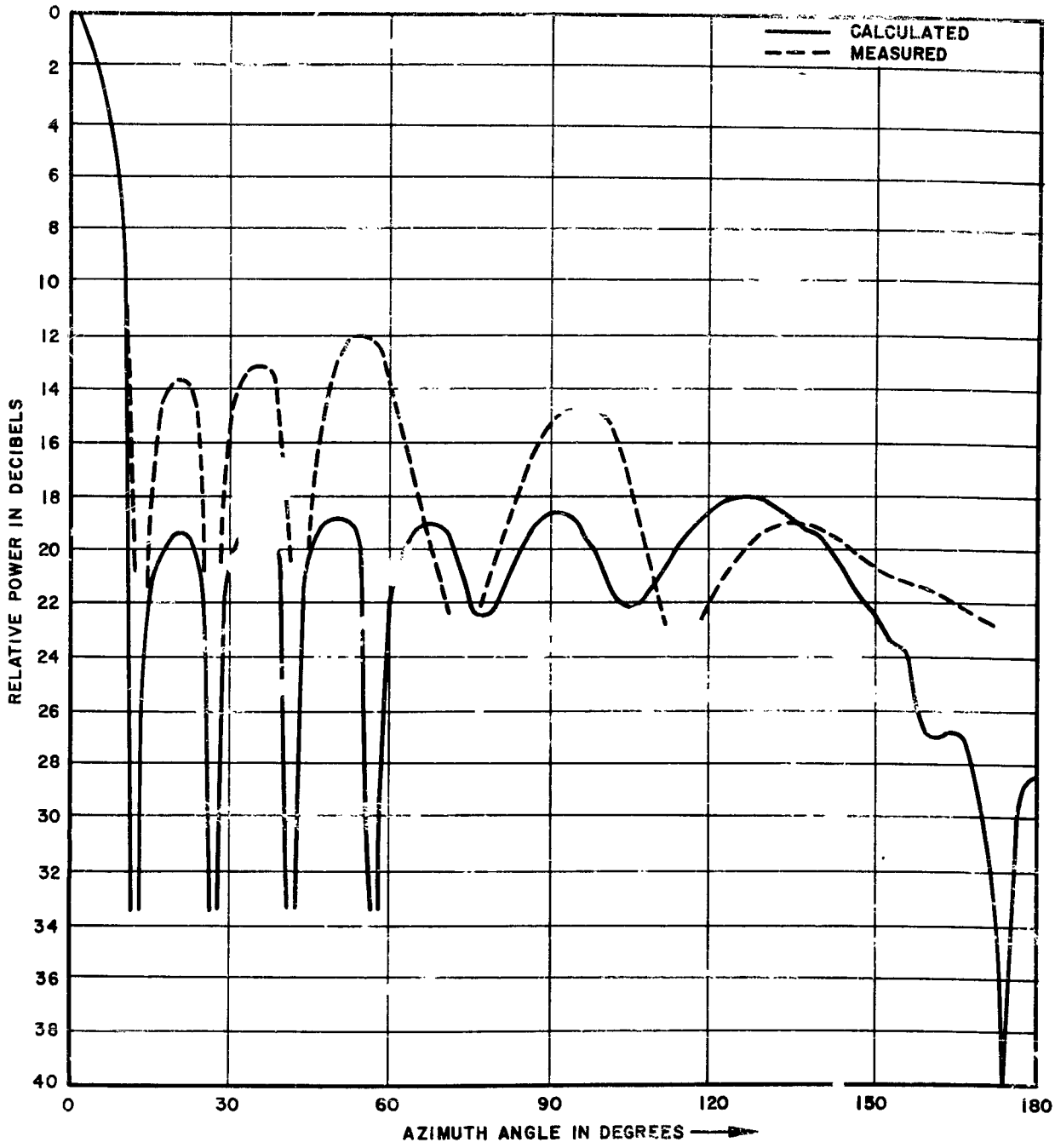

Figure III-42. Radiation Pattern of Circular Array

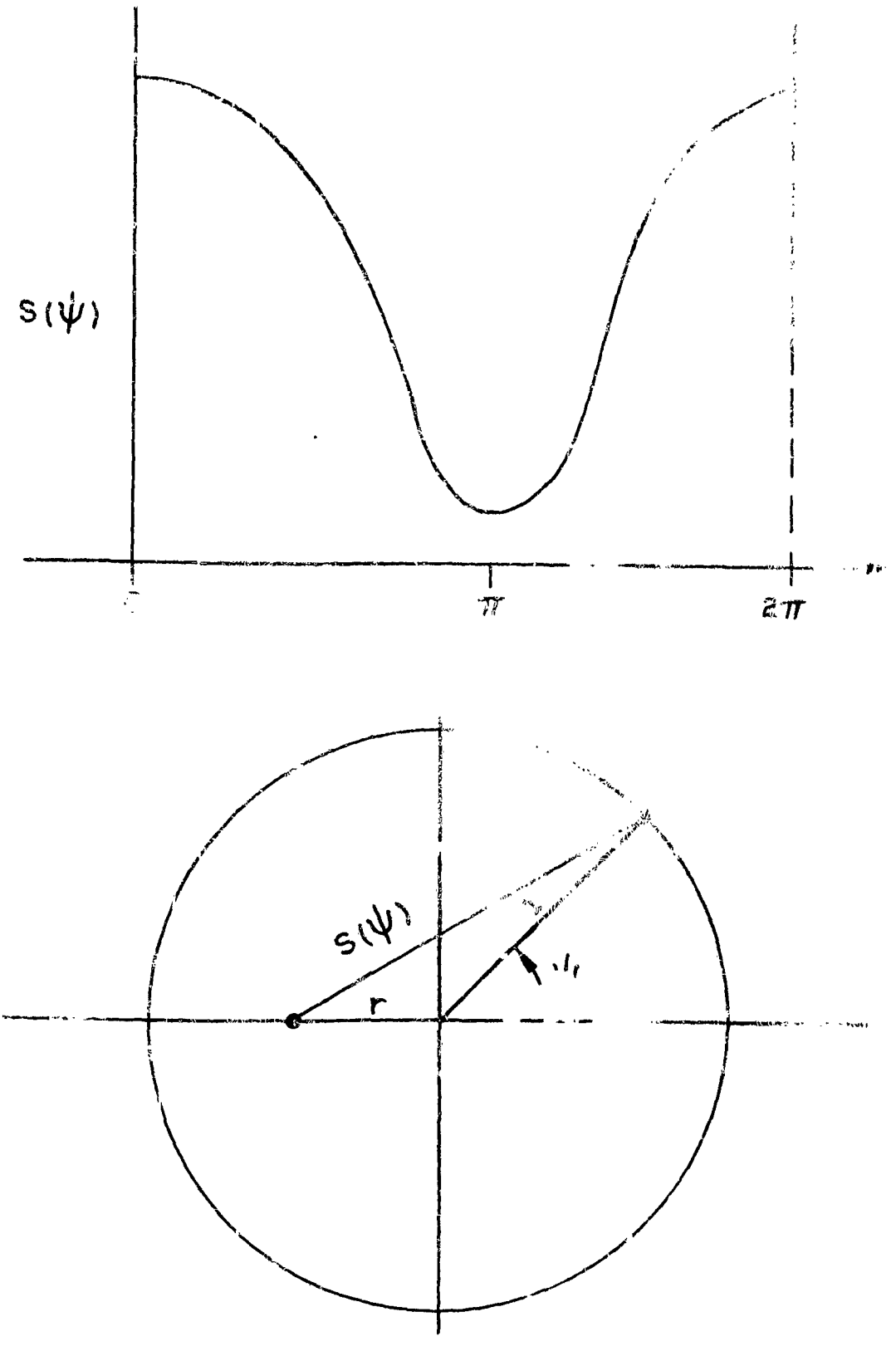

Figure A1-1. Pattern and Circle Diagram for Two-Element Array